



Department of Petroleum Engineering

Fluid Flow Projects

Seventy First Semi-Annual Advisory Board
Meeting Brochure and Presentation Slide
Copy

September 17, 2008

**Tulsa University Fluid Flow Projects
Seventy First Semi-Annual Advisory Board Meeting
Agenda
Wednesday September 17, 2008**

*Tuesday,
September 16, 2008*

***Tulsa University High-Viscosity Oil Projects
Advisory Board Meeting
Doubletree Hotel at Warren Place – Salon A
6110 South Yale Avenue
Tulsa, Oklahoma
8:00 – 11:30 a.m.***

***Tulsa University High-Viscosity Oil Projects, Tulsa University Hydrate Flow
Performance JIP and Tulsa University Fluid Flow Projects Workshop
Luncheon
Doubletree Hotel at Warren Place – Salon B
6110 South Yale Avenue
Tulsa, Oklahoma
12:00 – 1:00 p.m.***

***Tulsa University Fluid Flow Projects Workshop
Doubletree Hotel at Warren Place – Salon A
6110 South Yale Avenue
Tulsa, Oklahoma
1:00 – 3:00 p.m.***

***Tulsa University High-Viscosity Oil Projects, Tulsa University Hydrate Flow
Performance JIP, Tulsa University Fluid Flow Projects and Tulsa University
Paraffin Deposition Projects
Tour of Test Facilities
University of Tulsa North Campus
2450 East Marshall
Tulsa, Oklahoma
4:00 – 6:00 p.m.***

***Tulsa University High-Viscosity Oil Projects, Tulsa University
Hydrate Flow Performance JIP and Tulsa University Fluid Flow Projects
Reception
Doubletree Hotel at Warren Place – Salon C
6110 South Yale Avenue***

**Tulsa, Oklahoma
6:30 – 9:00 p.m.**

***Wednesday,
September 17, 2008***

***Tulsa University Fluid Flow Projects
Advisory Board Meeting
Doubletree Hotel at Warren Place – Tulsa Learning Center
6110 South Yale Avenue
Tulsa, Oklahoma
8:00 a.m. – 5:00 p.m.***

***Tulsa University Fluid Flow Projects and Tulsa University Paraffin
Deposition Projects
Reception
Doubletree Hotel at Warren Place – Parkview East
6110 South Yale Avenue
Tulsa, Oklahoma
6:00 – 9:00 p.m.***

***Thursday,
September 18, 2008***

***Tulsa University Paraffin Deposition Projects
Advisory Board Meeting
Doubletree Hotel at Warren Place – Salon A
6110 South Yale Avenue
Tulsa, Oklahoma
8:00 a.m. – 1:00 p.m.***

Tulsa University Fluid Flow Projects Seventy First Semi-Annual Advisory Board Meeting Agenda Wednesday September 17, 2008

8:00 a.m.	Breakfast – Tulsa Learning Center	
8:30	Introductory Remarks	Cem Sarica
	Executive Summary	Cem Sarica
9:00	TUFFP Progress Reports	
	An Experimental and Theoretical Investigation of Slug Flow for High Oil Viscosity in Horizontal Pipes	Bahadir Gokcal
	Liquid Entrainment in Annular Gas-Liquid Flow in Inclined Pipes	Kyle Magrini
10:30	Coffee Break	
10:45	TUFFP Progress Reports	
	Investigation of Three-Phase Gas-Oil-Water Flow in Hilly-Terrain Pipelines	Gizem Ersoy-Gokcal
	Modeling of Oil-Water Pipe Flow	Anoop Sharma
12:15 p.m.	Lunch – Parkview East	
1:15 p.m.	TUFFP Progress Reports	
	Modeling of Gas-Liquid Flow in an Upward Vertical Annulus	Tingting Yu
	Up-scaling Studies in Multiphase Flow	Abdel Al-Sarkhi
2:30	Coffee Break	
2:45	TUFFP Project Reports	
	Instrumentation Update – Capacitance Probe and Laser Sensors	Scott Graham
	Unified Model Update - A New Model for Wetted Wall Fraction and Gravity Center of Liquid Film in Gas-Liquid Pipe Flow	Holden Zhang
	TUFFPT 2008 Software Update	Holden Zhang
	TUFFP Questionnaire	Holden Zhang
4:00	TUFFP Business Report	Cem Sarica
4:30	Open Discussion	Cem Sarica
5:00	Adjourn	
6:00	TUFFP/TUPDP Reception – Parkview East	

Table of Contents

Executive Summary	1
Introductory Presentation	5
TUFFP Progress Reports	
Executive Summary	13
An Experimental and Theoretical Investigation of Slug Flow for High Oil Viscosity in Horizontal Pipes – Bahadir Gokcal	
Presentation	15
Report.....	47
Executive Summary	77
Liquid Entrainment in Annular Gas-Liquid Flow in Inclined Pipes – Kyle Magrini	
Presentation	79
Report.....	101
Executive Summary	117
Investigation of Three-Phase Gas-Oil Water Flow in Hilly Terrain Pipelines – Gizem Ersoy Gokcal	
Presentation	119
Report.....	147
Executive Summary	155
A Study on Oil-Water Flow Closure Relationships – Anoop Sharma	
Presentation	157
Report.....	175
Executive Summary	183
Modeling of Gas-Liquid Flow in Upward Vertical Annuli – Tingting Yu	
Presentation	185
Executive Summary	249
Up-Scaling Studies in Multiphase Flow – Abdel Alsarkhi	
Presentation	251
Report.....	271
Transient Modeling	
Executive Summary	287
Executive Summary	289
Capacitance Sensors – Scott Graham	
Presentation	291
Executive Summary	313
Unified Model - A Model for Wetted Wall Fraction and Gravity Center of Liquid Film in Gas-Liquid Pipe Flow – Holden Zhang	
Presentation	315
Report.....	329
TUFFPT Updates – Holden Zhang	
Presentation	339

2008 Questionnaire – Holden Zhang Presentation	341
TUFFP Business Report	
Presentation	343
Introduction	351
Personnel	353
Membership.....	357
Equipment and Facilities	359
Financial Status	361
Miscellaneous Information.....	367
Appendices	
Appendix A – Fluid Flow Projects Deliverables	371
Appendix B – 2007 Fluid Flow Projects Advisory Board Representatives.....	377
Appendix C – History of Fluid Flow Projects Membership.....	383
Appendix D – Contact Information.....	389

Executive Summary

Progress on each research project is given later in this Advisory Board Brochure. A brief summary of the activities is given below.

- “*Investigation of Gas-Oil-Water Flow*”. Three-phase gas-oil-water flow is a common occurrence in the petroleum industry. The ultimate objective of TUFFP for gas-oil-water studies is to develop a unified model based on theoretical and experimental analyses. A three-phase model has already been developed. There are several projects underway addressing the three-phase flow.
- “*Oil-Water Flow in Pipes*”. Our three-phase model requires knowledge on oil/water interaction. Moreover, oil-water flow is of interest for many applications ranging from horizontal well flow to separator design. The objectives of this study are to assess performance of current models by checking them against experimental data and improve the existing models through better closure relationships or develop new models if necessary.

After the completion of several experimental oil-water flow studies, efforts are concentrated on improvement of the modeling. A new modeling approach based on droplet formation mechanism is proposed.

- “*High Viscosity Oil Two-phase Flow Behavior*”. Oils with viscosities as high as 10,000 cp are produced from many fields around the world. Current multiphase flow models are largely based on experimental data with low viscosity fluids. The gap between lab and field data may be three orders of magnitude or more. Therefore, current mechanistic models need to be verified with higher liquid viscosity experimental results. Modifications or new developments are necessary.

An earlier TUFFP study conducted by Gokcal showed that the performances of existing models are not sufficiently accurate for high viscosity oils. It was found that increasing oil viscosity had a significant effect on flow behavior. Mostly, intermittent flow (slug and elongated bubble) was observed in his study. Based on his results, this study focuses on the slug flow.

Drift velocity measurements for a horizontal pipe configuration made last fall indicated that the drift velocity decreases with increasing liquid

viscosity. The drift velocity measurements were completed for the entire range of upward inclination angles for a viscosity range of 200 – 1200 cp and a drift flux model for horizontal flow was developed before Spring 2008 Advisory Board meeting. Since the spring Advisory Board meeting significant progress has been made in several fronts of this study. Air and highly viscous oil two-phase experiments have been performed with the 2-in. ID high viscosity indoor facility. Pressure drop and slug characteristics, including translational velocity, slug length and frequency, have been measured. A unified drift velocity for all inclination angles has been developed. New translational velocity and slug frequency correlations are developed including the viscosity effects. It is found that slug lengths follow a log-normal distribution, and the average slug length decreases as the liquid viscosity increases.

- “*Droplet Homo-phase Interaction Study*”. There are many cases in multiphase flow where droplets are entrained from or coalesced into a continuous homophase. For example, in annular mist flow, the liquid droplets are in dynamic equilibrium with the film on the walls, experiencing both entrainment and coalescence. Very few mechanistic models exist for entrainment rate and coalescence rate. Understanding the basic physics of these phenomena is essential to model situations of practical interest to the industry. Droplet homo-phase covers a broad range of possibilities.

A past sensitivity study of multiphase flow predictive models showed that, in stratified and annular flow, the variation of droplet entrainment fraction can significantly affect the predicted pressure gradient. Although better entrainment fraction correlations were proposed, a need was identified to experimentally investigate entrainment fraction for inclined pipes. The current study investigates entrainment fraction for various inclination angles. The 3-in. ID severe slugging facility is being utilized. A new device to measure entrainment fraction has been developed and constructed. Test will start following the Advisory Board meeting. On the modeling front, a new dimensionless group correlating the entrainment fraction for all inclination angles has been identified and verified with the experimental data from the open literature.

- “*Lagrangian-Eulerian Transient Two-Phase Model*”. The main motivation for this study comes from the need to mitigate hydrate formation

following cool-down of fluids and high pressure surge during shut-in. A study of the transient temperature variation along with phase redistribution is critical for the design of a flow line-riser system as well as for flow assurance during production cycle.

A two-phase transient model was first formulated and solved. The model is capable of simulating phase redistribution. There has not been much progress in this project since the graduate student had to go back to his home country to fulfill the requirements of his employer. The study will be attempted to be completed remotely. We will continue to report on this project as soon as we have significant progress.

TUFFP's simplified transient flow studies project proposal ranked #5 in our recent questionnaire. Therefore, it will be launched as a separate project as soon as we identify a fitting graduate student.

- “*Low Liquid Loading Gas-Oil-Water Flow in Horizontal and Near Horizontal Pipes*”. Low liquid loading exists widely in wet gas pipelines. These pipelines often contain water and hydrocarbon condensates. Small amounts of liquids can lead to a significant increase in pressure loss along a pipeline. Moreover, existence of water can significantly contribute to the problem of corrosion and hydrate formation problems. Therefore, understanding of flow characteristics of low liquid loading gas-oil-water flow is of great importance in transportation of wet gas.

Last year, large amount of data were collected on various flow parameters such as flow patterns, phase distribution, onset of droplet entrainment, entrainment fraction, and film velocity. The results revealed a new flow phenomenon.

This study has been continued with another MS student. Due to insufficient performance of the student, the project is put on temporary hold. A new graduate student has already been identified to take over the project. She will be starting January 2009. Moreover, we will have a visiting professor from China to spend his sabbatical with us. He will be working with us on this project. We hope to accelerate the project with his involvement.

- “*Multiphase Flow in Hilly Terrain Pipelines*”. Three-phase flow in hilly terrain pipelines is a

common occurrence. The existence of a water phase in the system poses many potential flow assurance and processing problems. Most of the problems are directly related to the flow characteristics. Although the characteristics of two-phase gas-liquid flow have been investigated extensively, there are very few studies addressing multiphase gas-oil-water flow in hilly terrain pipelines. The general objectives of this project are to thoroughly investigate and compare existing models, and develop closure relationships and predictive models for three-phase flow of gas-oil-water in hilly-terrain pipelines.

Since the Fall AB meeting, the facility modifications have been completed. The facility is instrumented with laser, conductance and capacitance sensors, pressure transducers, regular and high speed cameras and quick closing valves. We expect to acquire significant data to capture three-phase flow characteristics of a hilly terrain unit. The data will be used to identify new flow characteristics, to test the existing models and software, and to develop better models.

- “*Up-scaling Studies*”. One of the most important issues that we face in multiphase flow technology development is scaling up of small diameter and low pressure results to large diameter and high pressure conditions. Studies with a large diameter facility would significantly improve our understanding of flow characteristics in actual field conditions. Therefore, our main objective in this study is to investigate the effect of pipe diameter and pressures on flow behavior using a larger diameter flow loop.

The design of a high pressure (500 psi operating pressures) and large diameter (6 in. ID) facility were completed and presented at the last Advisory Board meeting. The facility P&ID is prepared by an independent engineering company. The final stage before construction will be the HAZOP exercise with the help of one of the member company HAZOP engineers. Major equipments with long lead time are expected to arrive soon. We are aiming to complete the construction of the facility by summer of 2009.

- “*Gas-Liquid Flow in an Upward Vertical Annulus*.” TUFFP has not conducted any study on this topic since Caetano's pioneering work in 1985. This project is initiated to improve our predictions for multiphase flow. Significant progress has been made by applying the unified modeling concepts to annulus flow. The comparisons with Caetano data shows improved performance. The efforts will continue to further improve the model.

- “*Unified Mechanistic Model*”. TUFFP maintains, and continuously improves upon the TUFFP unified model. A model is developed for predictions of wetted wall fraction and gravity center of liquid film in gas-liquid pipe flow under different flow conditions. This model is based on the instability of the liquid film in an equilibrium stratified flow. The relationship between the wetted wall fraction and the gravity center of the liquid film is based on the double circle model. The present model unifies the predictions of liquid wetted wall fraction, film gravity center and flow pattern transition between stratified and annular flows. It can also be used to predict the wetted wall fraction in the film region of a slug flow and stratified flow with droplet entrainment.
- “*Software Improvements*.” Several improvements have been made to TUFFPT, TUFFP’s multiphase flow prediction software. Improvements include: use of black oil model to update fluid properties for each segment during integration; better pressure drop prediction; living documentation describing the modeling details, and faster VBA interface.

Current TUFFP membership stands at 17 (16 industrial companies and MMS). DOE’s support of TUFFP in the development of new generation multiphase flow predictive tools for three-phase flow has officially ended in August 2008. DOE’s support translated into the equivalent of four additional members for five years, since July 2003. Efforts continue to further increase the TUFFP membership level. SPT will be joining TUFFP as soon as the legal documents signed. Drs Cem Sarica and Holden Zhang PetroChina and Chinese National Offshore Oil Company (CNOOC) in Beijing in June 2008. It is expected that CNOOC to join TUFFP. A detailed financial report is provided in this report. We thank our members for their continued support.

Several related projects are underway. The related projects involve sharing of facilities and personnel with TUFFP. The Paraffin Deposition consortium, TUPDP, is into its third phase with 11 members. The Center of Research Excellence (TUCoRE) initiated by Chevron at The University of Tulsa funds several research projects. TUCoRE activities in the area of Heavy Oil Multiphase Flow have resulted in a new Joint Industry Project (JIP) to investigate Heavy Oil Multiphase Flow in more detail. The JIP currently has three members. Chevron has already made \$680,000 commitment to upgrade an existing facility to be used in the project.



Fluid Flow Projects

71th Fluid Flow Projects Advisory Board Meeting

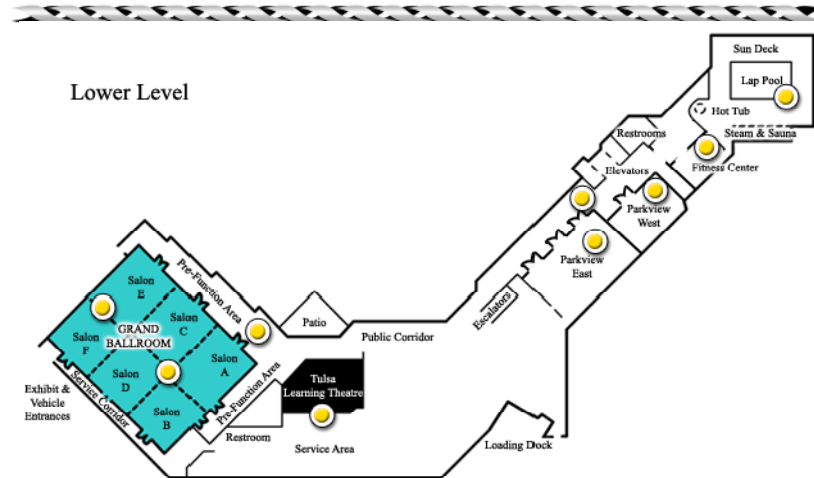
Welcome

Advisory Board Meeting, September 17, 2008

Safety Moment

- ◆ Emergency Exits
- ◆ Assembly Point
- ◆ Rest Rooms

Floor Plan



Introductory Remarks

- ◆ **71th Semi-Annual Advisory Board Meeting**
- ◆ **Handout**
 - **Combined Brochure and Slide Copy**
- ◆ **Sign-Up List**
 - **Please Leave Business Card at Registration Table**

Team

◆ Research Associates

- Cem Sarica (Director)
- Holden Zhang (Associate Director)
- Jim Brill (Director Emeritus)
- Abdel Salam Al-Sarkhi
 - ▲ Resigned Effective August 25, 2008
- Mingxiu (Michelle) Li

Team ...

◆ Project Coordinator

- Linda Jones

◆ Project Engineer

- Scott Graham

◆ Research Technicians/Flow Loop Operators

- Craig Waldron
- Brandon Kelsey

Team ...

- ◆ **Computer Manager and Web Master**

- **James Miller (On Military Service Leave)**

Team ...

- ◆ **TUFFP Research Assistants**

- **Kwonil Choi (Ph.D.) – Brazil**
- **Gizem Ersoy (Ph.D.) – Turkey**
- **Bahadir Gokcal (Ph.D.) – Turkey**
- **Ceyda Kora (MS) – Turkey**
- **Kyle Magrini (MS) – USA**
- **Anoop Sharma (MS) – India**
- **Tingting Yu (MS) - PRC**

Guests

- ◆ John Dobson, Advantica
- ◆ Geoff Fowler, BG Group
- ◆ Eva Habetinova, SINTEF
- ◆ Prof. Jing Gong, China University of Petroleum at Beijing

Agenda

- ◆ 8:30 **Introductory Remarks and Executive Summary**
- ◆ 9:00 **Progress Reports**
 - **An Experimental and Theoretical Investigation of Slug Flow for High Oil Viscosity in Horizontal Pipes**
 - **Liquid Entrainment in Annular Gas-Liquid Flow in Inclined Pipes**
- ◆ 10:30 **Coffee Break**

Agenda ...

- ◆ **10:45 Progress Reports**
 - Investigation of Three-Phase Gas-Oil-Water Flow in Hilly-Terrain Pipelines
 - Modeling of Oil-Water Pipe Flow
- ◆ **12:15 Lunch - Parkview East**
- ◆ **1:15 Progress Reports**
 - Modeling of Gas-Liquid Flow in an Upward Vertical Annulus
 - Up-scaling Studies in Multiphase Flow

Agenda ...

- ◆ **2:30 Coffee Break**
- ◆ **2:45 Progress Reports**
 - Instrumentation Update – Capacitance Probe and Laser Sensors
 - Unified Model Update - A New Model for Wetted Wall Fraction and Gravity Center of Liquid Film in Gas-Liquid Pipe Flow
 - TUFFPT 2008 Software Update
 - TUFFP Questionnaire

Agenda ...

- ◆ 4:00 TUFFP Business Report
- ◆ 4:30 Open Discussion
- ◆ 5:00 Adjourn
- ◆ 6:00 TUFFP/TUPDP Reception
(Park View East)

Other Activities

- ◆ September 16, 2008
 - TUHOP Meeting
 - TUFFP Workshop
 - ▲ Excellent Presentations
 - ▲ Beneficial for Everybody
 - Facility Tour
- ◆ September 18, 2008
 - TUPDP Meeting



Fluid Flow Projects

Executive Summary of Research Activities

Cem Sarica

Advisory Board Meeting, September 17, 2008

High Viscosity Multiphase Flow

- ◆ **Significance**
 - Discovery of High Viscosity Oil Reserves
- ◆ **Objective**
 - Development of Better Prediction Models
- ◆ **Past Studies**
 - **First TUFFP Study by Gokcal**
 - ▲ Existing Models Perform Poorly for Viscosities Between 200 and 1000 cp
 - ▲ Significantly Different Flow Behavior
 - + Dominance of Slug Flow
 - + Shorter Slugs
 - + Thicker Layer of Liquid in Gas Region
 - + Large and Small Size Bubbles in Slug Body

High Viscosity Multiphase Flow ...

◆ Current Study (Status)

- Drift Velocity Experiments are Completed at Inclinations Angles from 0° to 85°
- Horizontal and Inclined Flow Drift Velocity Models were Developed Based on Benjamin's Approach
- Slug Frequency, Length and Translational Velocity Data Acquired and Correlations Developed

High Viscosity Multiphase Flow ...

◆ Future Activities (With New Students)

- Remaining Closure Relationships
 - ▲ Liquid Holdup in the Slug
- Investigate Higher Viscosity Oils, $\mu > 1000$ cp
- Investigate Higher GOR Behavior



Fluid Flow Projects

An Experimental and Theoretical Investigation of Slug Flow for High Oil Viscosity in Horizontal Pipes

Bahadir Gokcal

Advisory Board Meeting, September 17, 2008

Outline

- ◆ **Significance**
- ◆ **Objectives**
- ◆ **Experimental Facility**
- ◆ **Modeling Study**
- ◆ **Project Schedule**

Significance

- ◆ **Increase in High Viscosity Oil Offshore Discoveries**
- ◆ **Current Multiphase Flow Models Developed for Low Viscosity Oils**
- ◆ **Multiphase Flows May Exhibit Significantly Different Behavior for Higher Viscosity Oils**

Significance ...

- ◆ **Gokcal (2005, TUFFP) Conducted Experimental Study**
- ◆ **Performance of Existing Models is not Sufficient**
- ◆ **Increasing Oil Viscosity has Significant Effect on Flow Behavior**

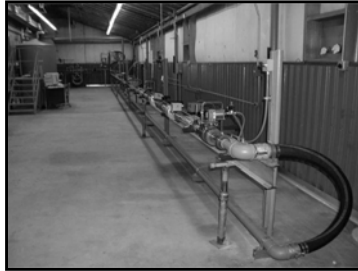
Objectives

- ◆ **Acquire Experimental Data on Characteristics of Slug Flow for High Viscosity Oil**
- ◆ **Develop Closure Models on Slug Flow for High Viscosity Oil in Horizontal Pipes**
 - **Translational Velocity and Drift Velocity**
 - **Slug Length/Frequency**
- ◆ **Validate Proposed Models with Experimental Results**

Experimental Facility

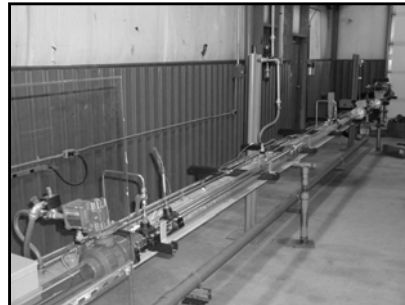
- ◆ **2-in ID High Viscosity Indoor Experimental Facility**
 - **Test Section**
 - **Metering Section**
 - **Heating System**
 - **Cooling System**

Experimental Facility ...



2-in ID High Viscosity Indoor Facility

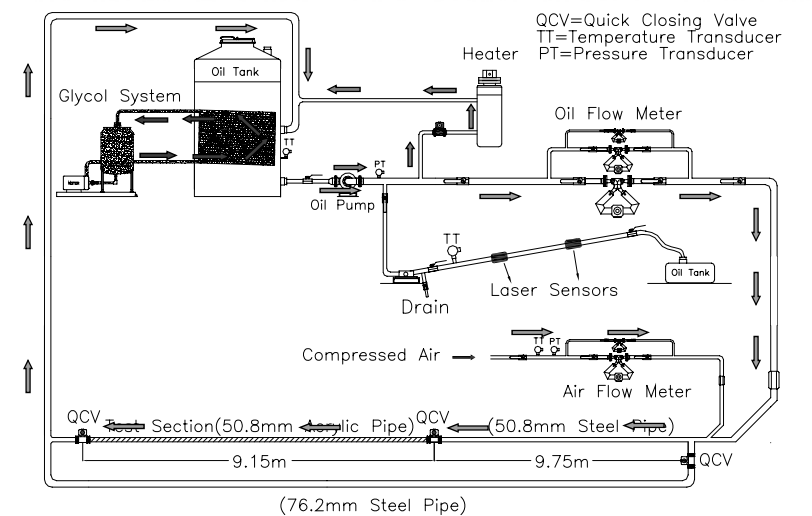
Test Section



 Fluid Flow Projects

Advisory Board Meeting, September 17, 2008

Experimental Facility...

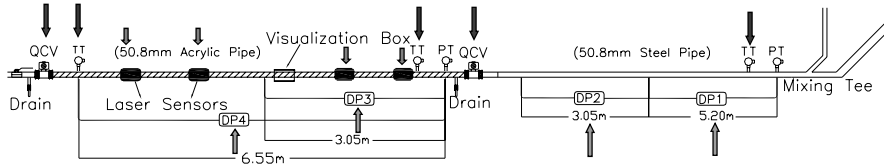


 Fluid Flow Projects

Advisory Board Meeting, September 17, 2008

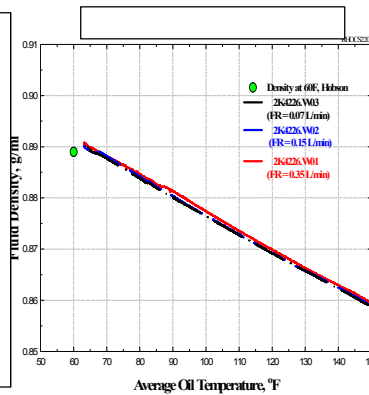
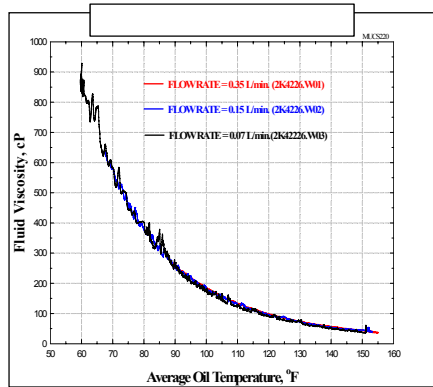
Experimental Facility...

Schematic of Test Section



Test Fluid

Company	Product Name	Grade	°API	Viscosity (40 °C)	Viscosity Index
Citgo	Sentry Oils	220	27.6	220 cp	95



Instrumentation and Data Acquisition

- ◆ **Four Laser Sensors**
 - **Commercially Available Instruments**
 - **Two of Them Used to Measure Translational Velocity**
 - **One Laser Sensor Enough to Determine Slug Frequency and Length**

Instrumentation and Data Acquisition...

- ◆ **Two Capacitance Sensors**
 - **Copper Ring, Electronic Circuit, Housing**
 - **Two of Them Necessary to Measure Translational Velocity**
- ◆ **Data Acquisition System**
 - **Maximum Scan Rate: 500Hz**
 - **8 Analog and 16 Digital Channels**

Data Processing

- ◆ **Data Processing Big Challenge**
- ◆ **Data Collected for 160 Seconds at 125 Hz**
- ◆ **Two Large Excel Macro Programs are Written to Process Data**

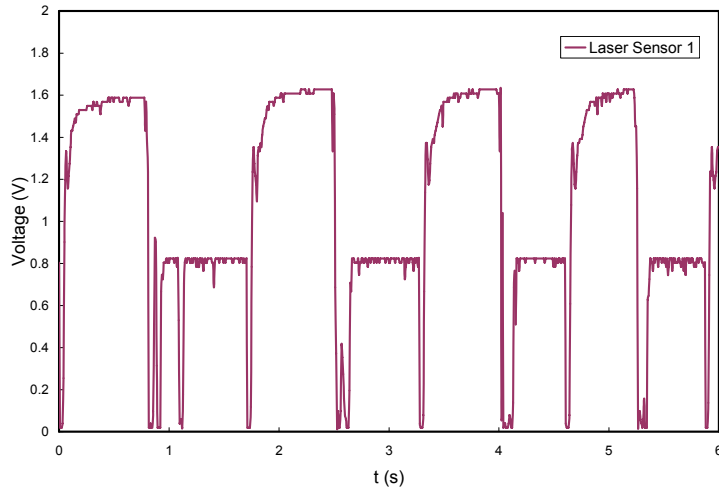
Data Processing...

- ◆ **First Macro**
 - **Clean Noise from Raw Signal**
 - **Count Number of Slugs**
 - **Calculate Slug Frequency**
 - **Record Time That Each Slug Passes from One Instrument**
- ◆ **Second Macro**
 - **Apply Cross-Correlation Technique on Raw Signal**
 - **Calculate Translational Velocity**

Data Processing...



Raw Output Signal



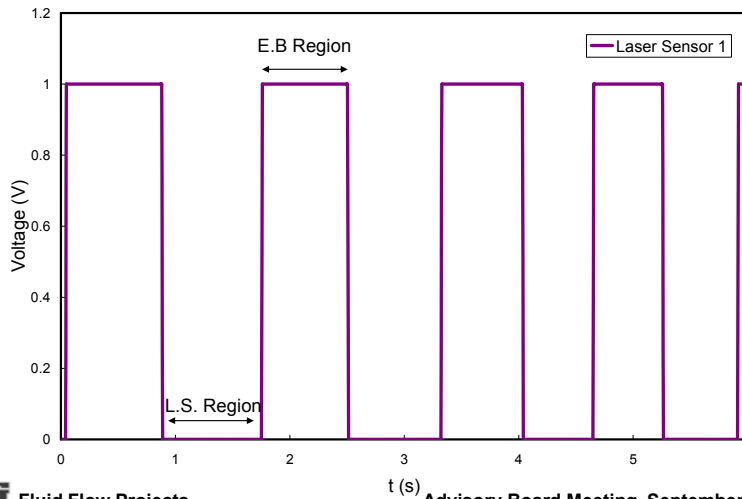
Fluid Flow Projects

Advisory Board Meeting, September 17, 2008

Data Processing...



Filtered Output Signal



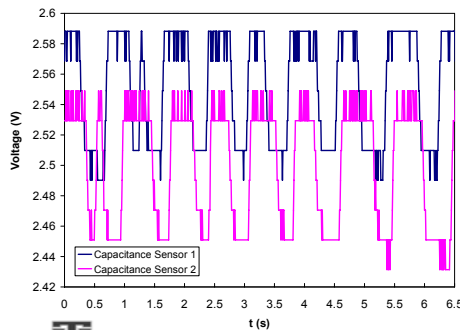
Fluid Flow Projects

Advisory Board Meeting, September 17, 2008

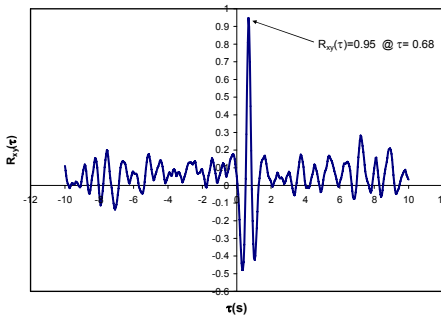
Data Processing...

◆ Cross-Correlation

- Measure of Similarity of Two Signals as Function of Time Lag Applied to One of Them



 Fluid Flow Projects



Advisory Board Meeting, September 17, 2008

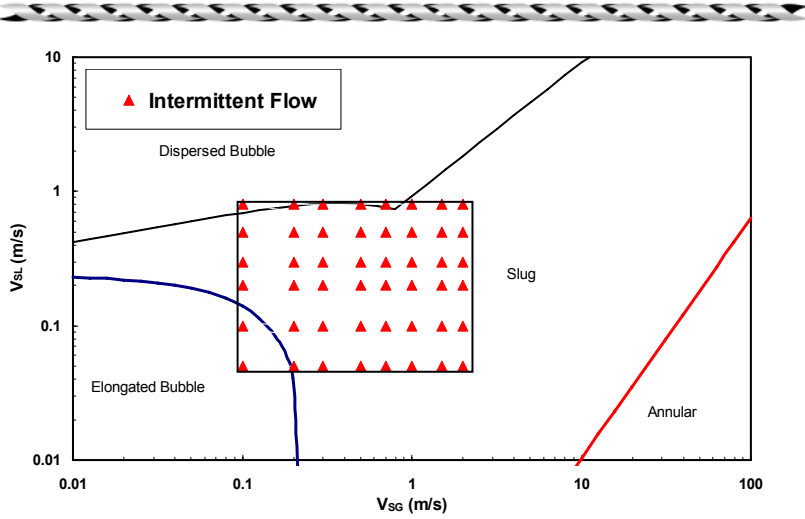
Testing Range

- ◆ Focused on Intermittent Flow (Elongated Bubble and Slug Flow)
- ◆ Significant Amount of Air Bubbles Entrained in Liquid with Increasing Gas Flow Rate
- ◆ New Mixture Appeared as Foam
- ◆ Critical Air Velocity Has to Be Known to Prevent Foaming
- ◆ Quality of Output Signals for Laser Sensors Decrease with Increase Air Bubbles in Liquid

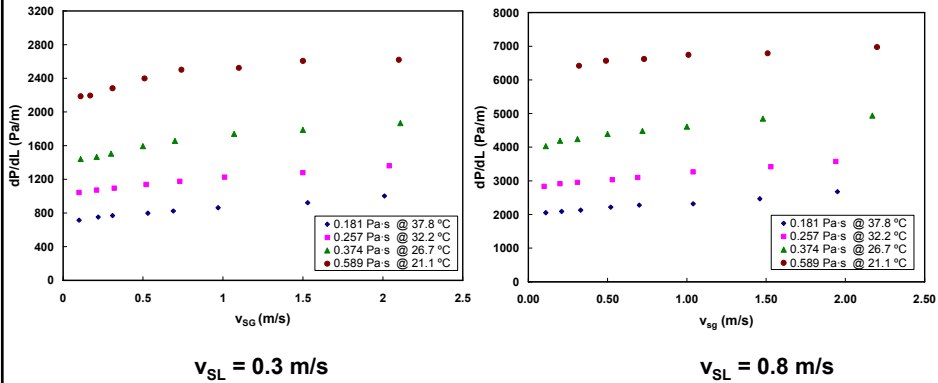
 Fluid Flow Projects

Advisory Board Meeting, September 17, 2008

Testing Range...



Pressure Gradients



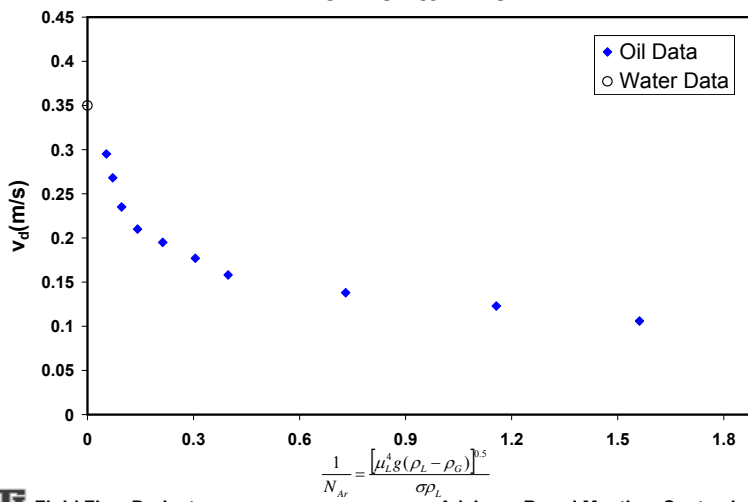
Drift Velocity...

- ◆ Experiments Performed for Horizontal and Inclined Pipes at Different Viscosities
 - Drift Velocity
 - Liquid Height
- ◆ Dimensionless Number Preferred in Graph
 - Archimedes Number

$$N_{Ar} = \frac{\sigma \rho_L}{[\mu_L^4 g (\rho_L - \rho_G)]^{0.5}}$$

Drift Velocity...

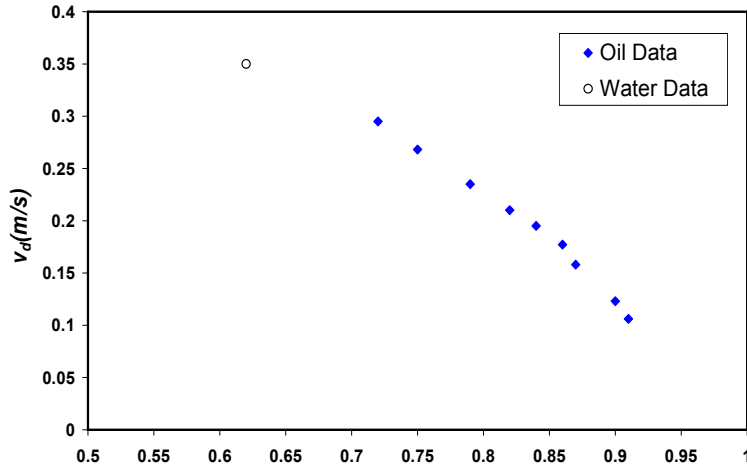
Horizontal Flow



Drift Velocity...



Horizontal Flow



Fluid Flow Projects

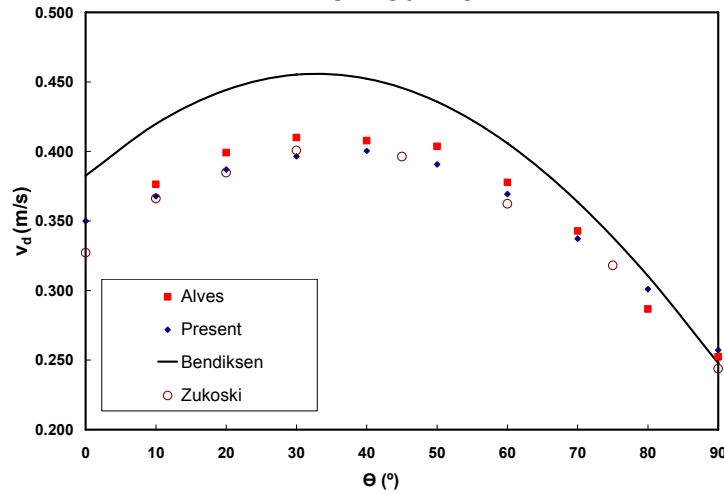
h/D

Advisory Board Meeting, September 17, 2008

Drift Velocity...



Inclined Flow



Fluid Flow Projects

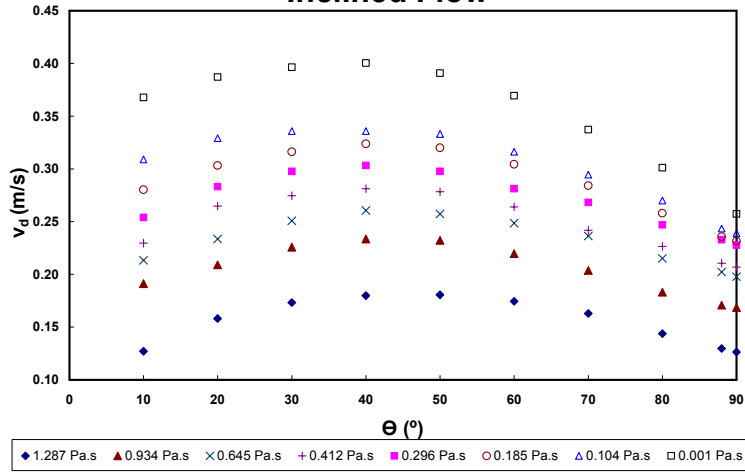
θ (°)

Advisory Board Meeting, September 17, 2008

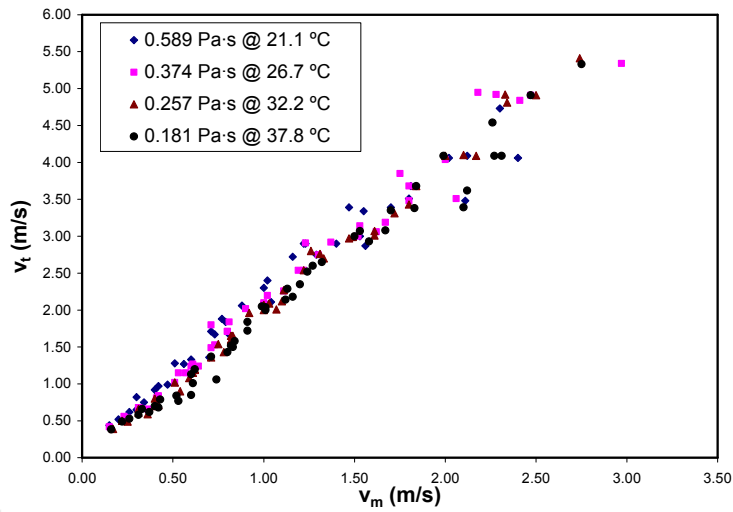
Drift Velocity...



Inclined Flow



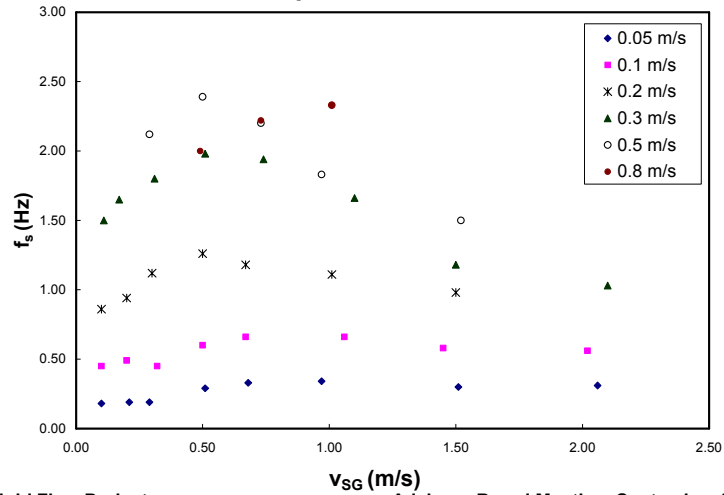
Translational Velocity



Slug Frequency



$\mu = 0.589 \text{ Pa}\cdot\text{s}$



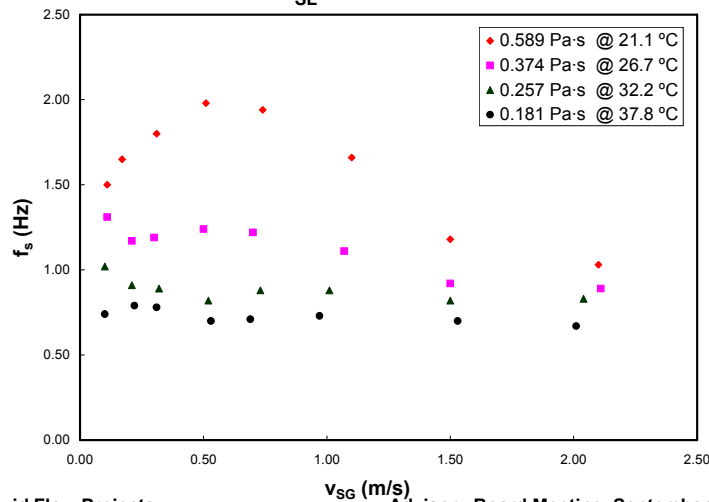
Fluid Flow Projects

Advisory Board Meeting, September 17, 2008

Slug Frequency...



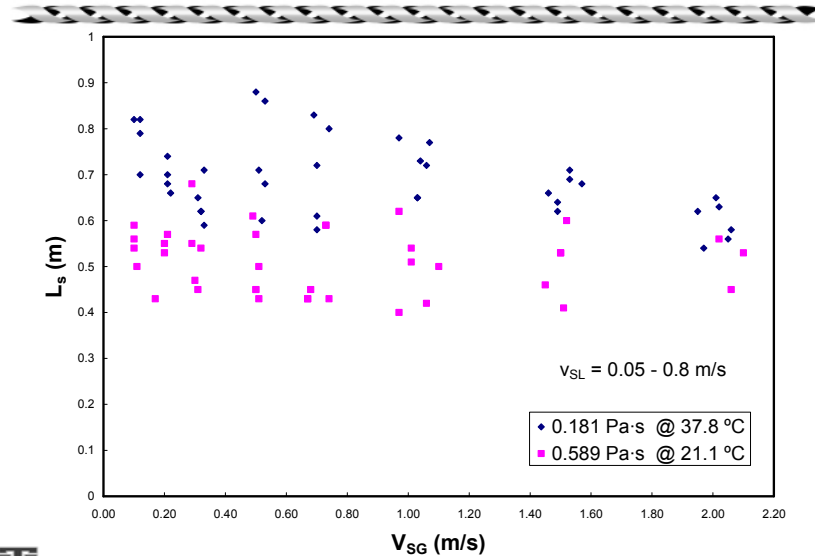
$v_{SL} = 0.8 \text{ m/s}$



Fluid Flow Projects

Advisory Board Meeting, September 17, 2008

Slug Length



Fluid Flow Projects

Advisory Board Meeting, September 17, 2008

Slug Length...

- ◆ **Slug Length Decreases with Increase of Liquid Viscosity**
- ◆ **Taitel et al. (1980) and Barnea and Brauner (1985) Proposed**
 - **Minimum Liquid Slug Length 32D for Horizontal Flow**
- ◆ **Slug Lengths Much Shorter than 32D They are Approximately 8D-13D.**



Fluid Flow Projects

Advisory Board Meeting, September 17, 2008

Slug Length...

- ◆ Slug Lengths are Log-Normally Distributed
- ◆ Easy Fit 3.0 Software Used to Determine Mean and Standard Deviation of Log-Normal Distribution

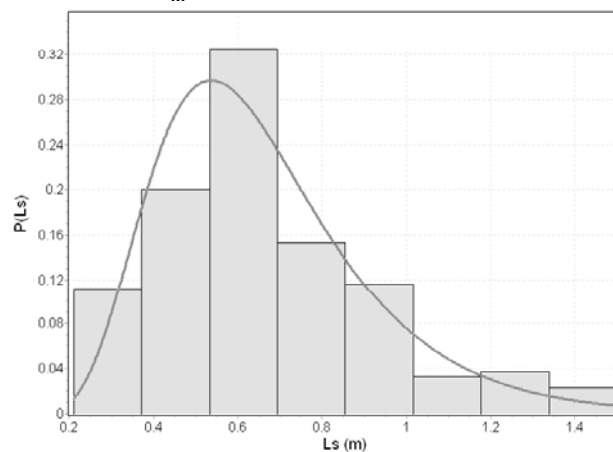
$$p(L_s) = \frac{1}{L_s \sigma_N \sqrt{2\pi}} \exp\left[\frac{-(\ln(L_s) - \mu_N)^2}{2\sigma_N^2}\right]$$

$$\mu_{L_s} = \int_{-\infty}^{\infty} L_s p(L_s) dL_s = e^{\mu_N + \frac{\sigma_N^2}{2}}$$

$$\sigma_{L_s}^2 = \int_{-\infty}^{\infty} (L_s - \mu_{L_s})^2 p(L_s) dL_s = e^{2\mu_N + \sigma_N^2} (e^{\sigma_N^2} - 1)$$

Slug Length...

$v_M = 1.5 \text{ m/s}$ and $\mu = 0.257 \text{ Pa}\cdot\text{s}$

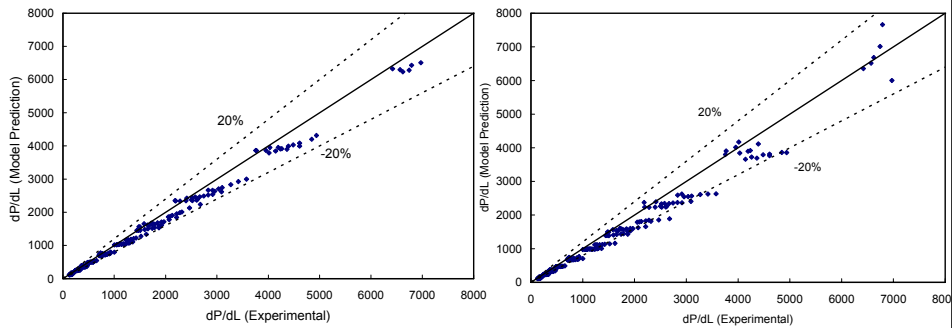


Experimental Data — Lognormal

Modeling Study

- ◆ Pressure Gradient Predictions
- ◆ Drift Velocity
- ◆ Translational Velocity
- ◆ Slug Frequency

Pressure Gradient Predictions



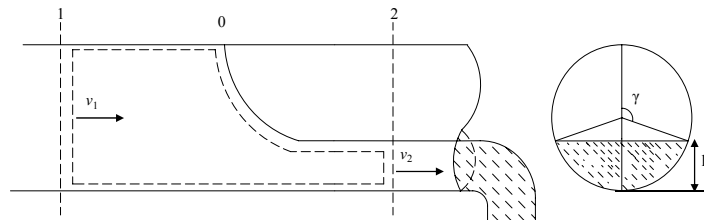
Model	No. of data	Statistical Parameters					
		ϵ_1 (%)	ϵ_2 (%)	ϵ_3 (%)	ϵ_4 (Pa/m)	ϵ_5 (Pa/m)	ϵ_6 (Pa/m)
TUFP Unified	190	-15	16.0	61	-131	141	79
Xiao	190	-18	19.0	121	-184	203	121

Drift Velocity

- ◆ From Experimental Results, Oil Viscosity Significant Effect on Drift Velocity
- ◆ New model to Predict Drift Velocity for High Viscosity Oils is Developed for Horizontal Flow
- ◆ Impossible to Extend Horizontal Configuration Model to Upward Flow
- ◆ New Model Based on Bendiksen Approach is Developed
 - Combination of Drift Velocities of Horizontal and Vertical Flows

Drift Velocity...

Horizontal Flow:



- ◆ Liquid Draining Out of Horizontal Pipe
- ◆ Point “0” Fixed and Point “1” Moving
- ◆ Point “0” Taken as Reference Point

Drift Velocity...

◆ Continuity Equation Over Control Volume

$$A_1 v_1 = A_2 v_2$$

where A_2 given by $A_2 = \left[\pi - \gamma + \frac{1}{2} \sin 2\gamma \right] r^2$

◆ Continuity Equation can be Expressed

$$\frac{v_1}{v_2} = \frac{A_2}{A_1} = 1 - \zeta \quad \zeta = \frac{\gamma - \frac{1}{2} \sin 2\gamma}{\pi}$$

Drift Velocity...

◆ Bernoulli Theorem Applied Between Point "1" and Stagnation Point "0"

$$P_1 = -\frac{v_1^2 \rho}{2}$$

◆ Bernoulli Theorem Applied Between Point "0" and Point "2" with Inclusion of Viscous Effect

$$v_2^2 = 2g[r(1 - \cos \gamma) - \Delta]$$

Δ = Uniform Loss of Total Head

Drift Velocity...

◆ Momentum Balance Between Points “1” and “2”

$$(P_1 + \rho g r) \pi r^2 - \int_0^h \rho g (h - y) b dy - F_f = \rho v_2 A_2 (v_2 - v_1)$$

where F_f given by $F_f = \rho g \Delta A_2$

◆ Second Term in Momentum Equation is Pressure Variation with Depth

$$\int_0^h \rho g (h - y) b dy = \rho g r (A_2 \cos \gamma + \frac{2}{3} r^2 \sin^3 \gamma)$$

Drift Velocity...

◆ Final Form of Momentum Balance

$$\frac{1}{2} (1 - \zeta)^2 v_2^2 - (1 - \zeta) v_2^2 = g r [(1 - \zeta) \cos \gamma + \frac{2}{3\pi} \sin^3 \gamma - 1] + \Delta g (1 - \zeta)$$

◆ Expression for v_2^2

$$v_2^2 = \frac{2 g r [1 - (1 - \zeta) \cos \gamma - \frac{2}{3\pi} \sin^3 \gamma] - 2 \Delta g (1 - \zeta)}{1 - \zeta^2}$$

Drift Velocity...

◆ Total Head Loss Δ

$$\Delta = k \frac{(1+\zeta)}{\zeta} \left\{ r(1-\cos\gamma) - \left[\frac{r[1-(1-\zeta)\cos\gamma] + \frac{2}{3\pi}\sin\gamma}{1-\zeta^2} \right] \right\}$$

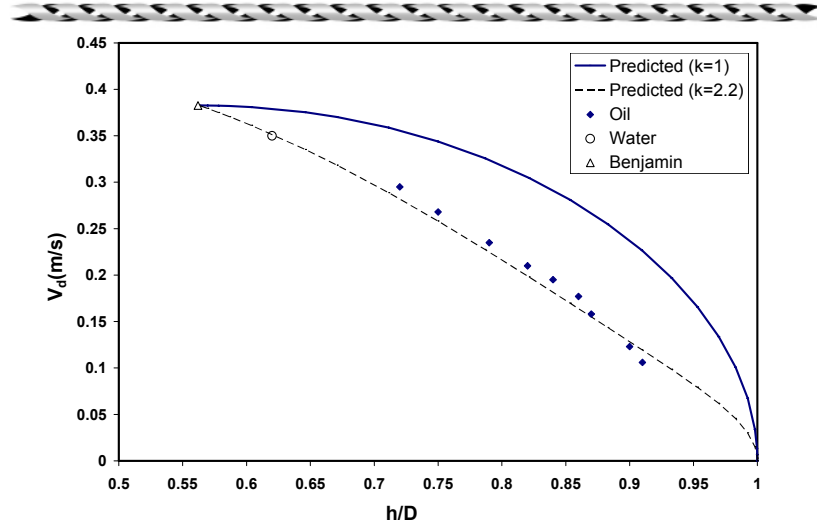
k = Total Head Loss Correction Factor

◆ Total Head Loss Solved Numerically for Given Angle γ

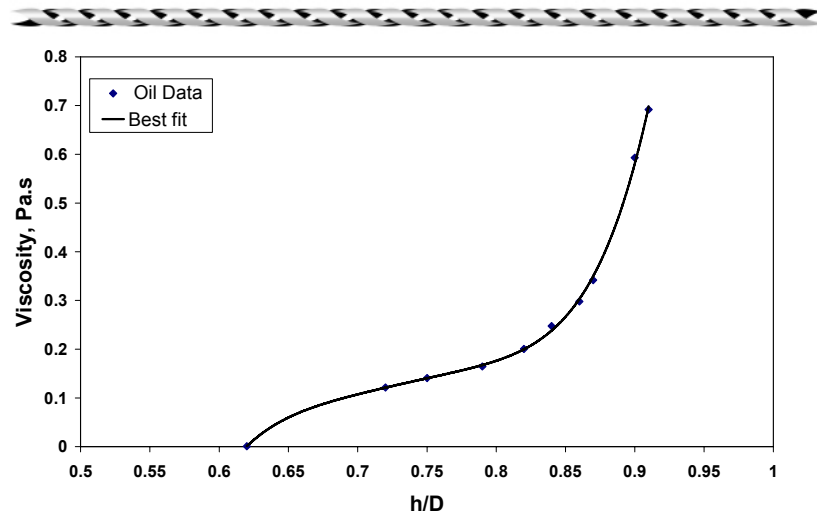
Drift Velocity...

- ◆ Δ Show Positive Values for $\gamma < 82.78^\circ$
 - Possible with Energy Loss
- ◆ Δ Show Negative Values for $\gamma > 82.78^\circ$
 - External Supply of Energy Necessary to Maintain Steady Flow
 - Impossible from Practical Point of View
- ◆ Δ Equal Zero for $\gamma = 82.78^\circ$
 - Solution Found By Benjamin for Inviscid Case

Drift Velocity...



Drift Velocity...



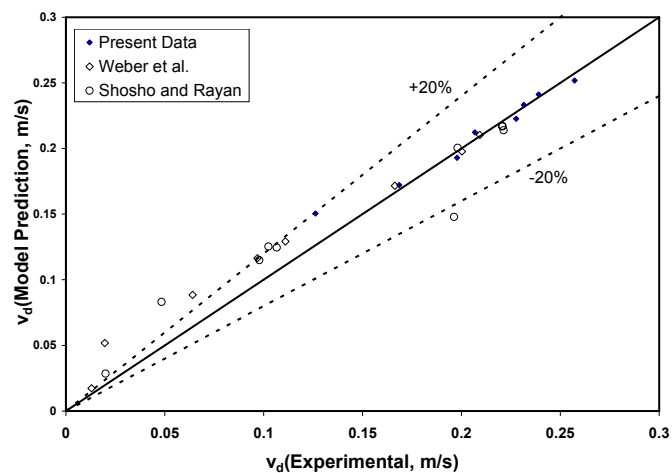
Drift Velocity...

Vertical Flow:

- ◆ Joseph (2003) Proposed Model for Drift Velocity in Vertical Flow Including
 - Viscosity, Surface Tension, Shape of Bubble Nose Effects
- ◆ From Experimental Results, Bubble Nose is Spherical

$$v_d = -\frac{4}{3} \frac{\mu}{\rho r} + \sqrt{\frac{4}{9} gr + \frac{16}{9} \frac{\mu^2}{(\rho r)^2}}$$

Drift Velocity...



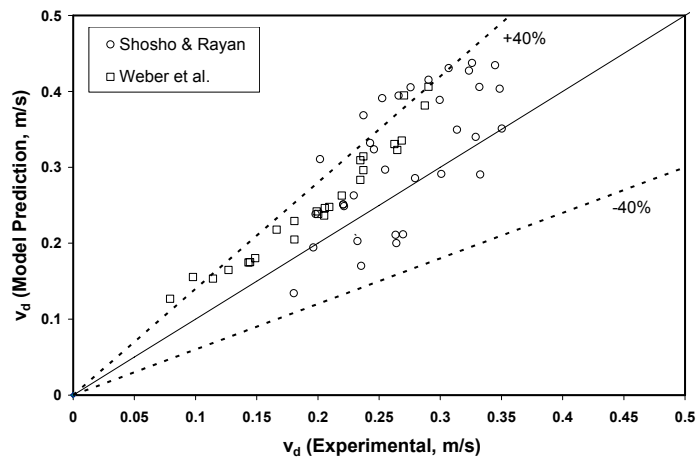
Drift Velocity...

Upward Inclined Flow:

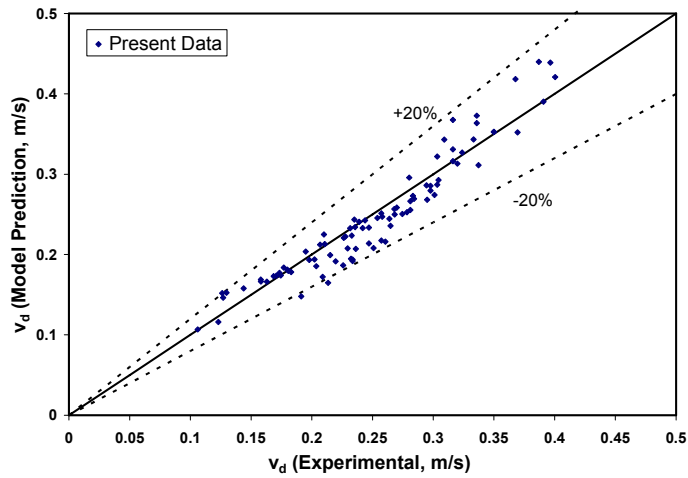
- ◆ New Model Similar to Bendiksen Approach is Developed for Upward Inclined Flow

$$v_d = v_d^v (\sin \theta)^{0.7} + v_d^h (\cos \theta)^{1.5}$$

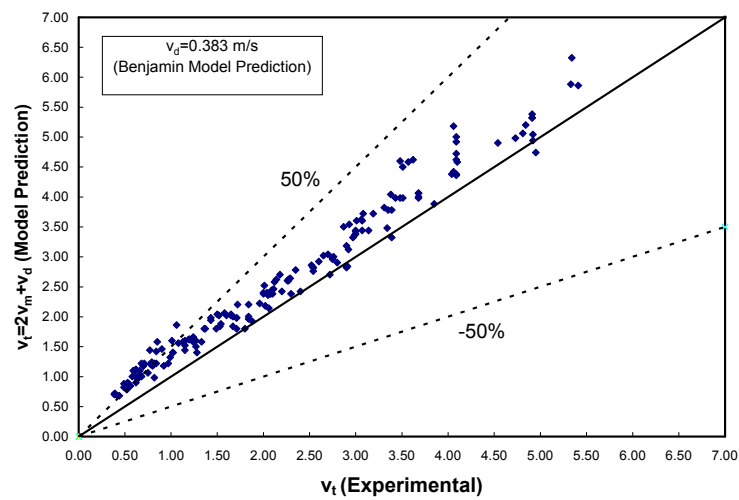
Drift Velocity...



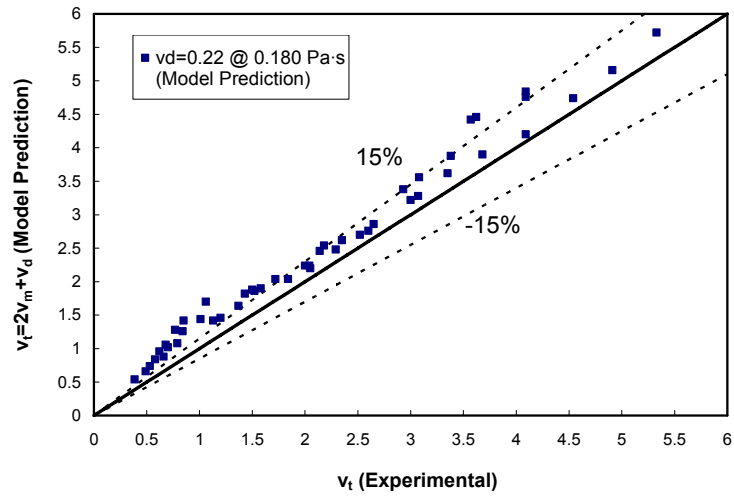
Drift Velocity...



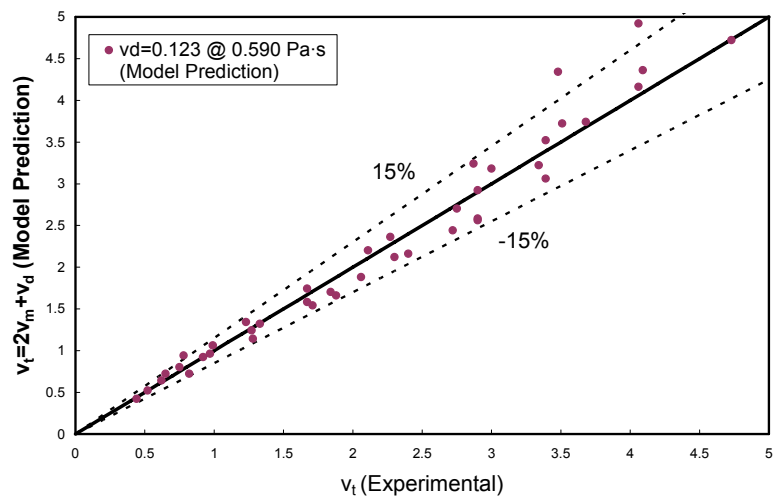
Translational Velocity



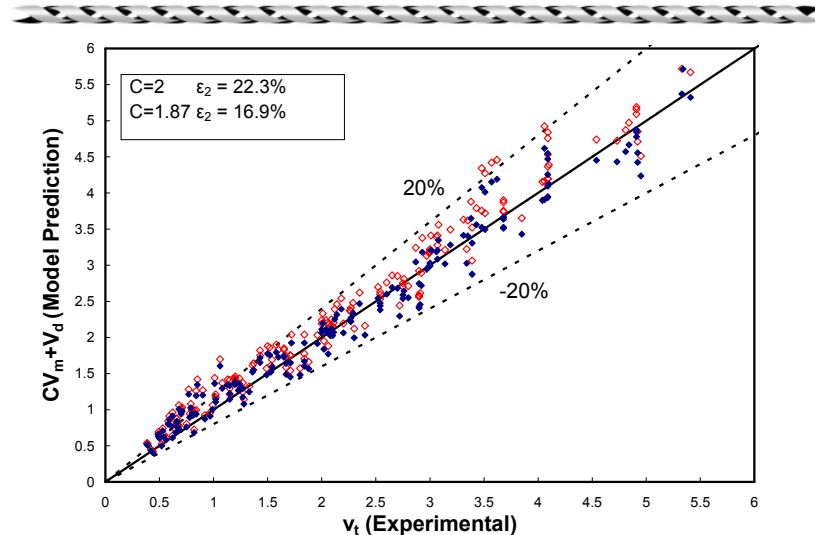
Translational Velocity...



Translational Velocity...



Translational Velocity...



Slug Frequency

- ◆ Dimensionless Analysis Approach Taken to Develop Slug Frequency Closure Model for Viscous Oil
- ◆ Intermittency, I , Defined as Fraction of Time Observed by Stationary Observer

$$I = \frac{f_s L_s}{C}$$

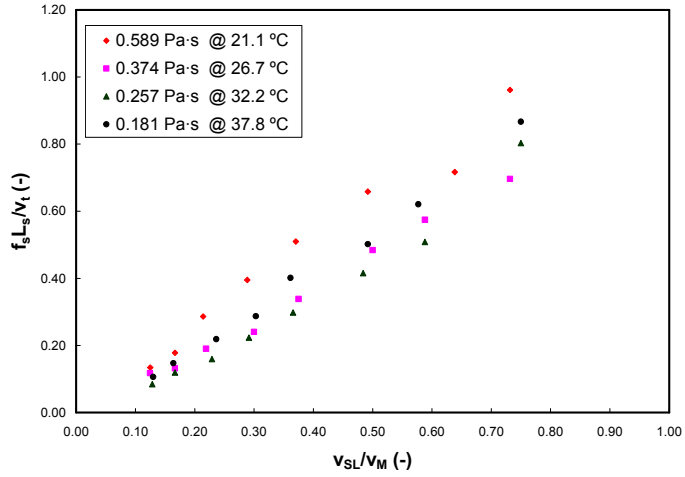
- ◆ Intermittency can be Correlated as Function of Velocity Ratio

$$\frac{f_s L_s}{v_t} \propto \frac{v_{SL}}{v_{SL} + v_{SG}}$$

Slug Frequency...



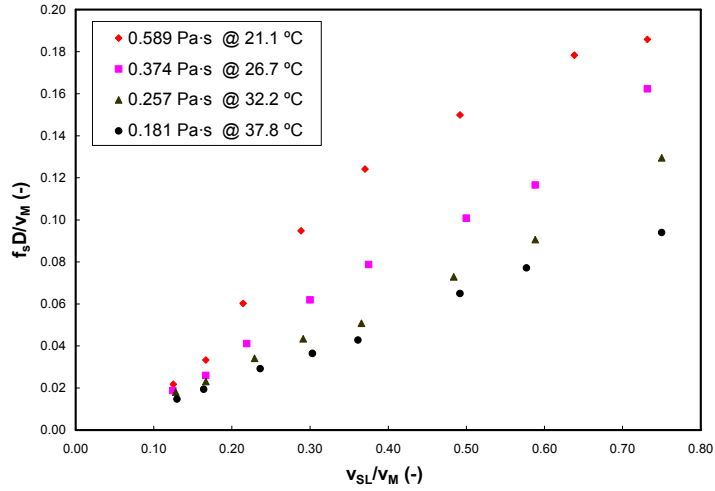
$v_{SL} = 0.3 \text{ m/s}$



Slug Frequency...



$v_{SL} = 0.3 \text{ m/s}$



Slug Frequency...

- ◆ Another Dimensionless Group Necessary to Include Effect of Viscosity into Slug Frequency

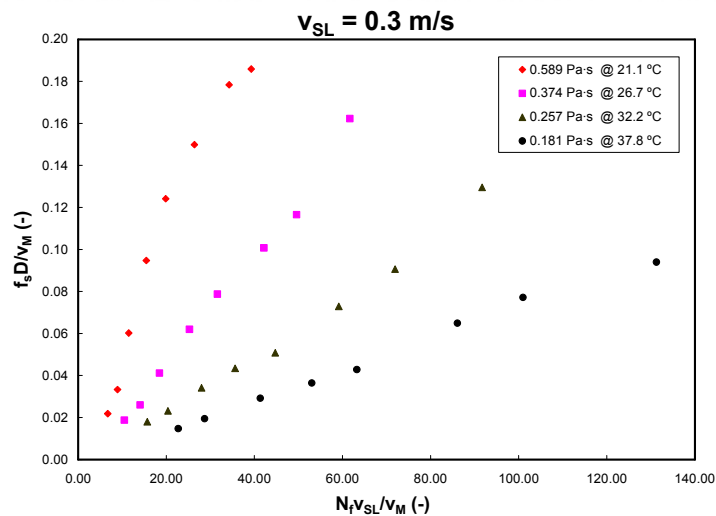
- ◆ N_f is Dimensionless Inverse Viscosity Defined by,

$$N_f = \frac{D^{3/2} \sqrt{\rho_L \Delta \rho g}}{\mu_L}$$

- ◆ Final Form of Relationship

$$\frac{f_s D}{v_m} \propto \frac{D^{3/2} \sqrt{\rho_L \Delta \rho g}}{\mu_L} \frac{v_{SL}}{v_m}$$

Slug Frequency...

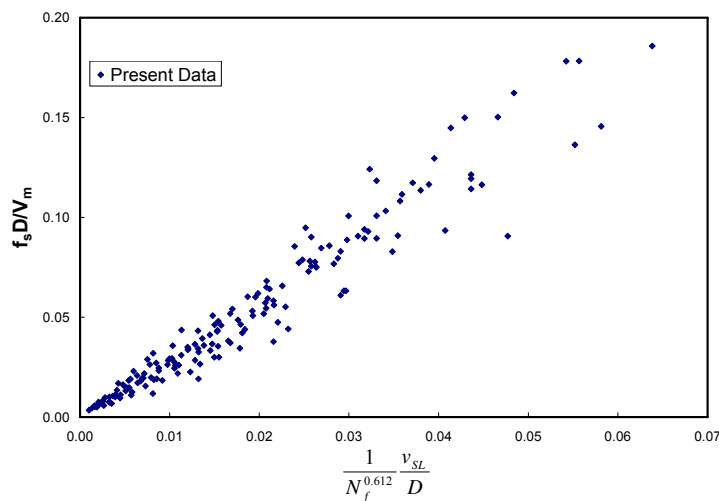


Slug Frequency...

- ◆ Simple Linear Relationship Exists between Dimensionless Groups
- ◆ Slope of Linear Relationship Increases with Increase of Liquid Viscosity
- ◆ Final Formula of Slug Frequency Model for High Oil Viscosity

$$f_s = 2.816 \frac{1}{N_f^{0.612}} \frac{v_{SL}}{D}$$

Slug Frequency...



Project Schedule

◆ Literature Review	Completed
◆ Facility Modifications	Completed
◆ Preliminary Testing	Completed
◆ Testing	Completed
◆ Model Development	Completed
◆ Model Validation	Completed
◆ Final Report	October 2008

Questions & Comments



An Experimental and Theoretical Investigation of Slug Flow for High Oil Viscosity in Horizontal Pipes

Bahadir Gokcal

PROJECTED COMPLETION DATES:

Literature Review	Completed
Facility Modifications	Completed
Preliminary Testing	Completed
Testing	Completed
Model Development	Completed
Model Validation	Completed
Final Report	October 2008

Objectives

The objectives of this study are:

- to acquire experimental data on characteristics of slug flow for high viscosity oil in horizontal pipes,
- to develop closure models on slug flow for high viscosity oils in horizontal pipes,
- to validate proposed models with experimental results.

Introduction

High viscosity oils are produced from many oil fields around the world. Oil production systems are currently flowing oils with viscosities as high as 10,000 cp. High viscosity or “heavy oil” has become one of the most important future hydrocarbon resources with the ever increasing world energy demand and the depletion of conventional oils.

Current multiphase flow models are largely based on experimental data with low viscosity liquids. Commonly used laboratory liquids have viscosities less than 20 cp. Thus, the gap between actual laboratory data and field data can be three orders of magnitude or more. Therefore, the current mechanistic models need to be verified with higher liquid viscosity experimental results. Modifications or new developments are necessary.

Almost all flow models have viscosity as an intrinsic variable. Multiphase flows are expected to exhibit significantly different behavior for higher viscosity oils. Many flow behaviors will be affected by the liquid viscosity, including flow pattern, droplet formation, surface waves, bubble entrainment, slug mixing zones, and even three-phase stratified flow.

Gokcal (2005) conducted an experimental study to investigate the effects of high oil viscosity on two-phase oil-gas flow behaviors. The comparison of experimental data against existing models showed that the performances of existing models are not sufficiently accurate for high viscosity oils. It was found that increasing oil viscosity had a significant effect on flow behaviors. Intermittent flow (slug and elongated bubble) was mostly observed in his study. Based on his results, this study is focused on the slug flow region for high viscosity oil. Knowledge of slug flow characteristics is crucial to design pipelines and process equipment. In order to improve the accuracy of slug characteristics for high viscosity oils, accurate closure models for slug flow are needed. The developed expressions will significantly improve the performance of existing two-phase flow models for high viscosity oil applications.

Air-highly viscous oil two-phase flow experiments were conducted at different temperatures and flow rates for horizontal pipe. Pressure drop and slug characteristics including translational velocity, slug length and frequency were measured and relevant closure models were developed.

Experimental Study

Facility

The existing indoor high viscosity test facility will be modified for this experimental study. The facility is comprised of an 18.9-m (62-ft) long, 50.8-mm (2-in.) ID pipe with a 9.15-m (30-ft) long transparent acrylic pipe section to visually observe the flow. The inclination angle can be changed from -2° to 2° from horizontal. A 76.2-mm (3-in.) ID return pipe is connected to the test section with a flexible hose. The return pipe goes to the oil storage tank. A metering section, test section, and heating and cooling systems are the major components of the facility, as shown in Fig. 1.

Compressed air was used as the gas phase, and was supplied by a dry rotary screw air compressor. Oil was pumped by a 20-hp screw pump from an oil storage tank. A motor frequency drive was installed to provide better flow rate control and reduce the amount of heat generated. The oil storage tank contained 3.03 m^3 of oil. Both air and oil flow rates were metered by Micro Motion™ mass flow meters. The fluids were mixed at a mixing tee, flowed through the test section and returned to the oil storage tank. The oil storage tank was also used as a separator. The separated air was discharged outside through a ventilation system.

There are four differential pressure transducers on the facility. Two of them are on the transparent acrylic pipe. The others are on the steel pipe. The purpose of DP1 and DP2 on the steel pipe is to monitor the development of the flow before it reaches the test section. DP3 spans 3.05-m (10-ft) of the transparent pipe is mainly used for high flow rates. DP4 spans 6.55-m (20-ft) of the transparent pipe and is used for low flow rates. Quick-closing valves are used for flow control and liquid trapping. Four laser beams and sensors and two capacitance sensors are used to measure translational velocity, slug frequency, and slug length. The location of each laser beam and sensor and capacitance sensor can be changed easily along the pipe. In addition, two Resistance Temperature Detector (RTD) temperature transducers located at the inlet and outlet of the test section are used to measure temperatures. The temperature measurements are imperative to determine the viscosity of the oil during experiments. A TUFFP high speed video system is used to identify the flow patterns. A visualization box is installed on the acrylic pipe to observe and record flow patterns in details. A schematic of the test section is shown in Fig. 2.

For drift velocity experiments, some additional modifications were made to the existing facility without changing the original structure. The objective of this modification is to determine the effect of high oil viscosity on the drift velocity for horizontal and upward inclined pipes. In order to measure drift velocity in horizontal pipe, one of the quick-closing valve located at the end of the test section was modified, and can be opened to the atmosphere manually. Therefore, the trapped oil can be drained from the horizontal pipe. The drift velocity is measured by two lasers. For drift velocity experiments at different inclination angles, a 3.05-m (10-ft) long transparent acrylic pipe with 50.8-mm (2-in.) ID was added to the existing facility temporarily, as shown in Fig. 1. The acrylic pipe is located close to the oil storage tank. The inclination angle can be changed from 0° to 90° . The oil pump is used to fill up the pipe at various temperatures corresponding to different viscosities. The oil can be captured by valves which are located at the inlet and outlet of the pipe. An air bubble from the bottom of the pipe is released into the stagnant liquid column. The drift velocity of the released air bubble is measured by two laser beams and sensors.

Testing Oil

The Citgo Sentry 220 oil used in the previous study is used. Following are typical properties of the oil:

- Gravity: 27.6°API
- Viscosity: 0.220 Pa·s @ 40°C
- Density: 889 kg/m³ @ 15.6°C

The oil viscosity and density vs. temperature behavior are shown in Figs. 3 and 4, respectively.

Instrumentation and Data Acquisition

Laser and capacitance sensors are used to determine slug flow characteristics including translational velocity, slug length and frequency. Both of the devices are designed and constructed by Tulsa University Fluid Flow Projects (TUFFP). Four laser and two capacitance sensors are used in this study. All of them are mounted on the acrylic pipe.

As an optical measurement method, commercially available laser beams from Premier-LC and laser sensing devices from Hawkeye were used. Laser beam is focused directly to sensor and glued inside the housing. Two laser sensors mounted on the test section by a distance of $\Delta L_{\text{Laser}} = 0.81\text{m}$ are used to measure the translational velocity. One laser sensor

is enough to determine slug frequency and length after measuring the translational velocity.

The principle of the capacitance method is based on the differences in the dielectric constants of gas-liquid phases in the flow. Each capacitance sensor has three major components: the copper ring around the pipe, the electronic circuit to filter, amplify and convert the measured capacitance to a voltage, and the housing. Two capacitance sensors are installed with a distance of $\Delta L_{\text{cap}}=1.0\text{m}$ to measure the translational velocity. The slug flow parameters obtained from laser sensors are compared against the results of capacitance sensors.

Both laser and capacitance sensors were connected to a portable data acquisition system using a scan rate of 500 Hz to measure the resulting voltage signals from sensors. Data acquisition system has 8 analog and 16 digital channels. In this study, six instruments are connected to analog channels. In order to obtain statistical information about liquid slugs, the output signals are sampled at a sampling frequency 125 Hz per instrument. Data acquisition system is locked for 160 seconds. As a result of sampling frequency and duration, 20,000 data points are collected for each channel in one experiment.

Data Processing

Data management is a big challenge for this study due to large amount of the data acquired. Therefore, the data processing has to be automated. Two large Excel macro programs are written to process the data obtained from laser and capacitance sensors. The first macro is worked for cleaning the noise from the raw signal, counting the number of slugs (Slug frequency equals to number of slugs divided by sampling time.), and recording the time that each slug passes from one instrument either laser or capacitance sensor. Before running the code, the raw output signal has to be examined. Voltage thresholds have to be specified at each capacitance sensor or laser sensor for each test run. It is found from the experimental results that the output signal for liquid slug region is lower than elongated bubble region. After setting the threshold value, program identifies liquid slug region as 0, and elongated bubble region as 1. Then, it counts the number of slugs from the filtered signal output. Figure 5 presents typical example of the raw output signal of laser sensor for time duration of 6 seconds. Voltage threshold is decided as 0.85 volt. Thus, the filtered signal output is obtained for laser sensor 1 as it can be seen in Fig. 6.

In the second macro, cross correlation technique is applied on the raw signal to find critical time lag. When the critical time lag is known, translational velocity can be easily calculated. Slug length is calculated by multiplying translational velocity with the time that is calculated from first macro program for each test.

Cross-Correlation Procedure:

The cross-correlation function is a measure of the extent to which two signals correlate with each other as a function of the time displacement between them. If the signals are identical, the cross correlation will be one, and if they are completely dissimilar, the cross correlation will be zero.

Consider two time series, $x(t_n)$ and $y(t_n)$, where $n = 0, 1, 2, \dots, N-1$. The cross-correlation coefficient is defined as:

$$R_{xy}(\tau) = \frac{C_{xy}(\tau)}{\sqrt{C_y(0)C_x(0)}}, \quad (1)$$

$$C_{xy}(\tau) = \frac{1}{N-\tau} \sum_{n=1}^{N-\tau} x(t_n)y(\tau+t_n). \quad (2)$$

In Eq. 2, $x(\tau)$ and $y(\tau)$ are time series data when τ is the temporal lag. When the time series $x(\tau)$ and $y(\tau)$ are identical, the correlation coefficient is called auto-correlation coefficient, as shown in Eq. 3,

$$C_x(0) = \frac{1}{N} \sum_{n=1}^N x(t_n)^2 = \overline{x^2}. \quad (3)$$

The raw output signals from laser and capacitance sensors are used for performing cross-correlation between different pairs of laser sensors and one pair of capacitance sensors, i.e between LS1-LS2, LS2-LS3, LS3-LS4, LS1-LS4 and CS1-CS2.

As an example, the output signals of capacitance sensors 1 and 2 are plotted against time in Fig. 7. The cross-correlation method is implemented to two time series. There is a strong correlation at a time lag of 0.68 as it can be seen in Fig. 8. The translational velocity is easily calculated from the following equation:

$$v_t = \frac{\Delta L_{LS2 \rightarrow LS1}}{\tau}. \quad (4)$$

Experimental Range

Elongated bubble and slug flows were mostly observed during high viscosity experiments. This study is focused on intermittent flow (elongated bubble and slug flow) for high viscosity oils.

It is known that a significant amount of air bubbles can be entrained in liquid with increasing gas flow rate. The diameter of air bubbles gets smaller with increasing gas flow rates and the color of the oil changes completely. The new mixture can exist as foam, and foam is a major challenge for separation. Therefore, a critical air velocity has to be known to prevent foam formation in the experimental study. Experimental observations will be used to determine the critical gas velocity that gives transition from air bubbles to foam.

Moreover, critical gas velocity needs to be determined by laser sensor. The laser beam interacts locally with the structure of the flow. It gives different signals on the presence of small air bubbles in liquid. The quality of signals decreases with increasing air bubbles in liquid.

It is found from preliminary study that the critical gas velocity should be 2 m/s. If the gas velocity is higher than this velocity, foaming will be observed and the laser sensors will not measure slug characteristics correctly.

Figure 9 shows the Barnea flow pattern map and the experimental observations for a liquid viscosity of 0.587 Pa·s. The marked area in the flow pattern shows the velocity limits for future high oil viscosity experiments. The superficial liquid and gas velocities can range from 0.05 to 0.8 m/s and from 0 to 2 m/s, respectively.

Experimental Results

In this study, a total of 190 tests were conducted for different superficial oil and gas velocities and temperatures for slug flow in horizontal pipe. The superficial liquid and gas velocities were varied from 0.05 m/s to 0.8 m/s and from 0.1 m/s to 2 m/s, respectively. The pressure gradient, translational velocity, slug length and frequency were measured in this study. Also, a total of 110 tests for drift velocity were performed at different temperatures for inclination angles of 0° to 90°.

Pressure Gradients:

Figures 10 and 11 present the measured pressure gradients at different oil viscosities and superficial

gas velocities for superficial oil velocities of 0.3 and 0.8 m/s, respectively. As expected, the pressure gradients increased with increasing superficial gas and liquid velocities. At the same superficial air and liquid velocities, the pressure gradient in the same cases increased more than 100% between the high and low viscosity values. It is seen that the effect of high viscosity played an important role on the pressure gradient. This effect became more significant with an increase of superficial oil and air velocities.

Drift Velocity:

Initially, an experiment is conducted with water for horizontal pipe to prove that the system is working properly. The results for water are compared with Benjamin's model prediction. The predictions of drift velocity and liquid height of the water from Benjamin's model show excellent agreement with the data. The calculated drift velocity and liquid height parameter (h/D) are 0.38 m/s and 0.563, respectively, while the measured drift velocity and liquid height for water are 0.35 m/s and 0.62.

The rest of the experiments are performed at temperatures between 19.2 °C and 45 °C using the oil. The oil viscosities corresponding to the above temperatures are 0.121 Pa·s and 0.692 Pa·s, respectively. The drift velocity and liquid height of the oil are measured at different oil viscosities.

Dimensionless Archimedes number, N_{Ar} , is applied to include viscosity, surface tension, fluid properties and gravitational acceleration parameters in one equation. Wallis (1969) proposed N_{Ar} , as

$$N_{Ar} = \frac{\sigma \rho_L}{[\mu_L^4 g (\rho_L - \rho_G)]^{0.5}} \quad (5)$$

Figure 12 shows the experimental results for drift velocity vs. Archimedes dimensionless number for horizontal flow. It is seen that the effect of high viscosity plays an important role on the drift velocity. The drift velocity decreases with the decrease of Archimedes dimensionless number and with the increase of oil viscosity.

The drift velocity vs. liquid height from the conducted experiments is plotted in Fig. 13. The drift velocity decreases with the increase of liquid height and oil viscosity. The lowest liquid height and the highest drift velocity are found for water. They also matched with the results obtained from Benjamin model by using inviscid flow theory.

Experiments were also conducted with water for inclined pipes to understand the reliability of the system. Water data are compared against the published data including Alves et al. (1993) and Zukoski (1966) as it can be seen in Fig. 14. The comparison of present data with the published ones matched well. Moreover, the data is compared against the Bendikson model (1984).

Experiments were performed at temperatures between 10.6 °C and 50 °C using viscous oil for inclination angles of 10° to 90°. The oil viscosities corresponding to the above temperatures are 0.107 Pa·s and 1.287 Pa·s, respectively. The change of drift velocity with inclination angle and viscosity is given in Fig. 15. Water data are shown in the same graph to understand the effect of high liquid viscosity. The results show that the dependence of drift velocity on viscosity is significant. The drift velocity decreases with the increase of oil viscosity. The Bendikson model is not valid when viscosity plays an important role on drift velocity. It increases with an increase in inclination angle, reaching a maximum at about 40° from horizontal, and then decreases to a lowest value for vertical pipe.

Translational Velocity:

Slug translational velocity was determined by dividing the distance between either two capacitance sensors or laser sensors by the most probable time lag Δt_{cr} . It was obtained from cross-correlating the output signals of the capacitance and laser sensors. (The cross-correlation method is discussed under the subsection of data processing.)

Figure 16 illustrates the linear relationship between the measured translational velocity and the mixture velocity at different temperatures in horizontal pipe. As expected, translational velocity increases with increasing mixture velocity. The slope of the linear relationship is almost 2.0. It is confirmed that experiments are laminar flow in this study.

Slug Frequency:

Slug frequency was measured by both capacitance and laser sensors. Good agreement was obtained between two different instruments. Moreover, the results are confirmed by visual observation. The number of slugs passing a given point on the test section is counted for certain time with a stopwatch.

Figure 17 show the slug frequencies against superficial gas velocity for different liquid superficial velocities at the liquid viscosity of 0.589 Pa·s. As

expected, the slug frequency increases with the increase in gas velocity.

The effect of viscosity on slug frequency is presented in Fig. 18. Slug frequency is plotted against superficial gas velocity at different viscosities for superficial liquid velocity of 0.3 m/s. The slug frequency increases with the increase of liquid viscosity. Also, similar trends are observed for different liquid velocities. It is concluded that slug frequency appears to be a strong function of liquid viscosity. However, existing slug frequency closure models do not show any explicit dependency on the liquid viscosity. A closure model taking into account viscosity effects on slug frequency needs to be developed. The model development of slug frequency will be discussed under the section of modeling study.

Slug Length:

The slug length and slug frequency are interrelated parameters and are very often used each other. Slug lengths are measured for a certain time by either capacitance or laser sensors.

Figure 19 shows the measurements of the mean value of slug length as a function of superficial gas velocity for superficial liquid velocities ranging from 0.05 to 0.8 m/s. The slug length is found to decrease with the increase of liquid viscosity. Taitel *et al.* (1980) and Barnea and Brauner (1985) proposed that a developed slug length is equal to a distance at which a jet has been absorbed by the liquid. Using this approach, the minimum liquid slug length is 32D for horizontal flow. However, it is noticed that slug lengths are much shorter than 32D. They are approximately 8D-13D for the viscosity value of 0.589 Pa·s.

It is found from the experimental results that, slug lengths are lognormally distributed. Also, measurements of Nydal (1991) showed that slug lengths in shorter pipelines are lognormally distributed. The Log-Normal distribution derives from the Normal or Gaussian distribution by replacing the random variable with the logarithm of the slug length. The Log-Normal probability density function of slug length distribution is expressed as,

$$p(L_s) = \frac{1}{L_s \sigma_N \sqrt{2\pi}} \exp \left[\frac{-(\ln(L_s) - \mu_N)^2}{2\sigma_N^2} \right], \quad (6)$$

where σ_N and μ_N are the average and standard deviation of normally transformed distribution, respectively.

The mean μ_{L_s} of the Log-Normal distribution is calculated by multiplying each value of L_s by its probability of occurrence. The variance, standard deviation squared, $\sigma_{L_s}^2$ is calculated by multiplying each of $(L_s - \mu_{L_s})^2$ by its probability of occurrence. μ_{L_s} and σ_{L_s} are expressed as,

$$\mu_{L_s} = \int_{-\infty}^{\infty} L_s p(L_s) dL_s = e^{\mu_N + \frac{\sigma_N^2}{2}} \quad (7)$$

$$\sigma_{L_s}^2 = \int_{-\infty}^{\infty} (L_s - \mu_{L_s})^2 p(L_s) dL_s = e^{2\mu_N + \sigma_N^2} (e^{\sigma_N^2} - 1) \quad (8)$$

EasyFit 3.0 software was used to determine the mean and standard deviation of Log-Normal distribution. Figure 20 shows comparison of experimental results and Log-Normal distribution. Log-Normal distribution matched well with experimental data.

Modeling Study

Slug flow closure models need to be investigated for high viscosity oil and gas two-phase flow. The closure models include translational velocity, slug length and frequency.

Pressure Gradient Predictions

The model evaluation results for pressure gradient are given in Table 1 for the TUFFP unified and Xiao mechanistic models, respectively. ϵ_1 , ϵ_2 , ϵ_3 , ϵ_4 , ϵ_5 , and ϵ_6 are average actual error, absolute actual average error, standard deviation for actual error, average relative error, absolute relative error, and standard deviation for relative error, respectively. The TUFFP unified model produced negative values of ϵ_1 and ϵ_4 indicating underestimation of the pressure gradient. When the entire dataset is compared against the TUFFP unified model, the average percentage relative and actual errors are -15 % and -131 Pa/m, respectively. The Xiao model predictions gave negative values of ϵ_1 and ϵ_4 indicating underestimation of the pressure. When the entire dataset is compared against the Xiao mechanistic model, the average percentage relative and actual errors are -18% and -184 Pa/m, respectively. Figures 21 and 22 show the predictions of the TUFFP Unified and Xiao models against the measured pressure gradient data within ± 20 % error band.

Drift Velocity

The literature review shows that there is no available study or model taking into account viscosity effects on the drift velocity. The drift velocity is expected to be affected significantly with increasing oil viscosity. A new model to predict the drift velocity for high viscosity oils has been developed for horizontal flow (Gokcal et al., 2008). The proposed model gave good agreement against experimental results.

It is experimentally found that as the pipe inclination increases from horizontal the shape of the rising bubble changes, after about 40 degrees a liquid film above the rising bubble start to form which pushes the location of the bubble toward the center of the pipe. At the highest degree of inclination (vertical) the bubble nose shape takes a spherical shape (approximately) and the bubble location is at the center of the pipe. Therefore, it is impossible to extend the horizontal configuration model for upward flow. Instead of using a single model for the drift velocity for all inclination angles, a new model based on the Bendiksen (1984) approach is developed. The new model gives the drift velocities for all pipe inclinations as a combination of drift velocities for horizontal and vertical flows.

Horizontal Flow:

By extending Benjamin (1968) analysis for horizontal case, a new model is developed for high viscosity oil to evaluate the drift velocity in horizontal pipe. Consider liquid draining out of a horizontal pipe as shown in Fig. 23. It is assumed that point "0" is a stagnation point and point "1" is moving. Moreover, point "0" is taken as a reference point. The value of pressure is zero along the free surface from points "0" to "2".

Continuity equation is written over the control volume shown in Fig. 23.

$$A_1 v_1 = A_2 v_2 \quad (9)$$

Where, A_2 is the cross sectional area covered by liquid and given by

$$A_2 = [\pi - \gamma + 0.5 \sin 2\gamma] r^2 \quad (10)$$

The continuity equation can also be expressed as follows:

$$v_1/v_2 = A_2/A_1 = 1 - \zeta \quad (11)$$

$$\zeta = (\gamma - 0.5 \sin 2\gamma)/\pi \quad (12)$$

Bernoulli theorem is applied between point “1” and stagnation point “0” along the upper boundary. The pressure at point “1” yields:

$$P_1 = -v_1^2 \rho / 2. \quad (13)$$

Bernoulli theorem is applied between points “0” and “2” with including the viscous effect similar to the procedure of Benjamin (1968) in his solution of the two dimensional flow between two infinite parallel plates. It is assumed that the flow undergoes a uniform loss of its total head, Δ . The pressure at stagnation point is the same as the pressure in the gas bubble. The velocity at point “2” is obtained as follows:

$$v_2^2 = 2g[r(1 - \cos \gamma) - \Delta]. \quad (14)$$

A momentum balance between points “1” and “2” is given by

$$(P_1 + \rho g r) \pi r^2 - \int_0^h \rho g (h-y) b dy - F_f = \rho v_2 A_2 (v_2 - v_1) \quad (15)$$

Where friction force F_f is given by,

$$F_f = \rho g \Delta A_2. \quad (16)$$

The second term in Eq. 15 is the pressure variation with depth which is hydrostatic. The integral term is solved explicitly,

$$\int_0^h \rho g (h-y) b dy = \rho g r (A_2 \cos \gamma + \frac{2}{3} r^2 \sin^3 \gamma) \quad (17)$$

The final form of the momentum balance can be written as,

$$\frac{1}{2} (1 - \zeta)^2 v_2^2 - (1 - \zeta) v_2^2 = \Delta g (1 - \zeta) + g r [(1 - \zeta) \cos \gamma + \frac{2}{3\pi} \sin^3 \gamma - 1] \quad (18)$$

An expression for v_2^2 is obtained as follows:

$$v_2^2 = \frac{2gr[1 - (1 - \zeta) \cos \gamma - \frac{2}{3\pi} \sin^3 \gamma] - 2\Delta g(1 - \zeta)}{1 - \zeta^2} \quad (19)$$

Equating Eqs. 14 and 19 for v_2^2 , the total head loss Δ can be written as:

$$\Delta = k \frac{(1 + \zeta)}{\zeta} \left\{ \begin{array}{l} r(1 - \cos \gamma) \\ - \left[\frac{r[1 - (1 - \zeta) \cos \gamma] + \frac{2}{3\pi} \sin^3 \gamma}{1 - \zeta^2} \right] \end{array} \right\} \quad (20)$$

where k is the total head loss correction factor. The importance of this factor is explained in the comparison with experiments section.

For a given angle γ , the head loss Δ can be calculated. The total head loss Δ is positive for angles less than 82.78° which corresponds to liquid height of 0.563 in 50.8 mm ID pipe. This appears to be possible with energy loss. For the angle greater than 82.78°, the head loss is negative, which implies that an external supply of energy would be necessary to maintain a steady flow. Therefore, the case for the angle greater than 82.78° is impossible from the practical point of view. The solution for the angle of 82.78° is the same as the solution found by Benjamin for inviscid case. For a given angle γ or liquid height h/D, the total head loss is obtained from Eq. 20. v_2 is calculated by using Eq. 14. Then, it is substituted in Eq.9 to calculate v_1 which is the drift velocity, v_d .

The drift velocity model for horizontal flow is developed in terms of h/D instead of liquid viscosity. However, liquid viscosity is needed to develop the model for upward inclined flow. Data for liquid viscosity as a function of h/D is not available in the literature. The liquid viscosity vs. liquid height from the conducted experiments is plotted in Fig. 24. The viscosity correlation is developed as a function of h/D based on experimental results as shown in Eq. 21. This relationship was found for single pipe diameter and range of viscosity up to 0.7 Pa·s. The correlation has to be expanded for different pipe diameters and wide range of liquid viscosity to obtain more accurate results.

$$\mu = 2236 \times \left(\frac{h}{D}\right)^5 - 8157.7 \times \left(\frac{h}{D}\right)^4 + 11914 \times \left(\frac{h}{D}\right)^3 - 8706.5 \times \left(\frac{h}{D}\right)^2 + 3184.9 \times \left(\frac{h}{D}\right) - 466.62 \quad (21)$$

Comparison with Experiments

In model prediction, the drift velocity decreases considerably with the increase in liquid height (h/D) and eventually reaches zero when the liquid height is one. It is apparent that the discrepancies between experimental results and model predictions of the drift velocities become considerable with the increase of oil viscosity. The possible reason for these discrepancies is the assumption of average velocity (constant profile). The liquid draining out of a pipe is

similar to an open channel flow. It is difficult to determine velocity distribution for laminar flow in this flow system. Therefore, the average velocity has to be assumed in the model to estimate the total head loss. For this reason, the calculated head loss from the model is simply modified by a correction factor, k , which is called the head loss correction factor to account for the use of the average velocity. The optimum total head loss correction factor for all experimental data at different liquid viscosities is found 2.2.

The comparison of model predictions with measured drift velocities for horizontal pipe can be seen in Fig. 25. Model predictions are shown with two curves; one curve is without the correction factor ($k=1$) and the other one is with the correction factor ($k=2.2$). The comparison of model predictions with the correction factor ($k=2.2$) with measured drift velocities for horizontal pipe shows good agreement. The model predictions with and without the correction factor also matched with the results obtained from Benjamin (1968) model by using inviscid flow theory.

Vertical Flow:

For vertical flow, a model is needed to take into account the effect of viscosity. Joseph (2003) proposed a model for the bubble rise velocity in vertical flow and taking viscosity, surface tension and shape of the bubble nose effects into consideration. From the experimental results, it is observed that the bubble nose is almost spherical. When the bubble nose is spherical (axisymmetric cap), the effect of the surface tension vanishes and the equation becomes only function of the fluid viscosity and the radius of the spherical cap bubble as shown in Eq. 22.

$$v_d = -\frac{4}{3} \frac{\mu}{\rho \cdot r} + \sqrt{\frac{4}{9} g \cdot r + \frac{16}{9} \frac{\mu^2}{(\rho \cdot r)^2}}, \quad (22)$$

where r is the radius of cap, ρ and μ are the density and viscosity of the liquid.

Comparison with Experiments

Figure 26 shows the comparison of the model predictions with experimental data from Weber et al.(1980), Shosho and Ryan (2001) and this study. The bubble radius and liquid viscosity must be known to calculate the drift velocity from Eq. 19. It is experimentally observed that the radius of bubble is approximately equal to 0.6 of the radius of the pipe. This value is used for the rest of calculations to compare model predictions with experimental results.

Weber et al. (1986) performed their experiments in 37.3 mm ID pipe for viscosities between 0.051 and 0.183 Pa·s. Shosho and Ryan experiments were also for same diameter for viscosities between 0.003 and 0.883 Pa·s. They are the only available dataset for higher viscosity range with comparable pipe diameter in the literature. When the data of the three studies were compared against the simplified model, it predicted the drift velocities within ± 20 % error band. Therefore, the simplified model for vertical flow is used in the proposed model for upward inclined flow.

Upward Inclined Flow:

A new model similar to Bendiksen (1984) approach is proposed for upward inclined flow. The drift velocity is expressed with Eq. 23. This equation is a unified drift velocity closure model including the effect of liquid viscosity is proposed for all inclination angles.

$$v_d = v_d^v (\sin \theta)^{0.7} + v_d^h (\cos \theta)^{1.5}, \quad (23)$$

where, v_d^h , v_d^v , and θ are drift velocities for horizontal and vertical flows, and the angle of inclination, respectively. The proposed horizontal drift velocity model is used for v_d^h in Eq. 20. The vertical drift velocity v_d^v is obtained from Eq. 22.

The accuracy of the drift velocity equation in horizontal flow depends on the accuracy of relationship between viscosity and liquid height (h/D). In the present study, the relationship is developed based on 50.8 mm ID pipe and within the range of viscosity between 0.1 and 0.7 Pa·s. Therefore, an extensive experimental study for drift velocity and liquid height (h/D) at different wide ranges of viscosity and different pipe diameters needs to be conducted to improve the accuracy of the model prediction.

Comparison with Experiments

A total of 100 drift velocity data are available for model evaluation. Figure 27 shows the comparison of model predictions with the data of Weber et al. (1986), and Shosho and Ryan (2001) for all inclination angles. It is seen that the difference between the model predictions and experimental results is within ± 40 % for most of the data. When the model is compared against the present study data, as shown in Fig. 28, the predictions are within ± 20 % error band.

Translational Velocity

Nicklin et al. (1962) proposed an equation for translational velocity as,

$$v_t = C_s v_s + v_d. \quad (24)$$

The experimental results are compared against the Nicklin model in Fig. 29. From the poor performance, it is concluded that the equation proposed by Nicklin is not valid with the increase of liquid viscosity. On the other hand, the experimental results have also revealed that translational velocity has a linear relationship with mixture velocity. Therefore, the discrepancy in results is found to be caused by drift velocity which was developed by using inviscid flow theory. A new drift velocity model is developed for high viscosity oils as explained above. The developed model is implemented into translational velocity equation.

Comparison with Experiments

Figures 30 and 31 show the comparison of model prediction against measured translational velocity for the viscosities of 0.181 and 0.587 Pa-s, respectively. The values of drift velocity at these viscosities are predicted from the developed model. The value of C_s is taken as 2 due to laminar flow. The comparison shows good agreement between model predictions and experimental measurements. The relative error is within $\pm 20\%$.

In the literature, the exact value of C_s is not clear. It changes for flow conditions. The value is 2 for laminar flow. In this study, the value of C_s is found as 1.87 by using a regression analysis. Figure 32 shows that the performances of translational velocity equation against experimental results when C_s is either 2 or 1.87. A much better agreement is obtained when C_s is 1.87.

Slug Frequency

A dimensionless analysis approach is taken in order to develop a slug frequency closure model for viscous oil. It is known that the slug length and slug frequency are interrelated parameters and are very often used each other. An intermittency, I , is defined as the fraction of the time is observed by a stationary observer,

$$I = \frac{f_s L_s}{C}, \quad (25)$$

where, C can be translational velocity, v_t . Experimental observations indicate that the intermittency can be correlated as a function of velocity ratio as shown in Eq. 26,

$$\frac{f_s L_s}{v_t} \propto \frac{v_{SL}}{v_{SL} + v_{SG}}. \quad (26)$$

The intermittency is plotted against velocity ratio at different viscosities for a constant liquid velocity of 0.3 m/s as it can be seen in Fig. 33. It gave a reasonable linear relationship. Similar trends are found for different liquid velocities. Using translational velocity and slug length in the same dimensionless group makes difficult to predict slug frequency. Especially, slug length has to be predicted by another closure model. Therefore, the intermittency is revised to dimensionless slug frequency, $(f_s D)/V_m$. The dimensionless slug frequency against velocity ratio at different viscosities for same liquid velocity is plotted in Fig. 34. The effect of viscosity on slug frequency is easily observed from the graph. The dimensionless slug frequency increases with the increase of liquid viscosity and velocity ratio.

Another dimensionless group is necessary to include the effect of viscosity into slug frequency closure model. Wallis (1969) completed an extensive dimensionless analysis for inertia, viscous and surface tension forces. The dimensionless Froude number for the inertia forces is defined as,

$$Fr_d = \frac{v_d}{(gD)^{0.5}} \sqrt{\frac{\rho_L}{(\rho_L - \rho_G)}}. \quad (27)$$

The dimensionless viscosity number for the viscous forces is defined as,

$$N_\mu = \frac{v_d \mu_L}{gD^2 (\rho_L - \rho_G)}. \quad (28)$$

The dimensionless inverse viscosity can be obtained by combining the first two dimensionless groups, as shown in Eq. 29

$$N_f = \frac{D^{3/2} \sqrt{\rho_L \Delta \rho g}}{\mu_L}. \quad (29)$$

It is decided that dimensionless slug frequency is correlated as a function of dimensionless inverse number. The final form of the relationship is,

$$\frac{f_s D}{v_m} \propto \frac{D^{3/2} \sqrt{\rho_L \Delta \rho g}}{\mu_L} \frac{v_{SL}}{v_m} \quad (30)$$

Figure 35 shows the dimensionless frequency against combination of dimensionless inverse viscosity and velocity ratio for the same liquid velocity that is used in Figs. 33 and 34. It is found that a simple linear relationship exists between the dimensionless groups. Furthermore, the slope of linear relationship increases with the increase of liquid viscosity.

Linear regression analysis is used to examine the relationship between the dimensionless slug frequency and the combination of dimensionless

inverse viscosity and velocity ratio. The value of R^2 indicates that the capability of the regression to capture the proportion of total variation of the dimensionless slug frequency. The summary of the results of linear regression analysis is presented in Table 2. The final equation of slug frequency model for high oil viscosity is developed by using the results of linear regression analysis as shown in Eq. 31. The dimensionless groups show linear relationship for all data as it can be seen in Fig. 36.

$$f_s = 2.816 \frac{1}{N_f^{0.612}} \frac{v_{SL}}{D} \quad (31)$$

References

- Alves, I.N., Shoham, O., Taitel Y.: "Drift Velocity of Elongated Bubbles in Inclined Pipes," Chem. Eng. Sci., Vol.48, pp.3063-3070 (1993).
- Barnea, D., and Brauner, N.: "Holdup of the Liquid Slug in Two-phase Intermittent Flow," Int. J. Multiphase Flow, Vol. 11, pp. 43-49 (1985).
- Benjamin, T. B.: "Gravity Currents and Related Phenomena," J. Fluid. Mech., Vol. 31, Part 2, pp. 209-248 (1968).
- Bendiksen, K. H.: "An Experimental Investigation of the Motion of Long Bubbles in Inclined Tubes," Int. J. Multiphase Flow, Vol.10, pp. 467-483 (1984).
- Gokcal, B.: "Effects of High Oil Viscosity on Two-Phase Oil-Gas Flow Behavior in Horizontal Pipes," M.S. Thesis, The University of Tulsa, Tulsa, OK (2005).
- Gokcal, B, Al-Sarkhi, A.S., and Sarica, C.: "Effects of High Oil Viscosity on Drift Velocity for Horizontal Pipes," Presented at BHRg Conference of Multiphase Production Technology, Banff, June 4-6, 2008.
- Joseph, D. D: "Rise velocity of a Spherical Cap Bubble," J. Fluid Mech., Vol. 488, pp. 213-223 (2003).
- Nicklin, D. J., Wilkes, J. O., Davidson, J. F.: "Two-Phase Flow in Vertical Tubes," Trans. Inst. Chem. Eng., Vol. 40, pp. 61-68 (1962).
- Nydal, O. J., Pintus, S., Andreussi, P.: "Statistical Characterization of Slug Flow in Horizontal Pipes," Int. J. Multiphase Flow, Vol. 18, No. 3, pp. 439-453 (1991).
- Shosho, C. E. and Ryan, M. E.: "An Experimental Study of the Motion of Long Bubbles in Inclined Pipes," Chem. Eng. Sci., Vol. 56, pp. 2191-2204 (2001).
- Taitel, Y., Barnea, D., and Dukler, A. E.: "Modeling Flow Pattern Transitions for Steady Upward Gas-Liquid Flow in Vertical Tubes," AIChE. Journal, Vol. 26, pp.345-354 (1980).
- Wallis, G. B.: *One Dimensional Two-Phase Flow*, McGraw-Hill, New York (1969).
- Weber, M.E.: "Drift in Intermittent Two-Phase Flow in Horizontal Pipes," Can. J. Chem. Eng., Vol. 59, pp. 398-399 (1981).
- Weber, M.E., Alarie, A., and Ryan, M. E.: "Velocities of Extended Bubbles in Inclined Tubes," Chem. Eng. Sci., Vol. 41, pp. 2235-2240 (1986).
- Xiao, J.J., Shoham, O., and Brill, J.P.: "A Comprehensive Mechanistic Model for Two-phase Model," SPE 20631, Presented at SPE Annual Meeting, New Orleans, LA, Sept. 1990.

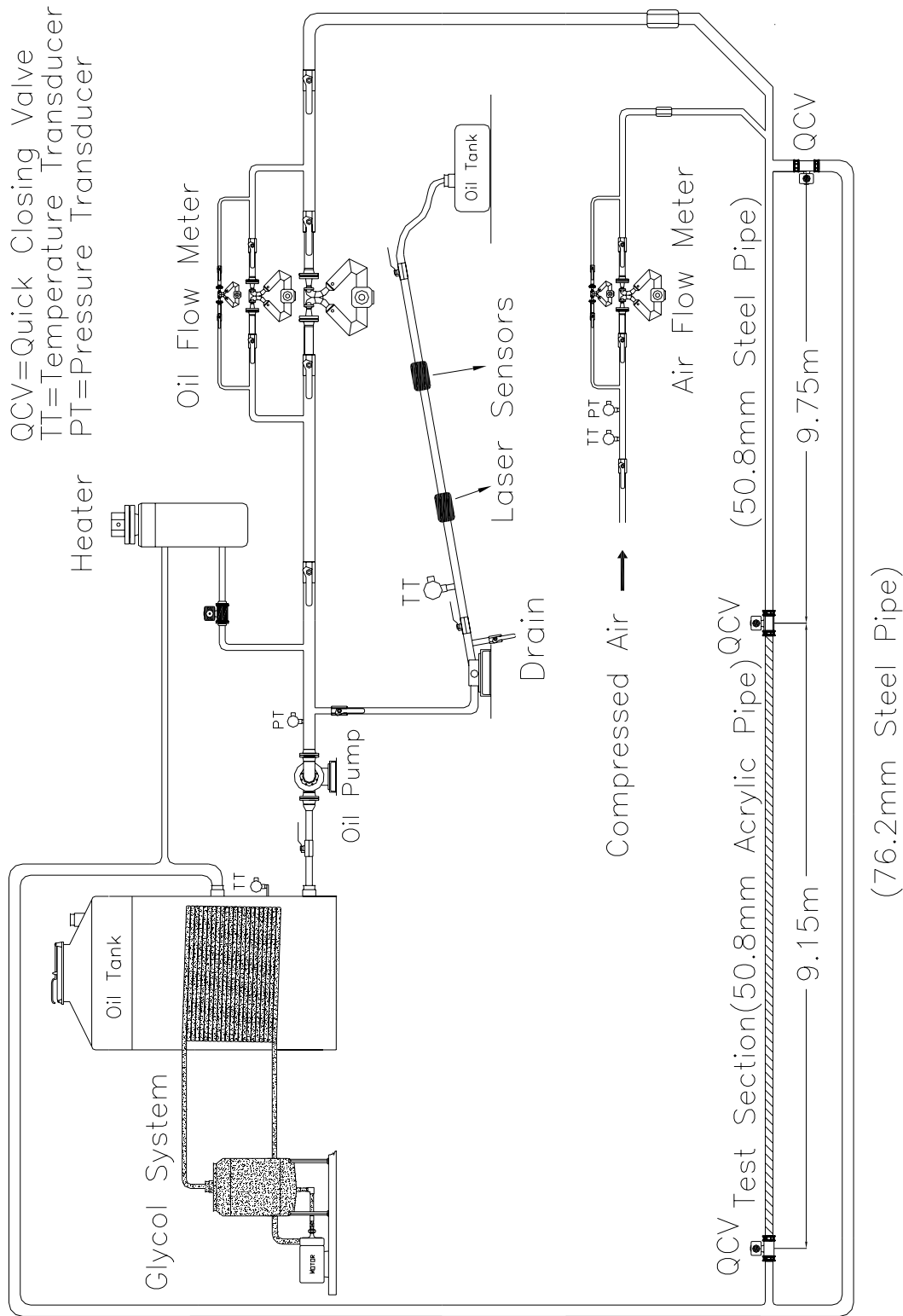
16. Zhang, H.-Q., Wang, Q., Sarica, C., and Brill, J.P.: “Unified Model for Gas-Liquid Pipe Flow via Slug Dynamics - Part 1: Model Development,” ASME, J. Energy Res. Tech., Vol. 125 (2003).
17. Zukoski, E. E.: “Influence of Viscosity, Surface Tension, and Inclination Angle on Motion of Long Bubbles in Closed Tubes,” J. Fluid Mech., Vol. 25, pp. 821-837 (1966).

**Table 1: Model Evaluation Using the Present
Study Pressure Gradient Data**

Model	No. of data	Statistical Parameters					
		ε_1 (%)	ε_2 (%)	ε_3 (%)	ε_4 (Pa/m)	ε_5 (Pa/m)	ε_6 (Pa/m)
TUFFP Unified Model	190	-15	16.0	61	-131	141	79
Xiao Model	190	-18	19.0	121	-184	203	121

Table 2: Linear Regression Analysis for Dimensionless Slug Frequency

Dataset	m	μ (Pa.s)	N_f	R^2
1	0.0046	0.589	53.6	0.92
2	0.0022	0.374	84.3	0.91
3	0.0012	0.257	122.3	0.97
4	0.0007	0.181	173.0	0.96



QC=Quick Closing Valve
 TT=Temperature Transducer
 PT=Pressure Transducer

Figure 1 - Schematic of Test Facility

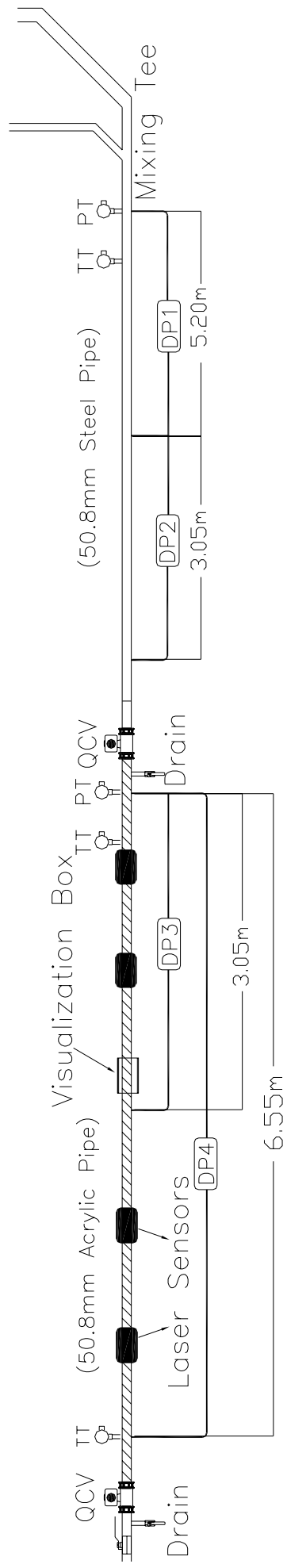


Figure 2 - Schematic of Test Section

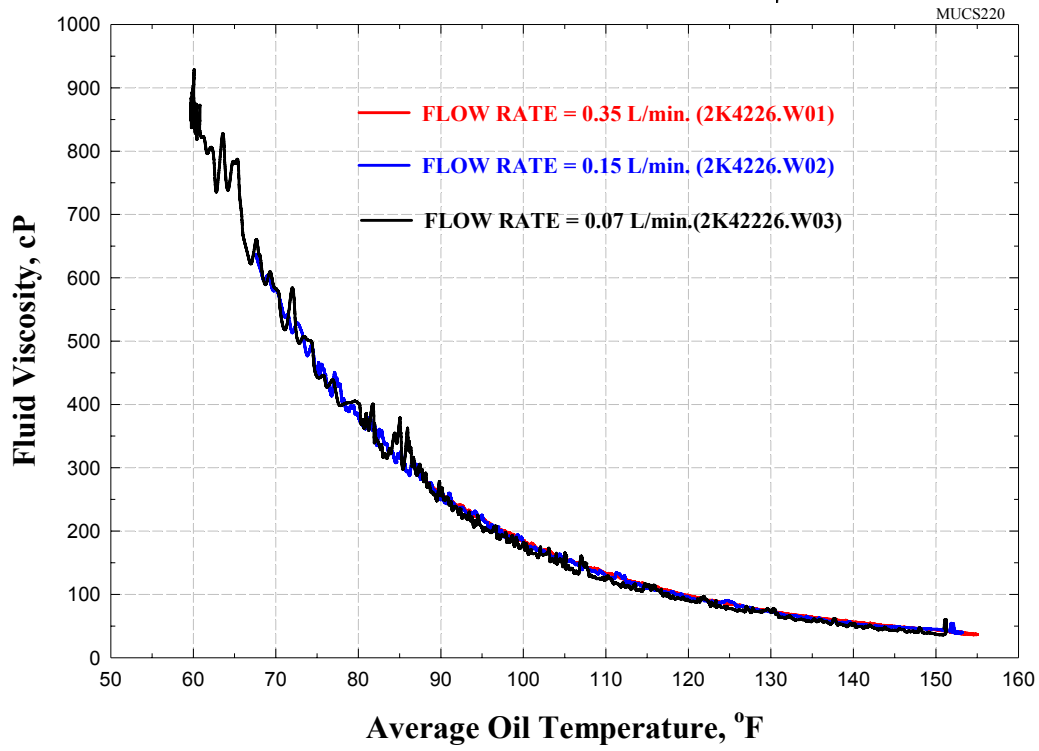


Figure 3 - Viscosity vs. Temperature for Citgo Sentry 220 Oil

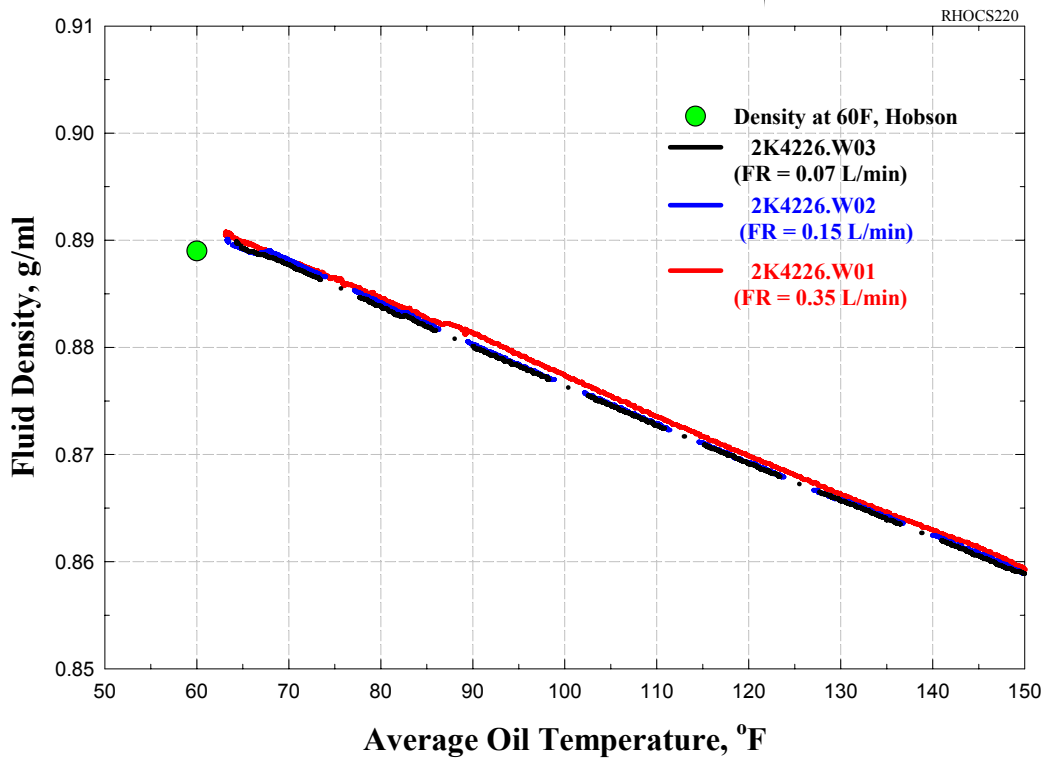


Figure 4 - Oil Density vs. Temperature for Citgo Sentry 220 Oil

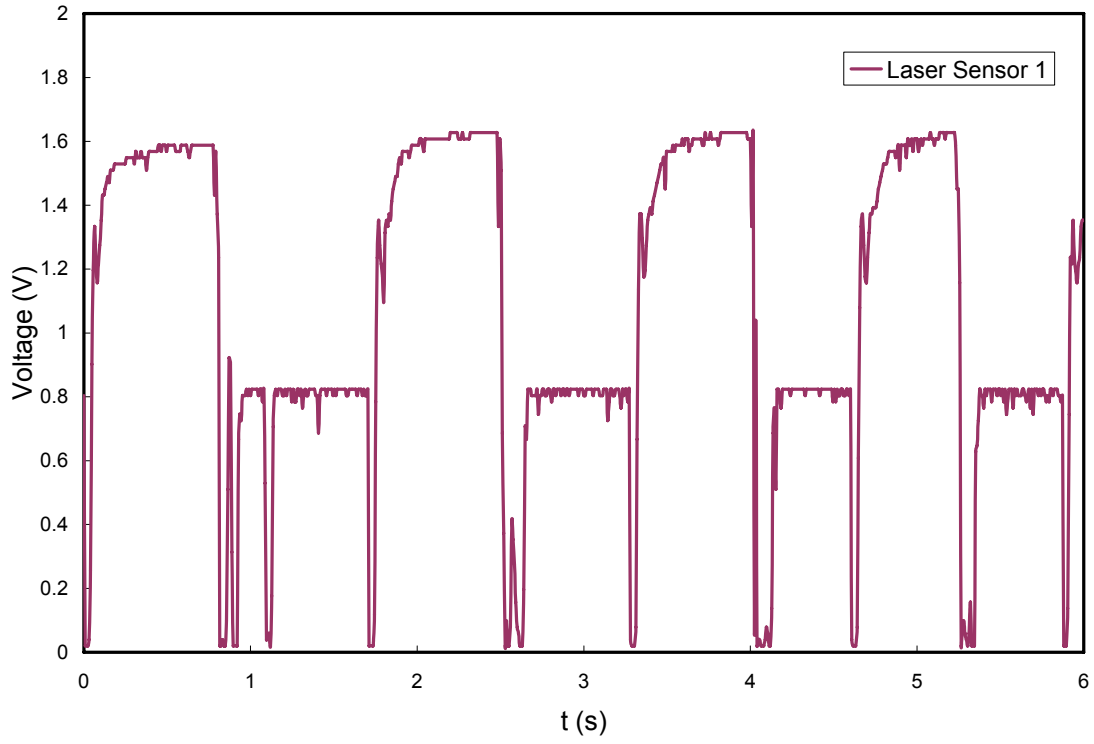


Figure 5 – The Raw Output Signal of Laser Sensor 1

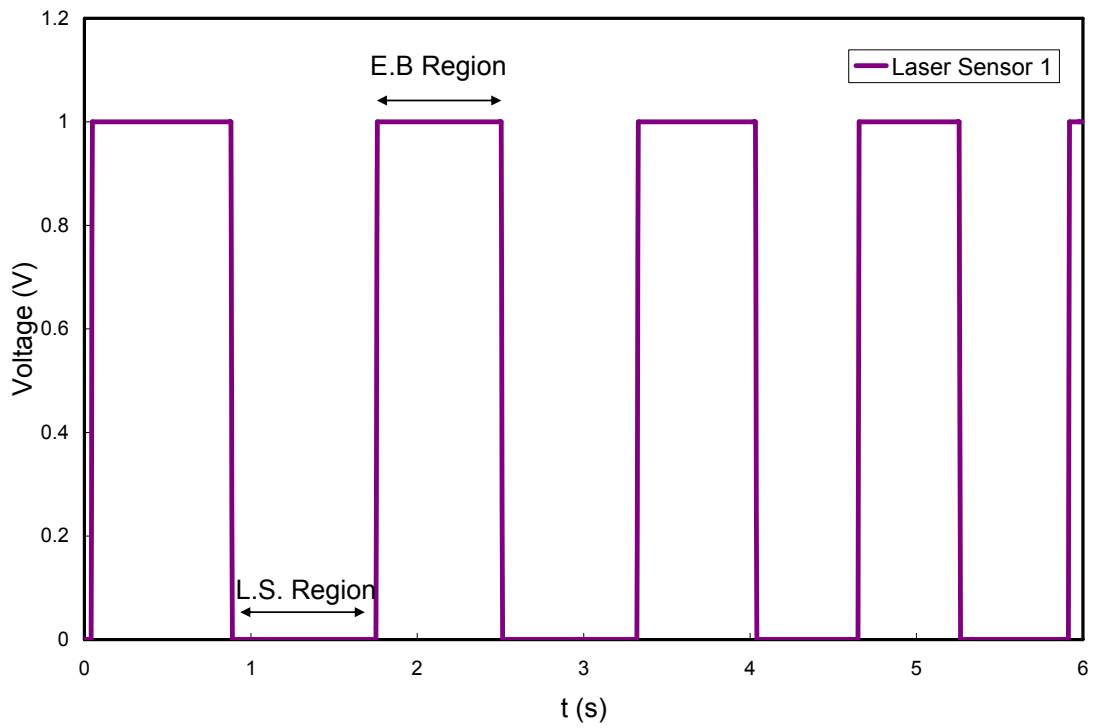


Figure 6 – The Filtered Output Signal of Laser Sensor 1

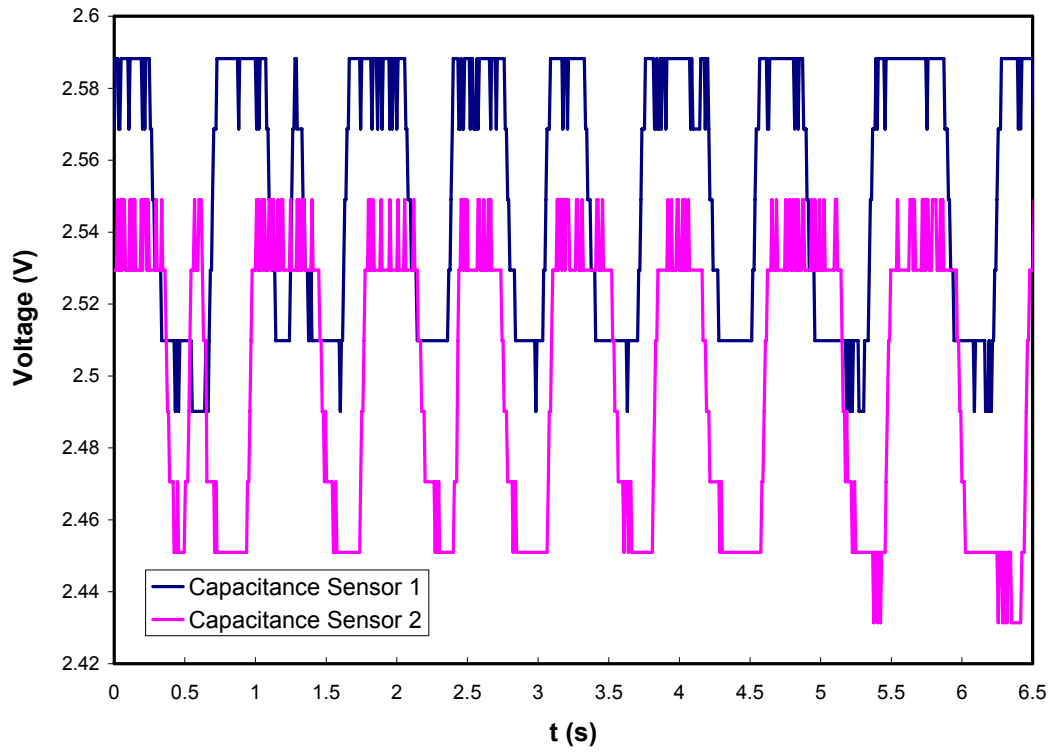


Figure 7 – Output Signals for Capacitance Sensors 1 and 2

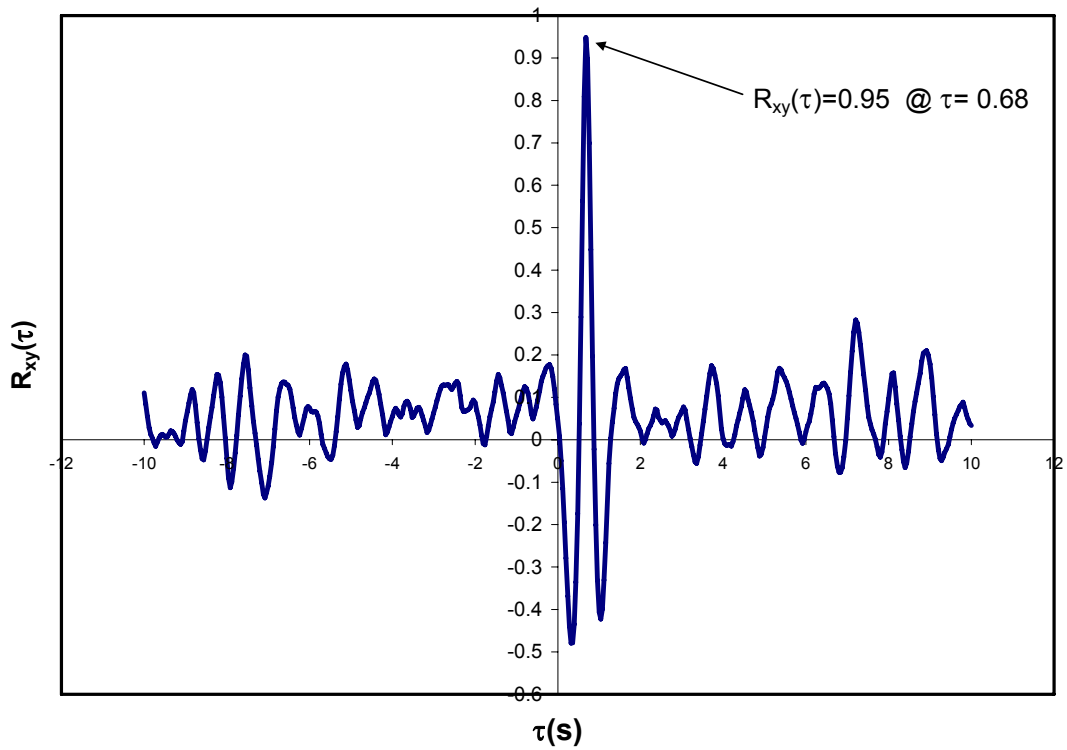


Figure 8 – Cross-Correlation Results between Capacitance Sensors 1 and 2

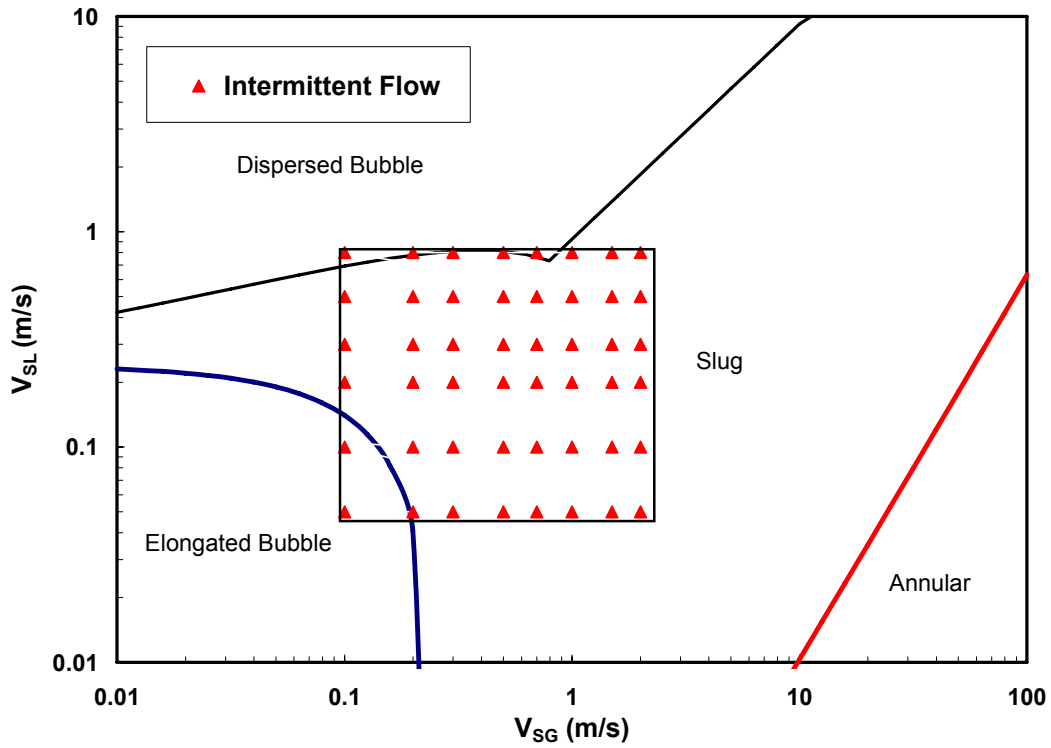


Figure 9 – Barnea Flow Pattern and Experimental Observation (0.589 Pa·s or 589 cP)

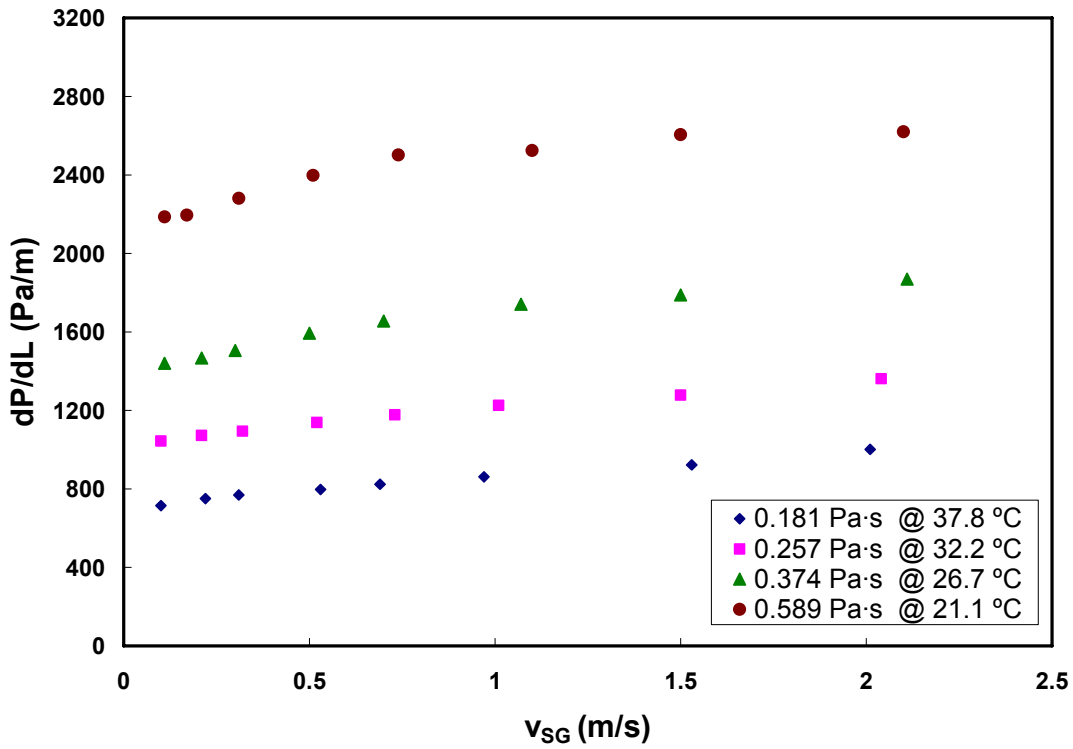


Figure 10 – Pressure Gradients at Different Viscosities and Superficial Gas Velocities for $v_{SL} = 0.3$ m/s

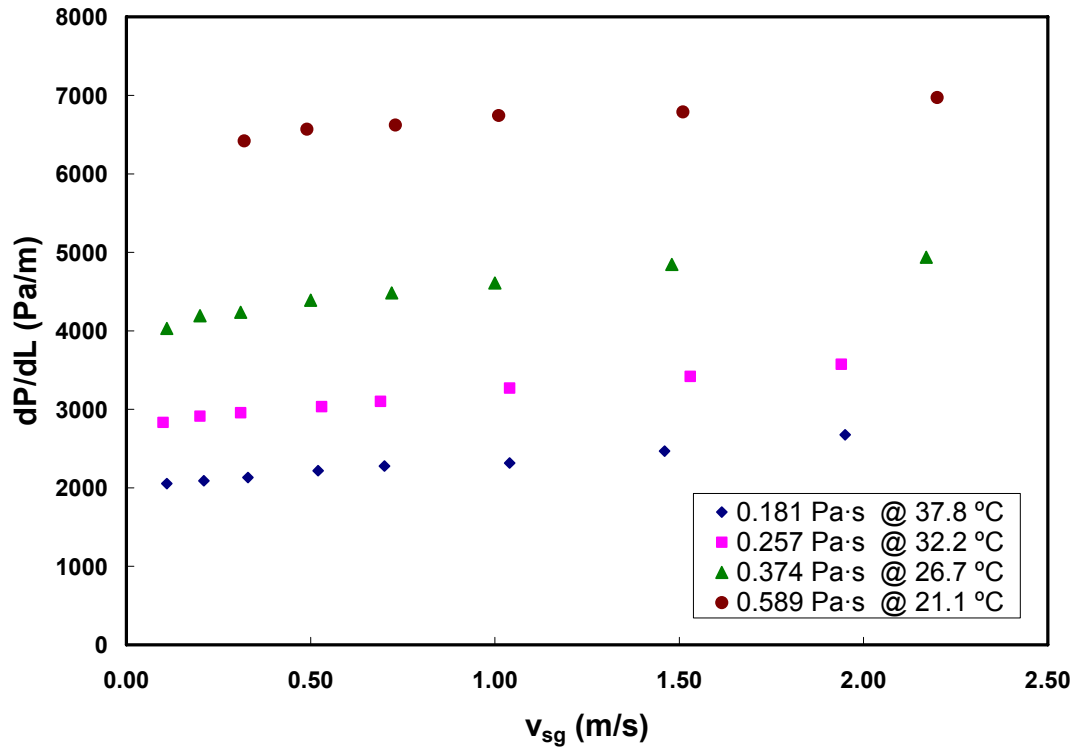


Figure 11 – Pressure Gradients at Different Viscosities and Superficial Gas Velocities for $v_{SL} = 0.8$ m/s

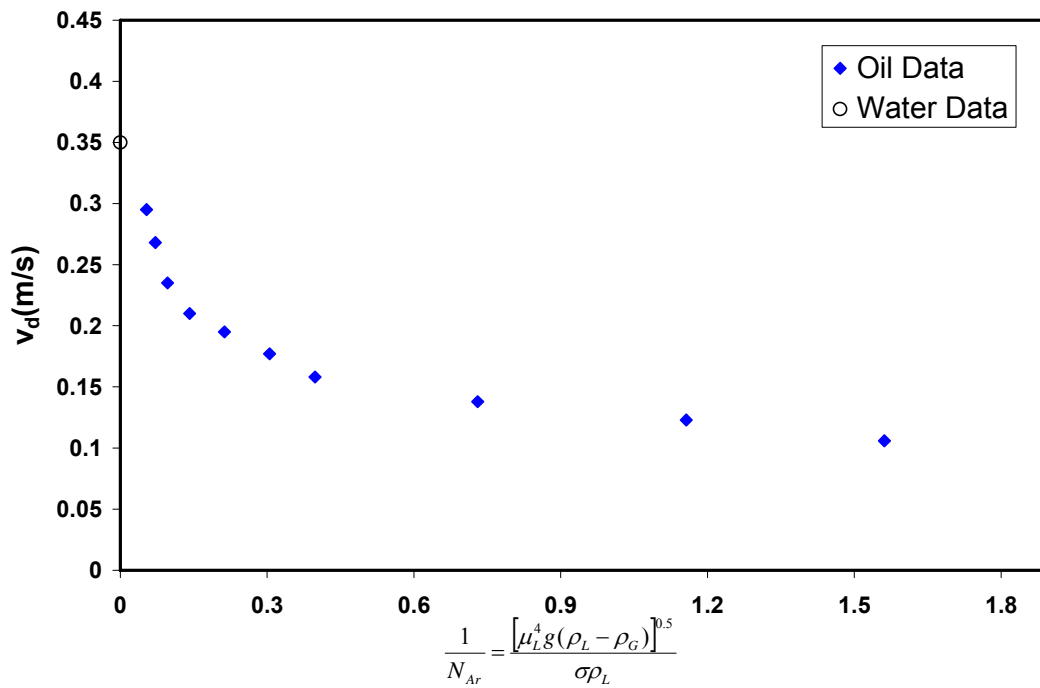


Figure 12 – Measured Drift Velocity vs. Inverse Arhmedes Number for Horizontal Flow

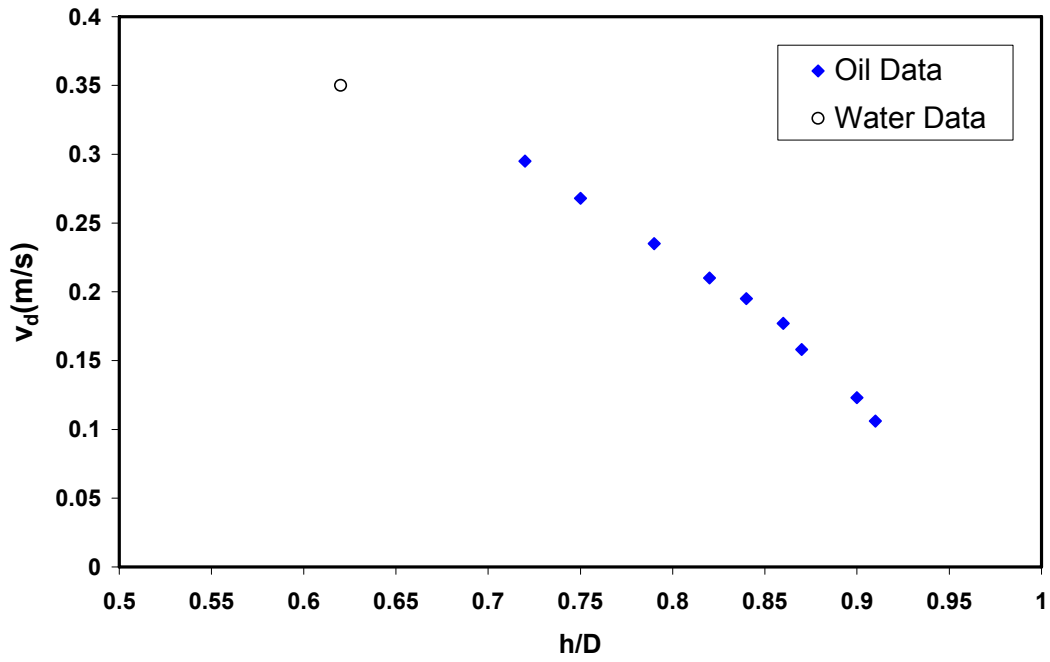


Figure 13 – Measured Drift Velocity vs. Liquid Height for Horizontal Flow

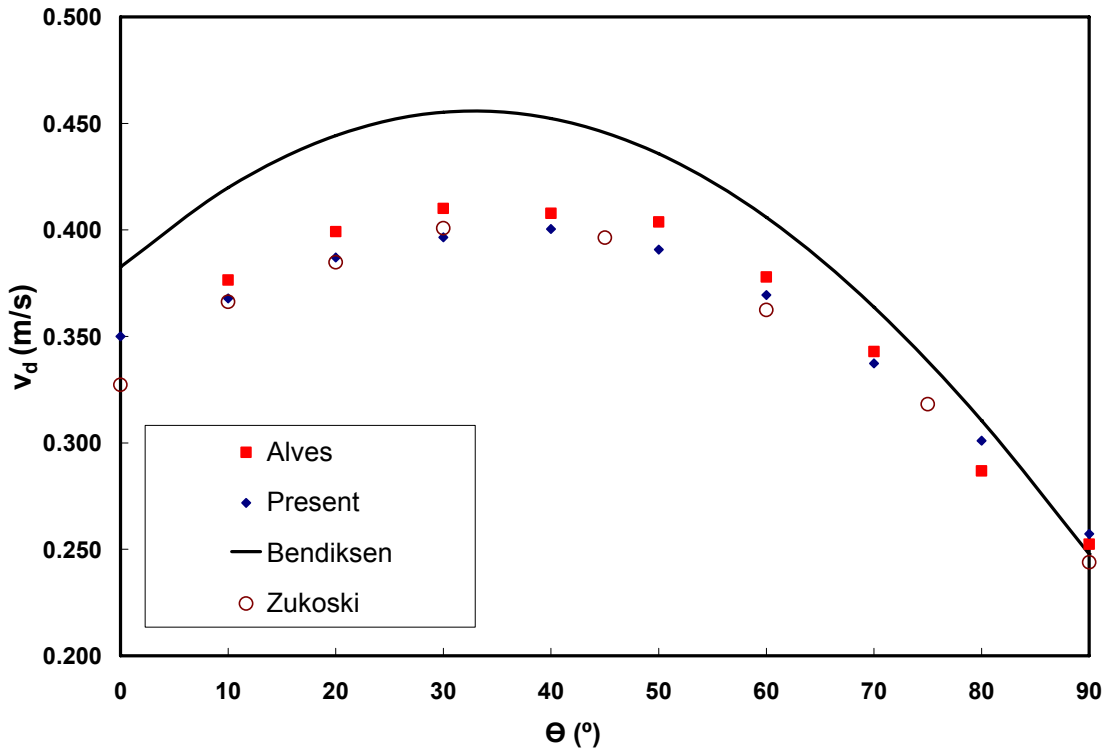


Figure 14 – Measured Drift Velocity vs. Inclination Angle for Water

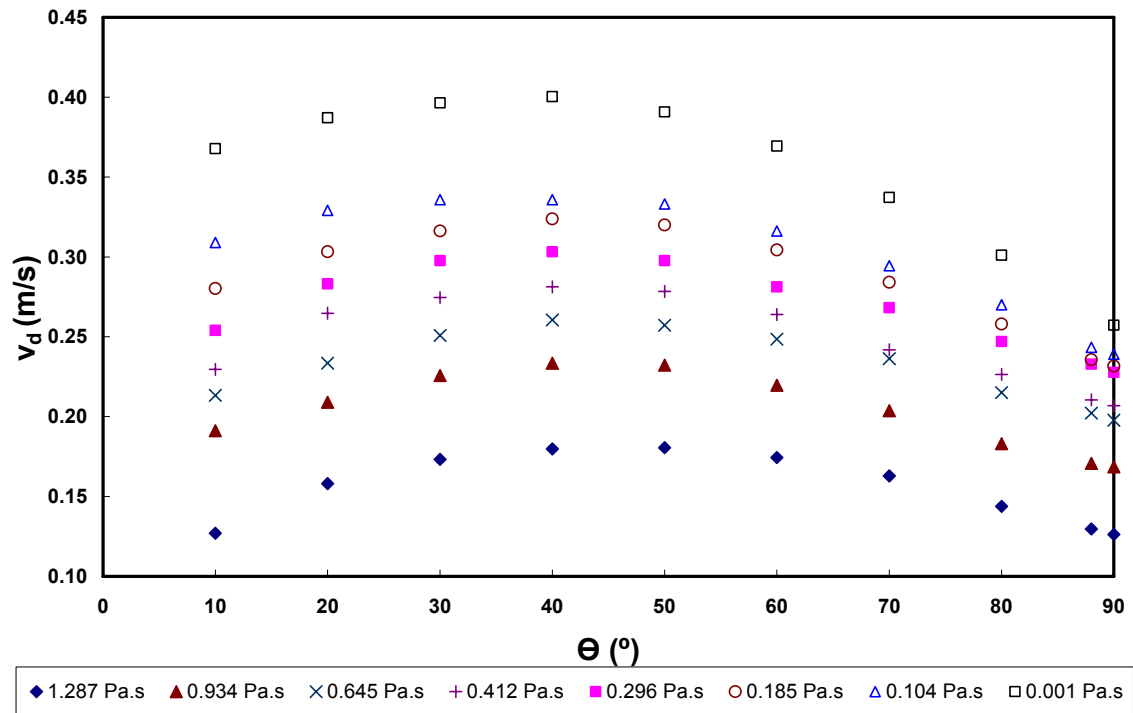


Figure 15 – Measured Drift Velocity vs. Inclination Angle for Different Oil Viscosities

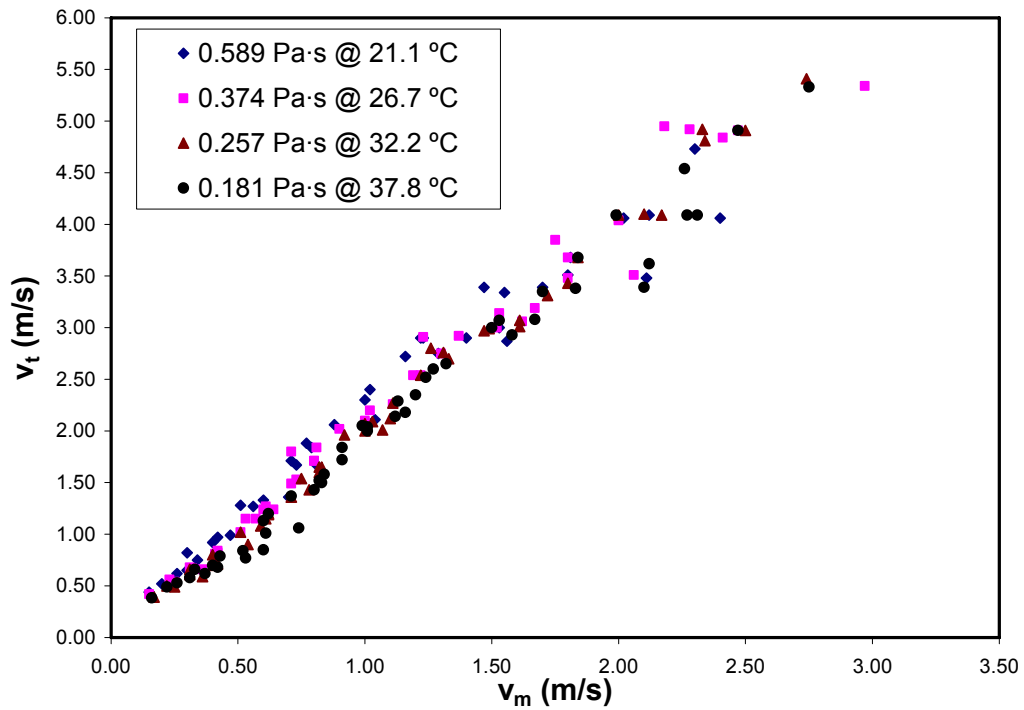


Figure 16 – Measured Translational Velocity vs. Mixture Velocity for Different Oil Viscosities

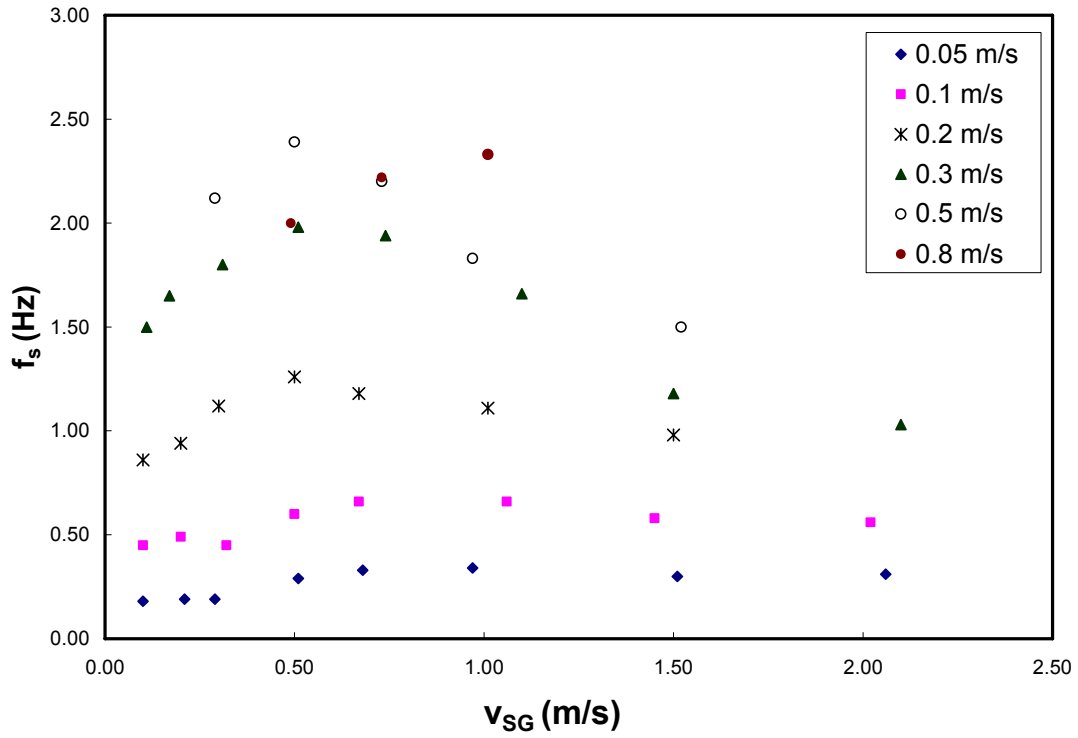


Figure 17 – Slug Frequency vs. Superficial Gas Velocity at $\mu = 0.589$ Pa·s

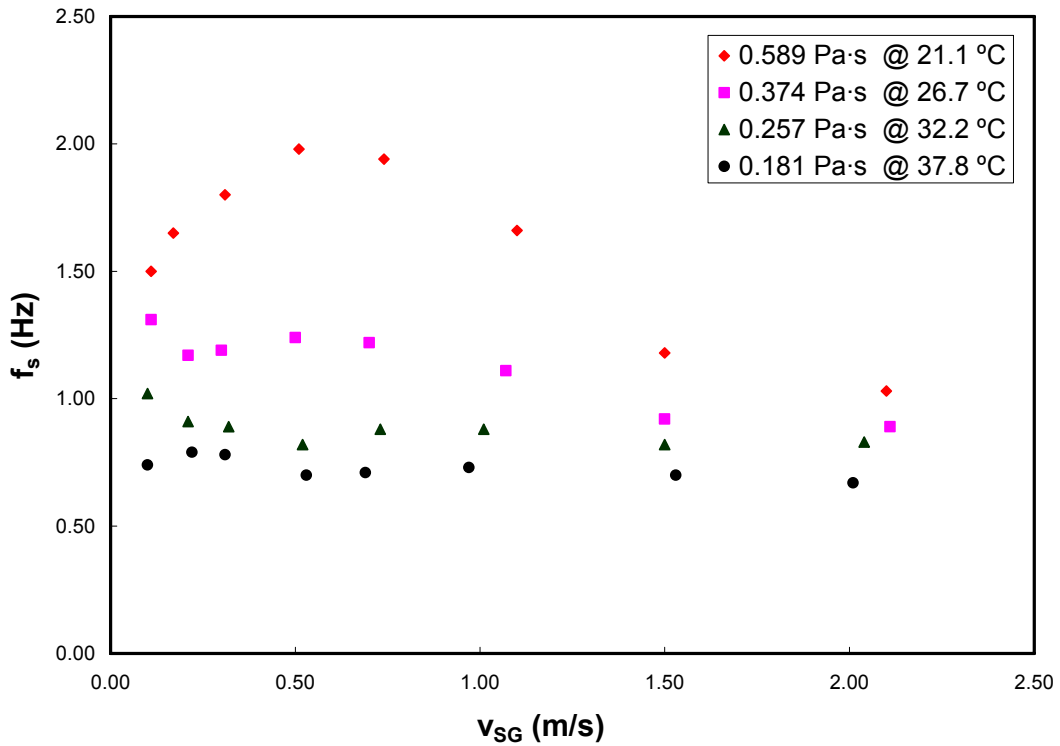


Figure 18 – Slug Frequencies at Different Viscosities and Superficial Gas Velocities for $v_{SL} = 0.3$ m/s

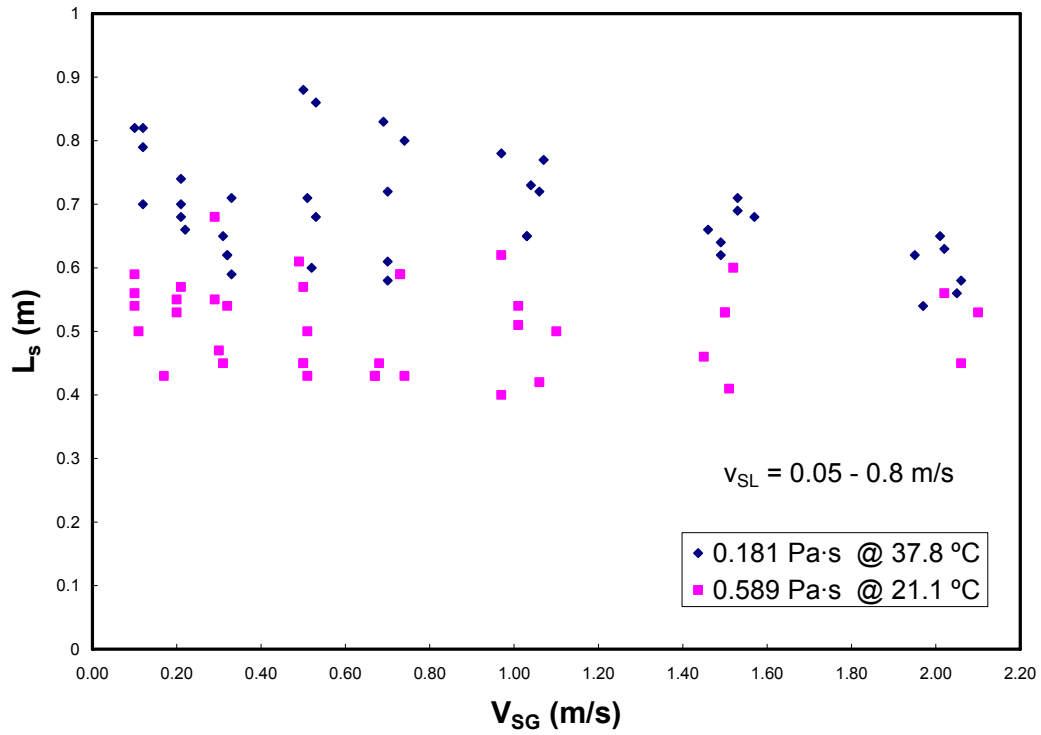


Figure 19 – Measured Mean Slug Lengths at $\mu = 0.181$ and $0.589 \text{ Pa}\cdot\text{s}$ for Different Velocities

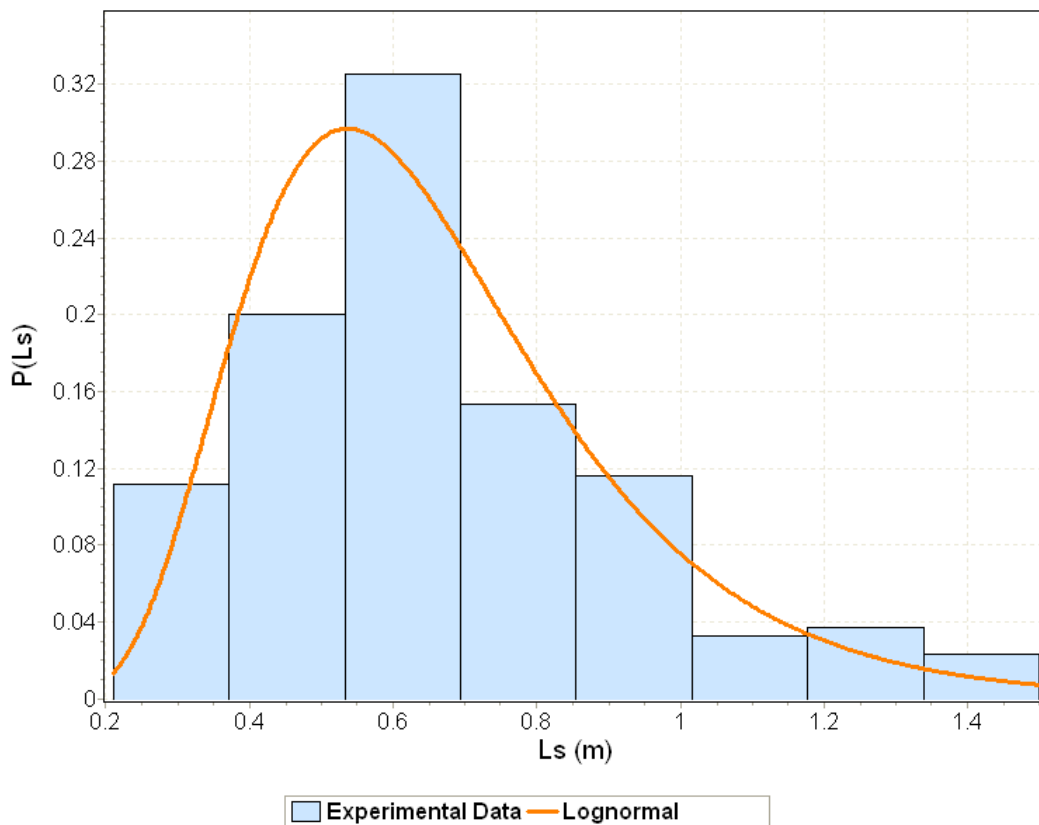


Figure 20 – Slug Length Distribution for $v_M = 1.5 \text{ m/s}$

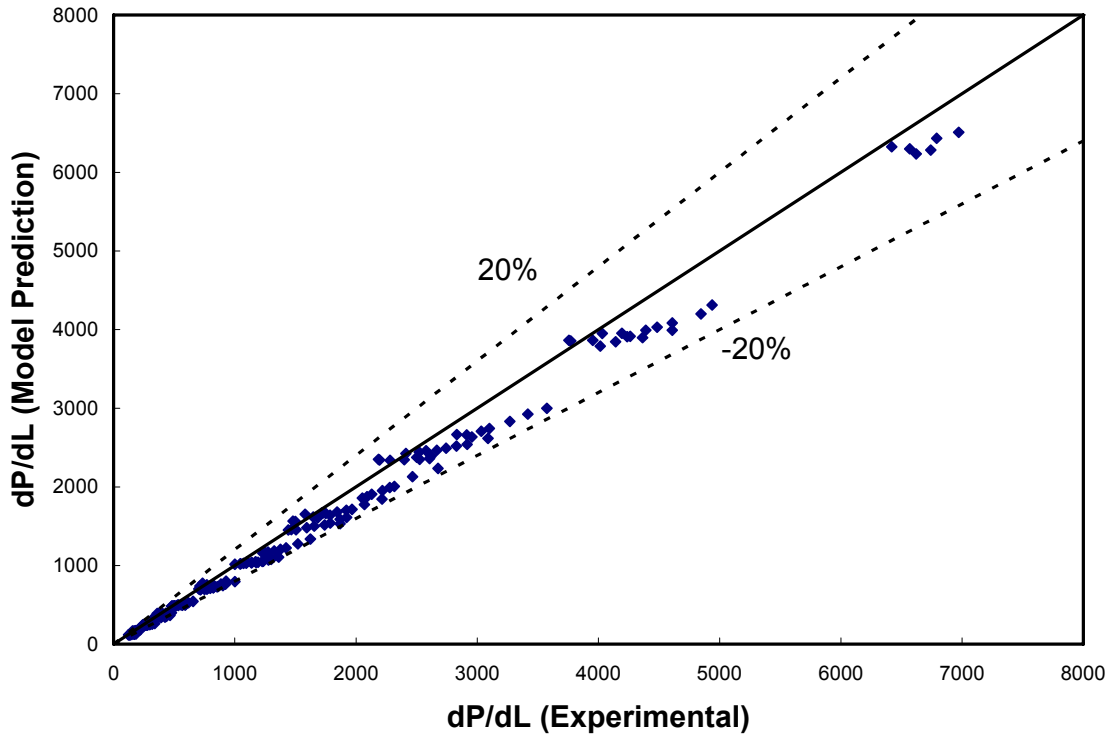


Figure 21 – Comparison of TUFFFP Unified Model Predictions and Measured Pressure Gradients

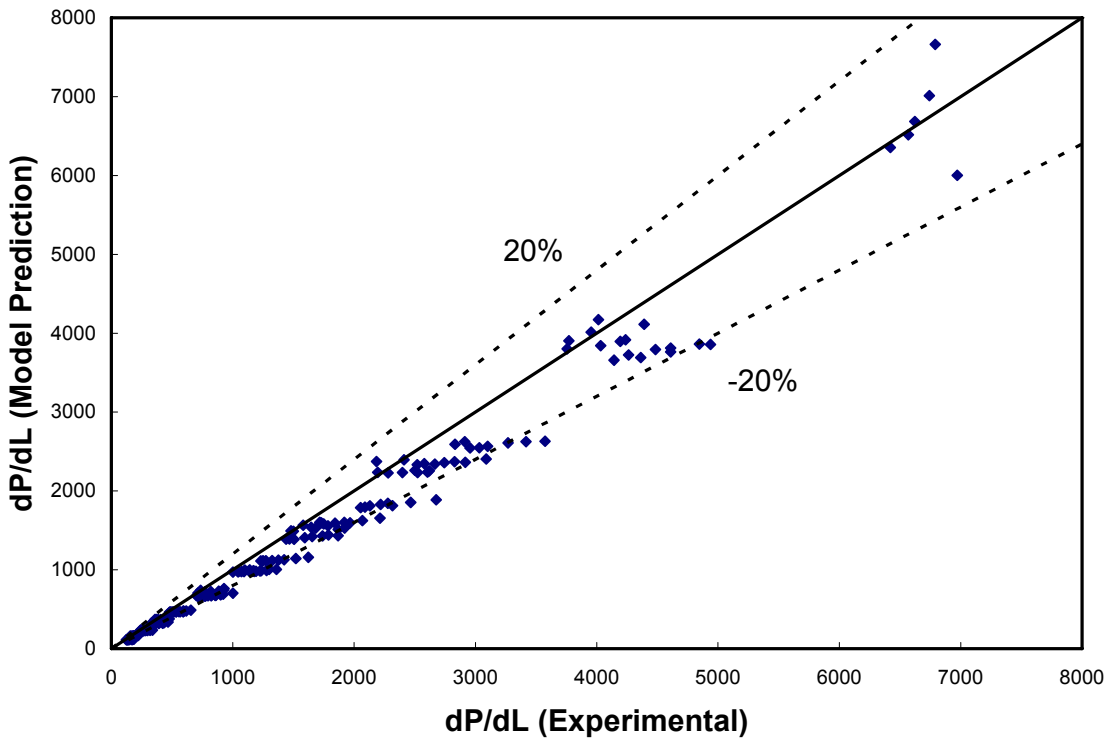


Figure 22 – Comparison of Xiao Model Predictions and Measured Pressure Gradients

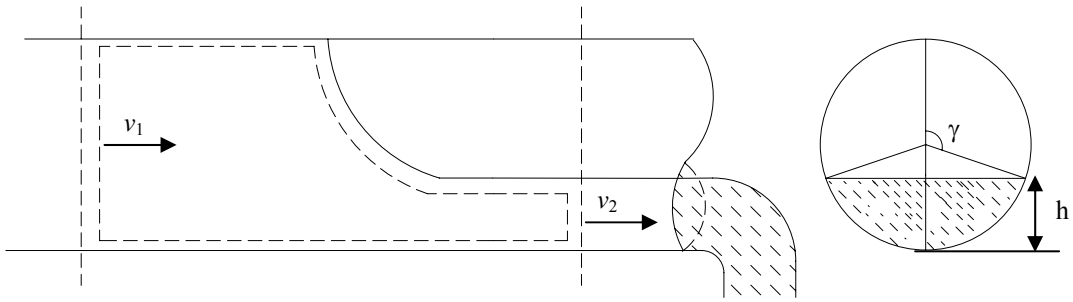


Figure 23 – Propagation of Gas Pocket in Draining Horizontal Pipe

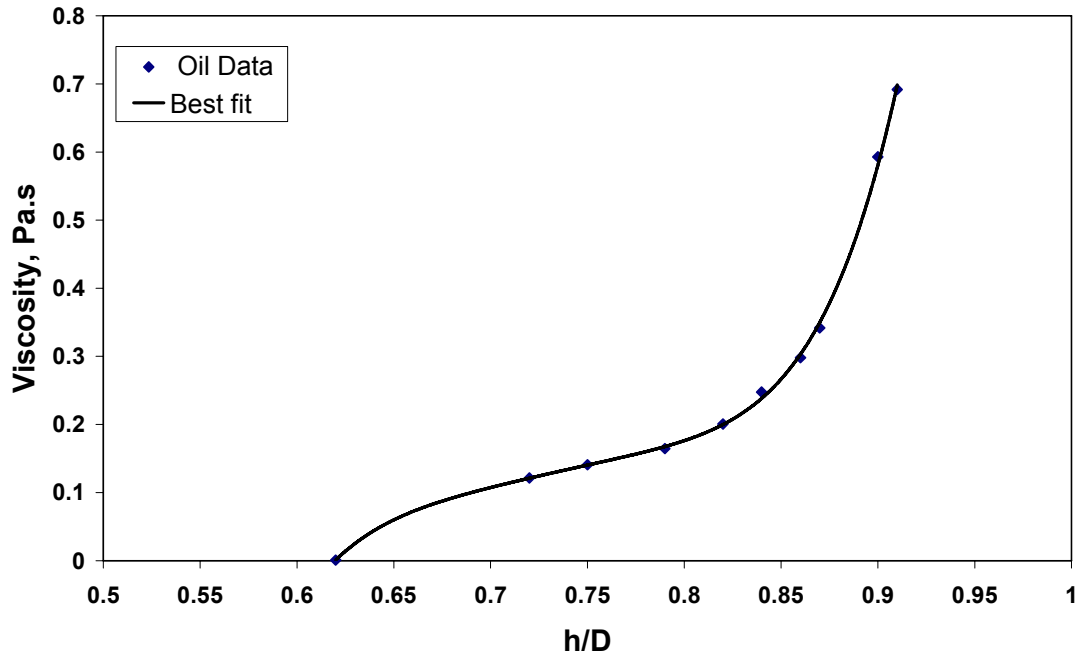


Figure 24 – Liquid Viscosity vs. Measured h/D

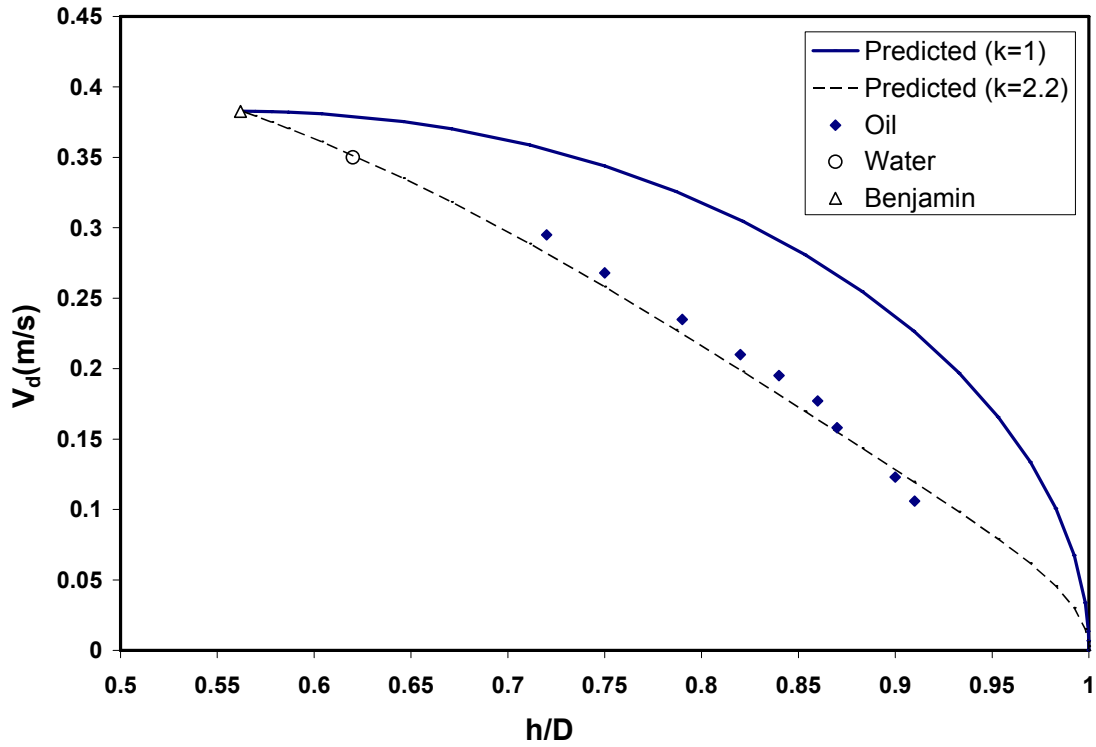


Figure 25 – Comparison of Predicted and Measured Drift Velocities for Horizontal Flow

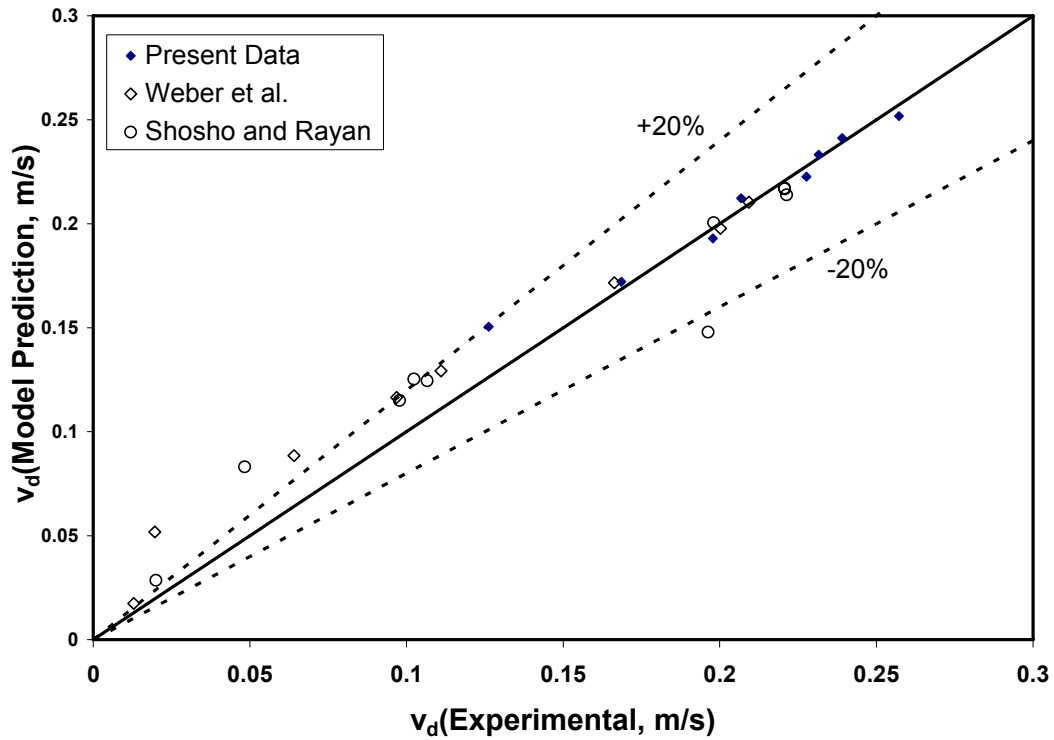


Figure 26–Measured vs. Predicted Drift Velocities for Vertical Flow

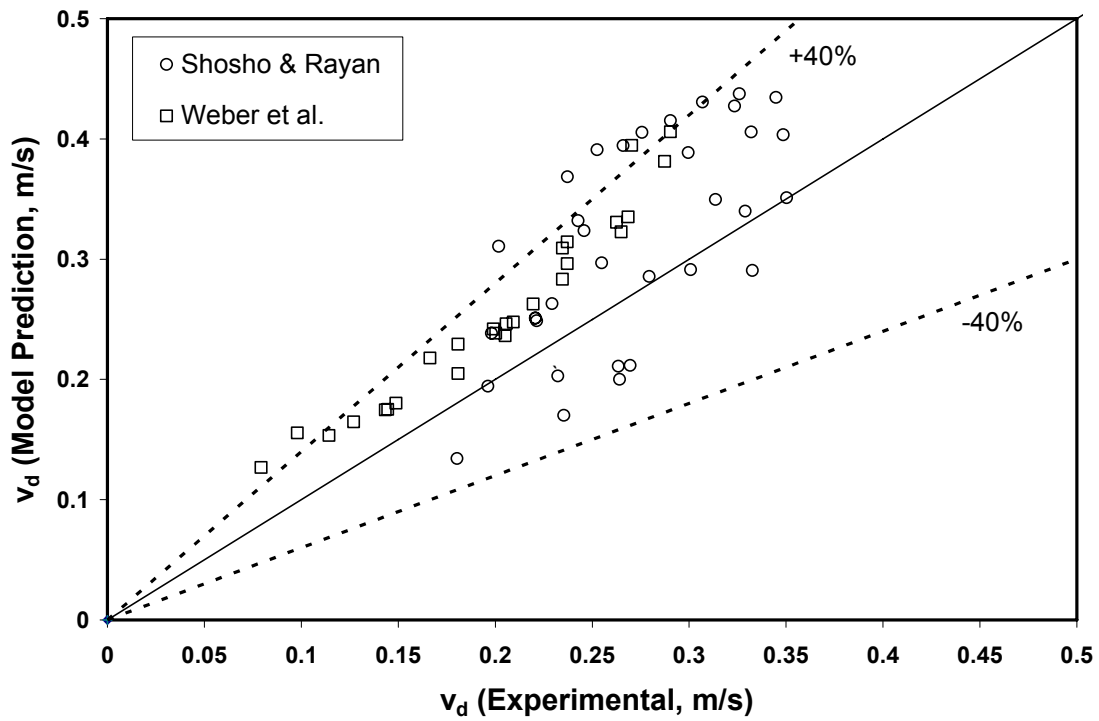


Figure 27 –Measured vs. Predicted Drift Velocities for All Inclination Angles

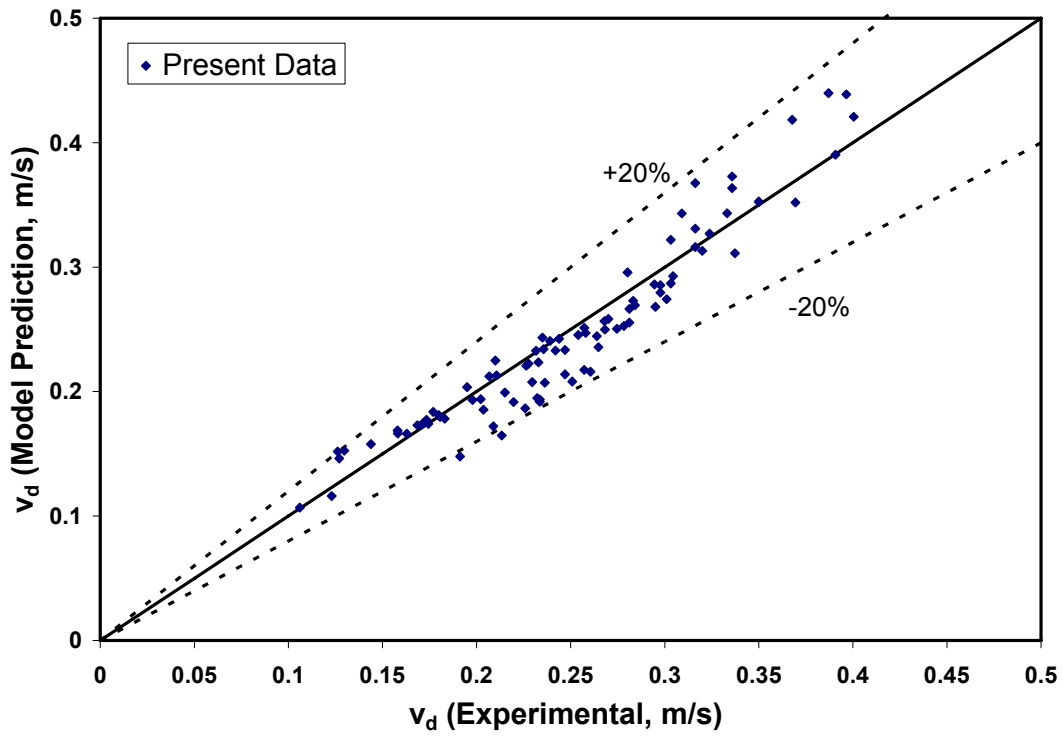


Figure 28 –Measured vs. Predicted Drift Velocities for All Inclination Angles

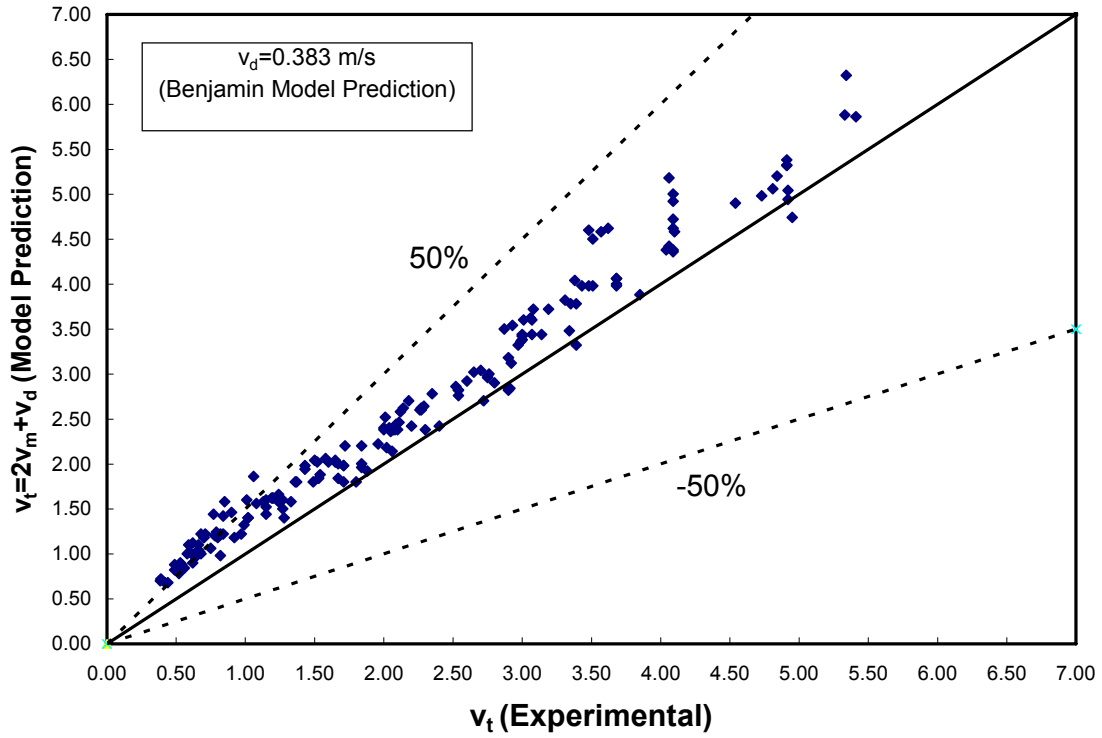


Figure 29 – Comparison of Nicklin Translational Velocity Predictions with Data

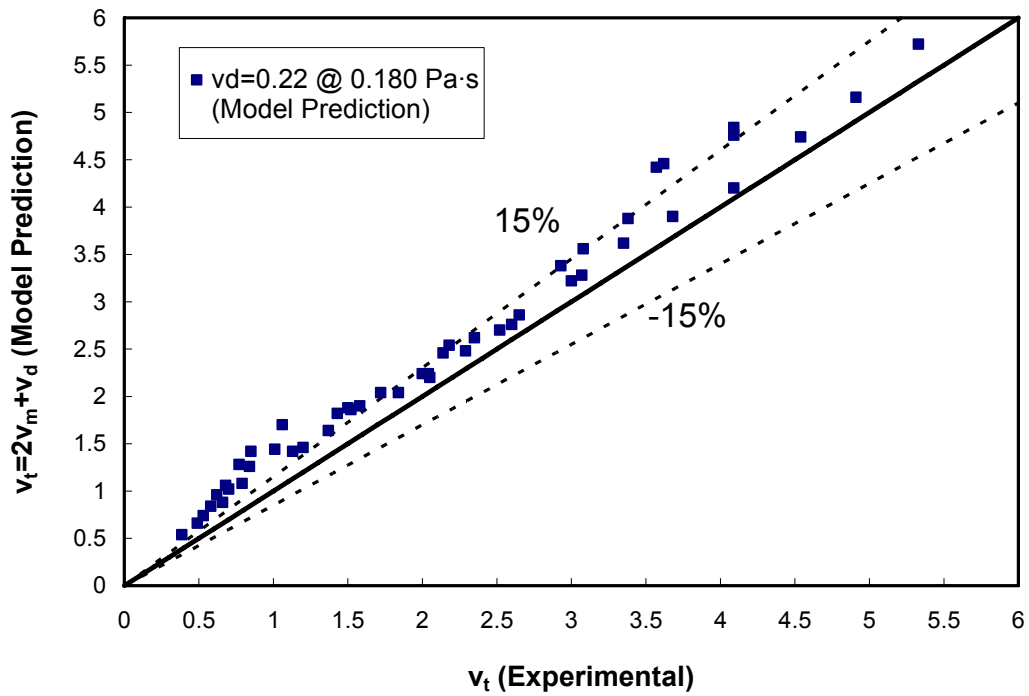


Figure 30 – Comparison of Model Translational Velocity Predictions with Data at $\mu = 0.181$ Pa·s

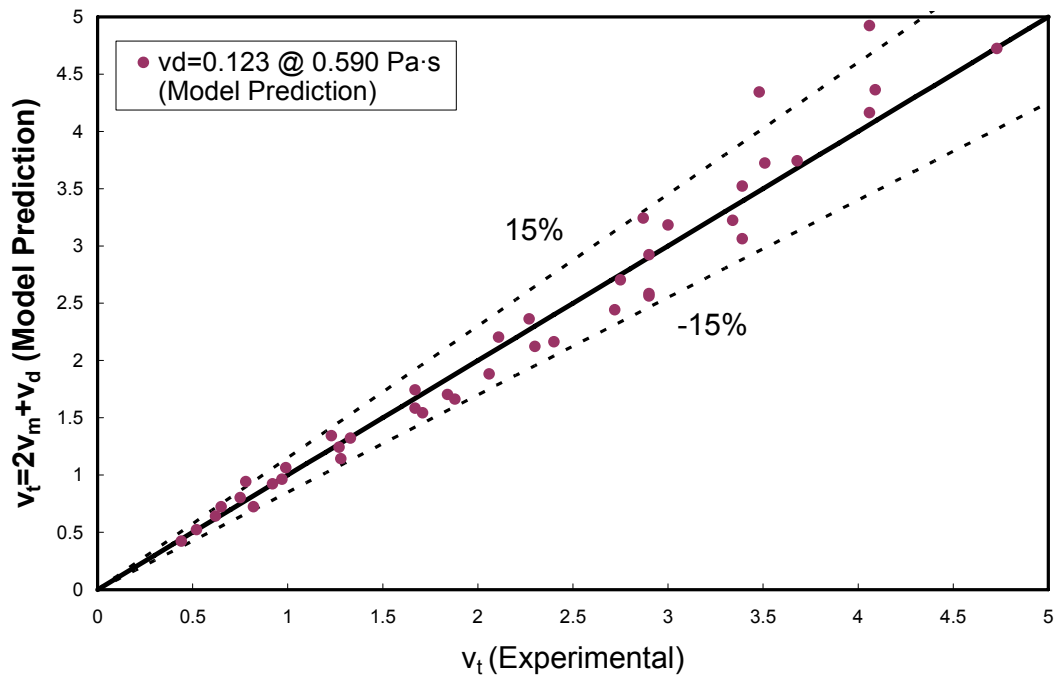


Figure 31 – Comparison of Model Translational Velocity Predictions with Data at $\mu = 0.589 \text{ Pa}\cdot\text{s}$

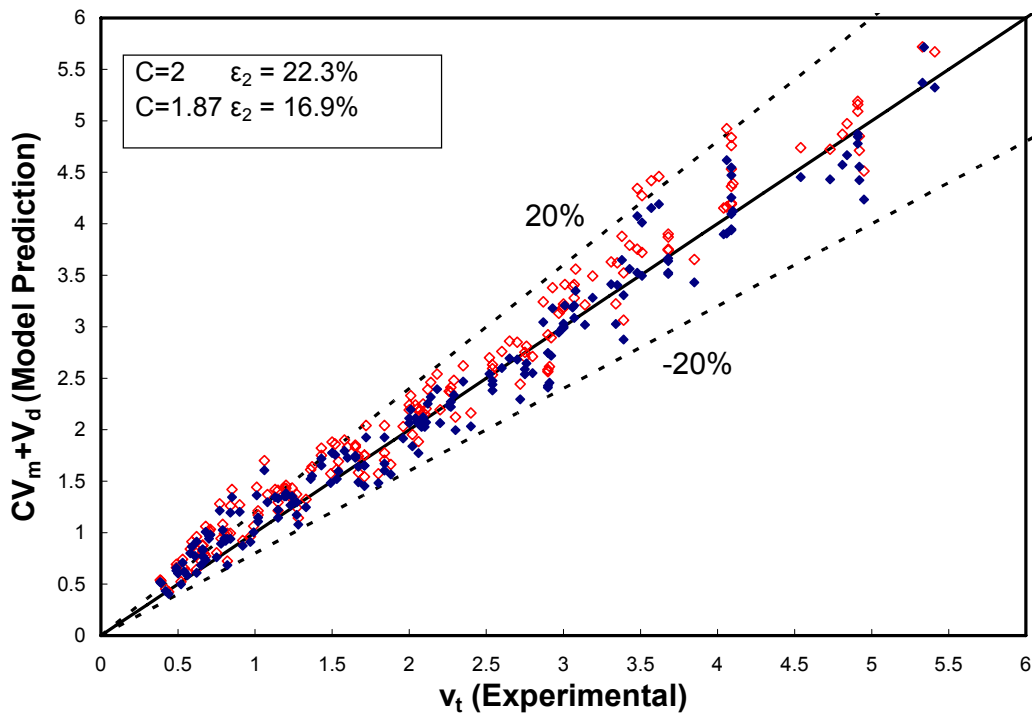


Figure 32 – Comparison of Predicted and Measured Translational Velocities

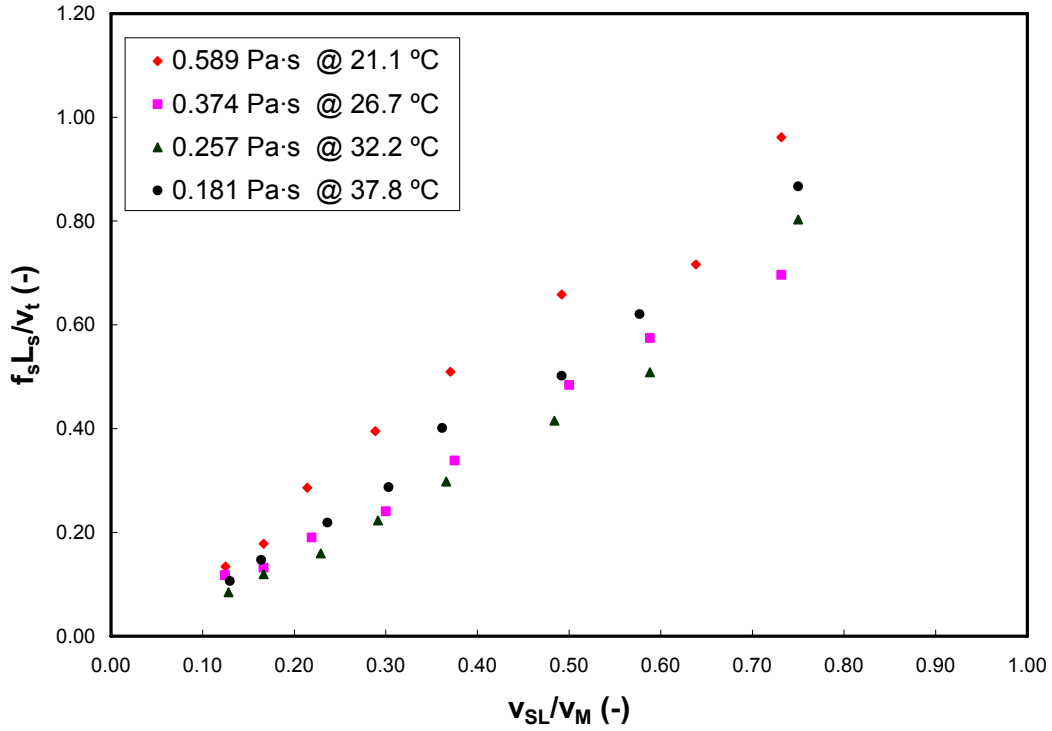


Figure 33 – Intermittency vs. Liquid Ratio at Different Viscosities for $v_{SL} = 0.3$ m/s

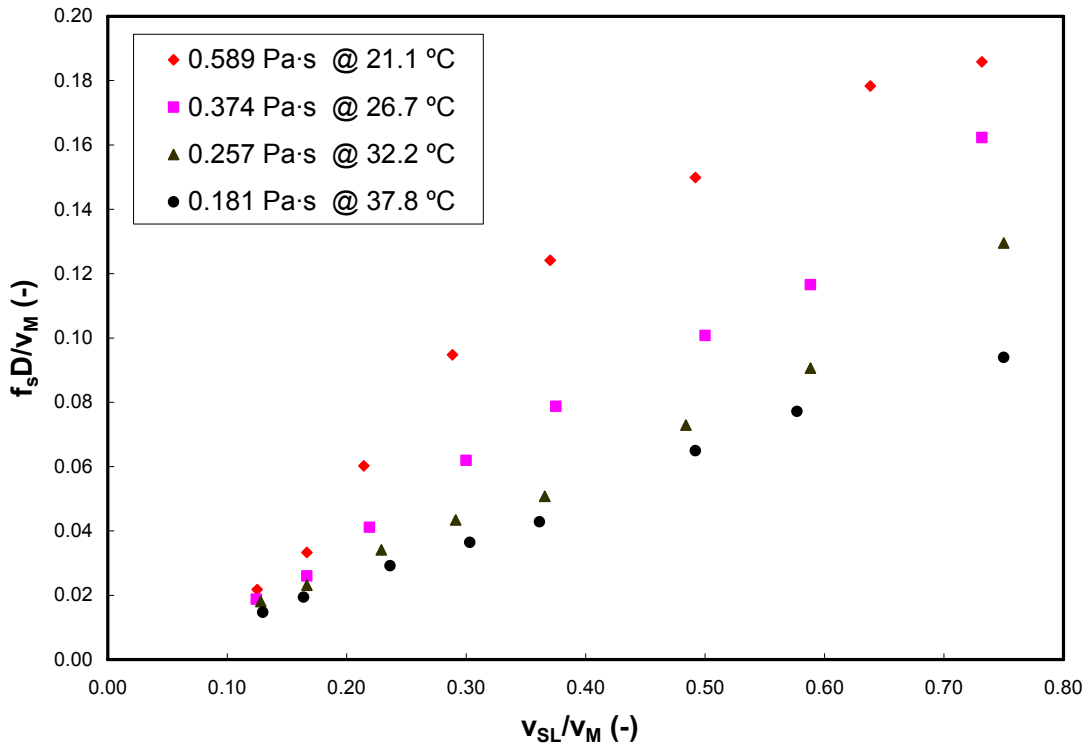


Figure 34 – Dimensionless Slug Frequency vs. Liquid Ratio at Different Viscosities for $v_{SL} = 0.3$ m/s

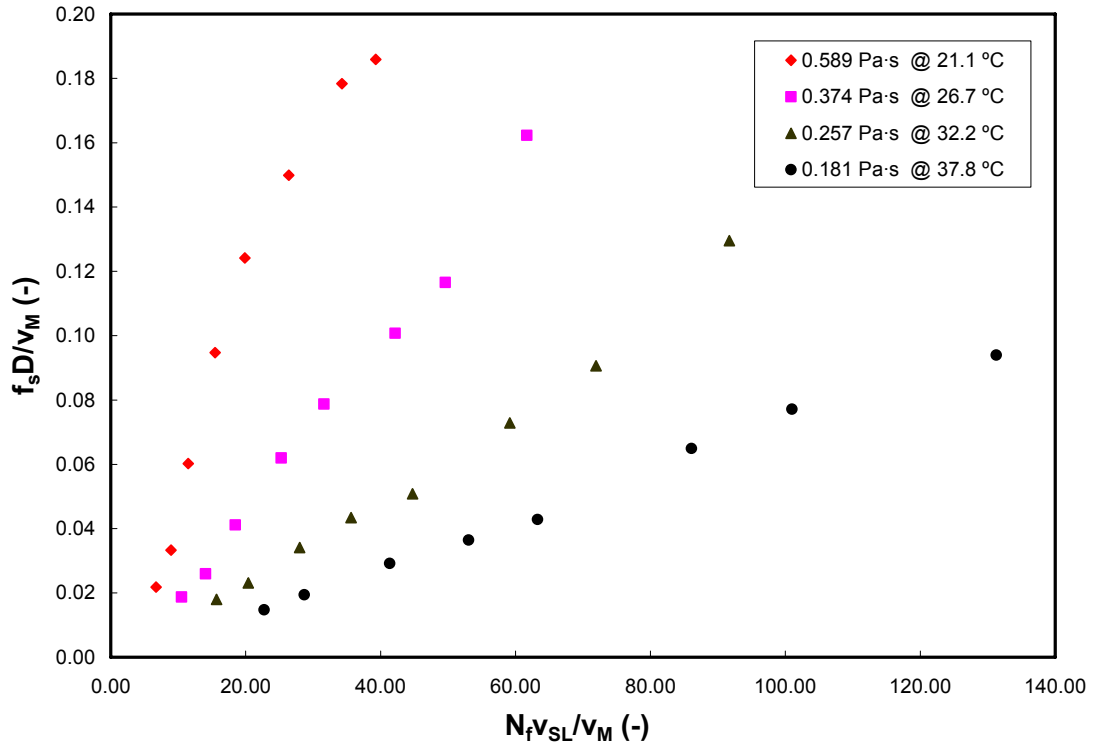


Figure 35– Dimensionless Slug Frequency vs. Liquid Ratio and Inverse Viscosity Number for $v_{SL} = 0.3$ m/s

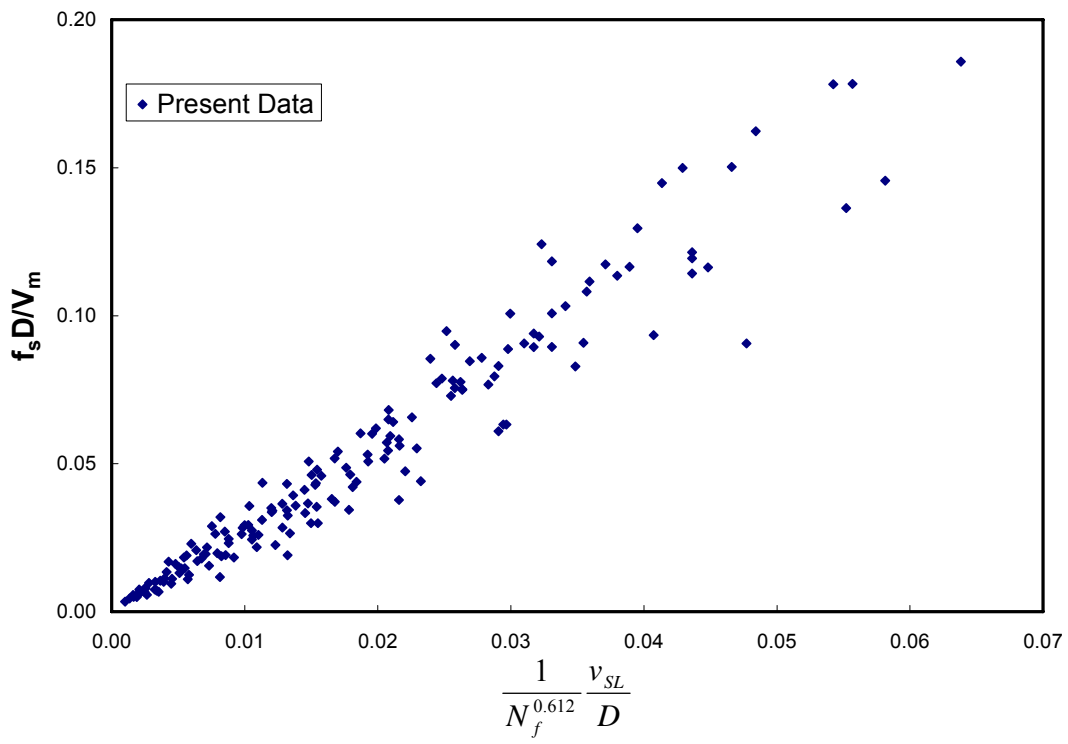


Figure 36– Dimensionless Slug Frequency vs. Liquid Ratio and Inverse Viscosity Number for All Data

Droplet Homo-phase Studies

- ◆ **Significance**
 - **Better Predictive Tools Lead to Better Design and Practices**
- ◆ **General Objective**
 - **Development of Closure Relationships**
- ◆ **Past Study**
 - **Earlier TUFFP Study Showed**
 - ▲ **Entrainment Fraction (FE) is Most Sensitive Closure Parameter in Annular Flow**
 - ▲ **Developed New FE Correlation**
 - ✦ **Utilizing In-situ Flow Parameters**
 - ✦ **Limited Data, Especially for Inclined Flow Conditions**

Droplet Homo-phase Studies ...

- ◆ **Current Study**
 - **Liquid Entrainment in Annular Two-Phase Flow in Inclined Pipes**
 - **Objectives**
 - ▲ **Acquire Data for Various Inclination Angles for 3-in. ID Pipe Using Severe Slugging Facility**
 - ✦ **Existing Data are for 1 and 1 ½ in.**
 - ▲ **Develop a New Closure Relationship**

Droplet Homo-phase Studies ...

◆ Status

- **Literature Search is Completed**
- **Experimental Study is Underway**
 - ▲ **New Entrainment Fraction Measurement Device is Constructed and Installed on the Facility**
 - ▲ **Facility Modifications are Completed**
 - ▲ **New Dimensionless Groups are Proposed to Correlate Entrainment Fraction**



Fluid Flow Projects

Liquid Entrainment in Annular Gas-Liquid Flow in Inclined Pipes

Kyle Magrini

Advisory Board Meeting, September 17, 2008

Outline

- ◆ Objectives
- ◆ Introduction
- ◆ Literature Review
- ◆ Preliminary Correlation Development
- ◆ Experimental Study
- ◆ Summary
- ◆ Future Work
- ◆ Project Schedule



Objectives

- ◆ **Acquire Experimental Data of Entrainment Fraction in Two-Phase Gas-Liquid Annular Flow for Inclination angles of 0°, 10°, 20°, 45°, 75°, and 90°**
- ◆ **Compare Data with Current Correlation and Model Predictions**
- ◆ **Improve Existing Models with New Correlation**

Introduction

- ◆ **Multiphase Flow Mechanistic Models are Tools in Multiphase Design and Applications**
 - **Pressure Gradient**
 - **Liquid Holdup**
 - **Temperature Gradient**
 - **Etc.**

Introduction ...

- ◆ **These Mechanistic Models (e.g. TUFFP Unified Model) Require Closure Relationships**
 - Interfacial Friction Factor
 - Droplet Entrainment Fraction
 - Slug Translational Velocity
 - Etc.

Introduction ...

- ◆ **Chen (2005a) Sensitivity Study Showed that for Annular Flow the TUFFP Unified Model and Xiao Model are Most Sensitive to Droplet Entrainment Fraction Compared to Other Closure Relationships**

Literature Review

- ◆ Vertical Flow Entrainment Fraction Correlations
- ◆ Horizontal Flow Entrainment Fraction Correlations
- ◆ Inclined Flow Entrainment Fraction Correlations

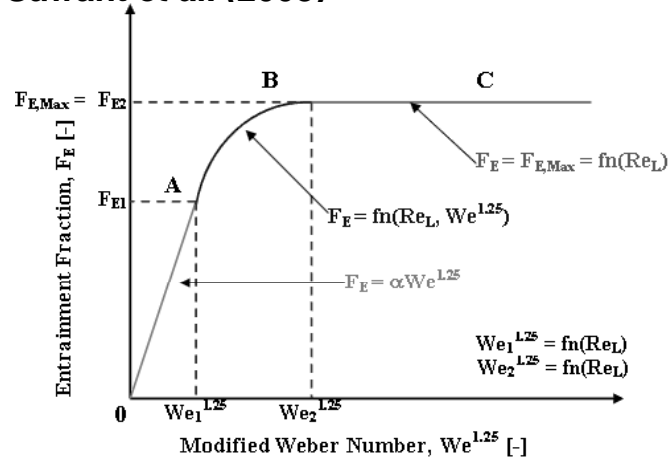
Vertical Flow

- ◆ Sawant *et al.* (2008)
 - Entrainment Measurements at High Pressure ($P_{\text{Max}} = 100$ psi) and High Flow Conditions ($v_{\text{SGmax}} = 100$ m/s & $v_{\text{SLmax}} = 0.75$ m/s)
 - Film Extraction Technique Implemented to Measure Entrainment Fraction
 - Developed Explicit Correlation Based on a modified Weber Number and Liquid Phase Reynolds Number

$$We = \frac{\rho_G v_{\text{SG}}^2 d}{\sigma} \left(\frac{\rho_L - \rho_G}{\rho_G} \right)^{1/3} \quad Re_L = \frac{\rho_L v_{\text{SL}} d}{\mu_L}$$

Vertical Flow ...

♦ Sawant *et al.* (2008)



Vertical Flow ...

♦ Sawant *et al.* (2008)

$$F_E = F_{E,Max} \tanh(2.31 \times 10^{-4} Re_L^{-0.35} We^{1.25})$$

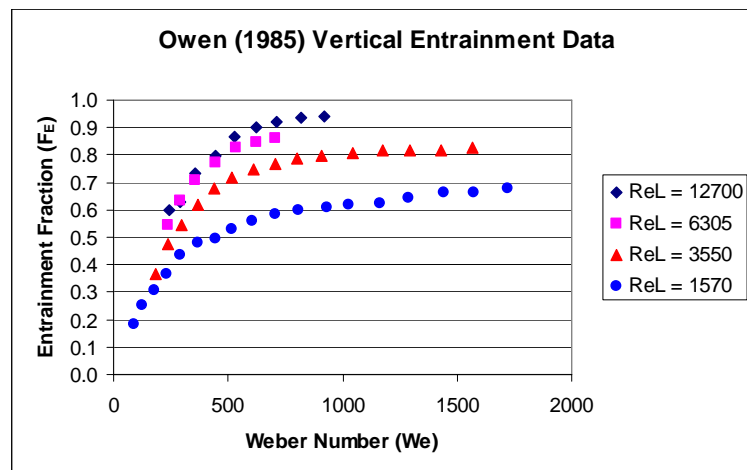
$$F_{E,Max} = 1 - \frac{Re_{F,Lim}}{Re_L}$$

$$Re_{F,Lim} = 250 \ln(Re_L) - 1265$$

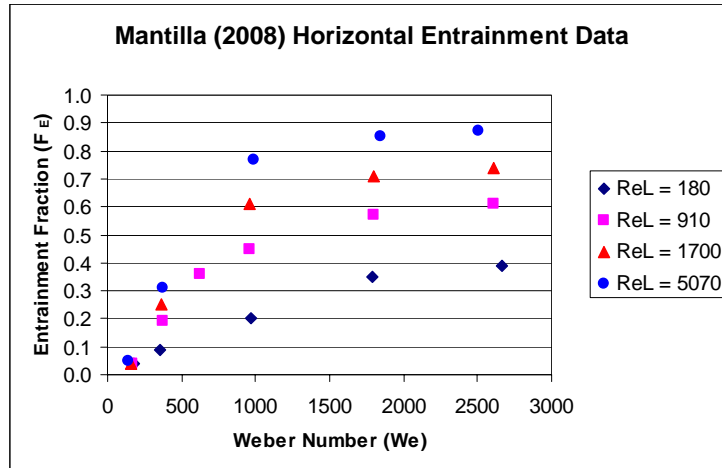
Preliminary Correlation Development

- ◆ Sawant *et al.* Approach
- ◆ Preliminary Correlation
- ◆ Data Used from Other Independent Sources
 - Vertical – Owen (1985)
 - Horizontal – Mantilla (2008)
- ◆ Data Used from Horizontal and Vertical Entrainment Data Banks

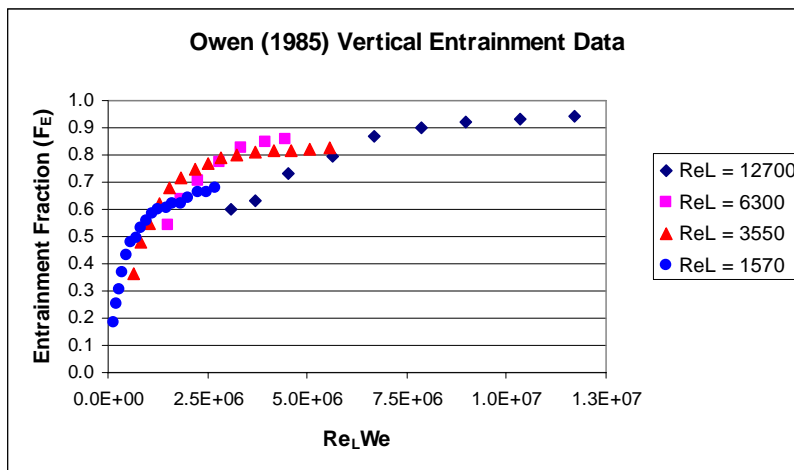
Preliminary Correlation Development ...



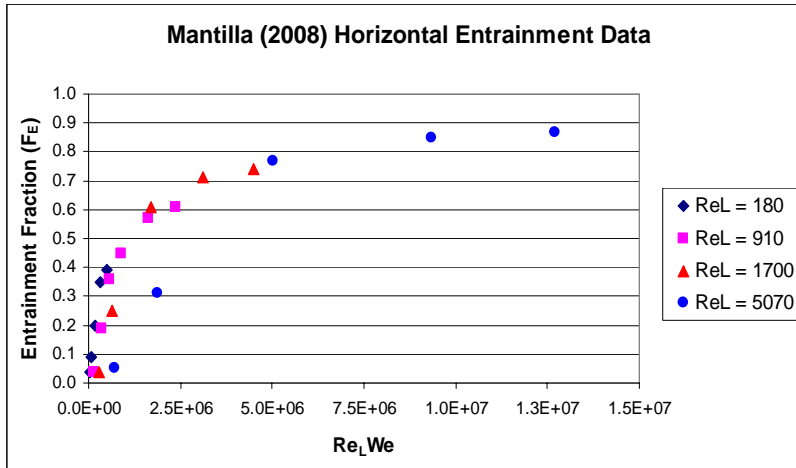
Preliminary Correlation Development ...



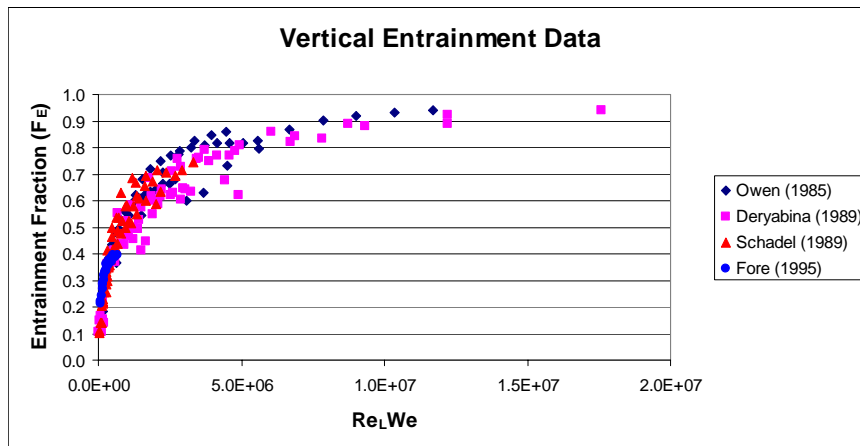
Preliminary Correlation Development ...



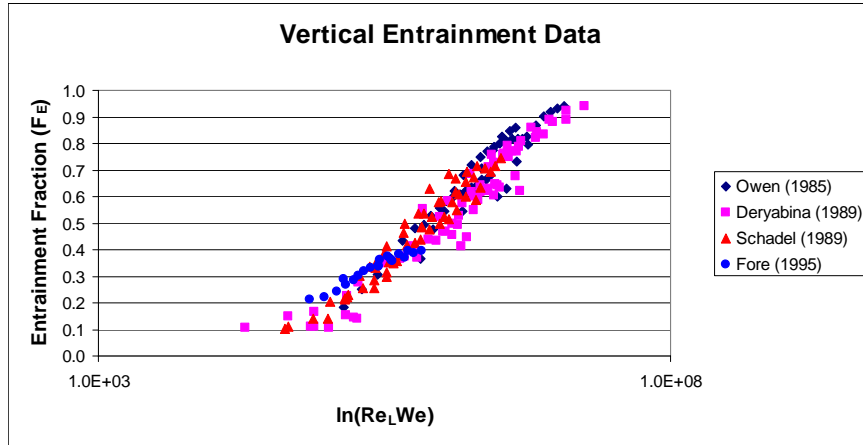
Preliminary Correlation Development ...



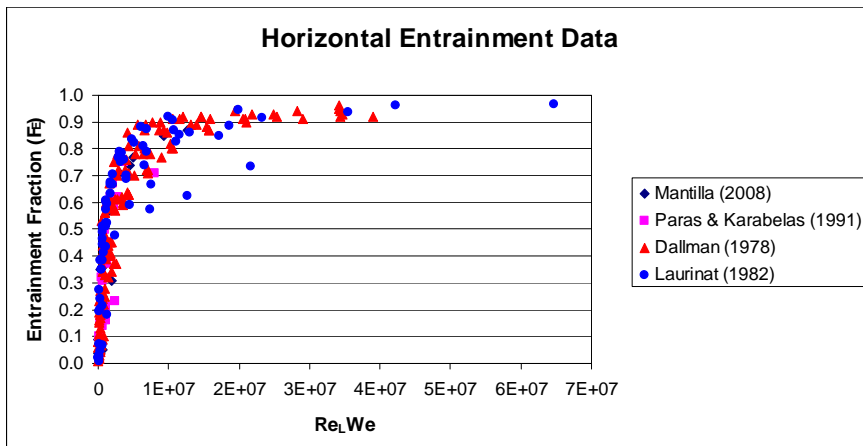
Preliminary Correlation Development ...



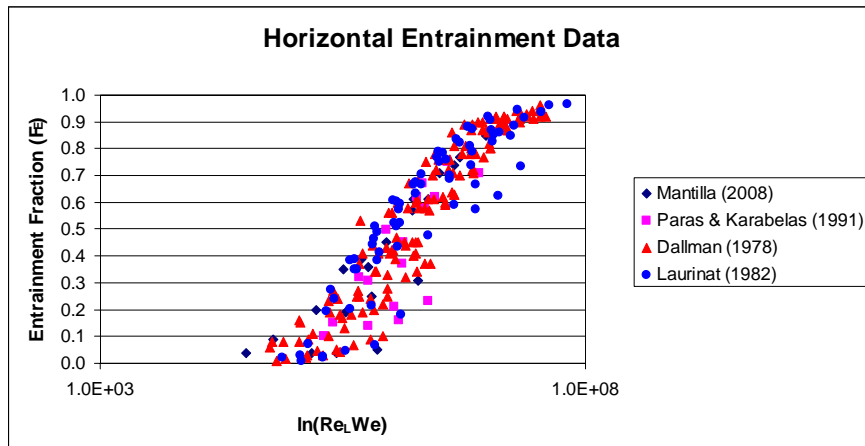
Preliminary Correlation Development ...



Preliminary Correlation Development ...



Preliminary Correlation Development ...



Correlation Development Summary

- ◆ **Explicit Correlation Introduced Based on Weber Number and Liquid Phase Reynolds Number**
- ◆ **Correlation Successfully Collapsed Entrainment Data at Horizontal and Vertical**
- ◆ **Further Work is Needed to Understand and Better Correlate the Data**

Experimental Facility

◆ 3 inch Severe Slugging Flow Loop



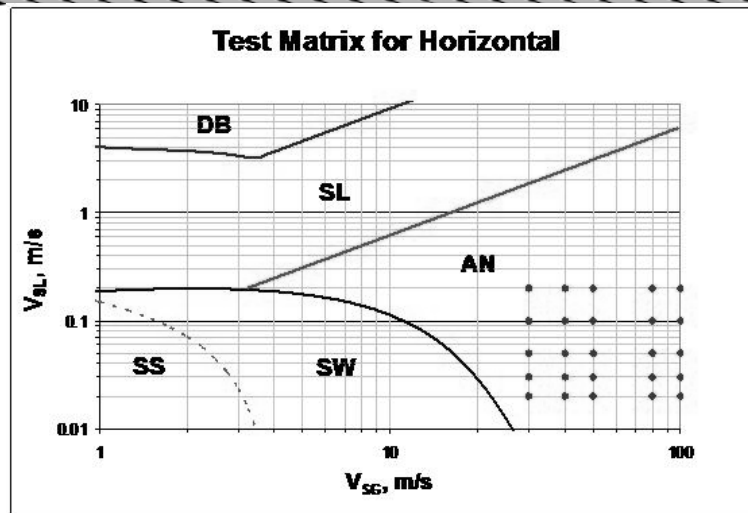
Experimental Facility

- ◆ Test Section 180 Diameters from Inlet to Ensure Fully Developed Flow
- ◆ Installation of Quick Closing Valves to Measure Local Liquid Holdup
- ◆ Conduct Tests at Horizontal and Inclination Angles of 10° , 20° , 45° , 75° , and 90°
- ◆ Measurement of Entrainment Fraction and Deposition Rate

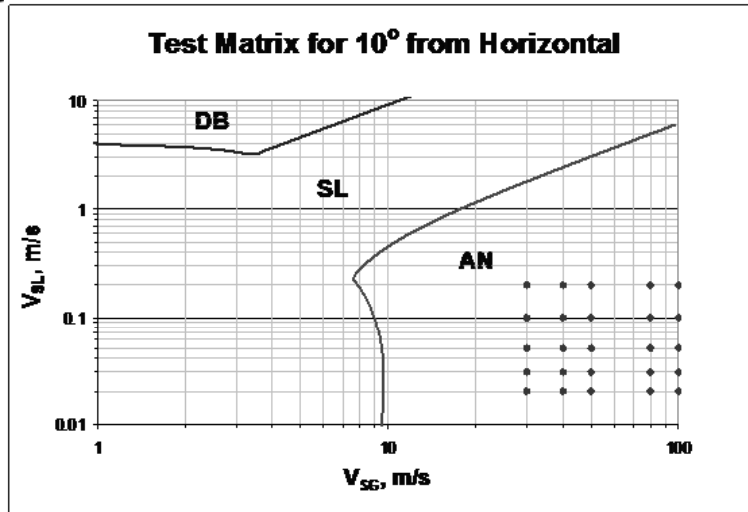
Testing Range

- ◆ Superficial Water Velocities Range from 0.02 to 0.2 m/sec
- ◆ Superficial Gas Velocities Range from 30 to 100 m/sec
- ◆ Maximum Entrainment Fraction will be Measured
- ◆ Surface Tension Measurements will be Conducted to Ensure Valid Results

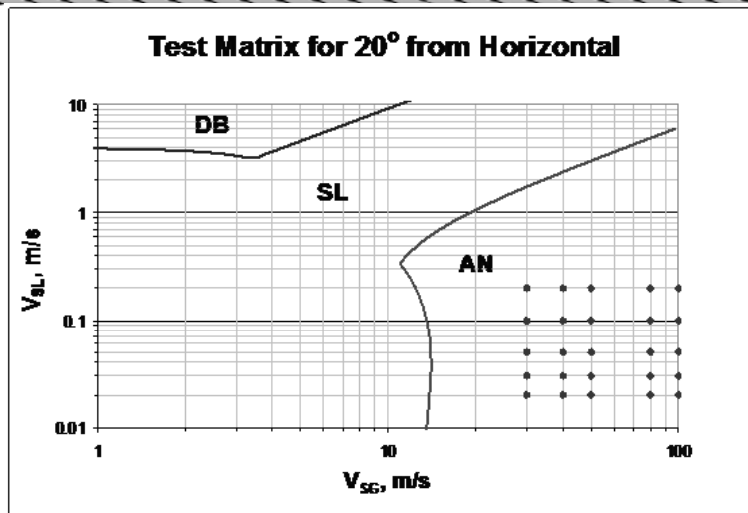
Testing Range ...



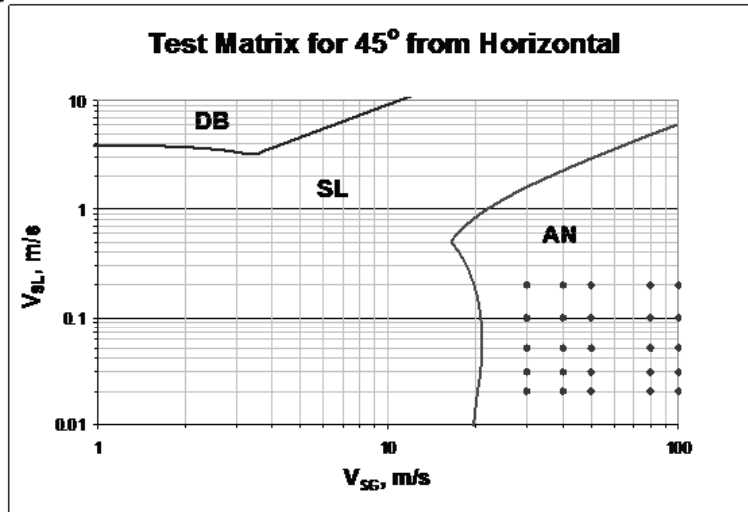
Testing Range ...



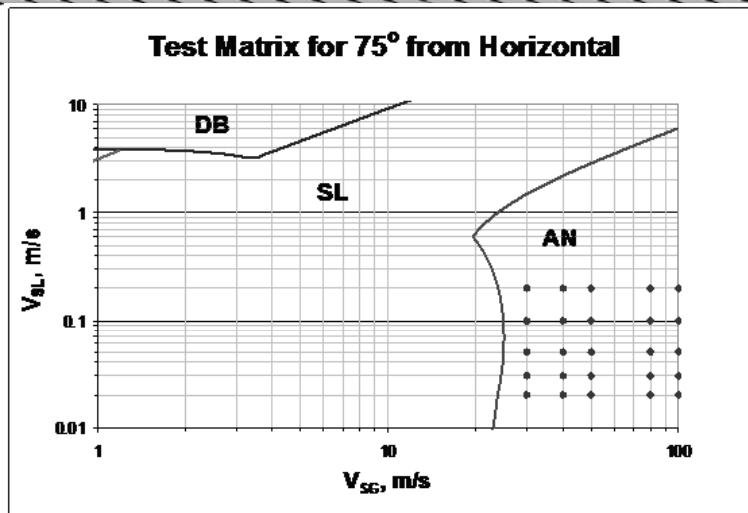
Testing Range ...



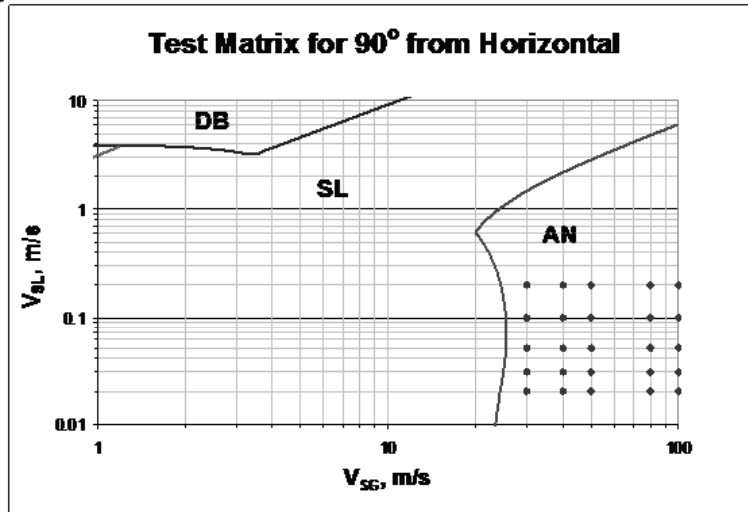
Testing Range ...



Testing Range ...



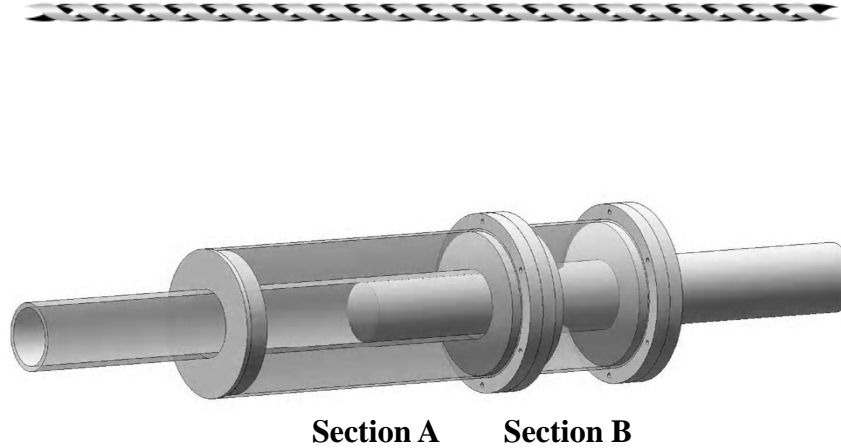
Testing Range ...



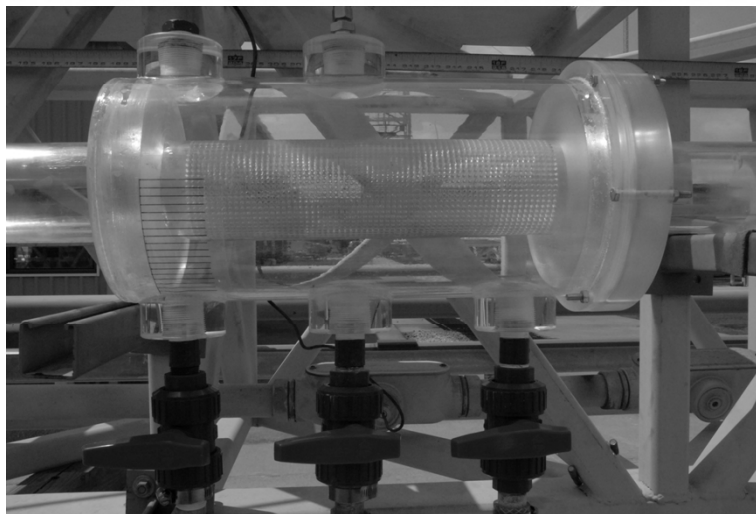
Measurement Techniques

- ◆ Film Removal Device
- ◆ Iso-kinetic Probe

Film Removal Device



Film Removal Device ...



Film Removal Device ...

◆ Film Removal Device Section A

- Measurement of Entrainment Fraction
- Liquid Film is Stripped through Porous Section
- Film Flow Rate will be Obtained
- Entrainment Fraction will be Obtained:

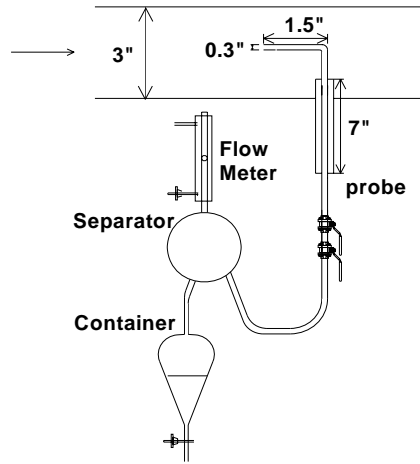
$$F_E = 1 - \frac{q_{Film}}{q_{Liquid}}$$

Film Removal Device ...

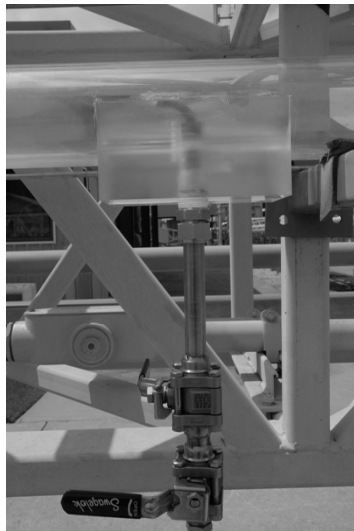
◆ Film Removal Device Section B

- Measurement of Droplet Deposition Rate
- Liquid Film is Stripped through Porous Section Similar to Section A
- Film Volume will be Measured Over Time to Determine Deposition Rate

Iso-kinetic Sampling Probe



Iso-kinetic Sampling Probe ...



Iso-kinetic Sampling Probe ...

- ◆ **Iso-kinetic Sampling Probe**
 - **Entrained Droplets are Sampled Over a Given Length of Time at Various Radial Distances**
 - **Entrainment Flux Profile is Created**
 - **Entrainment Fraction is Calculated by Integrating Flux Profile**
 - **Most Accurate Under Low Liquid Flow Rates**

Summary

- ◆ **Explicit, Non-Dimensional Correlation Introduced that Successfully Collapsed Entrainment Data**
- ◆ **Facility Modifications and Instrumentation have been Completed**
- ◆ **Entrainment Tests have Begun with Film Removal Device and Iso-kinetic Probe**

Future Work

- ◆ **Acquire Entrainment Data for Various Flow Rates and Inclination Angles**
- ◆ **Compare Results of Film Removal Device with Those Obtained from Iso-kinetic Probe**
- ◆ **Validate Existing Models with Experimental Data**
- ◆ **Improve Existing Models with New Correlation**

Project Schedule

- | | |
|--------------------------------|---------------------|
| ◆ Literature Review | Ongoing |
| ◆ Facility Construction | Completed |
| ◆ Data Acquisition | October 2008 |
| ◆ Model Comparison | March 2009 |
| ◆ Final Report | May 2009 |

Questions/Comments



Liquid Entrainment in Annular Gas-Liquid Flow in Inclined Pipes

Kyle Magrini

PROJECTED COMPLETION DATES:

Literature Review	Completed
Facility Modifications	Completed
Preliminary Correlation Development	Completed
Testing.....	October 2008
Model and Correlation Validation.....	March 2009
Final Report.....	May 2009

Objectives

The objectives of this study are:

- to acquire liquid entrainment data in two-phase gas-water annular flow through pipes from horizontal to near vertical,
- to validate current correlations and models with experimental results, and
- to improve current models, if necessary, or develop a new model.

Introduction

Annular flow usually occurs at high gas velocities and low to medium liquid velocities. The liquid flows as a film along the wall of the pipe and as droplets entrained in the gas core. The interface between the gas core and liquid film is usually very wavy, causing atomization and deposition of liquid droplets. Under equilibrium conditions, the rate at which the droplets atomize and deposit becomes equal, resulting in a steady fraction of the liquid being entrained as droplets, F_E . This critical parameter is crucial to understand and model the behavior of annular flow.

Most multiphase flow prediction models (including the TUFFP unified mechanistic models) are based on a simplified (one-dimensional) two-fluid model in which empirical closure relationships (i.e. interfacial friction factor, interfacial area, droplet entrainment fraction, etc.) are needed. The performance of the multiphase flow model is determined by the accuracy and physical completeness of these closure relationships. The literature reveals that sufficient

physics of multiphase flow may not be contained in these empirical closure relationships. Therefore, further refinements of these closure relationships can significantly improve the performance of multiphase mechanistic models.

Chen (2005a) conducted a sensitivity study to investigate the influence of individual closure relationships on the predictions of a multiphase mechanistic model. The study showed that in annular flow the variation in droplet entrainment fraction can substantially affect the predicted pressure gradient and liquid hold-up. Thus, the use of an accurate predictive model for entrainment fraction is imperative.

Literature Review

The liquid droplet entrainment phenomenon is very complicated. Various factors, such as pipe size, pipe orientation, velocity, and fluid properties, control the process. There are several studies devoted to understanding the different aspects of liquid entrainment. Many of these studies were presented at the October 2008 ABM meeting, along with the various correlations found in literature for different pipe orientations. The literature review will be an ongoing task.

A recent study by Sawant *et al.* (2008) concerning entrainment in vertical upward annular flow offered a simple, explicit correlation based on the Weber number and liquid phase Reynolds number. This correlation was verified with experimental data under high flow and high pressure conditions. The methodology for the modeling of entrainment fraction proposed by Sawant *et al.* is shown in Fig. 1.

In the figure, a curve is a representation of entrainment fraction variation with Weber number at a constant liquid phase Reynolds number. The entrainment curve is divided into three regions: a Weber number dependent region O-A, a transition region A-B and a liquid phase Reynolds number dependant region B-C.

Sawant *et al.* provided an explanation of the phenomenon based on the limited experimental data available in literature. In the region O-A, a relatively thick liquid film is present. As the superficial gas velocity increases, entrainment fraction also increases. Concurrently, liquid film flow rate decreases as more liquid is entrained into the gas core. Although the liquid film flow rate is decreasing, there is no affect on the disturbance wave characteristics. Therefore, entrainment fraction is unaffected, as long as a thick liquid film is present. As a result the entrainment fraction in this region is independent of the liquid phase Reynolds number.

As the superficial gas velocity is increased, a higher entrainment fraction results. At point A in Fig. 1, the first transition point, the liquid film flow rate decreases sufficiently and the interfacial momentum transfer is affected. Thus, in this part of the curve (A-B), the entrainment fraction depends on both the liquid phase Reynolds number and the Weber number. The liquid film flow rate decreases further with the increase in the superficial gas velocity. At point B, the second transition point, there is no more interaction between the gas core and the liquid film. The liquid film in this region (B-C) gets submerged in to the viscous sub-layer of the core gas flow, leading to the suppression of entrainment. In this region the further increase in the superficial gas velocity has no effect on the entrainment fraction which stays constant. Sawant *et al.* observed that the liquid film flow rate at both the transition points and at the limiting entrainment fraction region increases with the increase in the liquid phase Reynolds number.

Sawant *et al.* proposed the following correlation for the prediction of the entrainment fraction:

$$F_E = F_{E,Max} \tanh(\alpha We^{1.25}) \quad (1)$$

where $F_{E,Max}$ is the maximum entrainment fraction defined as a function of liquid phase Reynolds number and limiting liquid film Reynolds number,

$$F_{E,Max} = 1 - \frac{Re_{F,Lim}}{Re_L}, \quad (2)$$

where

$$Re_{F,Lim} = 250 \ln(Re_L) - 1265. \quad (3)$$

Coefficient α accounts for the dependence of the transition points A and B on liquid phase Reynolds number. Based on the current experimental data, the following correlation was obtained

$$\alpha = 2.31 \times 10^{-4} Re_L^{-0.35}. \quad (4)$$

Preliminary Correlation Development

Data from both vertical and horizontal experiments were plotted for the entrainment fraction against the Weber number for various liquid phase Reynolds number values, as suggested by Sawant *et al.* Figure 2 displays data collected by Owens (1985) for vertical annular flow. Figure 3 displays data collected by Mantilla (2008) for horizontal annular flow. These figures demonstrate the three regions described by Sawant *et al.* Building on the methodology presented by Sawant *et al.*, the entrainment fraction was plotted against the Weber number multiplied by the liquid phase Reynolds number. Figures 4 and 5 display the results for the data of Owen and Mantilla. Additional entrainment data for both horizontal and vertical orientations was also analyzed using the non-dimensional analysis presented. Figures 6 and 7 display the normal and semi-log plots for vertical entrainment data from several researchers. Figures 8 and 9 display the normal and semi-log plots for horizontal entrainment data from data sources. The normal plots display the curve mentioned by Sawant *et al.* The semi-log plots display the promising trend of the non-dimensional analysis. Although more work is needed to understand and better correlate the data, the data successfully collapses using the previously mentioned method.

Experimental Study

TUFFP's 76.2-mm (3-in.) diameter severe slugging facility (shown in Fig. 10) has been modified for this experimental study. The facility is capable of being inclined from horizontal to vertical. Pressure and temperature transducers will be placed near the test section to obtain fluid properties and flowing characteristics that are used in the entrainment fraction correlations. Quick-closing valves have been installed on the facility to measure the local liquid holdup of the flow.

The test section used to obtain entrainment fraction was placed 180d (15.24 m) from the entrance to ensure fully developed flow. Experiments for entrainment fraction will be conducted at inclination angles 0°, 10°, 20°, 45°, 75°, and 90° from horizontal. Iso-kinetic sampling and liquid film removal will be used to calculate the entrainment fraction.

Test Fluids

Compressed air and Tulsa city tap water will be used in this study. The surface tension of the tap water will be measured frequently to ensure accurate results.

Testing Range

In this study, a large number of data points will be collected at various conditions in terms of both fluid velocities and inclination angles. Superficial water velocities range from 0.02 to 0.2 m/sec. Superficial gas velocities range from 30 to 100 m/sec. The high gas superficial velocities will be essential to determine the maximum entrainment value which will be beneficial in the entrainment fraction correlation. Figure 11 displays the test matrix for the experiments to be conducted at horizontal. Figures 12 through 16 display the test matrices for experiments to be conducted at 10°, 20°, 45°, 75°, and 90° from horizontal.

Film Removal Device

The procedure for measuring entrainment fraction in the test section involves removing the liquid film from the wall of the pipe while allowing droplets entrained in the gas phase to continue to flow. The entrained liquid flow rate will be calculated by subtracting the liquid film flow rate from the total liquid flow rate. The specially designed test section is shown in Figs. 17 and 18. Section A is similar to the one used by Hay et al. (1996), Azzopardi et al. (1996), Simmons and Hanratty (2001), and Al-Sarkhi and Hanratty (2002). The flow passes through a porous section and the liquid film, traveling at a lower velocity than the gas core, is pushed through the porous section. The high inertia of the droplets in the gas core flowing close to the gas velocity prevents them from being removed through the porous section. To ensure no droplets will escape, a

long sleeve will be inserted close to where the liquid film dissipates. This sleeve will be moved in and out in the pipe to make sure the liquid film passes under the sleeve and only the gas core passes through the test section.

To ensure the accurate measurement of the entrainment fraction, the test section will be held at constant pressure. The liquid film will accumulate under the test section. Once a certain water level is reached, the liquid will be drained, ensuring little or no gas escapes. The volume of water and time will be measured to determine the film flow rate and entrainment fraction.

The deposition rate will also be measured after the liquid film is stripped in Section A of the test section. In Section B of Figs. 17 and 18, the film will once again be stripped from the flow through a porous section. The deposition rate of the droplets will be calculated based on the accumulation, liquid amount, and stripping area.

Iso-kinetic Sampling Probe

An iso-kinetic sampling probe (shown in Fig. 19) has also been installed in the facility to measure entrainment fraction. The iso-kinetic sampling probe will be inserted into the pipe at various radial distances. The liquid sampled from the gas core will be separated in a small gas-liquid separator and collected in a graduated cylinder. From these measurements, the droplet entrainment flux profile will be determined. The entrainment fraction can be calculated by integrating this flux profile. The iso-kinetic sampling probe works best under low liquid flow rates where a more distinct division between the gas core and liquid film exists. The results of the iso-kinetic sampling probe will be used in validating the results obtained from the film removal device.

Future Tasks

The main tasks for the future are:

- Conduct experiments,
- Compare entrainment measurement methods,
- Validate correlations,
- Modify or develop new correlations

Nomenclature

d	= pipe diameter [m]
F_E	= entrainment fraction
Re	= Reynolds number
v	= velocity [m/s]
We	= Weber number

Subscripts

E	= entrainment
F	= liquid film
G	= gas phase
L	= liquid phase
Lim	= limiting
Max	= maximum
SG	= superficial gas
SL	= superficial liquid

References

1. Al-Sarkhi, A. "Droplet-Homophase Interaction: Effect of Pipe Inclination on Entrainment Fraction," TUFFP ABM (November 6, 2007), pp. 271-288.
2. Al-Sarkhi, A., and Hanratty, T.J., 2002. "Effect of Pipe Diameter on the Drop Size in a Horizontal Annular Gas-Liquid Flow," *Int. J. Multiphase Flow*, 28(10), pp. 1617-1629.
3. Azzopardi, B.J., Zaidi, S.H., and Jepson, D.M., 1997. "Entrained fraction in inclined annular gas-liquid flow," ASME International Mechanical Engineering Congress and Exposition, Dallas, TX. 16–21 November 1997.
4. Chen, X. "Droplet-Homophase Interaction Study," TUFFP ABM (March 2005a), pp. 135-186.
5. Chen, X. "Droplet-Homophase Interaction - Development of an Entrainment Fraction Model," TUFFP ABM (October 2005b), pp. 149-178.
6. Dallman, J.C., 1978. "Investigation of Separated Flow Model in Annular Gas-Liquid Two-Phase Flow," PhD Dissertation, University of Illinois at Urbana, Champaign.
7. Mantilla, I., 2008. "Mechanistic Modeling of Liquid Entrainment in Gas in Horizontal Pipes," PhD Dissertation, University of Tulsa.
8. Paras, S.V., and Karabelas, A.J., 1991. "Droplet Entrainment and Deposition in Horizontal Annular Flow," *Int. J. Multiphase Flow*, 17(4), pp. 455-468.
9. Schadel, S.A., 1988. "Atomization and Deposition Rates in Vertical Annular Flow," PhD Dissertation, University of Illinois at Urbana, Champaign.
10. Sawant, P., Ishii, M., and Mori, M., 2008. "Droplet Entrainment Correlation in Vertical Upward Co-Current Annular Two-Phase Flow," *Nuclear Engineering and Design*, 238, pp. 1342-1352.

11. Zhang, H.Q., Wang, Q., Sarica, C., and Brill, J., 2003. "Unified Model of Gas-Liquid Pipe Flow via Slug Dynamics. Part I. Model Development," ASME J. of Energy Res. Tech., 125(4), pp. 266-273.

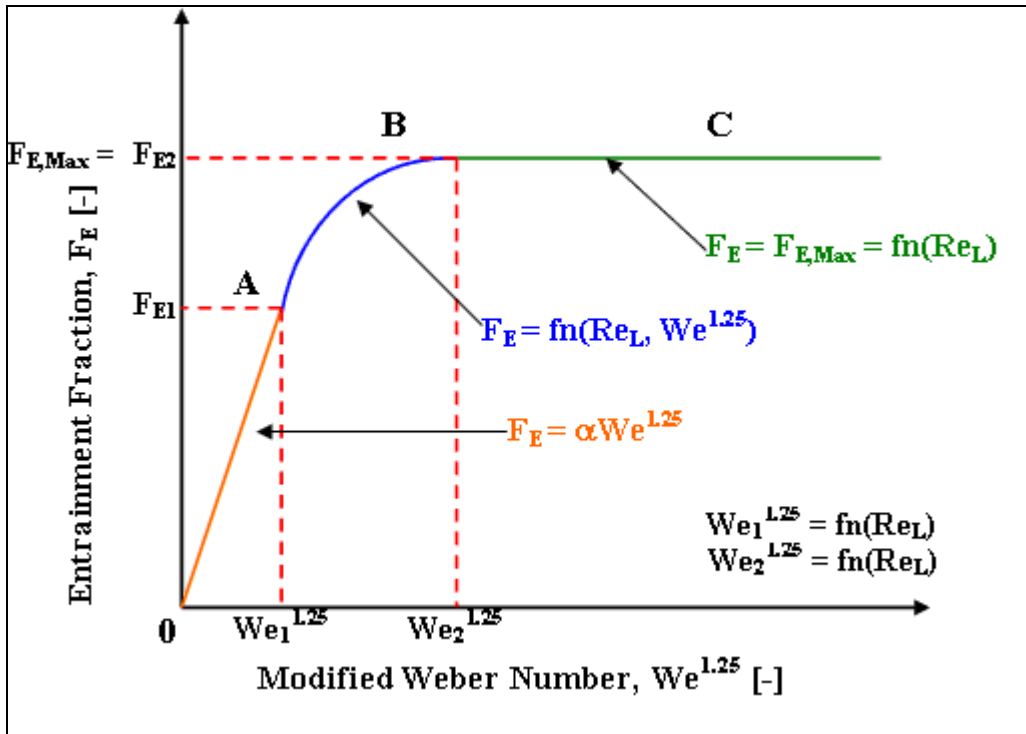


Figure 1. Sawant *et al.* (2008) Correlation Methodology.

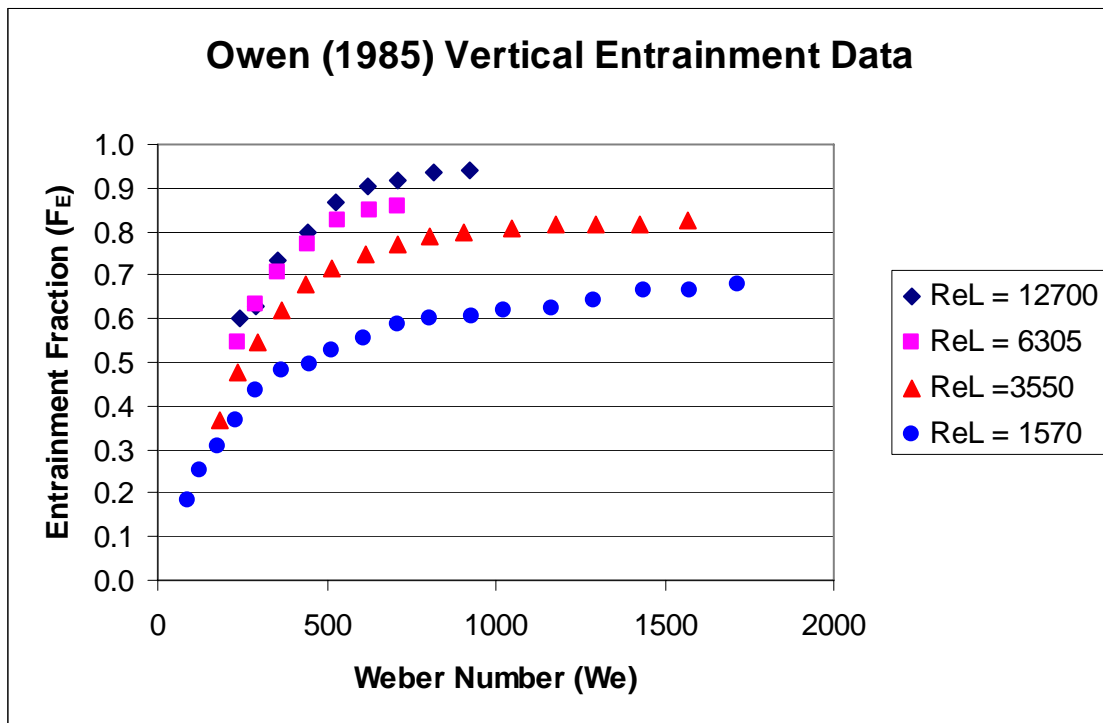


Figure 2. Entrainment Fraction vs. Weber Number for Owen (1985) Vertical Annular Flow Data.

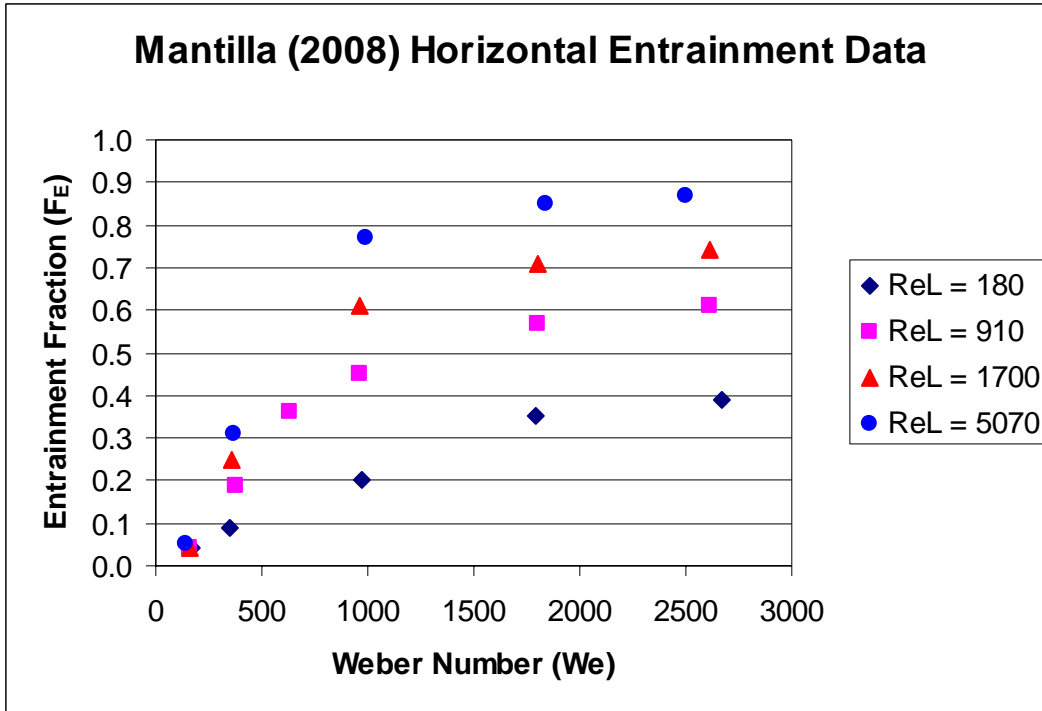


Figure 3. Entrainment Fraction vs. Weber Number for Mantilla (2008) Horizontal Annular Flow Data.

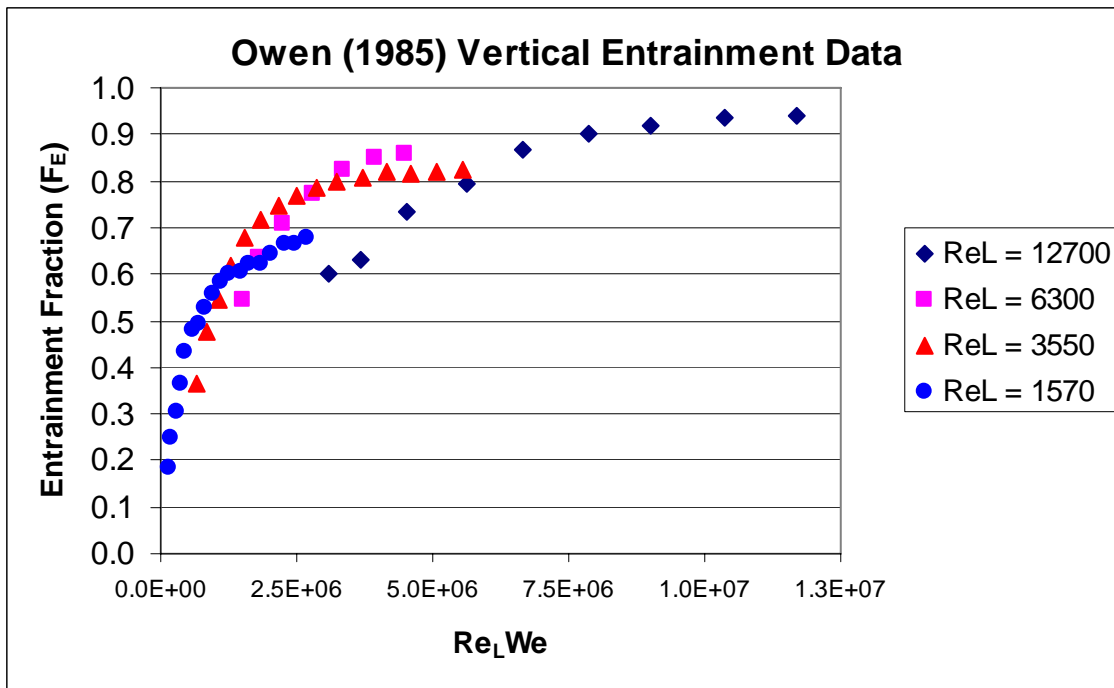


Figure 4. Entrainment Fraction vs. Weber - Reynolds Numbers for Owen (1985) Vertical Annular Flow Data.

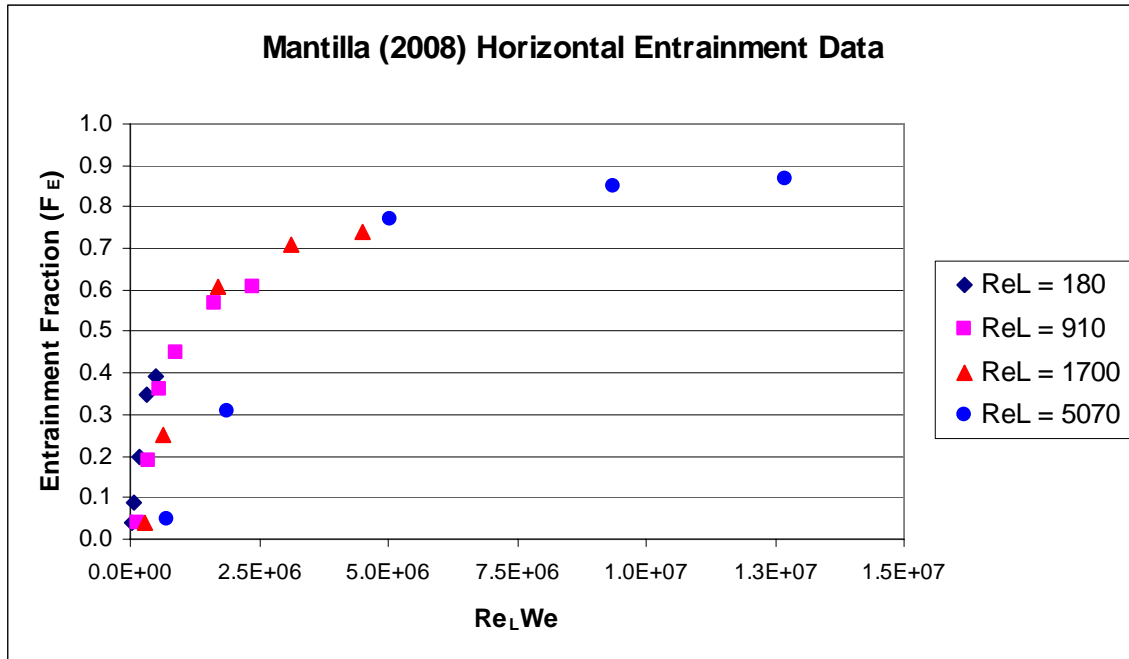


Figure 5. Entrainment Fraction vs. Weber - Reynolds Numbers for Mantilla (2008) Horizontal Annular Flow Data.

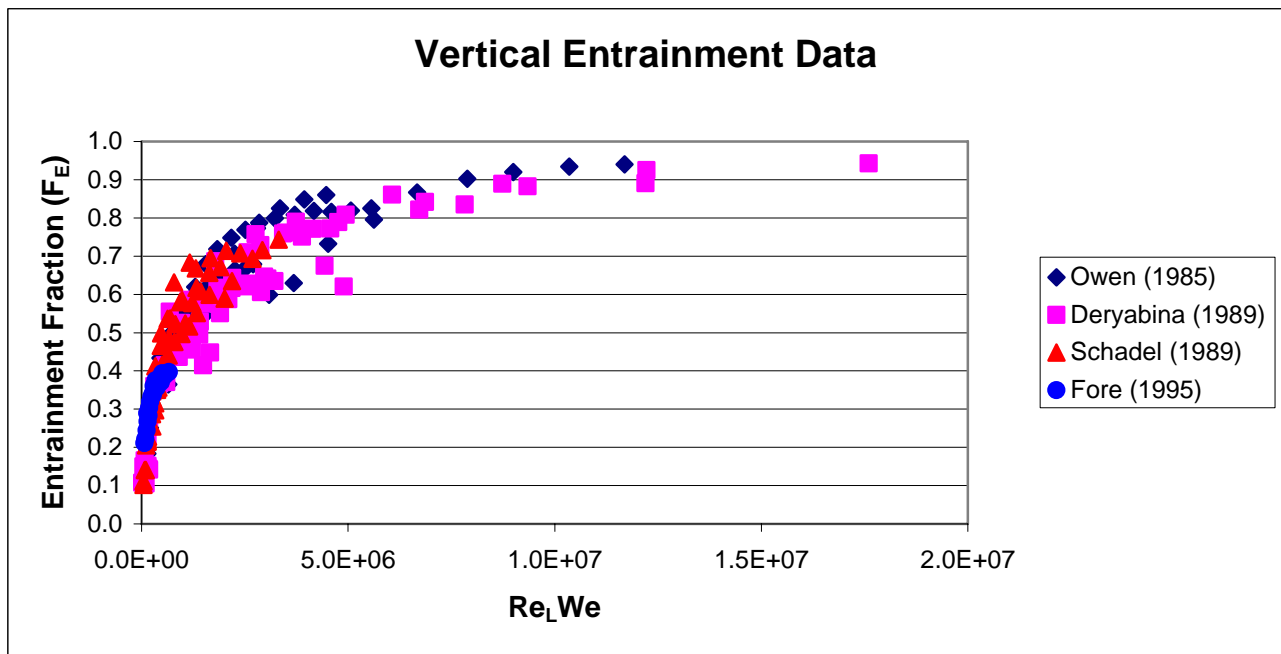


Figure 6. Entrainment Fraction vs. Weber - Reynolds Numbers for Vertical Entrainment Flow Data.

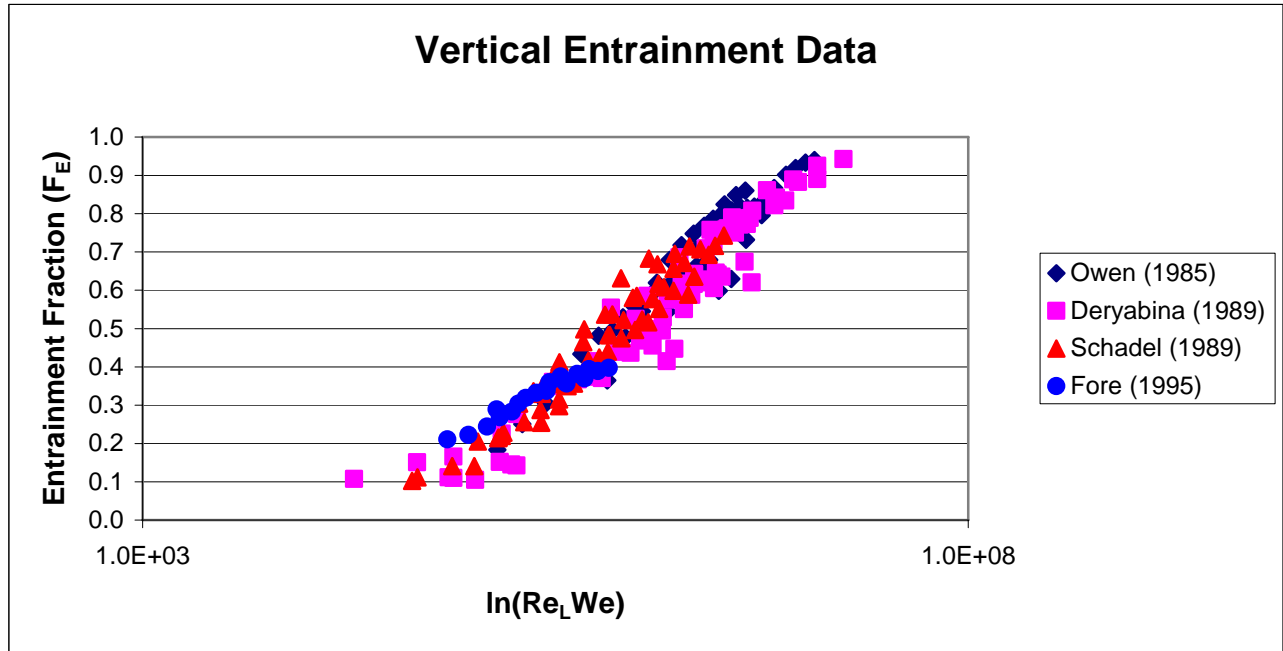


Figure 7. Semi-log Plot of Entrainment Fraction vs. Weber - Reynolds Numbers for Vertical Entrainment Flow Data.

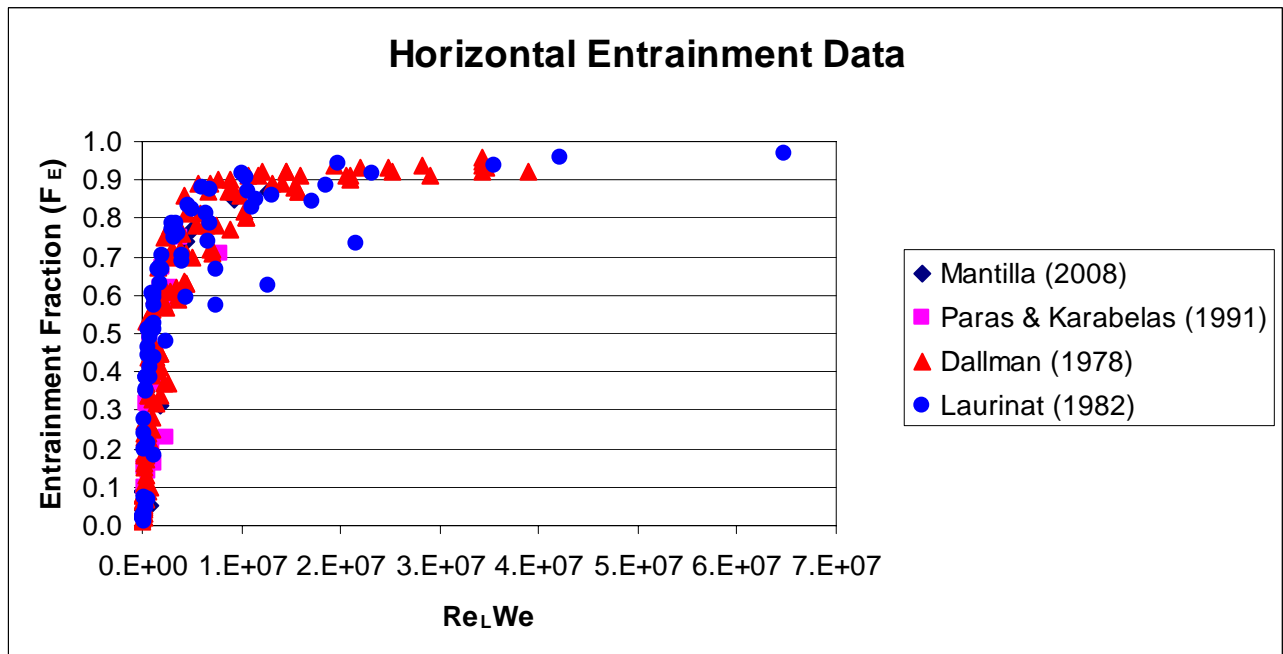


Figure 8. Entrainment Fraction vs. Weber - Reynolds Numbers for Horizontal Entrainment Flow Data.

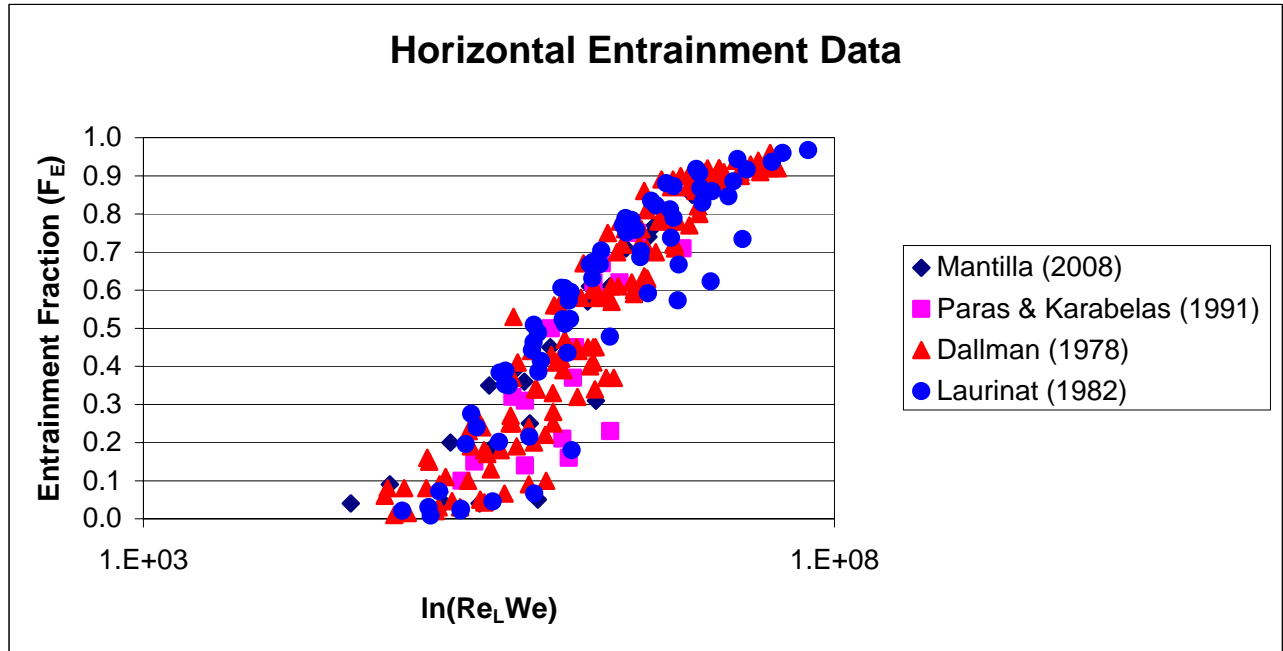


Figure 9. Semi-log Plot of Entrainment Fraction vs. Weber - Reynolds Numbers for Horizontal Entrainment Flow Data.

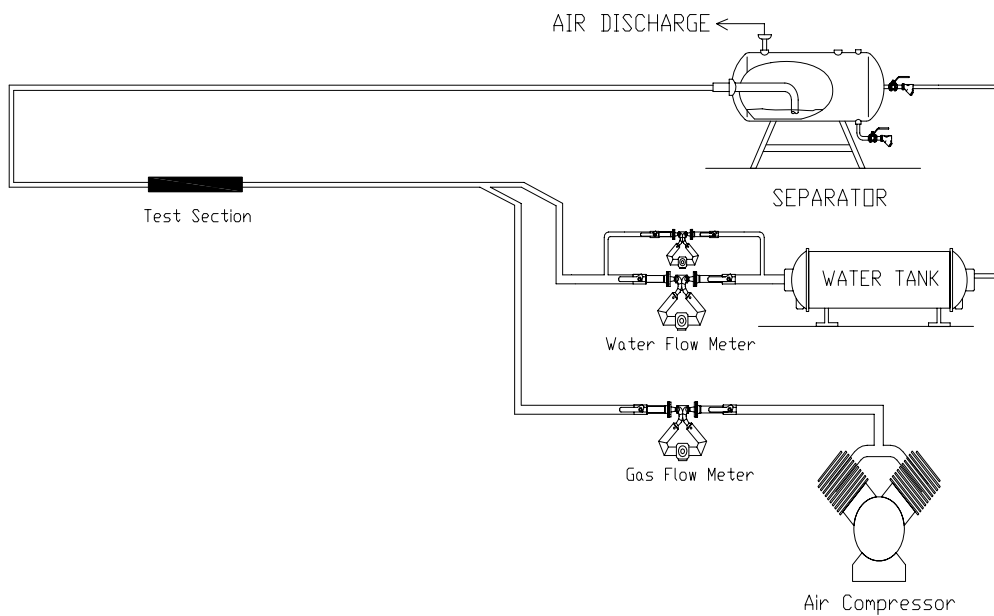


Figure 10. Facility Schematic

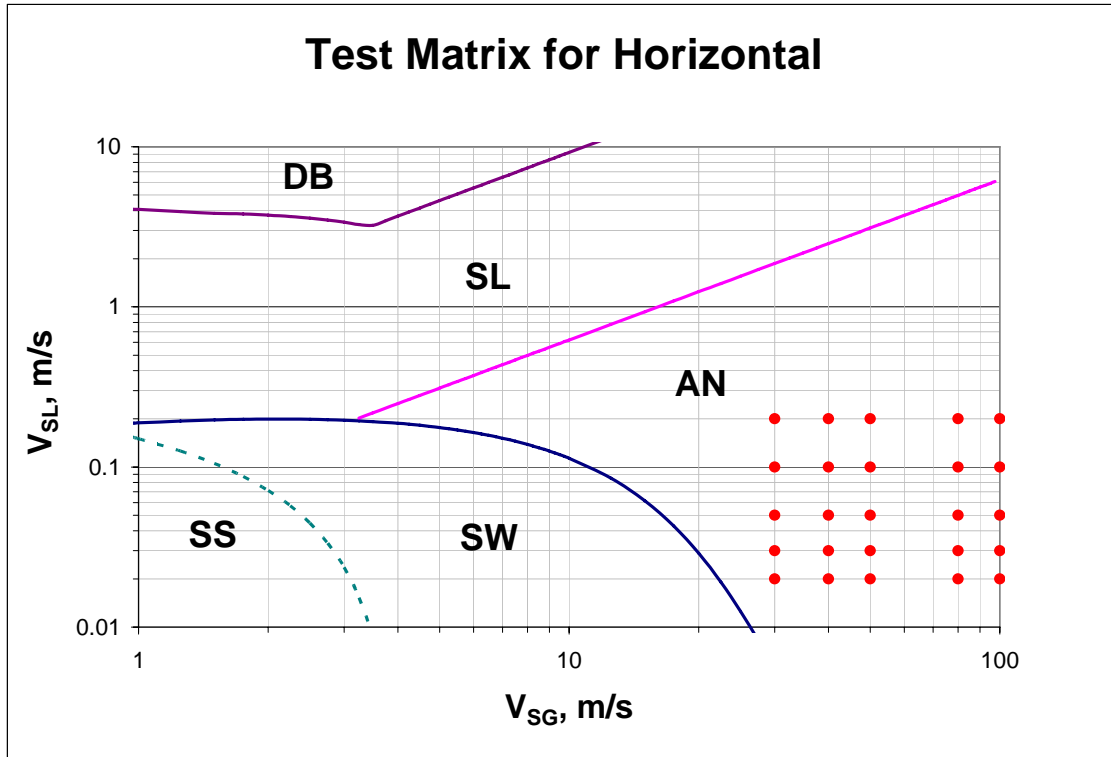


Figure 11. Test Matrix for Horizontal Flow.

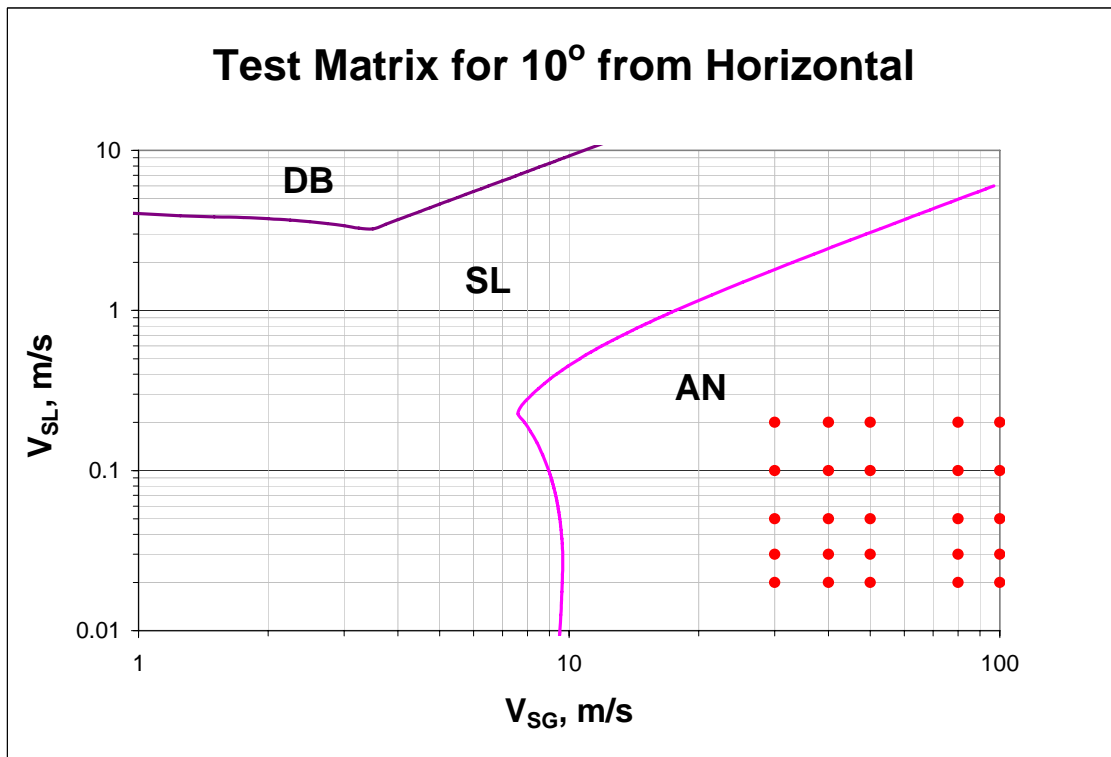


Figure 12. Test Matrix for 10° from Horizontal.

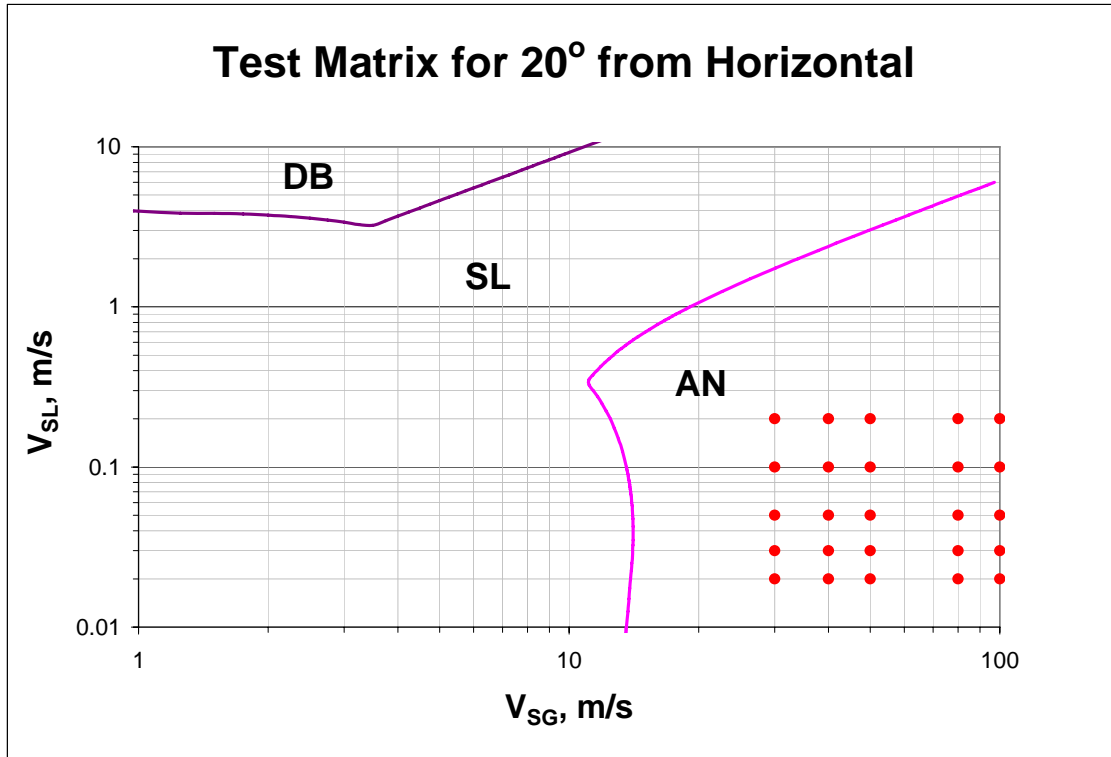


Figure 13. Test Matrix for 20° from Horizontal.

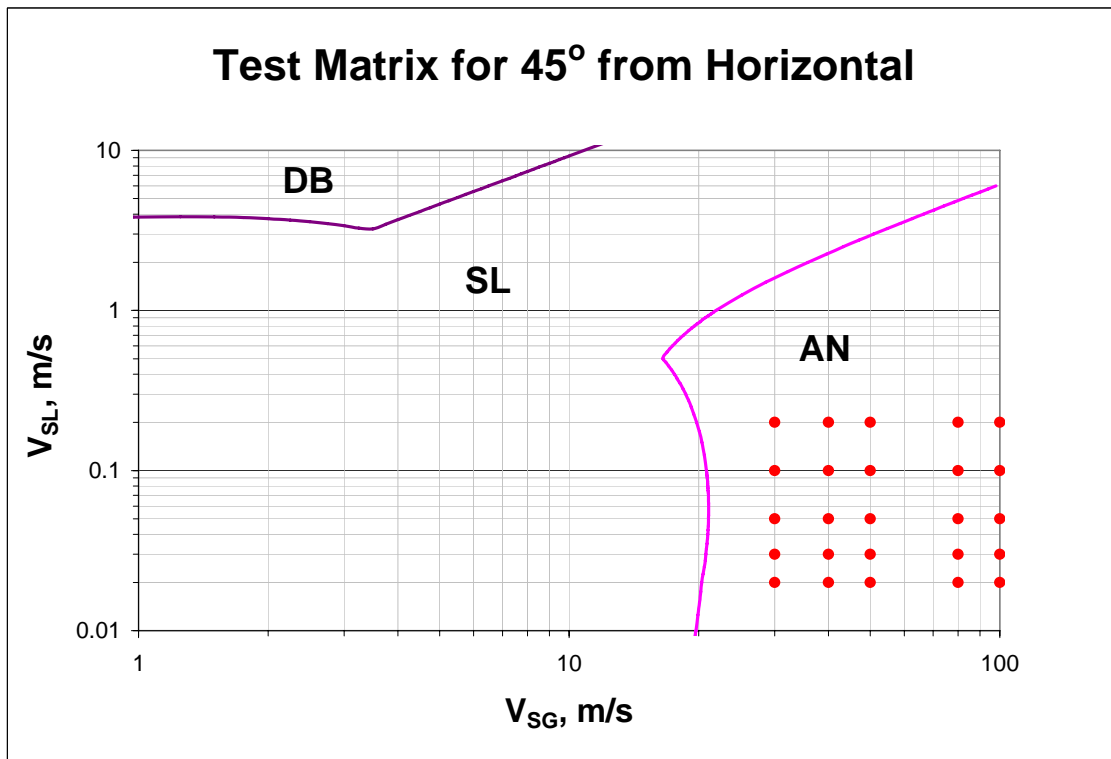


Figure 14. Test Matrix for 45° from Horizontal.

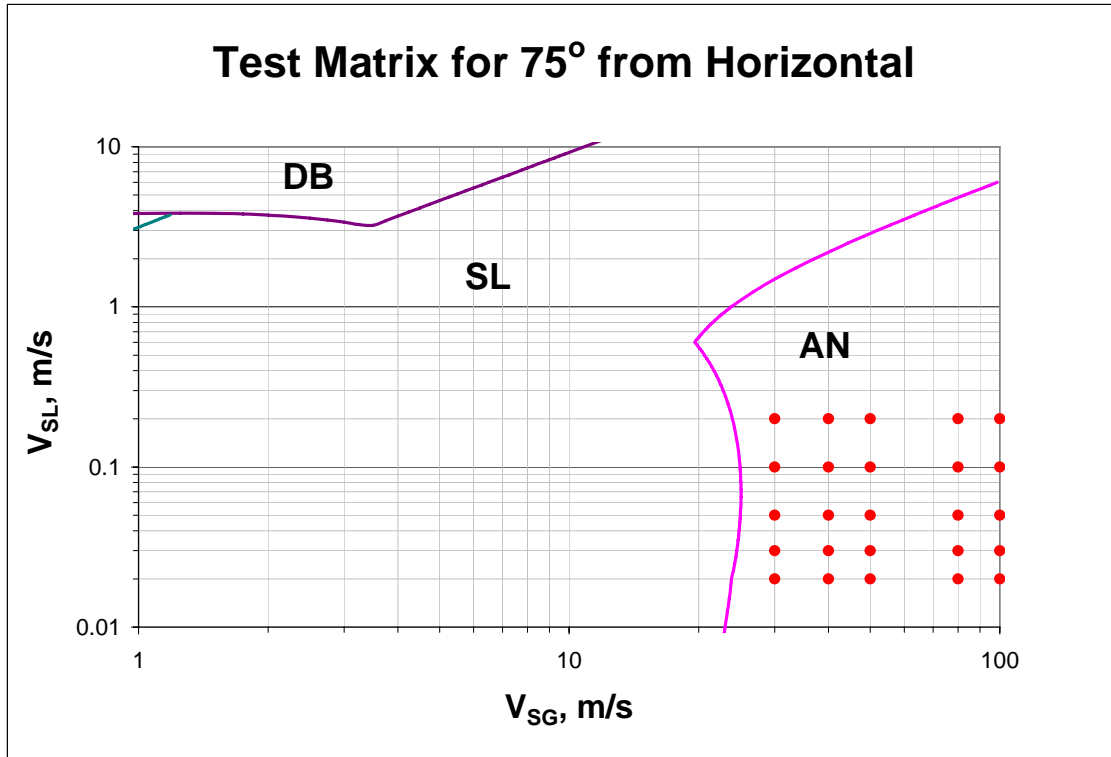


Figure 15. Test Matrix for 75° from Horizontal.

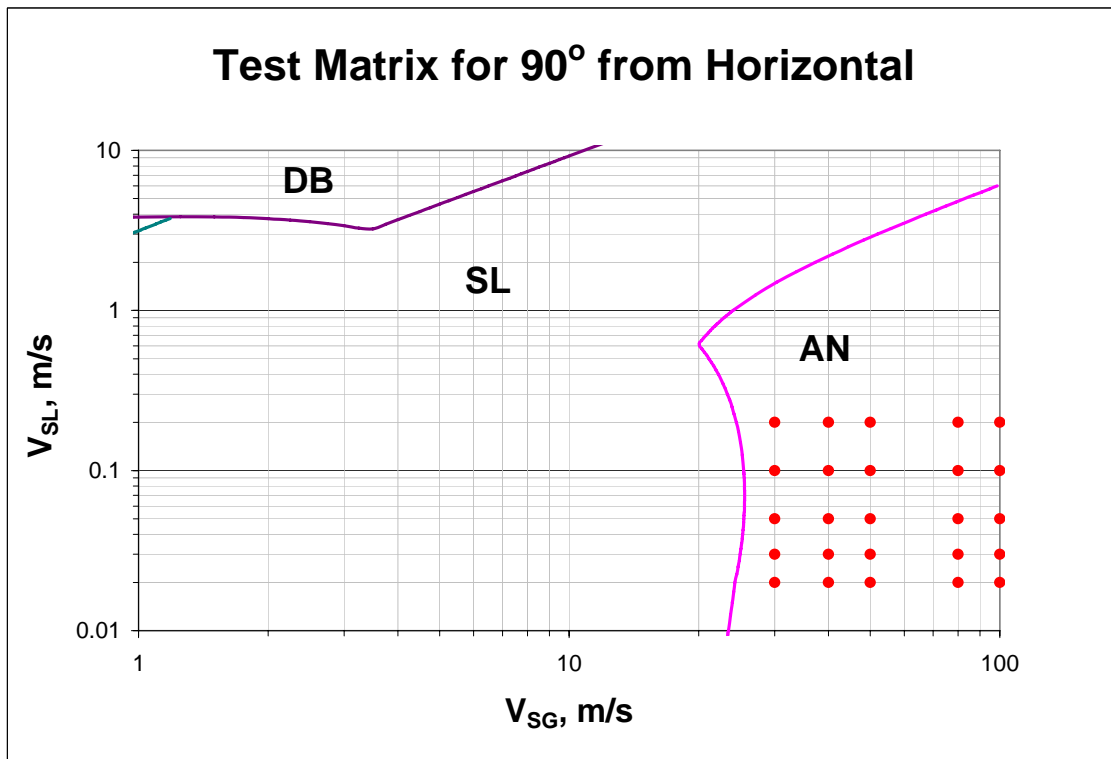


Figure 16. Test Matrix for 90° from Horizontal.

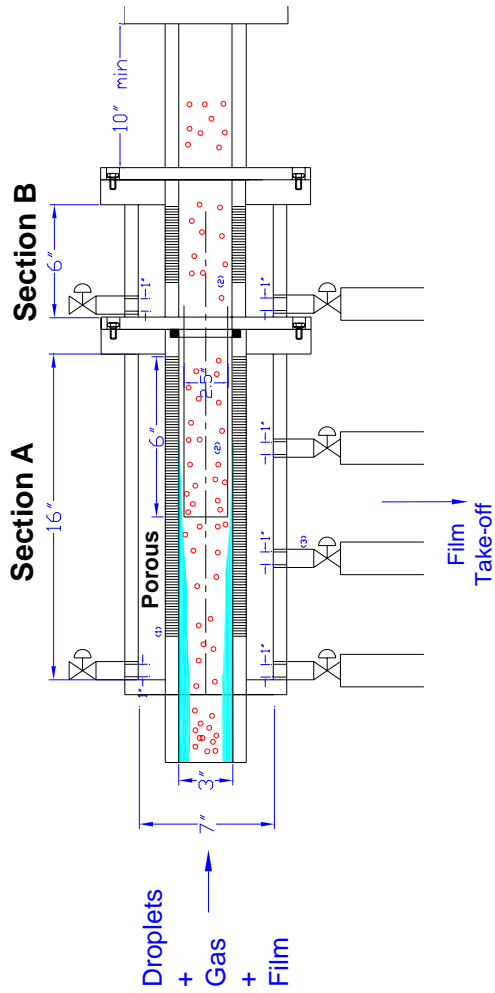


Figure 17. Film Removal Device Schematic

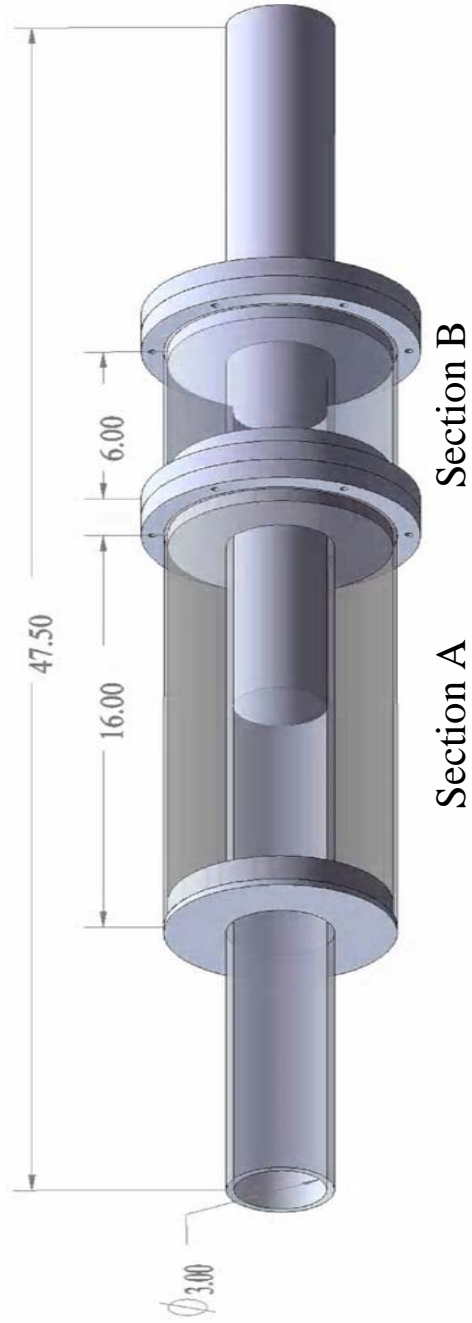


Figure 18. Film Removal Device Drawing

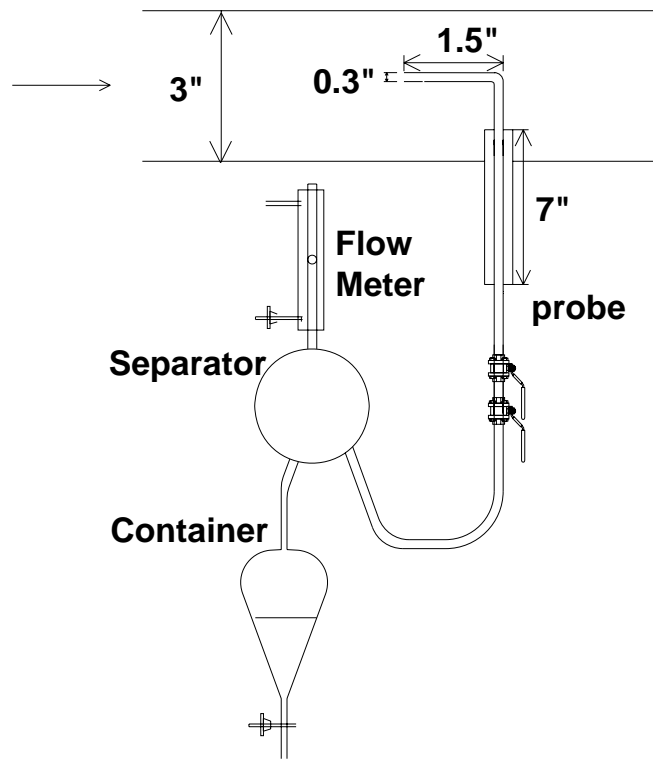


Figure 19. Iso-Kinetic Sampling System

Three-phase Hilly Terrain Flow

◆ Significance

- Valleys and Hills may Act as Local Separation Devices for Fluids
- Location, Amount and Residence Time of Water in a Pipe can have Significant Impact on Flow Assurance Issues such as Hydrate Formation and Corrosion

Three-phase Hilly Terrain Flow ...

◆ Past Studies

- Hilly Terrain Flow of Two Phases has been Studied Extensively
 - ▲ Al-Safran, 1999 and 2003
 - ▲ Others Outside of TUFFP
- No Available Research is Found on Three-phase Flow

Three-phase Hilly Terrain Flow ...

◆ Current Project

➤ Objectives

- ▲ Observe Flow Behavior and Identify Flow Characteristics
- ▲ Develop Predictive Tools (Closure Relationships or Models)

Three-phase Hilly Terrain Flow ...

◆ Status

- Facility Modification and Instrumentation is Complete
- Experiments are Underway



Fluid Flow Projects

Investigation of Three-Phase Gas-Oil-Water Flow in Hilly-Terrain Pipelines

Gizem Ersoy Gokcal

Advisory Board Meeting, September 17, 2008

Outline

- ◆ **Objectives**
- ◆ **Introduction**
- ◆ **Significance**
- ◆ **Three-Phase Flow Effects**
- ◆ **Experimental Study**
- ◆ **Preliminary Modeling**
- ◆ **Project Schedule**

Objectives

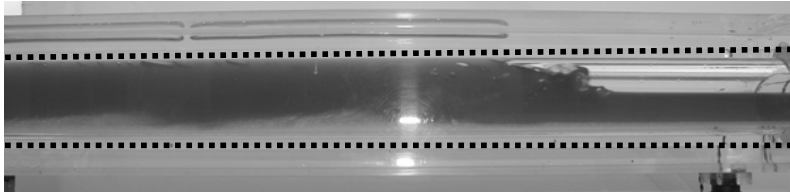
- ◆ **Investigate Three-Phase Gas-Oil-Water Flow in Hilly-Terrain Pipelines**
- ◆ **Develop Closure Models for Flow in Hilly-Terrain Pipelines on**
 - **Three-Phase Slug Initiation and Dissipation**
 - **Mixing Status of Phases**

Introduction

- ◆ **Oil-Water Distributions in Steady State Three-Phase Flow**
 - **Stratified Liquids**
 - **Oil Continuous**
 - **Water Continuous**

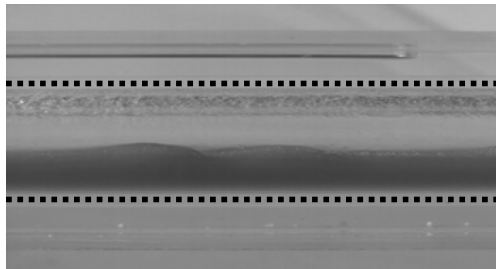
Introduction ...

◆ Stratified Liquids



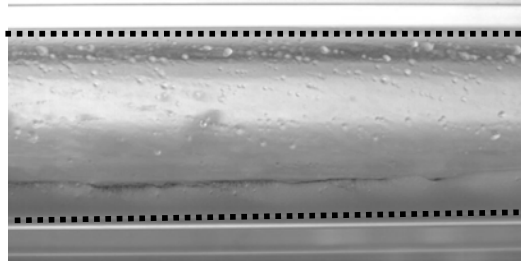
Introduction ...

◆ Oil Continuous



Introduction ...

◆ Water Continuous



Introduction ...



◆ Hilly-Terrain Pipelines Consist of Horizontal, Upward and Downward Inclined Sections

Introduction ...

- ◆ **Flow May Exhibit Different Behavior**



Significance

Hilly-Terrain Pipelines Cause

- ◆ **Operational Problems**
 - **Flooding of Downstream Facilities**
 - **Severe Pipe Corrosion**
 - **Structural Instability of Pipelines**
- ◆ **Poor Reservoir Management**
- ◆ **Production Loss**



Significance ...

◆ Change in Slug Characteristics

- Slug Length
- Slug Frequency
- Slug Translational Velocity
- Liquid Holdup

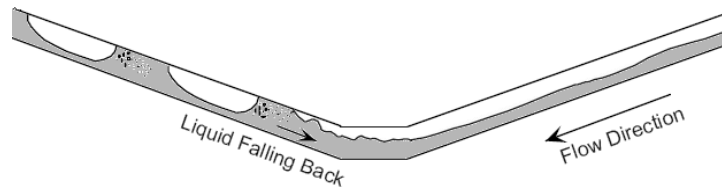
◆ Water Effects

- Flow Assurance Problems
 - ▲ Hydrates
 - ▲ Emulsions
 - ▲ Paraffin Deposition
 - ▲ Corrosion

Three-Phase Flow Effects

◆ Hydrodynamics

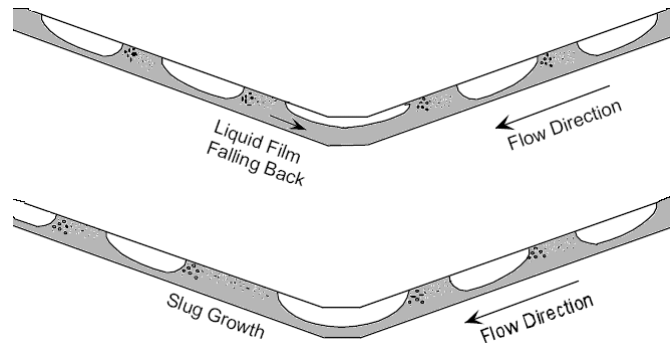
➢ Case-1



Three-Phase Flow Effects ...

◆ Hydrodynamics

➤ Case-2

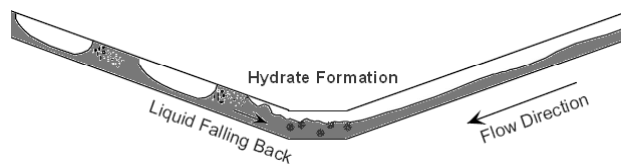


Three-Phase Flow Effects ...

◆ Flow Assurance:

➤ Hydrates

- ▲ Segregated Water Can Accelerate Hydrate Formation
- ▲ Oil-Water Dispersions/Emulsions Can Result in Hydrate Plugs

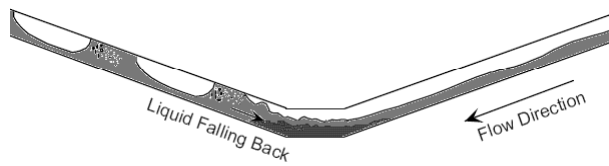


Three-Phase Flow Effects ...

◆ Flow Assurance:

➤ Emulsions

- ▲ Phase Distribution Can Change Continuous Phase and Liquid Characteristics

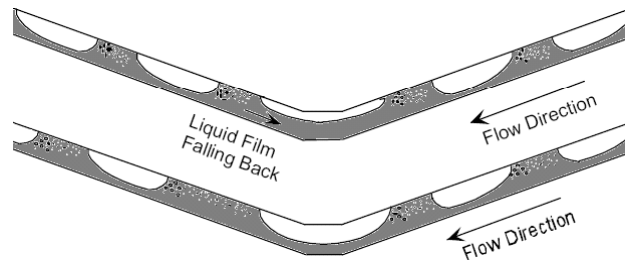


Three-Phase Flow Effects ...

◆ Flow Assurance:

➤ Paraffin Deposition

- ▲ Change in Hydrodynamics
- ▲ Change in Heat Transfer Characteristics

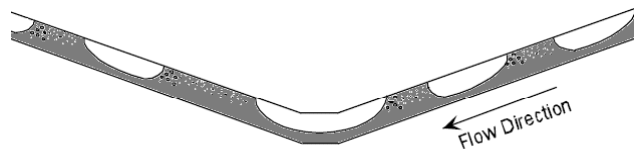


Three-Phase Flow Effects ...

◆ Flow Assurance:

➤ Corrosion

- ▲ Changes in Slug Length and Frequency
- ▲ Water Wet or Oil Wet Pipe?
- ▲ Accumulation of Water at Low Spots



◆ Prevention of Flow Assurance Problems

➤ Delivery and Distribution of Chemicals

Experimental Study

- ◆ Experimental Facility
- ◆ Instrumentation
- ◆ Data Acquisition System
- ◆ Test Fluids
- ◆ Testing Ranges
- ◆ Testing Procedure

Experimental Facility

- ◆ Previously Used by Atmaca (2007) for Oil-Water Flow
- ◆ Facility in Running Condition
- ◆ Relatively Small Modifications Required for Hilly-Terrain Study

Experimental Facility ...

- ◆ Extended to 69-m (226-ft) Long
- ◆ 50.8-mm (2-in.) ID Pipes
- ◆ Single Hilly-Terrain Unit
 - 9.7-m (32-ft) Long Downhill
 - 1.5-m (5-ft) Long Horizontal
 - 9.7-m (32-ft) Long Uphill Sections (L/D=413)
- ◆ $\pm 1^\circ$, $\pm 2^\circ$, $\pm 5^\circ$ of Inclination Angles

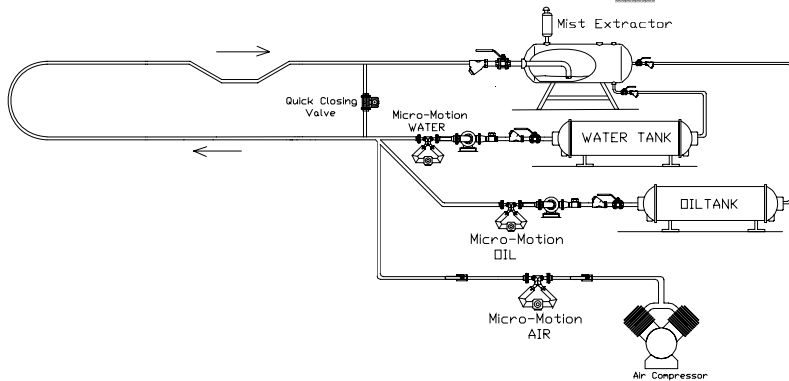
Experimental Facility ...



 Fluid Flow Projects

Advisory Board Meeting, September 17, 2008

Experimental Facility ...



 Fluid Flow Projects

Advisory Board Meeting, September 17, 2008

Experimental Facility ...



 Fluid Flow Projects

Advisory Board Meeting, September 17, 2008

Experimental Facility ...



 Fluid Flow Projects

Advisory Board Meeting, September 17, 2008

Experimental Facility ...

Water Pump

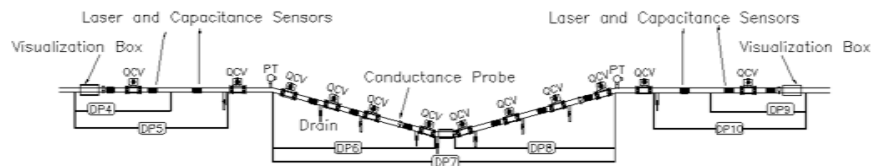


Oil Pump



Experimental Facility ...

Test Section



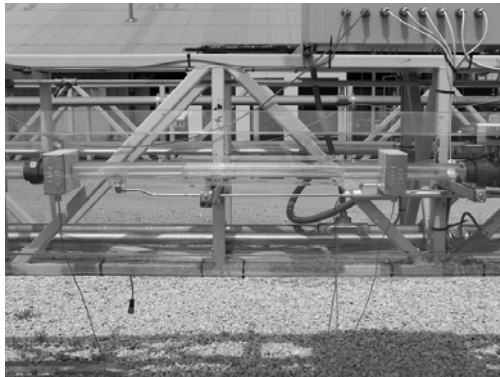
Experimental Facility ...



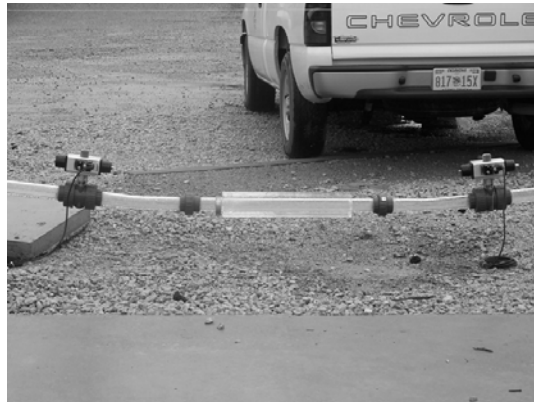
Test Section



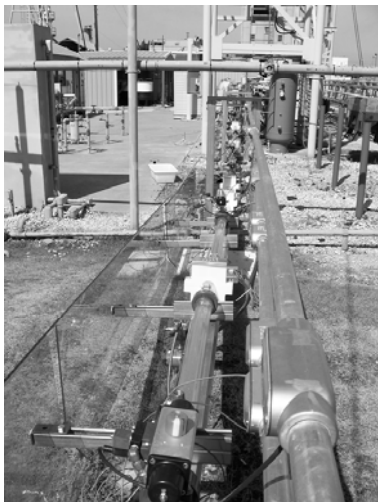
Experimental Facility ...



Experimental Facility ...



Experimental Facility ...



Instrumentation

◆ Pressure & Differential Pressure Transducers

- Pressure Drop
- Identification of Flow Patterns
- Connected to High-Speed DAQ

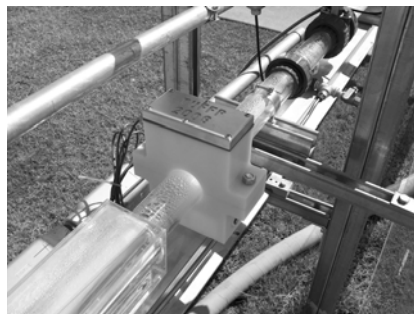
◆ Quick-Closing Valves

- Average Gas, Oil, Water Holdups

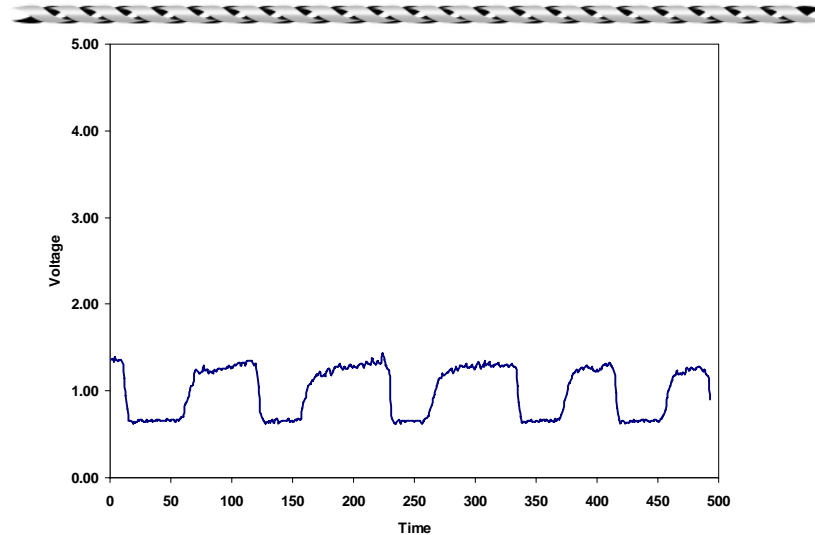
Instrumentation ...

◆ Laser Sensors

- Slug Flow Characteristics
- Connected to High-Speed DAQ
- Tested for Three-Phase Slug Flow



Instrumentation ...



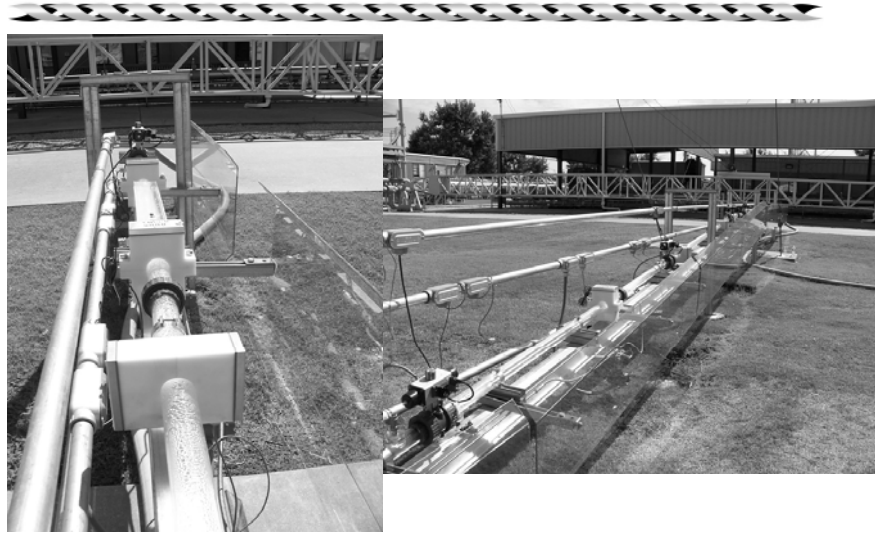
Instrumentation ...

◆ Capacitance Sensors

- Slug Flow Characteristics
- Connected to High-Speed DAQ
- Tested for Oil-Water and Three-Phase Slug Flow



Instrumentation ...



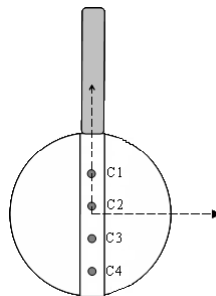
 Fluid Flow Projects

Advisory Board Meeting, September 17, 2008

Instrumentation ...

◆ Conductance Probes

➤ Phase Determination at a Point



**Insertion Type
Multi-point Probe**

 Fluid Flow Projects

Advisory Board Meeting, September 17, 2008

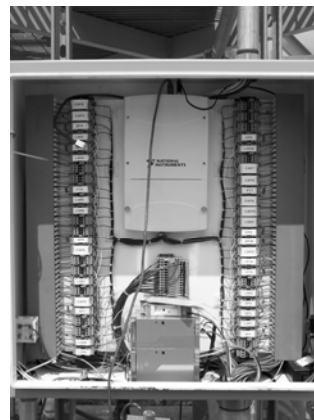
Instrumentation ...

- ◆ **High-Speed Video System**
 - Identification of Flow Patterns
 - Slug Characteristics
 - Oil-Water Mixing Status
- ◆ **Cameras**
 - Validation of Laser and Capacitance Sensors



Data Acquisition System

- ◆ **Lab VIEW™ 7.1 Software**
- ◆ **High-Speed Data Acquisition**



Test Fluids

- ◆ Air - Mineral Oil - Water
- ◆ Tulco Tech-80 Mineral Oil
 - API: 33.2°
 - Density: 858.75 kg/m³ @ 15.6 °C (60°F)
 - Viscosity: 13.5 cP @ 40 °C (104 °F)
 - Surface Tension: 29.14 dynes/cm @ 25.1 °C (77.2 °F)

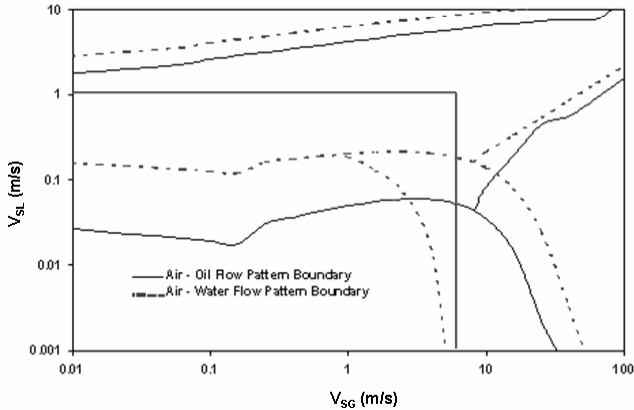
Testing Ranges

- ◆ Superficial Oil Velocity
 - 0.025 – 1.5 m/s
- ◆ Superficial Water Velocity
 - 0.025 – 1.5 m/s
- ◆ Superficial Gas Velocity
 - 0.1 – 7 m/s
- ◆ Water Fraction
 - 20%, 40%, 60%, 80%
 - 0% and 100% for Preliminary Tests
- ◆ Hilly-Terrain Unit
 - ±1°, ±2°, ±5°

Testing Ranges ...



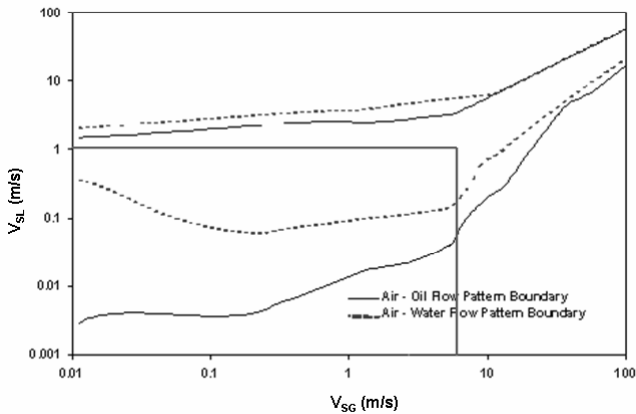
Taitel & Dukler Flow Pattern Map for Horizontal Flow



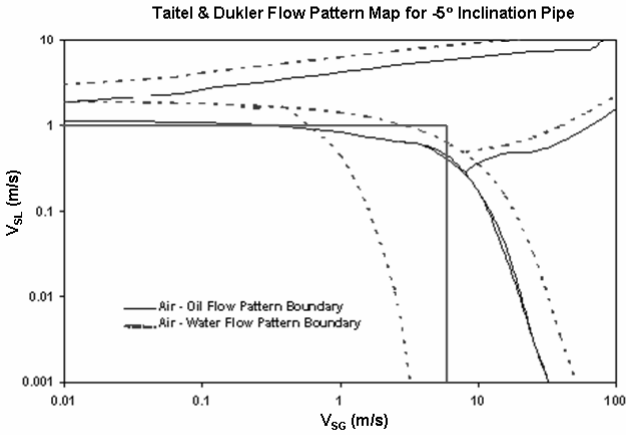
Testing Ranges ...



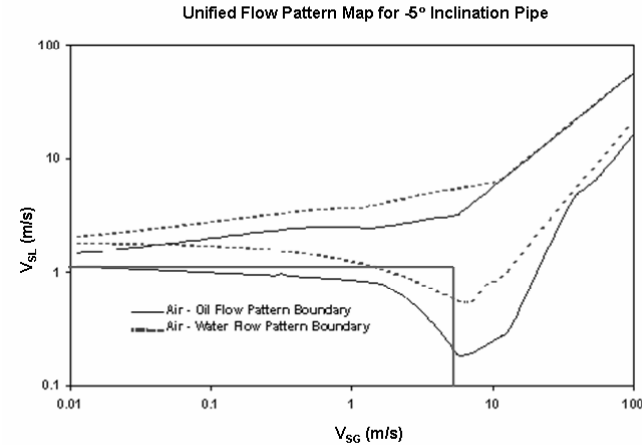
Unified Flow Pattern Map for Horizontal Flow



Testing Ranges ...



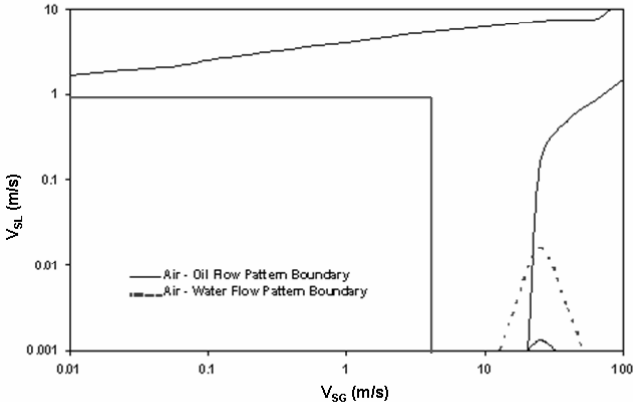
Testing Ranges ...



Testing Ranges ...



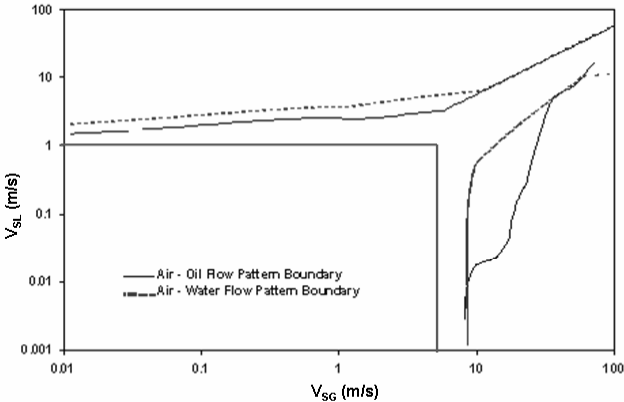
Taitel & Dukler Flow Pattern Map for +5° Inclination Pipe



Testing Ranges ...



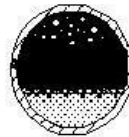
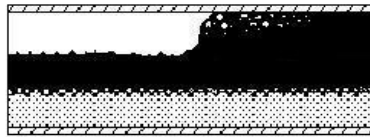
Unified Flow Pattern Map for +5° Inclination Pipe



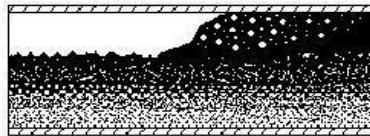
Testing Ranges ...

Three-Phase Gas-Oil-Water Slug Flow

Intermittent-Stratified (IN-ST)



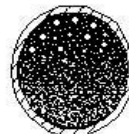
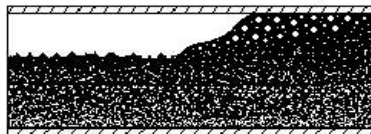
Intermittent-Dual Continuous (IN-DC)



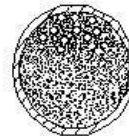
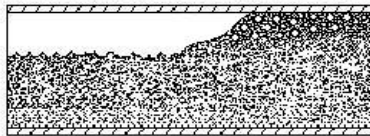
Testing Ranges ...

Three-Phase Gas-Oil-Water Slug Flow

Intermittent-Oil Continuous (IN-OC)



Intermittent-Water Continuous (IN-WC)



Testing Procedure

- ◆ **Vary Gas Flow Rate Keeping Oil and Water Flow Rates Constant**
- ◆ **Repeat Above Tests for Several Oil and Water Flow Rates at Constant Water Fraction**
- ◆ **Repeat Above Tests with Different Water Fractions and Inclination Angles**

Preliminary Modeling

- ◆ **Challenges:**
 - **Lack of Studies Addressing Three-Phase Gas-Oil-Water Flow in Hilly-Terrain Pipelines**
 - **Significance of Experimental Data**
 - ▲ **Observation of Physical Phenomena**
 - ▲ **Validation of Models**
- ◆ **Comparison of Developed Models with Multiphase Flow Simulator, OLGA[®]**

Preliminary Modeling ...

- ◆ **Development of Closure Models for Three-Phase Slug Flow on:**
 - **Slug Length/Frequency**
 - **Translational Velocity**
 - **Phase Distribution**
 - **Average Slug Holdup**

Preliminary Modeling ...

- ◆ **Identifying Flow Regions of Slug Initiation, Growth and Dissipation with Mixing Status of Liquid Phases**
- ◆ **Testing and Modification of Existing Two-Phase Slug Initiation and Dissipation Models**

Preliminary Modeling ...

- ◆ **Investigation of Water Phase at Hilly-Terrain Unit**
 - **Water Level in Downhill and Uphill Sections of Hilly-Terrain Unit**
 - **Water Accumulation at Elbow**
 - **Critical Values**

Project Schedule

- | | |
|--------------------------------|----------------------|
| ◆ Ph.D Proposal Defense | October 2008 |
| ◆ Testing | December 2008 |
| ◆ Model Development | March 2009 |
| ◆ Model Validation | April 2009 |
| ◆ Final Report | May 2009 |

Questions & Comments



Investigation of Three-Phase Gas-Oil-Water Flow in Hilly-Terrain Pipelines

Gizem Ersoy Gokcal

PROJECTED COMPLETION DATES:

Literature Review	Completed
Facility Modifications	Completed
Preliminary Testing	Completed
Testing.....	December 2008
Model Development.....	March 2009
Model Validation.....	April 2009
Final Report.....	May 2009

Objective

The general objectives of this project are:

- to conduct experiments on three-phase gas-oil-water flow in hilly-terrain pipelines,
- to develop closure models for three-phase slug initiation, dissipation and mixing status of phases,
- to validate developed closure models with experimental results.

Introduction

A hilly-terrain pipeline is a pipeline consisting of horizontal, upward inclined, and downward inclined sections. Hilly-terrain pipelines are common in both onshore and offshore production and transportation systems.

In the petroleum industry, slug flow is the dominant flow pattern in horizontal and near-horizontal pipes. Numerous studies have been carried out on slug flow in pipelines. Although slug flow in horizontal and inclined pipes has been studied extensively, slug flow in hilly-terrain pipelines is still not completely understood. In hilly terrain pipelines, the standard engineering design method has been to divide a pipeline into various sections of constant slopes, and apply steady state flow models to simulate flow behavior in each section. Hydrodynamic slugs

generated in uphill sections may or may not decay in following downhill sections, causing uncertainties in pressure behavior. Such configurations can also result in terrain induced slugs that are much longer than those normally encountered in horizontal pipelines. These long slugs often cause operational problems, flooding of downstream facilities, severe pipe corrosion, and structural instability of the pipeline, as well as production loss and poor reservoir management due to unpredictable wellhead pressures.

In the petroleum industry, three-phase gas-oil-water flow can occur in surface gathering lines and sub-sea production lines. The understanding of three-phase flow is crucial for flow assurance problems such as hydrates, emulsions and paraffin deposition. Corrosion and erosion also depend on the characteristics of three-phase flow in pipes.

In the open literature, no studies addressing three-phase flow in hilly-terrain pipelines could be found. Since slug flow is frequently encountered in three-phase flow, a study of slug characteristics for three-phase flow in hilly-terrain pipelines is very crucial for production and pipeline transportation. However, the complexity of slug flow increases significantly from two-phase to three-phase flow. The increased complexity in slug flow necessitates transient solutions, supported by closure models. These closure models should focus especially on the phase distribution throughout the flow, and oil-water

interactions, as well as the slug flow characteristics. In this study, these models will be examined and studied.

Experimental Study

Experimental Facility and Flow Loop

The experimental work is being conducted using the TUFFP facility for gas-oil-water flow located at the University of Tulsa North Campus Research Complex. The gas-oil-water facility was previously used by Atmaca (2007) for characterization of oil-water flow in inclined pipes. The facility consists of a closed circuit loop with storage tanks, progressive cavity pumps, heat exchangers, metering sections, filters, test section and separator.

For oil and water phases, there are two storage tanks equipped with valves to control the flow rates. Two progressive cavity pumps are used to maintain the liquid flow rates. There are manual bypass valves after the pumps to obtain low flow rates, and pressure relief valves for excessive pressure control. Copper-tube type heat exchangers are used to control the temperature of the fluid during the tests. After the heat exchangers, manual bypass valves allow the fluids to be pumped back to the respective tanks.

Two separate metering sections are equipped with Micro Motion™ Coriolis flow meters to measure mass flow rates and densities of the fluids, and with temperature transducers for monitoring the temperatures of the fluids. Oil and water flow through filters after the metering section. At the inlet of the test section gas, oil and water flow through the mixing tee to form the gas-oil-water three-phase co-current flow. After the fluids flow through the test section, the mixture is directed to the separator where pressure is set at 20 psig.

The test section is attached to an inclinable boom that makes inclined flow in the loop possible. However, during the three-phase hilly-terrain study, the boom will not be used and the part of the flow loop that is mounted on the boom stay horizontal.

Significant modifications are needed to flow loop to make enough space for the hilly-terrain section and instrumentation. The original gas-oil-water flow loop consisted of two 21.1-m (69.3-ft) long runs connected with a U-shaped bend to reduce the disturbance of the flow pattern due to a sharp turn. The current test section consists of a 21.1-m (69.3-ft) long upstream branch and a 46.7-m (153.2-ft) long downstream branch connected with a 1.2-m (4-ft) long U-shaped

PVC bend as shown in Fig. 1. Both of the branches are made of transparent pipes with 50.8-mm (2-in.) diameter.

The upstream branch of the test section consists of a 13.8-m (45.3-ft) long flow developing section ($L/D=272.0$), two pressure drop sections 1.17-m (3.83-ft) and 2.79-m (9.3-ft) long, one long pressure drop section combining the two short sections, and one 3.1-m (10.2-ft) long fluid trapping section ($L/D=108$). The entire upstream branch is placed on the boom.

The downstream branch of the test section consists of a 13.8-m (45.3-ft) long flow developing section ($L/D=272.0$), a 6-m (19.7-ft) long horizontal section with two short pressure drop sections 4.2-m (14-ft) and 2.13-m (7-ft) long, in addition to a 21-m (68.9-ft) long hilly-terrain section ($L/D=413.4$) followed by a 6-m (19.7-ft) long horizontal section.

The hilly-terrain section simulates a hilly-terrain unit of 9.5 m (31.3 ft) downhill followed by a 1.9 m (6.2 ft) horizontal and 9.5 m (31.3 ft) uphill sections. The inclination angles are $\pm 1^\circ$, $\pm 2^\circ$ and $\pm 5^\circ$ for the valley configurations.

The horizontal section immediately downstream of the hilly-terrain section was designed and built similar to the horizontal section immediately upstream of the hilly-terrain section.

The 21.1-m long section of the downstream branch is placed on the inclined boom as in the original gas-oil-water facility. The rest of the downstream branch, which is 25.6 m long, is supported by an aluminum base. Schematic diagram of the test section is given in Fig. 2.

Some hazards have been identified through a facility hazard analysis. Polycarbon protective glass is installed around the test section to provide protection in case of a rupture. In addition, the existing equipment such as pumps, flow meters, separator and storage tanks are checked and made operational.

Instrumentation and Data Acquisition

Instruments on the transparent pipes measure the operating temperature, pressure, differential pressure, total liquid holdup and spatial distribution of the phases.

The facility is divided into four segments. The horizontal section at the upstream branch is the first

segment. The horizontal section before the hilly-terrain unit, the hilly-terrain unit and the horizontal section after the hilly-terrain unit are segments two, three and four, respectively. Conductance probes, capacitance sensors, quick closing valves, laser sensors, and pressure and differential pressure transducers are installed on each segment of the facility. Two temperature transducers are also installed at the inlet of the flow loop and at the beginning of the hilly-terrain unit.

Absolute and differential pressure transducers are used to monitor the flow behavior. Absolute pressure transducers are located at the inlet, before and after the PVC bend and before and after the hilly-terrain unit. The aim of the pressure transducers before and after the PVC bend is to monitor and examine the effects of the bend on the flow. Although early studies on gas-oil-water facility showed that the effects of PVC bend are negligible, an additional developing section for the flow at the downstream branch is included in this study. There are three differential pressure transducers installed on the horizontal section at the upstream branch and at the hilly-terrain unit. On each of the other segments, two differential pressure transducers are installed. Pressure gradients over segments are measured with the high-speed data acquisition system to compare the results with laser and capacitance sensors for each test.

Previously developed laser sensors are modified to be used in three-phase slug flow in hilly-terrain pipelines. A new housing design is developed to use the laser sensors at outside conditions. The in-house developed laser sensors are installed on each segment of the facility to obtain translational velocity, slug frequency and slug length. The laser sensors are very sensitive to changes in flow characteristics. A preliminary testing on laser sensors is conducted to test their ability to respond to three-phase slug flow. Since the optical properties of test fluids (water and mineral oil) are very similar to each other, laser sensors are found to be applicable to determine only translational velocity, slug frequency and length. The locations of the laser sensors can be changed easily along the pipe. This enables to monitor slug initiation, slug growth and slug dissipation more easily with the change in operational conditions. The laser sensors are connected to the high-speed data acquisition system to monitor the changes in three-phase slug characteristics. There are two laser sensors installed on each horizontal section of the flow loop. There are three laser sensors on each branch of the hilly-terrain section. Using laser sensors with a high speed data acquisition system

makes the analysis of slug characteristics easier and more accurate.

Quick-closing valves will be used for liquid trapping to measure phase fractions and obtain holdup for each flowing condition. The liquid trapped by the quick-closing valves is drained into graduated cylinders to measure the volumes of water and oil phases. There are two quick-closing valves placed in sections one, two and three of the flow loop. The hilly-terrain test section is divided into seven trapping sections to observe the change in liquid holdups with inclination angles. An air tank is also added to keep the air pressure required to operate the QCV.

Previously designed conductance probes are modified. They consist of three probes across the pipe from top to bottom for determining the location of water phases at three different points. The objective of this configuration is to obtain different data points in the cross-sectional area of the pipe and to determine the continuous phase for all of the flow conditions. Conductance probes are installed on each segment of the facility to differentiate the conducting water phase from the non-conducting gas-oil phases. There is a conductance probe at the end of the downstream section and at the end of the upstream section of the hilly-terrain unit.

New capacitance sensors are designed and built in house. They work with the high speed data acquisition system. By using capacitance sensors, translational velocity, slug length and frequency can be measured. Two capacitance sensors are installed for each trapping section. The data obtained from capacitance sensors are going to be analyzed along with the data from laser sensors. The locations of capacitance sensors can also be changed along the flow loop to obtain slug characteristics at different flow conditions. The capacitance sensors are made weatherproof in order to eliminate the moisture effect.

A high speed video system is used to identify the flow patterns and determine the oil-water mixing status at the dip of the hilly-terrain section. The videos are taken through visualization boxes. The high speed video system is capable of recording at frames up to 100000 fps and electronic shutter speed of $4\mu\text{s}$.

Throughout the downstream section of the flow loop, cameras are also placed to investigate the details of three-phase slug characteristics in hilly-terrain pipelines. They are also used to validate the responses of laser and capacitance sensors.

For data acquisition, Lab View™ 7.1 is used. The existing program is updated for three-phase gas-oil-water flow in hilly-terrain studies. New hardware, including a high speed data acquisition system, is installed for the absolute and differential pressure transducers, laser and capacitance sensors. With the instruments connected to high speed data acquisition system, slug flow characteristics is captured and compared more efficiently. For the high-speed data acquisition system, a separate computer is utilized. The high-speed data acquisition system enables data sampling rates as high as 10000 samples/second. However, to optimize data quality and required time to data analysis, different sampling rates are going to be tested. A sampling rate of 1 sample/s is selected to collect data for this study and data acquisition lasts about three to four minutes for each test.

Test Fluids

For the experiments of three-phase flow in a hilly-terrain pipeline, fresh water, air and refined mineral oil were chosen as the testing fluids. The refined oil, Tulco Tech 80, was chosen based on its easy separation. The physical properties of Tulco Tech 80 are given below:

- API gravity: 33.2°
- Density: 858.75 kg/m³ @ 15.6°C
- Viscosity: 13.5 cp @ 40°C
- Surface tension: 29.14 dynes/cm @ 25.1°C
- Interfacial tension with water: 16.38 dynes/cm @ 25.1°C
- Pour point temperature: -12.2°C
- Flash point temperature: 185°C

The properties of Tulco Tech 80 were measured by Chevron labs. As shown in Figs. 3 and 4, the density and viscosity changes with temperature at three different flow rates were measured, respectively.

Experimental Ranges

The testing ranges for the three-phase hilly-terrain experiments on the gas-oil-water flow loop are as follows:

- Superficial gas velocity: 0.1-7.0 m/s
- Superficial oil velocity: 0.02-1.5 m/s
- Superficial water velocity: 0.02-1.5 m/s
- Water fraction: 20, 40, 50, 60 and 80%

The lower limits of superficial velocities were decided on by the accuracies of the Micro Motion™ flow meters. The higher limits were set by the pressure gradient and facility limits.

Within the testing ranges, three-phase slug flow and transition to stratified flow are going to be analyzed. As observed by Keskin et al. intermittent-stratified, intermittent-dual continuous, intermittent-oil continuous and intermittent-water continuous flow patterns are expected to be observed with various water cuts.

For every water-cut, twenty five data points will be taken from the three-phase slug flow region. The experimental work is expected to be finished by December 2008 by taking one hundred twenty five data point altogether.

The hilly-terrain branch of the flow loop can be modified for inclination angles $\pm 1^\circ$, $\pm 2^\circ$ and $\pm 5^\circ$. Due to time restriction for operation of the facility, only inclination angle of $\pm 5^\circ$ will be tested for the hilly-terrain effects on three-phase gas-oil-water flow. This inclination angle is chosen for the tests to observe the changes in flow conditions easily.

Test Program

A typical test program for gas-oil-water flow in a hilly-terrain pipeline starts with varying the gas flow rate, keeping the oil and water flow rates and water fraction constant. Then, tests will be repeated for several oil and water flow rates at constant water fraction and continue with various water fractions.

Preliminary Testing

After the facility construction is completed, several single phase and two-phase tests are conducted to check the facility condition and instruments. The high speed data acquisition system is also checked with these tests.

Laser sensors are found to be successfully working with both two-phase and three-phase slug flow. Capacitance sensors are tested for both oil-water and gas-oil-water flow.

Data Analysis Procedure

The three-phase slug flow characteristics are investigated by using laser and capacitance sensors in addition to the cameras.

Slug frequency is determined by dividing the number of slugs detected by the laser or capacitance sensors by the test duration. Times for the slug front and back to travel from the first laser sensor to the second one can be obtained. Since the distance between two sensors is known, the slug front and back velocities can be calculated. The slug translational velocity can be obtained by taking the average of the slug front and back velocities. If the time difference between a slug front and back passing one of the laser sensors can be determined, slug length can be calculated using the translational velocity.

Preliminary Modeling Study

As reported in the previous ABM, the literature review shows a lack of studies that address modeling of three-phase gas-oil-water flow in hilly-terrain pipelines. The following areas will be studied. The resulting models will be validated with experimental data and compared with a multiphase flow simulator, OLGA®.

Hilly-Terrain Effects on Three-Phase Slug Flow Characteristics

Three-phase gas-oil-water slug flow will be observed in the experiments with changes in water cut. Using the experimental findings, closure models for slug length and frequency, translational velocity, slug holdup and phase distributions will be investigated.

Three-Phase Effects on Slug Growth and Initiation Mechanisms

In the previous studies of two-phase hilly-terrain pipelines, different cases of flow were identified for slug dissipation, initiation and growth along the hilly-terrain section (Al-Safran, 2003). In the three-phase study, these flow cases will be improved by including the three-phase flow patterns.

Existing two-phase slug initiation and dissipation models will be tested and modified for the improved three-phase gas-oil-water flow cases.

Water Accumulation in Hilly-Terrain Pipelines

Accumulation of water at low spots in pipelines can cause serious corrosion and hydrate problems. Water level in downward and upward flow in the hilly-terrain section will be analyzed and modeled. At the elbow of the hilly-terrain unit, the water accumulation and critical values of mixture velocity to sweep the water phase will be studied with different inclination angles, water cuts and mixture velocities. A detailed modeling approach will be developed right after the Advisory Board Meeting.

Near Future Activities

Ph.D Dissertation Proposal Defense will be held on October 17th, 2008. Experiments are planned to be completed in December 2008. The data analysis is planned to be done parallel to the tests. The modeling study including the model validation is expected to be finished by April 2009. The final report will be submitted by May 2009.

References

1. Al-Safran, E.: "An Experimental and Theoretical Investigation of Slug Flow Characteristics in the Valley of a Hilly Terrain Pipeline," Ph.D. Dissertation, U. of Tulsa, Tulsa, OK (2003).
2. Zhang, H.-Q., Al-Safran, E., Jayawardena, S., Redus, C., Sarica, C. and Brill, J.: "Modeling of Slug Dissipation and Generation in Gas-Liquid Hilly-Terrain Pipe Flow," ASME J. Energy Res. Tech., vol. 125, pp. 161-168 (2003).
3. Zhang, H.-Q. and Sarica, C.: "Unified Modeling of Gas/Oil/Water Pipe Flow – Basic Approaches and Preliminary Validation," SPE 95749, presented at SPE ATCE, Dallas, TX (2005).
4. Zhang, H.-Q., Wang, Q., Sarica, C. and Brill, J.P.: "Unified Model for Gas-Liquid Pipe Flow via Slug Dynamics-Part 1: Model Development," ASME J. Energy Res. Tech., vol. 125 (4), pp.266 (2003).

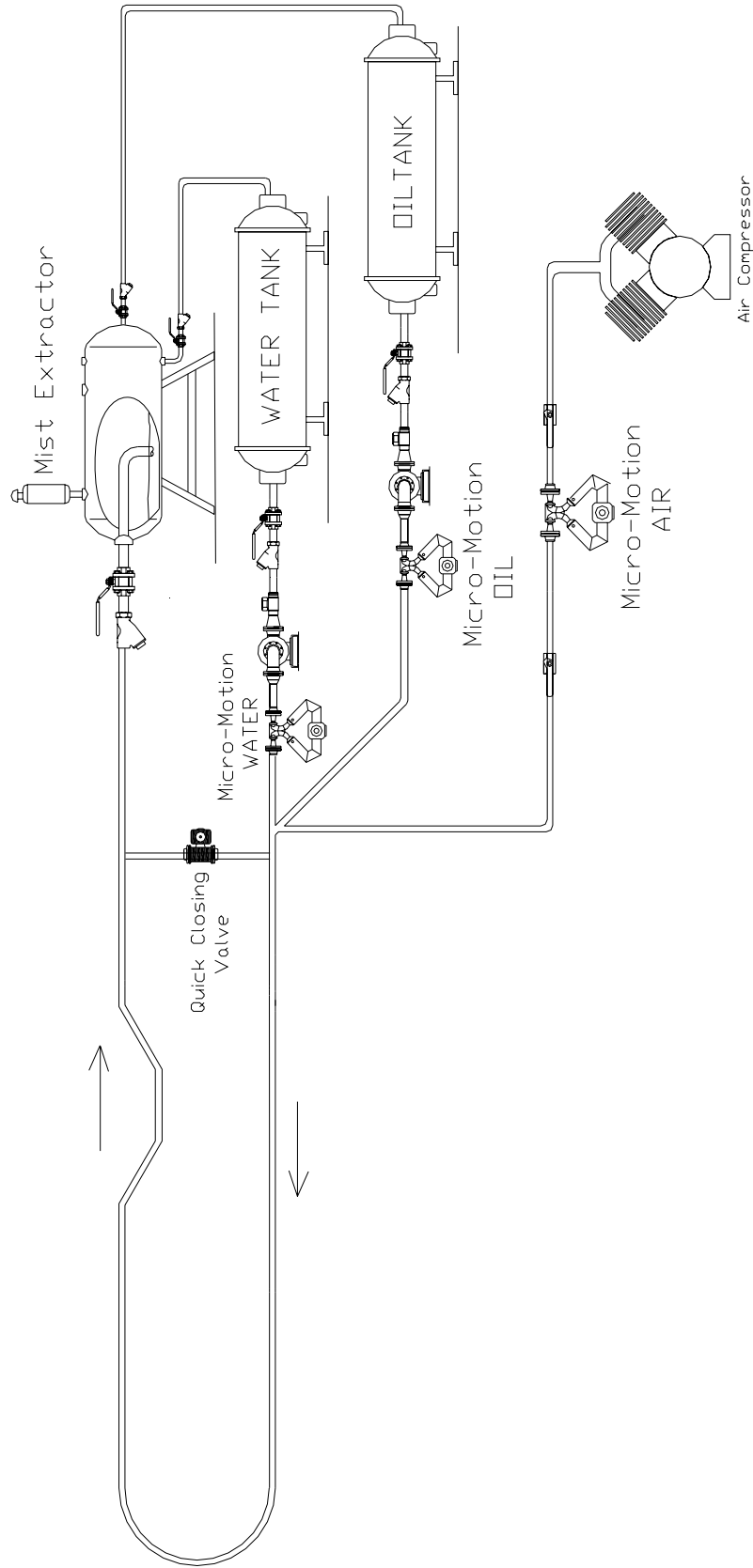


Figure 1: Gas-Oil-Water Facility Schematic

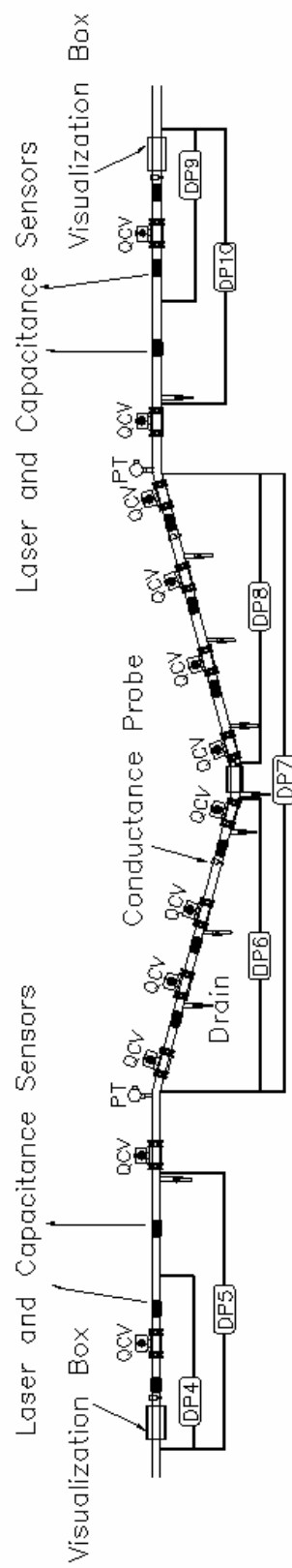


Figure 2: Schematic of Downstream Branch of Test Section

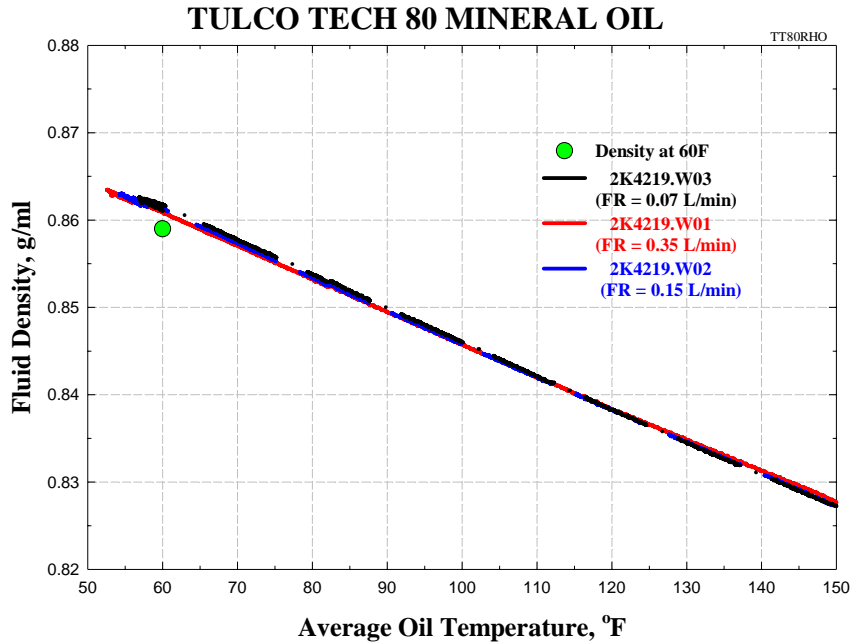


Figure 3: Tulco Tech 80 Oil Density vs. Temperature

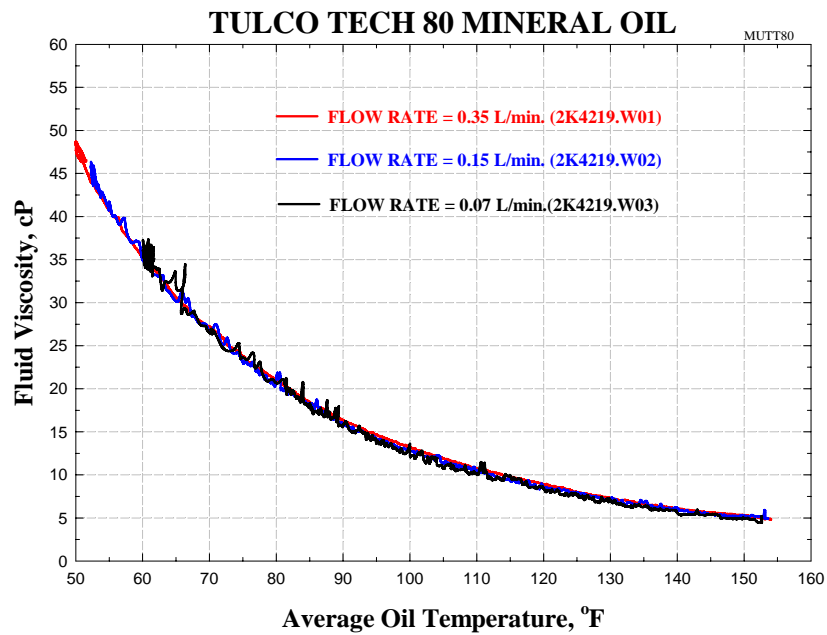


Figure 4: Tulco Tech 80 Oil Viscosity vs. Temperature

Three-phase Flow Studies

- ◆ **Significance**
 - Good Understanding of Gas-Oil Flow
 - Poor Understanding of Gas-Oil-Water Flow
- ◆ **Objective**
 - Development of Improved Prediction Models
- ◆ **Past Studies**
 - Oil-Water
 - ▲ Trallero (1994), Horizontal
 - ▲ Flores (1996), Vertical and Deviated
 - ▲ Alkaya (1999), Inclined

Three-phase Flow Studies ...

- ◆ **Past Studies ...**
 - Three-phase
 - ▲ Keskin (2007), Experimental Horizontal Three-phase Study
 - ▲ Zhang and Sarica (2005), Three-phase Mechanistic Model Development
 - ▲ Need to More Research on Oil-Water Flow
 - Recent Oil-Water Studies with Emphasis on Droplets
 - ▲ Vielma (2006), Horizontal Flow
 - ▲ Atmaca (2007), Inclined Flow

Three-phase Flow Studies ...

- ◆ **Current Study (Oil-Water Flow Modeling)**

- **Progress**

- ▲ **New Modeling Approach Based on Droplet Formation**



Fluid Flow Projects

Modeling of Oil-Water Pipe Flow

Anoop Kumar Sharma

Advisory Board Meeting, September 17, 2008

Outline

- ◆ Objectives
- ◆ Significance
- ◆ Preliminary Model
- ◆ Near Future Tasks

Objectives

- ◆ **Development of Better Model for Oil-water Flow**
- ◆ **Validation of Model Using Available Present Experimental Data**

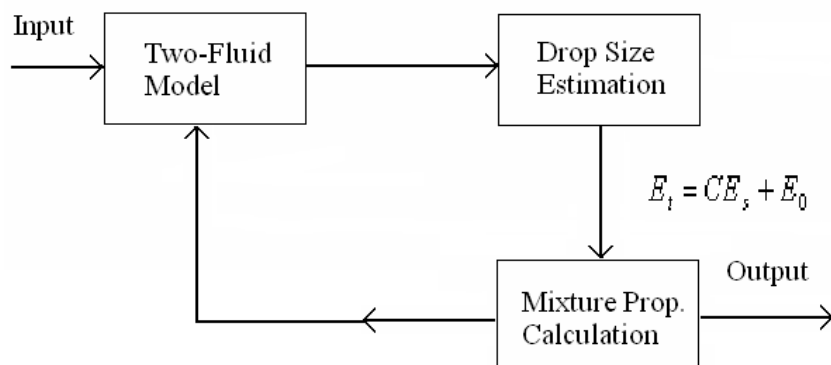
Significance

- ◆ **Oil-water Flow is Encountered in Various Processes in Petroleum Industry**
- ◆ **Existing Predictive Models**
 - **Do not Properly Represent Physics**
 - **Can not Capture Gradual Transition Between Flow Patterns**

Preliminary Model

- ◆ Consists of 3 Sub-models
 - Two-Fluid Model
 - Drop Size Estimation
 - Mixture Properties Calculation

Preliminary Model ...



Two-fluid Model

◆ Trallero Oil-Water (1995)

$$-A_1 \left(\frac{dP}{dL} \right)_1 - \tau_{w1} S_1 \pm \tau_i S_i - \rho_1 A_1 g \sin \theta = 0$$

$$-A_2 \left(\frac{dP}{dL} \right)_2 - \tau_{w2} S_2 \mp \tau_i S_i - \rho_2 A_2 g \sin \theta = 0$$

Two-Fluid Model ...

◆ Interfacial Friction Factor

➤ Wahaibi and Angeli (2007)

$$f_i = C \left(\frac{S_i}{\pi} \frac{v_i \rho_i}{\mu_i} \right)^{-n}$$

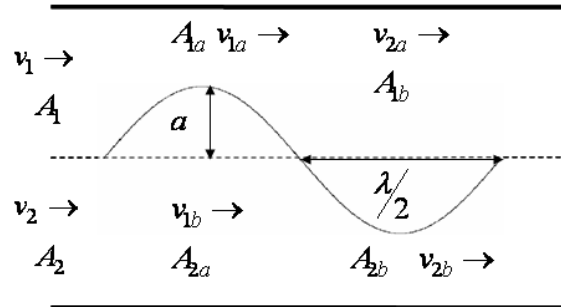
Drop Size Estimation

- ◆ **Sauter Mean Diameter**
 - **Rigorous Model**
 - **Angeli and Hewitt Method**
 - **Martinez-Bazan et al. Method**
 - **Hinze Method**

Rigorous Model

- ◆ **Wavelength and Amplitude Estimation**
- ◆ **Volume of Crest**
- ◆ **Minimum and Maximum Drop Size Estimation**
- ◆ **Estimation of SMD**

Rigorous Model ...



Formation of Waves in Stratified Flow

Rigorous Model ...

◆ Energy Balance – Wahaibi and Angeli (2007)

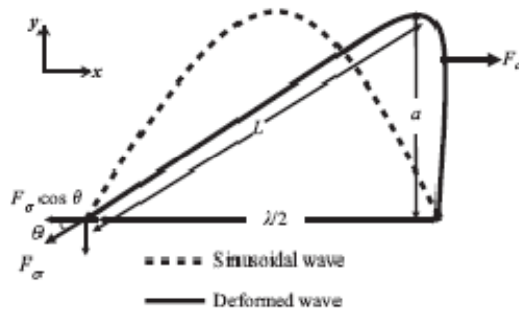
$$\frac{1}{2} \rho_2 \left[(v_2 - C_v) \times \left(\left(\frac{A_2}{A_{2b}} \right)^2 - \left(\frac{A_2}{A_{2a}} \right)^2 \right) \right] +$$

$$\frac{1}{2} \rho_1 \left[(v_1 - C_v) \times \left(\left(\frac{A_1}{A_{1a}} \right)^2 - \left(\frac{A_1}{A_{1b}} \right)^2 \right) \right]$$

$$- 2ga(\rho_2 - \rho_1) = \frac{8\pi^2 a \sigma}{\lambda^2}$$

Rigorous Model ...

◆ Force Balance on Deformed Wave – Wahaibi and Angeli (2007) ...



Rigorous Model ...

◆ Force Balance

➤ Drag vs. Surface Forces

$$F_d = C_d A_{wave} \rho_2 \frac{(v_2 - v_1)^2}{2}$$

$$F_\sigma = 2\sigma S_l \left(\frac{\lambda/2}{L} \right)$$

$$C_d A_{wave} \rho_2 \frac{(v_2 - v_1)^2}{2} - 2\sigma S_l \left(\frac{\lambda/2}{L} \right) = 0$$

Rigorous Model ...

- ◆ Wahaibi and Angeli (2007) Used Energy and Force Balance as Flow Pattern Transition Criteria
- ◆ In This Study, Energy and Force Balance Used to Find Wavelength and Amplitude to Calculate Volume of Crest (Largest Drop Volume Possible)

Rigorous Model ...

- ◆ Initial Drop Formation

$$V_d = \frac{1}{2} a \frac{\lambda}{2} S_I$$

$$D_o = \left(\frac{3}{4\pi} V_d \right)^{1/3}$$

- D_o will be Used in Minimum Droplet Diameter Calculation

Rigorous Model ...

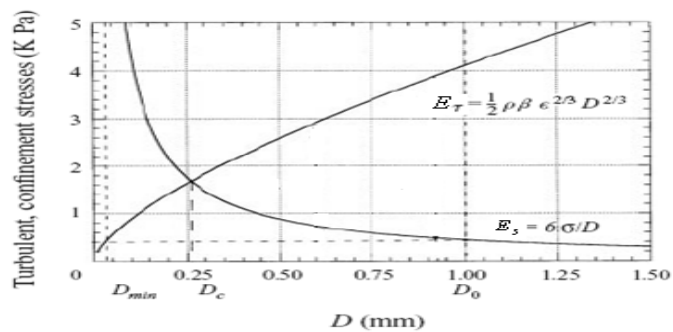
◆ Martinez-Bazan *et al.* (1999)

$$E_{\tau} = \frac{1}{2} \rho_c \beta \epsilon^{2/3} D_{drop}^{2/3}$$

$$E_s = \frac{6\sigma}{D_{drop}}$$

Rigorous Model ...

◆ Turbulent and Surface Stresses vs. Droplet Diameter Martinez-Bazan *et al.* (1999)



Rigorous Model ...

◆ Critical and Minimum Diameter

$$D_c = \left(\frac{12\sigma}{\beta\rho} \right)^{3/5} \varepsilon^{-2/5}$$

$$D_{\min} = \left(\frac{12\sigma}{\beta\rho D_0} \right)^{3/2} \varepsilon^{-1}$$

Rigorous Model ...

◆ Log Normal Distribution (Vielma (2006) and Atmaca (2007))

$$\text{Log}(D_{sm}) = \frac{1}{2} \text{Log}(D_{05} D_{95})$$



$$\text{Log}(D_{sm}) = \frac{1}{2} \text{Log}(D_{\min} D_c)$$

Angeli and Hewitt Method

◆ Angeli and Hewitt (2000) SMD Correlation

$$D_{SM} v_c^{1.8} = 2 \times 10^{-2} f^{-3.12}$$

Where: v_c is continuous phase velocity.
 f is wall friction factor for continuous phase.

Martinez-Bazan *et al.* Method

◆ Martinez-Bazan *et al.* (1999)

$$D_c = \left(\frac{12\sigma}{(\beta\rho)} \right)^{3/5} \varepsilon^{-2/5} = D_{MAX}$$

◆ Hesketh *et al.* (1987)

$$D_{SM} = 0.62 D_{MAX}$$

Hinze Method

◆ Hinze (1955) Model

$$D_{MAX} \left(\frac{\rho_c}{\sigma} \right)^{3/5} \varepsilon^{2/5} = 0.725$$

◆ Hesketh *et al.* (1987)

$$D_{SM} = 0.62 D_{MAX}$$

Mixture Properties Calculation

◆ Zhang *et al.* (2003)

➤ Total Surface and Turbulent Energy for a Control Volume

$$E_S = \frac{6\sigma}{D_{SM}} A(1 - H_C)$$

$$E_\tau = \frac{3}{2} \rho_C (v^*)^2 A H_C$$

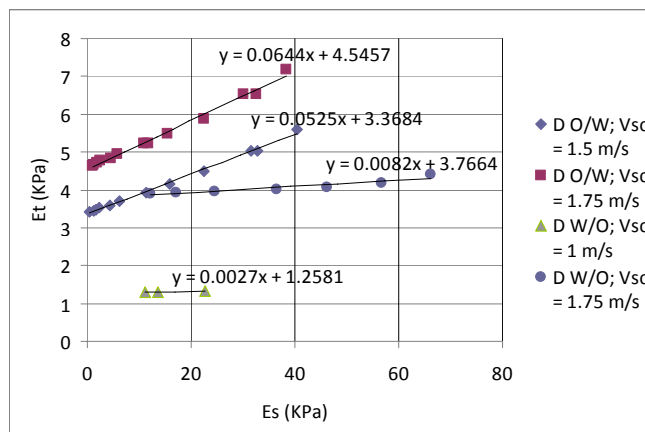
Mixture Properties Calculation ...

◆ Conventional Energy Balance

$$E_{\tau} = CE_S$$

Mixture Properties Calculation ...

Turbulent Energy and Surface Energy Correlation for Vielma (2006) Data



Mixture Properties Calculation ...

- ◆ **Modification to Energy Balance**
 - **Addition of Threshold Energy**

$$E_{\tau} = CE_S + E_0$$

Mixture Properties Calculation ...

- ◆ **Shi (2001)**

$$\mu_M = (H_{pack} \pm 10\%) (We)^{-1/8} \mu_C (1 - H_D)^{-2.5}$$

$$We = \frac{D_H \rho_M v_M^2}{2\sigma}$$

Mixture Properties Calculation ...

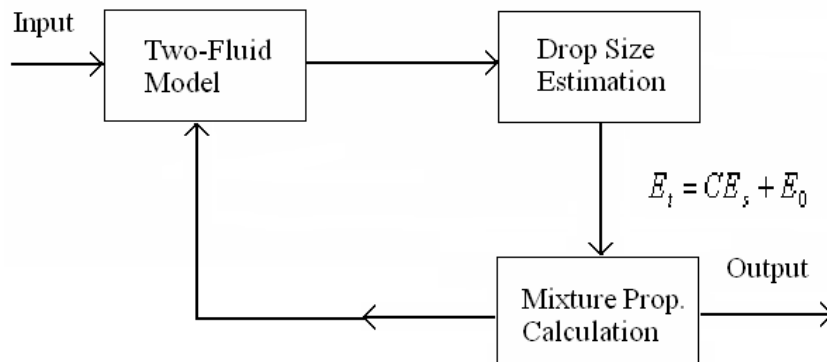
$$\rho_M = \rho_D(1 - H_D) + \rho_D H_D$$

$$q_{1,T} = A_1(1 - H_{D1})v_1 + A_2 H_{D2}v_2$$

$$q_{2,T} = A_2(1 - H_{D2})v_2 + A_1 H_{D1}v_1$$

$$v_{SL1} = v_1 \frac{A_1}{A_p}$$

Preliminary Model



Near Future Tasks

- ◆ Development of Computer Code for Model
- ◆ In Depth Analysis of Turbulent Energy and Surface Energy Relationship
- ◆ Validation of Model With Experimental Results

Schedule

- ◆ Literature Review.....Completed
- ◆ Model Development...November 2008
- ◆ Model Validation.....January 2009
- ◆ Final Report and Thesis.....May 2009

Questions & Comments



Modeling of Oil-Water Pipe Flow

Anoop Kumar Sharma

PROJECT COMPLETION DATES:

Literature Review.....	Completed
Model Development.....	November 2008
Model Validation.....	January 2009
Final Report and Thesis.....	May 2009

Objectives

The objectives of this study are:

- To develop better model for oil-water flow that captures the physics.
- To validate the model using available present experimental data.

Introduction

The flow of two immiscible liquids is encountered in a diverse range of processes and equipment, particularly in the petroleum industry, where mixtures of oil and water are often transported in pipes over long distances. Accurate prediction of oil-water flow characteristics, such as flow pattern, water holdup and pressure gradient is important in many engineering applications. However, despite their importance, liquid-liquid flow has not been explored to the same extent as gas-liquid flow. The density difference between the phases in a liquid-liquid system is relatively small. However, the viscosity ratio encountered can extend over several many orders of magnitude. Oil and oil-water emulsions can show either a Newtonian or non-Newtonian rheological behavior. Therefore, concepts of gas-liquid two-phase flow cannot be readily applied to liquid-liquid systems.

Moreover, existing models predict on the basis of flow pattern which is defined by certain criteria. Because of this the transition prediction between the

flow patterns is abrupt not capturing the gradual nature of the transition. The present study will focus onto this aspect along with more accurate prediction of pressure drop.

Preliminary Modeling

The following model developed for the prediction of the flow pattern and pressure gradient consists of three sub-modules, namely, two-fluid model, estimation of drop size and mixture properties calculation. These constitute the backbone of the model and are iterated until the convergence is achieved. The basic process of the model is:

- Initially, assuming segregated flow, the velocities and other flow characteristics of each segregated layer are calculated by using the two-fluid model.
- The turbulence energy associated with each phase can cause dispersion hence, accommodating the droplets of another phase in it. Estimation of the drop size can be done by any of the methods discussed later. Then, the holdup of dispersed phase can be calculated by performing energy balance for each phase, between turbulent energy and the surface energy.
- New mixture properties of each phase can be calculated using holdup information.
- These new properties will then be used in two-fluid model again. This iterative process will continue until the convergence is reached.

If turbulence in both the layers is not enough to cause any dispersion, the flow pattern will remain

segregated. When interface height falls below 1% of diameter or rises above 99% of diameter of pipe, the thinner phase can be neglected leaving one phase dispersed fully in the other. In between, either partial dispersion flow pattern or dual dispersion flow pattern will exist. Two-fluid model will be used to calculate the pressure gradient, except for full dispersion, where homogeneous model will be used.

Two-Fluid Model

Trallero (1995) presented a two fluid model to predict pressure drop in two-phase segregated flow. Assuming equilibrium stratified flow, the following momentum balance equations can be derived for each phase (phase 1 and 2):

$$-A_1 \left(\frac{dP}{dL} \right)_1 - \tau_{W1} S_1 \pm \tau_I S_I - \rho_1 A_1 g \sin \theta = 0, \quad (1)$$

$$-A_2 \left(\frac{dP}{dL} \right)_2 - \tau_{W2} S_2 \pm \tau_I S_I - \rho_2 A_2 g \sin \theta = 0. \quad (2)$$

Where, A, ρ, S and (dp/dL) denotes area, density, perimeter and pressure gradient, respectively. While, subscript 1, 2 and I represents respective oil phase, water phase and interface between them. $\tau_{W1}, \tau_{W2}, \tau_I$ are oil, water and interfacial shear stresses, respectively. These can be expressed in terms of the corresponding fluid friction factors f_1, f_2 and f_I .

$$\tau_{W1} = \frac{f_1 \rho_1 v_1^2}{2}. \quad (3)$$

$$\tau_{W2} = \frac{f_2 \rho_2 v_2^2}{2}. \quad (4)$$

The Fanning friction factor is used and can be expressed for any phase j assuming smooth pipe wall.

$$f_j = C \left(\frac{D_j v_j \rho_j}{\mu_j} \right)^{-n}. \quad (5)$$

Where, coefficient C and exponent n are equal to 16 and 1 for laminar flow and to 0.046 and 0.2 for turbulent flow. Equivalent hydraulic diameters are determined on the basis of which phase is faster.

For $v_1 > v_2$

$$D_1 = \frac{4A_1}{S_1 + S_I}. \quad (6)$$

$$D_2 = \frac{4A_2}{S_2}. \quad (7)$$

For $v_1 < v_2$

$$D_1 = \frac{4A_1}{S_1}. \quad (8)$$

$$D_2 = \frac{4A_2}{S_2 + S_I}. \quad (9)$$

For $v_1 \approx v_2$

$$D_1 = \frac{4A_1}{S_1}. \quad (10)$$

$$D_2 = \frac{4A_2}{S_2}. \quad (11)$$

The interfacial shear stress can be given by

$$\tau_I = f_I \frac{\rho_I (v_1 - v_2) |v_1 - v_2|}{2}. \quad (12)$$

The interfacial friction factor used in this model is same as the one used by Wahaibi and Angeli (2007).

$$f_I = C \left(\left(\frac{S_I}{\pi} \right) \frac{v_I \rho_I}{\mu_I} \right)^{-n}. \quad (13)$$

Where, v_I, ρ_I and μ_I corresponds to the properties of faster phase.

Sauter Mean Diameter (SMD) Estimation

Information about SMD in dispersed flow is important for mixture properties and pressure gradient predictions. It can be used to estimate holdup which in turn will be used to calculate mixture properties. There are several ways to estimate SMD. Method 1 is more elaborate and captures the physics behind but it is complicated and can have significant uncertainties. Methods 2, 3 and 4 are based more or less on correlations.

Method 1

As the flow rates of oil and water increase, interfacial waves start to appear. These waves will grow until the wave length and the amplitude reach the threshold at which their crest will break due to shear force and form droplets. In the model, a finite sinusoidal wave is assumed at the interface in a moving coordinate system with wavelength λ and amplitude a as shown in Fig. 1. Wahaibi and Angeli (2007) in their study performed energy balance in such system;

$$\begin{aligned} & \frac{1}{2} \rho_2 \left[(v_2 - C_v) \times \left(\left(\frac{A_2}{A_{2b}} \right)^2 - \left(\frac{A_2}{A_{2a}} \right)^2 \right) \right] + \\ & \frac{1}{2} \rho_1 \left[(v_1 - C_v) \times \left(\left(\frac{A_1}{A_{1a}} \right)^2 - \left(\frac{A_1}{A_{1b}} \right)^2 \right) \right] . \quad (14) \\ & -2ga(\rho_2 - \rho_1) = \frac{8\pi^2 a \sigma}{\lambda^2} \end{aligned}$$

Where,

$$A_{1a} = A_1 - A_{wave} . \quad (15)$$

$$A_{1b} = A_1 + A_{wave} . \quad (16)$$

$$A_{2b} = A_2 - A_{wave} . \quad (17)$$

$$A_{2a} = A_2 + A_{wave} . \quad (18)$$

A_1 , A_2 , v_1 , and v_2 are obtained from the solution of two-fluid model mentioned before. Assuming $a \ll S_b$, A_{wave} can be given by

$$A_{wave} = S_I \times a . \quad (19)$$

In Eq. 14, σ represents the interfacial tension between oil and water and C_v the wave velocity. A general relationship for wave velocity is developed by Wallis (1969) which is the derivative of the liquid flux with respect to the in-situ liquid hold-up. Wahaibi and Angeli (2007) estimated the wave velocity directly from the equilibrium condition of the two-fluid model.

$$C_v = \frac{(\partial F / \partial H_2)_{v_{S1}, v_{S2}}}{(\partial F / \partial v_{S1})_{v_{S2}, H_2} - (\partial F / \partial v_{S2})_{v_{S1}, H_2}} . \quad (20)$$

Where, v_{S1} and v_{S2} are the oil and water superficial velocities, respectively. H_2 is water holdup and F is given by the combined momentum equation of the system.

$$F = -\frac{\tau_{W2} S_2}{A_2} + \frac{\tau_{W1} S_1}{A_1} + \tau_I S_I \left(\frac{1}{A_1} + \frac{1}{A_2} \right) = 0 . \quad (21)$$

The derivatives in Eq. 20 can be evaluated numerically by perturbing H_2 , v_{S1} and v_{S2} in Eq. 21 by very small amounts, e.g. $\pm 1\%$.

Wahaibi and Angeli (2007) also performed force balance on the wave for horizontal flow, considering the deformation of the wave. Wahaibi and Angeli (2007) assumed that the deformed wave will be triangular in shape with height, a , and base, $\lambda/2$, as shown in Fig. 2. The drag force is given by

$$F_d = C_d A_{wave} \rho_2 \frac{(v_2 - v_1)^2}{2} . \quad (22)$$

Where,

$$C_d = 4.9 \times 10^{-8} \text{Re}_o^{0.77} \text{Re}_w^{0.86} \left(\frac{\mu_o}{\mu_w} \right) . \quad (23)$$

Re_o and Re_w are Reynolds numbers for oil and water, respectively. The surface force due to wave deformation is estimated as

$$F_\sigma = \sigma (2S_I) \left(\frac{\lambda/2}{L} \right) . \quad (24)$$

Where,

$$L = \left((a^2) + \left(\frac{\lambda/2}{2} \right)^2 \right)^{0.5} . \quad (25)$$

From Eq. 22 and Eq. 24,

$$C_d A_{wave} \rho_2 \frac{(v_2 - v_1)^2}{2} - \sigma (2S_I) \left(\frac{\lambda/2}{L} \right) = 0 . \quad (26)$$

Finally, Eq. 14 and Eq. 26 can be solved simultaneously for a and λ . This analysis can be applied to both water waves and oil waves. It is assumed that the crest of the wave will be sheared out by the drag force and will form a droplet with volume equal to the volume of the wave crest. Since, it is

already assumed that $a \ll S_l$, the volume of the droplet can be estimated as

$$V_d = \frac{1}{2} \times a \times \frac{\lambda}{2} \times S_l. \quad (27)$$

Hence the equivalent drop diameter will be

$$D_o = \left(\frac{3}{4\pi} V_d \right)^{1/3}. \quad (28)$$

Martinez-Bazan *et al.* (1999) studied the breakup phenomenon of the droplets in turbulent flow. Assuming a horizontal flow, only two energies will come into play, i.e. deformation energy (turbulent energy) and confinement energy (surface energy). The average deformation energy per unit volume acting on the surface of the drop is

$$E_\tau = \frac{1}{2} \rho_c \beta \varepsilon^{2/3} D_{drop}^{2/3}. \quad (29)$$

Where, ρ_c is the density of the continuous phase, β is the constant obtained by integrating the difference between the velocity fluctuations and it is estimated by Batchelor (1956) to be equal to 8.2. ε is the dissipation rate of turbulent kinetic energy and it is given by

$$\varepsilon = \frac{fv_c^3}{2D_h}. \quad (30)$$

Where, f is the friction factor, v_c is the velocity of continuous phase and D_h is the equivalent hydraulic diameter of the continuous phase. The confinement energy (surface energy) of the droplet per unit volume is given by

$$E_s = \frac{6\sigma}{D_{drop}}. \quad (31)$$

Martinez-Bazan *et al.* (1999) concluded in their study that all droplet diameters in the turbulent flow will lie in between the minimum diameter D_{min} and the critical diameter D_c as shown in Fig. 3. D_{min} and D_c are given below:

$$D_c = \left(\frac{12\sigma}{\beta\rho} \right)^{3/5} \varepsilon^{-2/5}. \quad (32)$$

$$D_{min} = \left(\frac{12\sigma}{\beta\rho D_o} \right)^{3/2} \varepsilon^{-1}. \quad (33)$$

Vielma (2006) and Serdar (2007) in their respective experimental studies reported that log-normal distribution is predominant in droplet size distribution for dispersed flow. Assuming, $D_{05} = D_{min}$, $D_{95} = D_c$ and log normal distribution, SMD (D_{SM}) can be estimated as

$$\text{Log}(D_{SM}) = \frac{1}{2} \text{Log}(D_{05} D_{95}). \quad (34)$$

Method 2

Instead of using the entrainment model and SMD estimation model, a closure relationship can be used. Angeli and Hewitt (2000) developed a correlation for SMD based on their experimental data.

$$D_{SM} v_c^{1.8} = 2 \times 10^{-2} \times f^{-3.12}. \quad (35)$$

Where, v_c is the velocity of continuous phase and f is friction factor of the corresponding phase.

Method 3

The critical droplet diameter can also be estimated using the Martinez-Bazan *et al.* (1999) method

$$D_c = \left(\frac{12\sigma}{\beta\rho} \right)^{3/5} \varepsilon^{-2/5}. \quad (36)$$

Where,

$$\varepsilon = \frac{fv_c^3}{2D_h}. \quad (37)$$

Since only turbulent forces and surface forces are considered, it can be assumed that,

$$D_{MAX} = D_c. \quad (38)$$

Hesketh *et al.* (1987) related the maximum and the SMD with a factor of 0.62.

$$D_{SM} = 0.62 \times D_{MAX}. \quad (39)$$

Method 4

The maximum droplet size can also be estimated using the Hinze (1955) model,

$$D_{MAX} \left(\frac{\rho_c}{\sigma} \right)^{3/5} \varepsilon^{2/5} = 0.725. \quad (40)$$

Then, the SMD can be estimated using Hesketh *et al.* (1987) relation (Eq. 39).

Mixture Properties Calculation

Zhang *et al.* (2003) proposed a unified model for slug liquid holdup. In their study, energy balance between turbulent energy and surface energy was used to predict the slug holdup. Same approach is used in the present model wherein the energy balance is done in each phase. The surface energy per unit length of pipe and turbulent energy per unit length, in either phase are

$$E_s = \frac{6\sigma}{D_{SM}} A(1 - H_C). \quad (41)$$

$$E_\tau = \frac{3}{2} \rho_C (v^*)^2 A H_C. \quad (42)$$

Where, H_C is the holdup of continuous phase and A is the cross sectional area of the segregated layer. v^* is friction velocity. In the present model it is also assumed that E_τ and E_s have a linear relationship with C as slope and E_0 as constant.

$$E_\tau = C E_s + E_0. \quad (43)$$

The values of C and E_0 can be determined by plotting E_τ against E_s . In Fig. 4, Vielma (2006) data is plotted for E_τ vs. E_s . It can be inferred that there is a linear relationship between turbulent energy and surface energy. E_0 is the threshold turbulent energy regarding to the onset of entrainment. Below this turbulent energy there will be no entrainment. Further analysis is required to determine the value of C and E_0 . Equation 43 can be used to predict the dispersed phase holdup for each segregated layer.

Then, this holdup information can be used to calculate the new mixture properties of each segregated layer using following equations.

$$\rho_M = \rho_D(1 - H_D) + \rho_C H_D. \quad (44)$$

$$\mu_M = (\eta_{pack} \pm 10\%) (We)^{-1/8} \mu_C (1 - \eta_D)^{-2.5}. \quad (45)$$

$$We = \frac{D_H \rho_M v_M^2}{2\sigma}. \quad (46)$$

$$q_{1,T} = A_1(1 - H_{D1})v_1 + A_2 H_{D2} v_2. \quad (47)$$

$$q_{2,T} = A_2(1 - H_{D2})v_2 + A_1 H_{D1} v_1. \quad (48)$$

$$v_{SL1} = v_1 \frac{A_1}{A_p}. \quad (49)$$

To incorporate the effect of droplet size and emulsification Shi (2001) modified the Brinkman viscosity correlation. In Eq. 45, η_{pack} is the phase inversion point water concentration while “+” applies when input water cut is greater than η_{pack} and “-” applies when input water cut is less than η_{pack} . We is the Weber number associated with the segregated layer and is defined as Eq. 46. Equations 47 and 48 are steady state continuity equation for oil and water, respectively. Solving Eqs. 47 and 48 simultaneously will give the new velocity of each segregated mixed phase. The corresponding new superficial velocity of each layer mixed phase can be calculated from Eq. 49.

These mixture properties are again used in two-fluid model to get new value of interface height and hence to get new set of flow parameters for each segregated phase layer. This will cause an iteration which will go on until the convergence is reached.

Near Future Tasks

The main tasks for the future are:

- Development of computer code for the model.
- In depth analysis of turbulent energy and surface energy relationship.
- Validation of the model with experimental results.

References

- Al-Wahaibi, T., Angeli, P., “Transition between Stratified and Non-stratified Horizontal Oil-water Flows. Part I: Stability Analysis. *Chemical Engineering Science* (2007), **62**, 2915-2928.
- Al-Wahaibi, T., Smith, M., Angeli, P., “Transition Between Stratified and Non-stratified Horizontal Oil-water Flows. Part II: Mechanism of Drop Formation,” *Chemical Engineering Science* (2007), **62**, 2929-2940.
- Angeli, P. and Hewitt, G.F., “Drop Size Distribution in Horizontal Oil-Water Dispersed Flows,” *Chemical Engineering Science* (2000), **55**, 3133-3143.
- Hesketh, R.P., Russell, T.W.F., and Etchells, A. W. (1987), “Bubble Size in Horizontal Pipelines,” *AIChE J.* (1987), **33**, 663-667.
- Hinze, J.O., “Fundamentals of the Hydrodynamic Mechanism of Splitting in Dispersion Processes,” *AIChE J.*(1955), **3**, 289–295.
- Martinez-Bazan, C., Montanes, J.L. and Lasheras, J.C., “On the Break-up of Air Bubble Injected into A Fully Developed Turbulent Flow, Part I: Break-up Frequency,” *J. Fluid Mechanics* (1999), **401**, 157–182.
- Martinez-Bazan, C., Montanes, J.L. and Lasheras, J.C., “On the Break-up of Air Bubble Injected into A Fully Developed Turbulent Flow, Part II: Size Population Density Function of the Resulting Daughter Bubbles,” *J. Fluid Mechanics* (1999), **401**, 183–207.
- Shi H.: “A Study of Oil-Water Flows in Large Diameter Horizontal Pipelines,” Ph.D. Dissertation, Ohio University (2001).
- Trallero, J.L.: “Oil-Water Flow Patterns in Horizontal Pipes,” Ph.D. Dissertation, University of Tulsa, Tulsa, Oklahoma (1995).
- Vielma, M.: “Characterization of Oil-Water Flow in Horizontal Pipes,” M.S. Thesis, University of Tulsa (2007).
- Zhang, H.-Q., Wang, Q., Sarica, C. and Brill, J.P., “A Unified Mechanistic Model for Slug Liquid Holdup and Transition Between Slug and Dispersed Bubble Flows,” *Int. J. Multiphase Flow* (2003), **29**, 97-107.

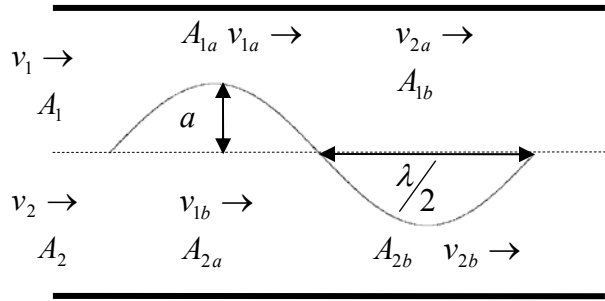


Figure 1: Formation of Waves in Stratified Flow

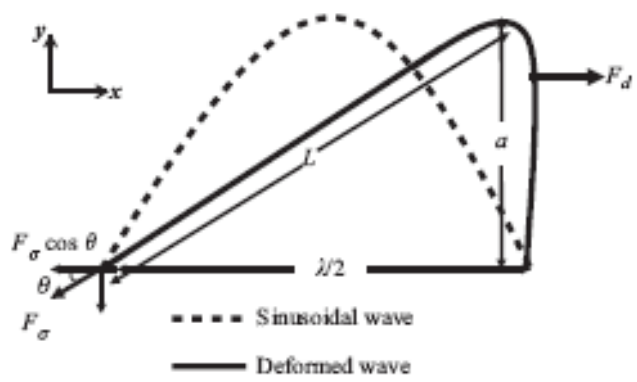


Figure 2: Force Balance on Deformed Wave (Wahaibi and Angeli, 2007)

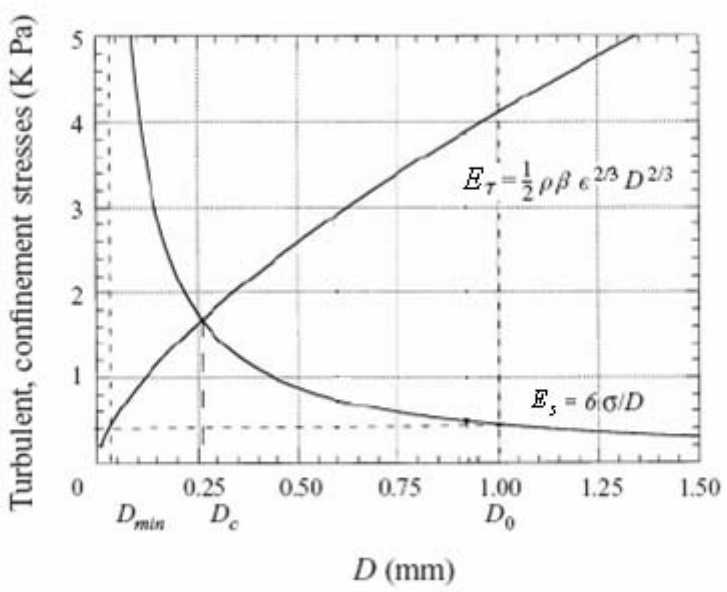


Figure 3: Turbulent and Surface Stresses vs. Droplet Diameter (Martinez-Bazan et al., 1999)

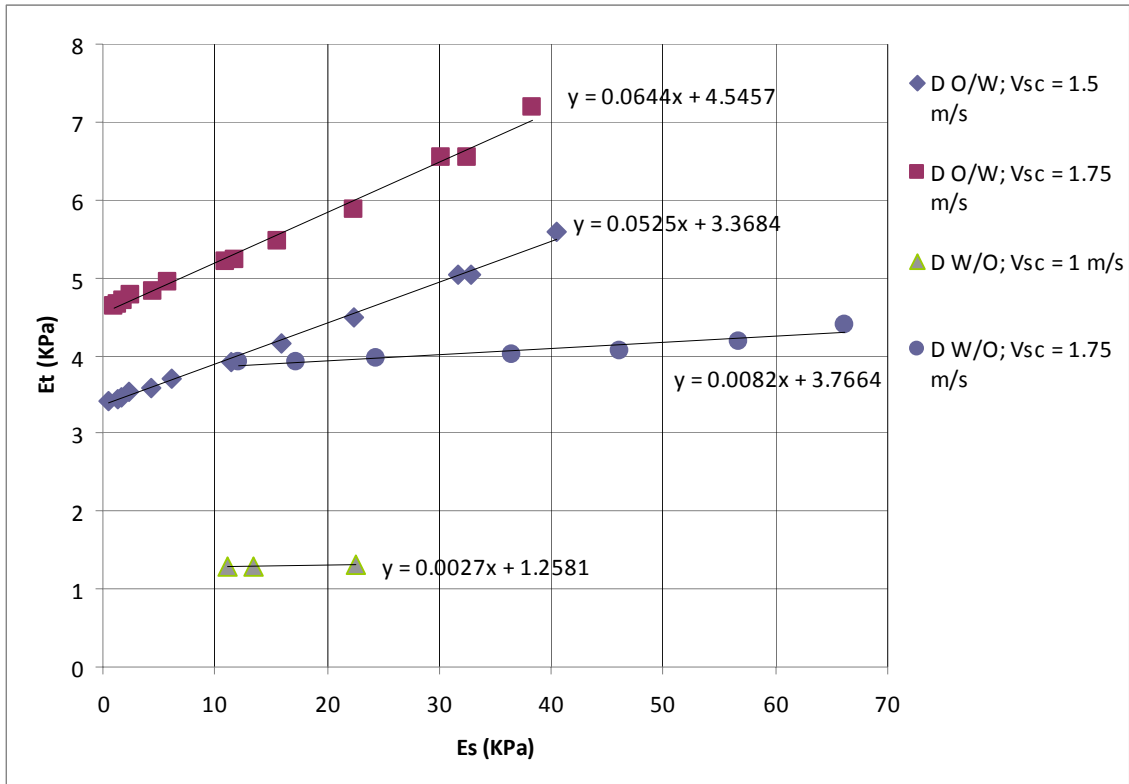


Figure 4: Turbulent Energy and Surface Energy Correlation (Vielma, 2006)

Upward Multiphase Flow in a Vertical Annulus



- ◆ **Significance**
 - Production Through Annulus
 - Liquid Loading Problem
- ◆ **Objective**
 - Significant Improvements in Multiphase Flow Modeling Since 1985
 - Development of an Improved Mechanistic Model for Vertical Annulus
- ◆ **Past Studies**
 - Caetano
 - ▲ Thorough Experimental and Modeling Study in 1985

Upward Multiphase Flow in a Vertical Annulus ...



- ◆ **Current Study**
 - Tingting Yu Completed a Literature Search
 - Studied Caetano Work Thoroughly
 - Developed a New Model Based on Unified Modeling Approach
 - New Model Outperforms the Original Unified Model
- ◆ **Near Future Tasks**
 - Refinement of the Model



Fluid Flow Projects

Modeling of Gas-Liquid Flow in Upward Vertical Annuli

Tingting YU

Advisory Board Meeting, September 17, 2008

Outline

- ◆ Objectives
- ◆ Introduction
- ◆ Hydrodynamic Models for Individual Flow Patterns
- ◆ New Model and Unified Model Performances
- ◆ Research Plan
- ◆ Schedule

Objectives

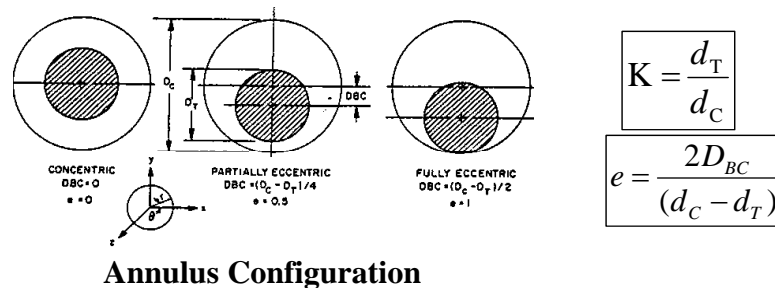
- ◆ **Theoretically Investigate Gas-Liquid Flow in Upward Vertical Concentric and Eccentric Annuli**
- ◆ **Develop a New Model and Validate Model with Experimental Data**

Significance

- ◆ **Flow through Annuli Encountered in Many Applications**
 - **Gas Well Production**
 - **Wells under Various Types of Artificial Lifts**
- ◆ **Oil Wells of High Production Rates Produce through Casing-Tubing Annulus**

Introduction

- ◆ Annulus Formed by Two Circular Pipes, One in the Other
- ◆ Two Geometrical Parameters:



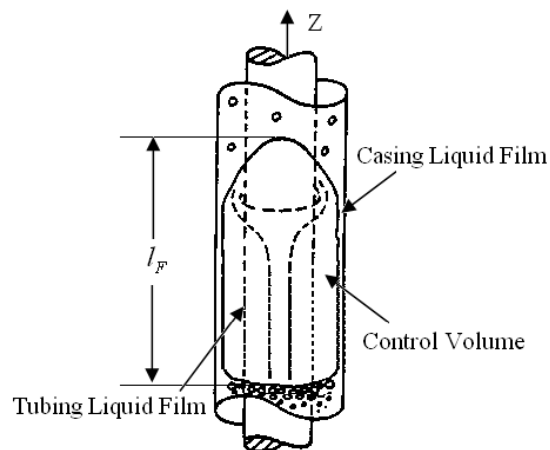
Literature Review Summary

- ◆ No Modeling for Vertical Annulus Flow After Caetano (1986)
- ◆ Lage et al. (2000) and Omurlu et al. (2007) Developed Mechanistic Models for Horizontal Annulus Flow
- ◆ Several Advances in Upward Pipe Flow Modeling to be Applied in Annulus Flow

Modeling of Annulus Flow

- ◆ Unified Model Predictions of Liquid Holdup and Pressure Gradient of Annulus Flow Not Satisfactory
- ◆ New Model Developed by Taking Annulus Configuration into Account
- ◆ Model Based on Zhang et al. (2003) Unified Modelling Approach

Control Volume



Slug Flow Model

◆ Mass Conservation

➤ Liquid in Film Zone

$$H_{LS}(v_T - v_S) = H_{LFC}(v_T - v_{FC}) + H_{LFT}(v_T - v_{FT})$$

➤ Gas in Liquid Film Zone

$$(1 - H_{LS})(v_T - v_S) = (1 - H_{LFC} - H_{LFT})(v_T - v_C)$$

Slug Flow Model...

◆ Continuity Equations

➤ Liquid in Slug Unit

$$l_U v_{SL} = l_S H_{LS} v_S + l_F (H_{LFC} v_{FC} + H_{LFT} v_{FT})$$

➤ Gas in Slug Unit

$$l_U v_{SG} = l_S (1 - H_{LS}) v_S + l_F (1 - H_{LFC} - H_{LFT}) v_C$$

Slug Flow Model...

◆ Momentum Equation for Liquid Film

➤ Casing Film

$$\frac{(P_2 - P_1)}{l_F} = \frac{\rho_L (v_{FC} - v_T)(v_{FC} - v_S) - \rho_L \frac{H_{LFT}}{H_{LFC}} (v_{FC} - v_T)v_S}{l_F} + \frac{\tau_{IC} S_{IC} - \tau_{FC} S_{FC}}{H_{LFC} A} - \rho_L g \sin \theta$$

➤ Tubing Film

$$\frac{(P_2 - P_1)}{l_F} = \frac{\rho_L (v_{FT} - v_T)(v_{FT} - v_S) - \rho_L \frac{H_{LFC}}{H_{LFT}} (v_{FT} - v_T)v_S}{l_F} + \frac{\tau_{IT} S_{IT} - \tau_{FT} S_{FT}}{H_{LFT} A} - \rho_L g \sin \theta$$

Slug Flow Model...

◆ Momentum Equation for Gas Core

$$\frac{(P_2 - P_1)}{l_F} = \frac{\rho_C (v_T - v_C)(v_S - v_C)}{l_F} + \frac{\tau_{IT} S_{IT} + \tau_{IC} S_{IC}}{(1 - H_{LFT} - H_{LFC}) A} - \rho_C g \sin \theta = 0$$

Slug Flow Model...

◆ Combined Momentum Equation for Casing Film

$$\frac{\rho_L(v_{FC}-v_T)(v_{FC}-v_S)-\rho_L \frac{H_{LFT}}{H_{LFC}}(v_{FT}-v_T)v_S-\rho_C(v_C-v_T)(v_C-v_S)}{l_F} - \frac{\tau_{FC}S_{FC}}{H_{LFC}A} + \frac{\tau_{IT}S_{IT}}{(1-H_{LFC}-H_{LFT})A} + \tau_{IC}S_{IC} \left(\frac{1}{H_{LFC}A} + \frac{1}{(1-H_{LFC}-H_{LFT})A} \right) + (\rho_C - \rho_L)g \sin\theta = 0$$

Slug Flow Model...

◆ Combined Momentum Equation for Tubing Film

$$\frac{\rho_L(v_{FT}-v_T)(v_{FT}-v_S)-\rho_L \frac{H_{LFC}}{H_{LFT}}(v_{FC}-v_T)v_S-\rho_C(v_C-v_T)(v_C-v_S)}{l_F} - \frac{\tau_{FT}S_{FT}}{H_{LFT}A} + \frac{\tau_{IC}S_{IC}}{(1-H_{LFC}-H_{LFT})A} + \tau_{IT}S_{IT} \left(\frac{1}{H_{LFT}A} + \frac{1}{(1-H_{LFC}-H_{LFT})A} \right) + (\rho_C - \rho_L)g \sin\theta = 0$$

Slug Flow Model...

◆ Combined Momentum Equations for Tubing, Casing Liquid Films and Gas Core

$$\frac{\rho_L \frac{H_{LFT}}{H_{LFC}} (v_{FT} - v_T) v_S - \rho_L \frac{H_{LFC}}{H_{LFT}} (v_{FC} - v_T) v_S}{l_F} - \frac{\tau_{IC} S_{IC}}{H_{LFC} A} + \frac{\tau_{FC} S_{FC}}{H_{LFC} A} - \frac{\tau_{FT} S_{FT}}{H_{LFT} A} + \frac{\tau_{IT} S_{IT}}{H_{LFT} A} + (\rho_C - \rho_L) g \sin \theta = 0$$

Annular Flow Model

◆ Momentum Equation for Tubing and Casing Films

➤ Casing Film

$$\frac{\tau_{IC} S_{IC}}{(1 - H_{LFC} - H_{LFT}) A} - \frac{\tau_{FT} S_{FT}}{H_{LFT} A} + \tau_{IT} S_{IT} \left(\frac{1}{H_{LFT} A} + \frac{1}{(1 - H_{LFC} - H_{LFT}) A} \right) + (\rho_C - \rho_L) g \sin \theta = 0$$

➤ Tubing Film

$$\frac{\tau_{IT} S_{IT}}{(1 - H_{LFC} - H_{LFT}) A} - \frac{\tau_{FC} S_{FC}}{H_{LFC} A} + \tau_{IC} S_{IC} \left(\frac{1}{H_{LFC} A} + \frac{1}{(1 - H_{LFC} - H_{LFT}) A} \right) + (\rho_C - \rho_L) g \sin \theta = 0$$

Churn Flow Model

- ◆ Apply Slug Flow Model from Zhang et al. (2003) Unified Model in Churn Flow by Using Representative Diameter
- ◆ Different Slug Liquid Holdup Used in Present Model
- ◆ Concentric Annulus

$$H_{LS} = 0.8$$

Fully Eccentric Annulus

$$H_{LS} = 0.88$$

Shear Stresses

Film

$$\tau_F = f_F \frac{\rho_L |v_F| v_F}{2}$$

Gas core

$$\tau_C = f_C \frac{\rho_C |v_C| v_C}{2}$$

Interface

$$\tau_{IC} = f_I \frac{\rho_C (v_C - v_F) |v_C - v_F|}{2}$$

Closure Relationships

- ◆ Wall Friction Factor
- ◆ Interfacial Friction Factors
- ◆ Film Liquid Holdup Ratio
- ◆ Liquid Entrainment Fraction in Gas Core
- ◆ Slug Liquid Holdup
- ◆ Slug Translational Velocity
- ◆ Slug Length
- ◆ Reference Diameter

Wall Friction Factor

- ◆ Friction Factor for Shear Stress at Wall

$$f = C \text{Re}^{-n}$$

$$C = 16, n = 1 \quad \text{Laminar}$$

$$C = 0.046, n = 0.2 \quad \text{Turbulent}$$

- ◆ Caetano's Friction Factor

$$f_{CA} = \frac{16}{\text{Re}} \frac{(1-K)^2}{\left[\frac{1-K^4}{1-K^2} - \frac{1-K^2}{\ln(1/K)} \right]} \quad \text{Laminar}$$

Wall Friction Factor

◆ Caetano's Friction Factor

$$\frac{1}{\left\{ f_{CA} \left(\frac{F_P}{F_{CA}} \right)^{0.45 \exp[-(\text{Re}-3000)/10^6]} \right\}^{1/2}} = \text{Turbulent}$$

$$4.0 \log \left\{ \text{Re} \left[f_{CA} \left(\frac{F_P}{F_{CA}} \right)^{0.45 \exp[-(\text{Re}-3000)/10^6]} \right]^{1/2} \right\} = 0.40$$

Interfacial Friction Factor

Annular Flow – Ambrosini et al. (1991)

$$f_I = f_S \left[1 + 13.8 We_G^{0.2} Re_G^{-0.6} \left(h_F^+ - 200 \sqrt{\rho_G / \rho_L} \right) \right]$$

$$We_G = \frac{\rho_G v_G^2 d}{\sigma} \quad Re_G = \frac{\rho_G v_G d}{\mu_G}$$

$$h_F^+ = \frac{\rho_G h_F v_G^*}{\mu_G} \quad v_G^* = \sqrt{\tau_I / \rho_G}$$

$$f_S = 0.046 Re_G^{-0.2}$$

Film Liquid Holdup Ratio

◆ Caetano's (1986) Liquid Film Holdup Equations

$$H_{LFT} = \frac{4\delta_T}{d_c} K \frac{\left(1 + \frac{\delta_T}{d_T}\right)}{(1-K^2)} \quad H_{LFC} = \frac{4\delta_C}{d_c} \frac{\left(1 + \frac{\delta_C}{d_C}\right)}{(1-K^2)}$$

$$\frac{H_{LFT}}{H_{LFC}} = \frac{\delta_T}{\delta_C} K \quad \frac{\delta_T}{\delta_C} = \frac{W_T'}{(2\pi - W_T')K}$$

$$W_T' = \frac{1}{(1-K^2)} \left(2 \sin^{-1}(K) + 2K\sqrt{1-K^2} - K^2\pi \right)$$

Liquid Entrainment Fraction

◆ Oliemans et al. (1986) and Zhang et al. (2003) Correlation

$$\frac{F_E}{1-F_E} = 0.003 We_{SG}^{1.8} Fr_{SG}^{-0.92} Re_{SL}^{0.7} Re_{SG}^{-1.24} \left(\frac{\rho_L}{\rho_G}\right)^{0.38} \left(\frac{\mu_L}{\mu_G}\right)^{0.97}$$

$$We_{SG} = \frac{\rho_G v_{SG}^2 d}{\sigma} \quad Fr_{SG} = \frac{v_{SG}}{\sqrt{gd}}$$

$$Re_{SL} = \frac{\rho_L v_{SL} d}{\mu_L} \quad Re_{SG} = \frac{\rho_G v_{SG} d}{\mu_G}$$

Slug Liquid Holdup

Zhang et al. (2003) Model

$$H_{LS} = \frac{1}{1 + \frac{T_{sm}}{3.16[(\rho_L - \rho_G)g\sigma]^{1/2}}}$$

$$T_{sm} = \frac{1}{C_e} \left[\frac{f_S}{2} \rho_S v_S^2 + \frac{d_r}{4} \frac{\rho_F H_{LF} (v_T - v_F)(v_S - v_F) + \rho_C (1 - H_{LF})(v_T - v_C)(v_S - v_C)}{l_S} \right]$$

$$C_e = \frac{2.5 - |\sin(\theta)|}{2}$$

Slug Translational Velocity

◆ Nicklin (1962) and Hasan and Kabir (1900)

$$v_T = C_S v_S + v_D$$

Drift velocity

$$v_D = 0.345(1 + 0.1K) \sqrt{gd_c(\rho_L - \rho_G) / \rho_L}$$

Slug Length

- ◆ Taitel et al. (1980) and Barnea and Brauner (1985)

$$l_s = (32.0 \cos^2 \theta + 16.0 \sin^2 \theta) d_r$$

Reference Diameter

- ◆ Representative Diameter

$$d_r = \sqrt{d_C^2 - d_T^2}$$

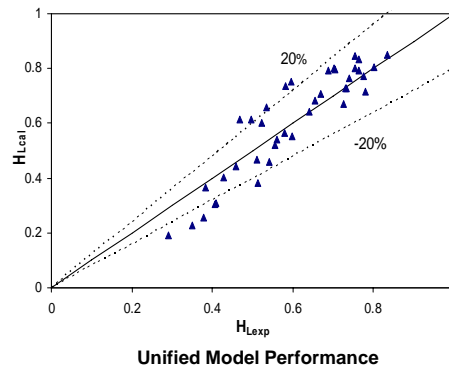
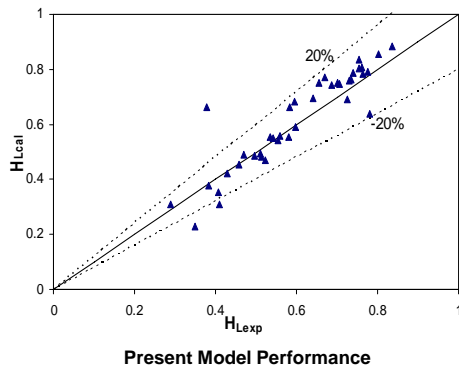
- ◆ Hydraulic Diameter

$$d_H = d_C - d_T$$

Liquid Holdup – Slug Flow Concentric Annulus



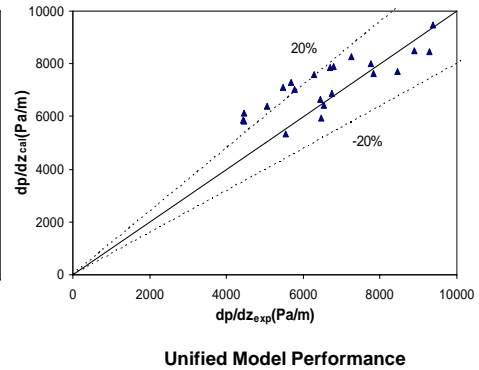
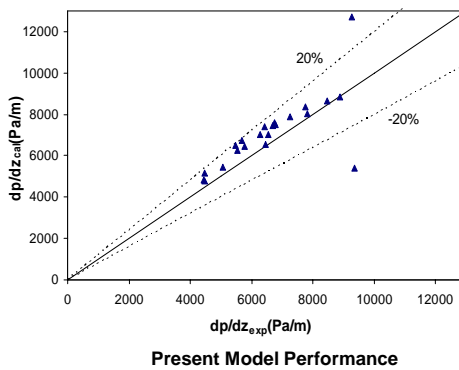
Air and water



Pressure Gradient – Slug Flow Concentric Annulus



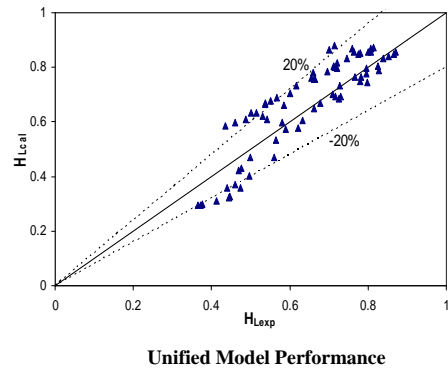
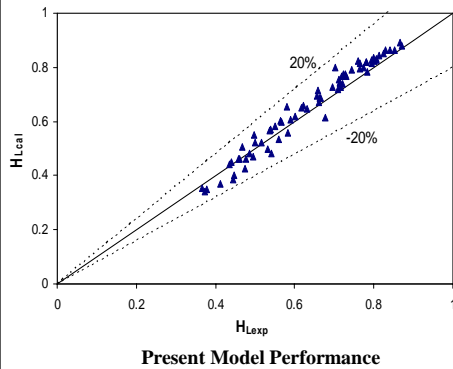
Air and water



Liquid Holdup – Slug Flow Fully Eccentric Annulus



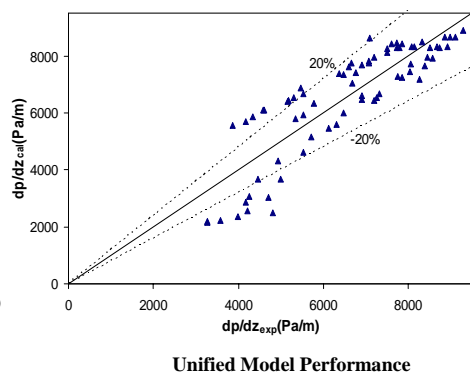
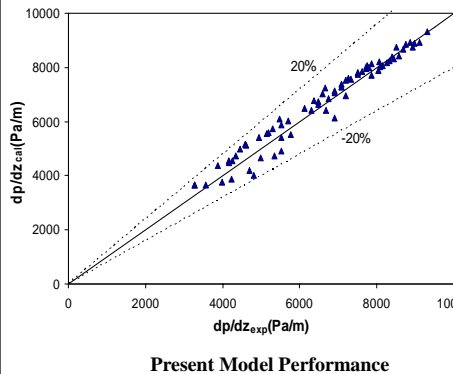
Air and water



Pressure Gradient – Slug Flow Fully Eccentric Annulus



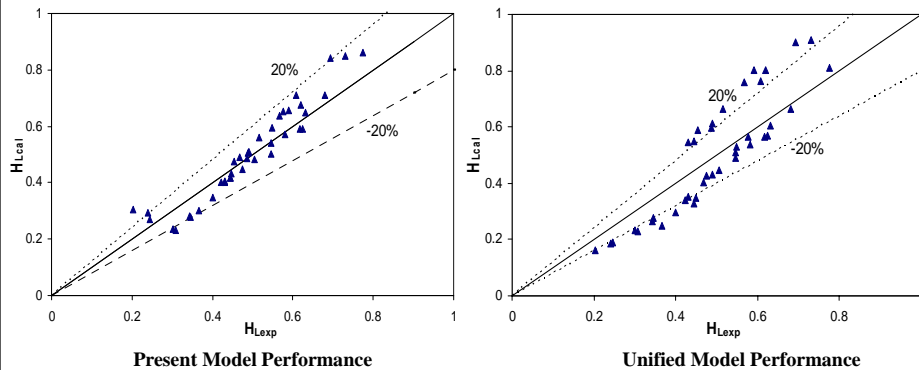
Air and Water



Liquid Holdup – Slug Flow Concentric Annulus



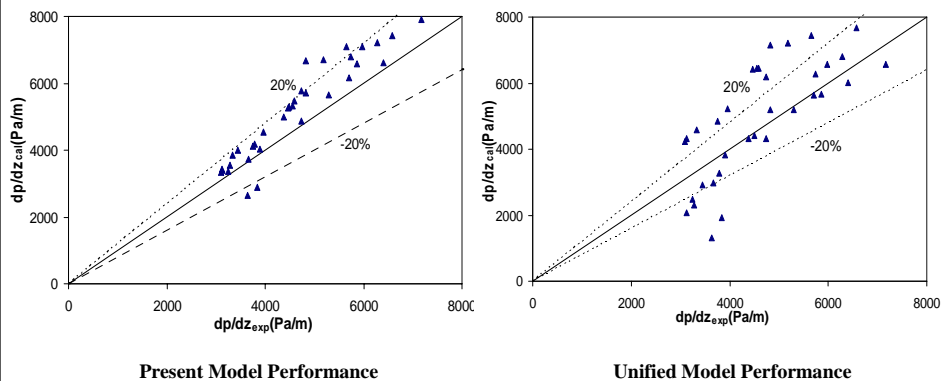
Air and Kerosene



Pressure Gradient – Slug Flow Concentric Annulus



Air and Kerosene



Slug Flow Model Performance

- ◆ **Slug Flow Model Performs Well Using Representative Diameter for Fully Eccentric Annulus Flow**
- ◆ **Pressure Gradient Over Prediction Exists for Concentric Annulus Flow**
- ◆ **Further Improvement Needed**

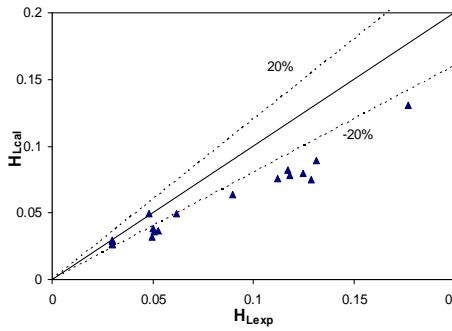
Annular Flow

- ◆ **Four Combinations of Reference Diameters and Friction Factors Used for Each Case in Present Model**
- ◆ **Combination Performances are Different**
- ◆ **Results from Representative Diameter/Unified Model Friction Factor Combination Presented**

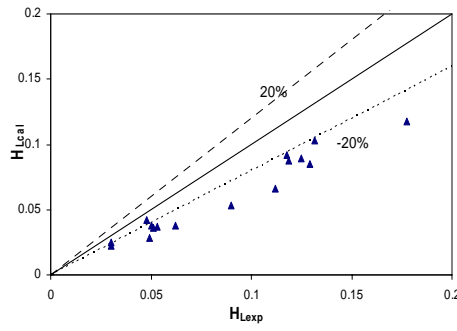
Liquid Holdup – Annular Flow in Concentric Annulus



Air and Water



Present Model Performance

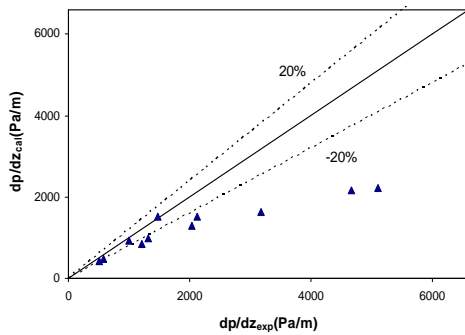


Unified Model Performance

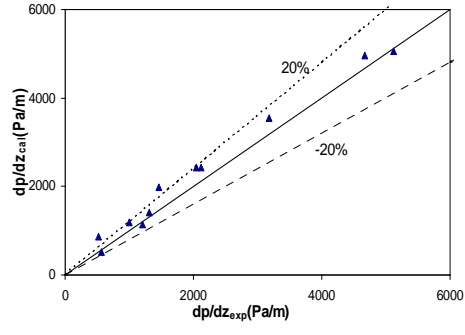
Pressure Gradient – Annular Flow Concentric Annulus



Air and Water



Present Model Performance

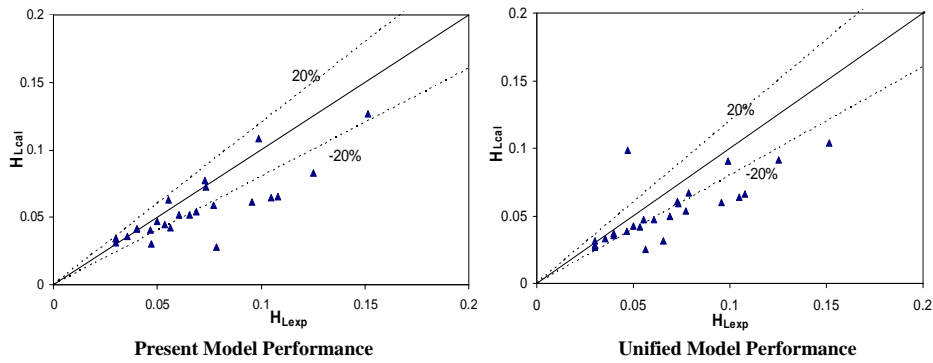


Unified Model Performance

Liquid Holdup – Annular Flow Fully Eccentric Annulus



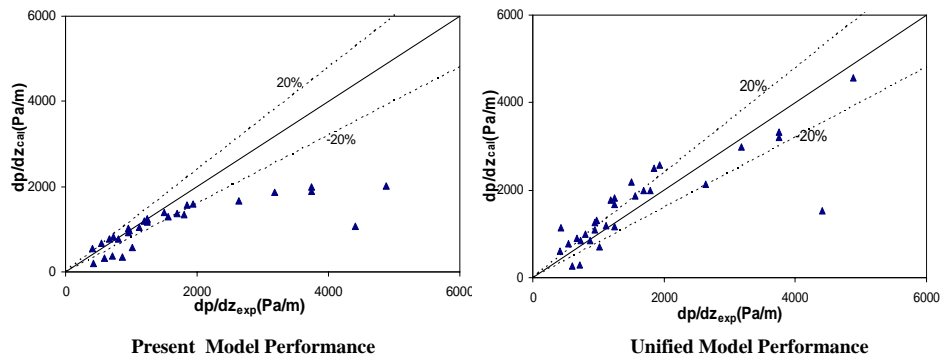
Air and Water



Pressure Gradient – Annular Flow Fully Eccentric Annulus



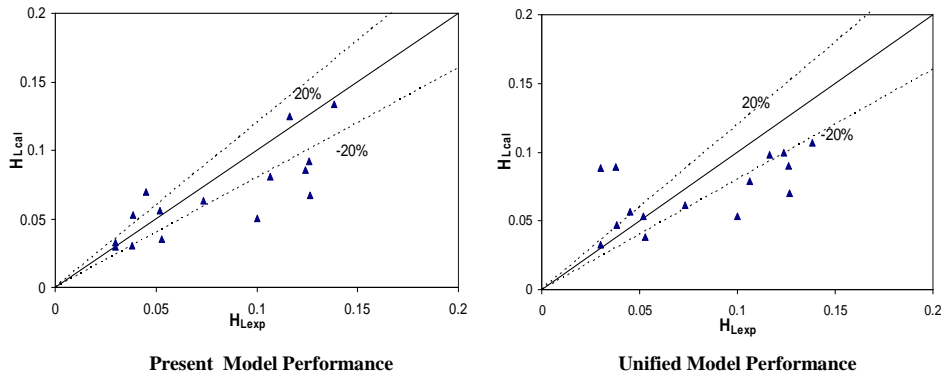
Air and Water



Liquid Holdup – Annular Flow Concentric Annulus



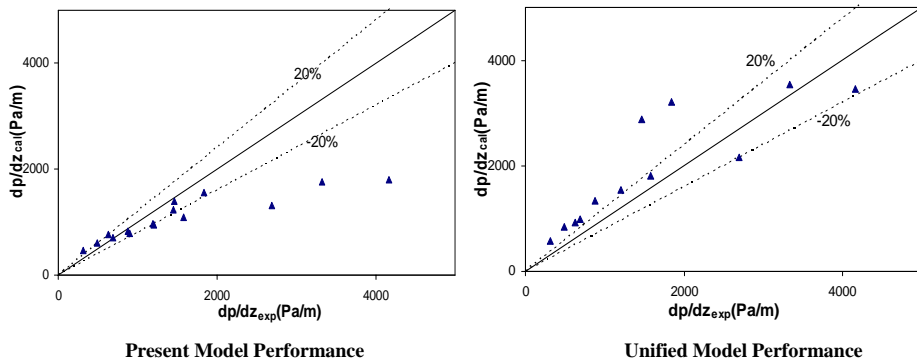
Air and Kerosene



Pressure Gradient – Annular Flow Concentric Annulus



Air and Kerosene

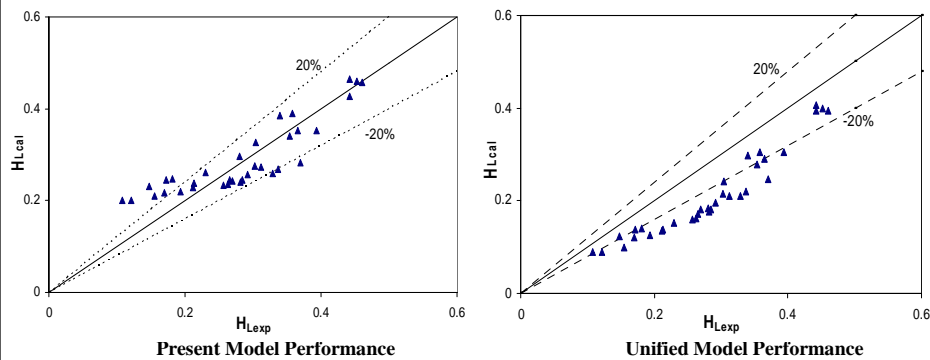


Annular Flow Model Performance

- ◆ Annular Flow Model Performance not as Good as Slug Flow Model
- ◆ Uncertainties in Measurements of Liquid Holdup and Pressure Gradient
- ◆ Model Needs to be Improved

Liquid Holdup – Churn Flow Concentric Annulus

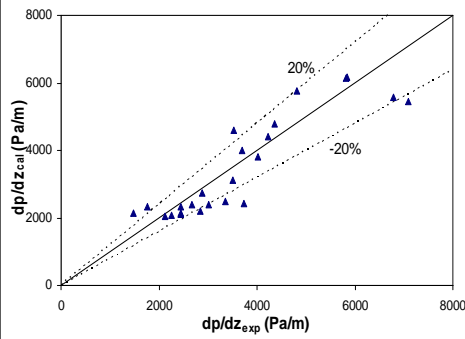
Air and Water



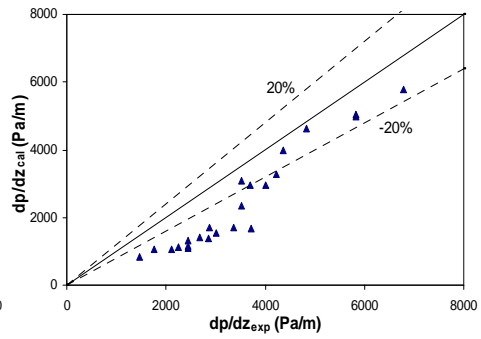
Pressure Gradient – Churn Flow Concentric Annulus



Air and Water



Present Model Performance

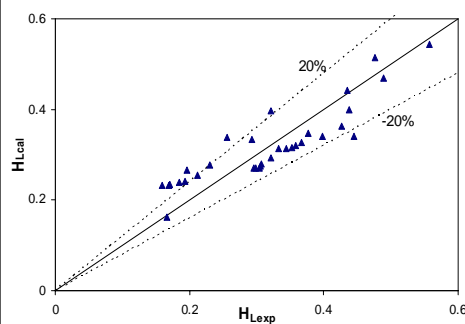


Unified Model Performance

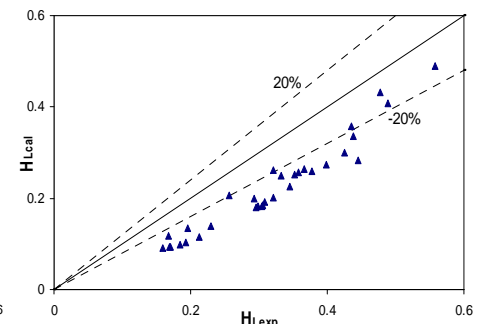
Liquid Holdup – Churn Flow Fully Eccentric Annulus



Air and Water



Present Model Performance

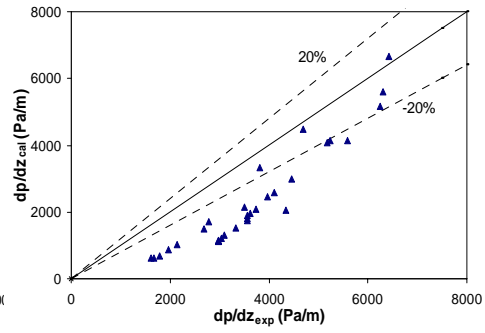
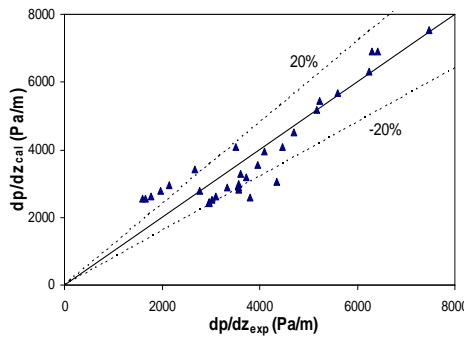


Unified Model Performance

Pressure Gradient – Churn Flow Fully Eccentric Annulus



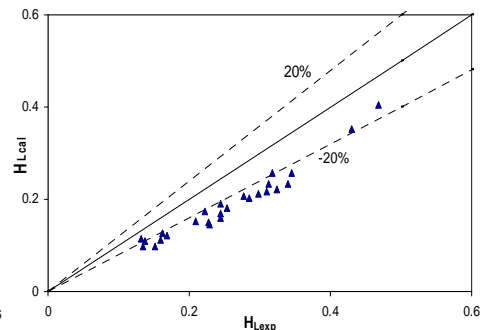
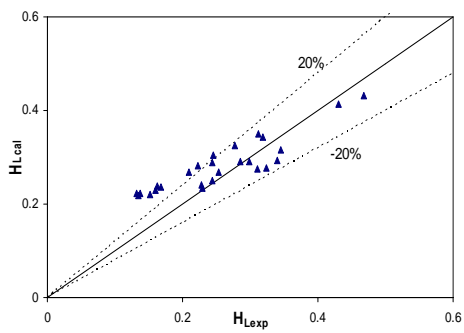
Air and Water



Liquid Holdup – Churn Flow Concentric Annulus

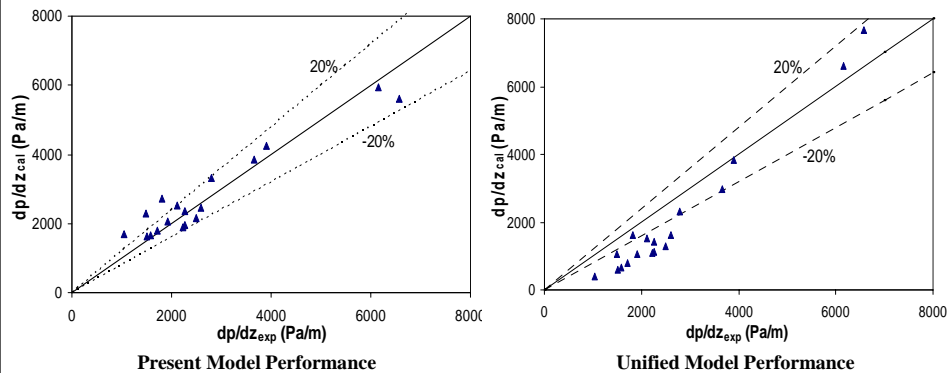


Air and Kerosene



Pressure Gradient – Churn Flow Concentric Annulus

Air and Kerosene



Churn Flow Model Performance

- ◆ Better Prediction than Unified Model
- ◆ Constant Slug Liquid Holdup Used in Model May Cause Scattering
- ◆ Further Improvement Needed

Research Plan

- ◆ **Improve Hydrodynamic Models**
- ◆ **Develop Flow Pattern Transition Models**
- ◆ **Validate New Model**
- ◆ **Final Report**

Project Schedule

- ◆ **Model Development** **October 2008**
- ◆ **Model Verification** **February 2009**
- ◆ **Final Report** **May 2009**

Questions & Comments



Questions?

Modeling of Gas-Liquid Flow in an Upward Vertical Annulus

Tingting YU

PROJECTED COMPLETION DATES:

Literature Review.....	Completed
Model Development.....	October 2008
Model Validation.....	December 2008
Final Report.....	May 2009

Objectives

The objectives of this study are:

- Theoretically investigate upward gas-liquid two-phase flow in concentric and eccentric annuli
- Analyze data from a previous experimental study (Caetano, 1986) and develop a new model for gas-liquid two-phase flow in annuli

Introduction

As shown in Figure 1, an annulus is formed by a pipe being located inside a larger pipe. Fluid flows through the area bounded by the outer pipe casing inner wall and the tubing inner pipe outer wall. There are two important parameters to identify this configuration: annulus pipe diameter ratio and the degree of eccentricity.

The pipe diameter ratio is given by:

$$K = \frac{d_T}{d_C}, \quad (1)$$

where d_T is the outer diameter of the tubing and d_C is the inner diameter of the casing. The degree of eccentricity accounts for the displacement of the inner pipe center from the outer pipe center and is expressed by

$$e = \frac{2DBC}{(d_C - d_T)}. \quad (2)$$

DBC is the distance between the two pipe centers.

In the petroleum industry, multiphase flow in wells normally occurs in a tubing string. However, many oil wells with high production rates produce through the casing-tubing annulus. This trend can be dictated by economics, multiple completions and regulated production rates. Although the number of these wells is small compared with all producing wells, these “casing flow” wells still account for a significant part of the world oil production.

Many applications of casing flow in the oil industry are also found in various types of artificial lift. In sucker rod pumping wells, a rod string is installed inside the tubing string to connect the prime mover unit on the surface to the pump at the bottom of the well. The fluids are pumped upward through the tubing-rod string annulus.

Another application of flow through an annulus is found in gas well production. In order to remove or “unload” undesirable liquids that can accumulate at the bottom of these wells, a siphon tube is often installed inside the tubing string. The normal permanency of the siphon tube in the tubing string requires the fluids to flow upward through the tubing string-siphon tube annulus.

Most researchers have treated the annulus based on the hydraulic diameter concept. The hydraulic diameter is four times the area for flow divided by the wetted perimeter. For annulus configurations,

$$d_H = d_C - d_T, \quad (3)$$

where d_H is hydraulic diameter.

However, the hydraulic diameter is not always the most representative characteristic dimension for flow in an annulus. Omurlu and Evren (2007) introduced

a “representative diameter” d_r for a fully eccentric annulus, which they claimed worked better than hydraulic diameter. For annular configurations:

$$d_r = \sqrt{d_C^2 - d_T^2} . \quad (4)$$

where d_r is representative diameter.

The Zhang *et al.* (2003) unified model was tested first against Caetano’s (1986) experimental data using hydraulic diameter and representative diameter, respectively. The results were dissatisfactory due to the wrong prediction of flow patterns and large errors in slug flow and annular flow.

Considering the limitation of the previous models for annulus flow, new flow pattern transition models and hydrodynamic models will be developed based on annulus configuration. The model results will be compared with Caetano’s (1986) experimental data.

Model Development

The new hydrodynamic models will be developed following the approach of the Zhang *et al.* (2003) unified model by taking the annulus configuration into account.

Modeling of Slug Flow

Mass Balance Equations in Film Zone

The hydrodynamic model developed for slug flow in annuli considers two liquid films, and the entire liquid film zone of a slug unit is considered to be the control volume, as shown Figure 2. The input mass flow rate at the upper boundary of the film zone is equal the output mass flow rate at the lower boundary of the film zone. The analysis is carried out using Lagrangian coordinate system.

Assuming the incompressible flow at a given point, the mass balances can be expressed in terms of volumetric flow rates. The mass balance for the liquid phase in the film zone can be written as

$$H_{LS}(v_T - v_S) = H_{LFC}(v_T - v_{FC}) + H_{LFT}(v_T - v_{FT}), \quad (5)$$

where H_{LFC} and H_{LFT} are the liquid holdup in the casing film and tubing film, respectively. The fluid velocity in the slug body is,

$$v_S = v_{SL} + v_{SG} . \quad (6)$$

Similarly, the mass balance for gas phase can be written as

$$(1 - H_{LS})(v_T - v_S) = (1 - H_{LFC} - H_{LFT})(v_T - v_C). \quad (7)$$

Overall Mass Balances

Considering the gas and liquid flow along the slug unit and the incompressibility of gas and liquid, the mass balance equations for liquid and gas can be written, respectively.

$$l_U v_{SL} = l_S H_{LS} v_S + l_F (H_{LFC} v_{FC} + H_{LFT} v_{FT}) \quad (8)$$

$$l_U v_{SG} = l_S (1 - H_{LS}) v_S + l_F (1 - H_{LFC} - H_{LFT}) v_C . \quad (9)$$

The slug unit length is

$$l_U = l_S + l_F . \quad (10)$$

Momentum Equations

In the Zhang *et al.* (2003) unified model., the forces acting on the left and right boundaries of the liquid film include momentum exchange between slug body and liquid film, frictional forces acting at the wall, static pressure differences between left and right boundaries, frictional forces acting at the interface and also gravitational forces. In this study, the same forces are considered in deriving the momentum equations for annulus flow except that two liquid films are considered in the derivation process.

The momentum exchange between casing film and gas pocket is

$$\rho_L A H_{LFC} (v_{FC} - v_T) v_{FC} .$$

The frictional force acting on casing film at the wall is

$$-\tau_{FC} S_{FC} l_F .$$

The frictional force acting on the interface between casing film and gas pocket is

$$-\tau_{IC} S_{IC} l_F .$$

All forces acting on the casing liquid film should be in balance and hence the momentum equation for the casing film can be written as

$$\begin{aligned} & H_{LFC} A P_1 - H_{LFC} A P_2 + \rho_L A H_{LFC} (v_{FC} - v_T) v_{FC} \\ & - \rho_L A H_{LS} (v_S - v_T) v_S + \tau_{CF} S_{CF} l_F \\ & - \tau_{CF} S_{CF} l_F - \rho_L H_{LFC} l_F A g \sin \theta = 0. \end{aligned} \quad (11)$$

Similarly, the momentum equation for the tubing film can be written as

$$\begin{aligned} & H_{LFT}AP_1 - H_{LFT}AP_2 + \rho_L AH_{LFT}(v_{TF} - v_T)v_{FT} \\ & - \rho_L AH_{LS}(v_S - v_T)v_S + \tau_{IT}S_{IT}l_F \\ & - \tau_{TF}S_{TF}l_F - \rho_L H_{LFT}l_F g \sin \theta = 0. \end{aligned} \quad (12)$$

Rearrange Eqs. (5) and (6) and apply Eq. (1) to get the momentum equations for the casing film and tubing film, respectively,

$$\begin{aligned} \frac{(P_2 - P_1)}{l_F} &= \frac{\tau_{IC}S_{IC} - \tau_{FC}S_{FC}}{H_{LFC}A} - \rho_L g \sin \theta + \\ & \frac{\rho_L(v_{FC} - v_T)(v_{FC} - v_S) - \rho_L \frac{H_{LFT}}{H_{LFC}}(v_{FC} - v_T)v_S}{l_F}, \end{aligned} \quad (13)$$

$$\begin{aligned} \frac{(P_2 - P_1)}{l_F} &= \frac{\tau_{IT}S_{IT} - \tau_{FT}S_{FT}}{H_{LFT}A} - \rho_L g \sin \theta + \\ & \frac{\rho_L(v_{FT} - v_T)(v_{FT} - v_S) - \rho_L \frac{H_{LFC}}{H_{LFT}}(v_{FT} - v_T)v_S}{l_F}. \end{aligned} \quad (14)$$

Similarly, the momentum equation for the gas pocket can be written as:

$$\begin{aligned} \frac{(P_2 - P_1)}{l_F} &= \frac{\rho_C(v_T - v_C)(v_S - v_C)}{l_F} \\ & + \frac{\tau_{IT}S_{IT} + \tau_{IC}S_{IC}}{(1 - H_{LFT} - H_{LFC})A} - \rho_C g \sin \theta = 0. \end{aligned} \quad (15)$$

Equating Eqs. (13) and (15), and Eqs. (14) and (15) yield the combined equations for the casing and the tubing, respectively.

$$\begin{aligned} & \frac{\rho_L(v_{FC} - v_T)(v_{FC} - v_S) - \rho_L \frac{H_{LFT}}{H_{LFC}}(v_{FC} - v_T)v_S - \rho_C(v_C - v_T)(v_C - v_S)}{l_F} \\ & + \frac{\tau_{IT}S_{IT}}{(1 - H_{LFC} - H_{LFT})A} + \tau_{IC}S_{IC} \left(\frac{1}{H_{LFC}A} + \frac{1}{(1 - H_{LFC} - H_{LFT})A} \right) \\ & - \frac{\tau_{FC}S_{FC}}{H_{LFC}A} + (\rho_C - \rho_L)g \sin \theta = 0, \end{aligned} \quad (16)$$

$$\begin{aligned} & \frac{\rho_L(v_{FT} - v_T)(v_{FT} - v_S) - \rho_L \frac{H_{LFC}}{H_{LFT}}(v_{FT} - v_T)v_S - \rho_C(v_C - v_T)(v_C - v_S)}{l_F} \\ & + \frac{\tau_{IC}S_{IC}}{(1 - H_{LFC} - H_{LFT})A} + \tau_{IT}S_{IT} \left(\frac{1}{H_{LFT}A} + \frac{1}{(1 - H_{LFC} - H_{LFT})A} \right) \\ & - \frac{\tau_{FT}S_{FT}}{H_{LFT}A} + (\rho_C - \rho_L)g \sin \theta = 0. \end{aligned} \quad (17)$$

The casing and tubing liquid film velocities in annulus slug flow are assumed the same for slug flow in concentric annulus. Thus, the overall combined momentum equation for both casing and tubing films and gas pocket can be derived using Eqs. (16) and (17).

$$\begin{aligned} & \frac{\rho_L \frac{H_{LFT}}{H_{LFC}}(v_{FT} - v_T)v_S - \rho_L \frac{H_{LFC}}{H_{LFT}}(v_{FC} - v_T)v_S}{l_F} \\ & - \frac{\tau_{IC}S_{IC}}{H_{LFC}A} + \frac{\tau_{FC}S_{FC}}{H_{LFC}A} - \frac{\tau_{FT}S_{FT}}{H_{LFT}A} + \frac{\tau_{IT}S_{IT}}{H_{LFT}A} \\ & + (\rho_C - \rho_L)g \sin \theta = 0. \end{aligned} \quad (18)$$

Modeling of Annular flow

For annulus, the momentum equation for casing and tubing can be obtained by removing momentum exchange term from Eqs. (16) and (17),

$$\begin{aligned} & \frac{\tau_{IC}S_{IC}}{(1 - H_{LFC} - H_{LFT})A} + \tau_{IT}S_{IT} \left(\frac{1}{H_{LFT}A} + \frac{1}{(1 - H_{LFC} - H_{LFT})A} \right) \\ & - \frac{\tau_{FT}S_{FT}}{H_{LFT}A} + (\rho_C - \rho_L)g \sin \theta = 0, \end{aligned} \quad (19)$$

$$\begin{aligned} & \frac{\tau_{IT}S_{IT}}{(1 - H_{LFC} - H_{LFT})A} + \tau_{IC}S_{IC} \left(\frac{1}{H_{LFC}A} + \frac{1}{(1 - H_{LFC} - H_{LFT})A} \right) \\ & \frac{\tau_{FC}S_{FC}}{H_{LFC}A} + (\rho_C - \rho_L)g \sin \theta = 0. \end{aligned} \quad (20)$$

For fully eccentric annulus, the casing and tubing film velocities are assumed the same. Thus, the combined momentum equation for annular flow in fully eccentric annulus is

$$\begin{aligned} & \frac{(\tau_{IC}S_{IC} - \tau_{IT}S_{IT})}{(1 - H_{LFC} - H_{LFT})A} - \frac{\tau_{FT}S_{FT}}{H_{LFT}A} + \frac{\tau_{FC}S_{FC}}{H_{LFC}A} \\ & + \frac{\tau_{IT}S_{IT} - \tau_{IC}S_{IC}}{(1 - H_{LFC} - H_{LFT})A} + \frac{\tau_{IT}S_{IT}}{H_{LFT}A} - \frac{\tau_{IC}S_{IC}}{H_{LFC}A} = 0. \end{aligned} \quad (21)$$

The relationships between superficial velocities and the fluid velocities are

$$v_{SL} = H_{LFC}v_{FC} + H_{LFT}v_{FT} + H_{LC}v_C, \quad (22)$$

$$v_{SG} = (1 - H_{LFC} - H_{LFT} - H_{LC})v_C. \quad (23)$$

Liquid entrainment fraction in the gas core is defined as

$$F_E = \frac{H_{LC}v_C}{H_{LFC}v_{FC} + H_{LFT}v_{FT} + H_{LC}v_C}. \quad (24)$$

Modeling of Churn Flow

Annulus churn flow is similar to annulus slug flow, but it looks much more chaotic, frothy and disordered. The bridging of the pipe is shorter and frothy comparing to slug flow. This is because of the higher gas phase concentration in liquid slug which breaks the continuity of the liquid in the liquid slug between successive Taylor bubbles. As this happens, the slug collapses, falls back and merges with the following slug. The bullet-shaped Taylor bubble is then distorted and churn flow occurs. Churn flow is independent of annulus configuration and is similar to the churn flow in pipes.

There is no available mechanistic model to predict hydrodynamic behaviors of churn flow in pipes. Most researchers apply slug flow model in churn flow without any modifications.

Caetano (1986) described the flow characteristics of churn flow, but no relevant churn flow models were given. Kelessidis (1988) tried to predict the slug/churn flow pattern transition in concentric and eccentric annuli based on Taitel's (1972) slug/churn flow pattern transition in pipes. However, no hydrodynamic model for annulus churn flow has been developed.

In this study, the hydrodynamic model for annulus churn flow will be developed based on the slug flow model in the Zhang *et al.* (2003) unified model with necessary modifications. Only one liquid film is considered in this model by using representative diameter.

Barnea (1986) proposed that churn flow occurs when the gas void fraction within the liquid slug reaches the maximum value above which occasional collapse of the liquid slug occurs. In the present study, the liquid holdup at the slug/churn flow transition in concentric annulus is considered to be constant and

the liquid holdup for churn flow has a constant value. Using the experimental results for concentric annulus, the liquid holdup in the liquid slug zone in churn flow is: $H_{LS} = 0.8$. Similarly, the liquid holdup in liquid slug body in fully eccentric annulus is: $H_{LS} = 0.88$. The higher value of liquid holdup of churn flow in fully eccentric annulus is due to the migration of the small bubbles in the wide gap region of eccentric annulus. This creates a higher local void fraction in the wide gap region of the liquid slug and makes slug-churn flow transition happens in this area, while the overall gas void fraction is less than the transition value.

Shear Stress

The shear stress in the combined momentum equations are evaluated as

$$\tau_{FC} = f_{FC} \frac{\rho_L v_{FC}^2}{2}, \quad (25)$$

$$\tau_{FT} = f_{FT} \frac{\rho_L v_{FT}^2}{2}, \quad (26)$$

$$\tau_{IC} = f_{IC} \frac{\rho_C (v_C - v_{FC}) |v_C - v_{FC}|}{2}, \quad (27)$$

$$\tau_{IT} = f_{IT} \frac{\rho_C (v_C - v_{FT}) |v_C - v_{FT}|}{2}. \quad (28)$$

The friction factors f_{CF} and f_{TF} are estimated in two different ways. The common way to predict friction factor is the application of hydraulic diameter in the Fanning friction factor calculation

$$f = C \text{Re}^{-n}, \quad (29)$$

where $C=16$, $n=1$ for laminar flow, if the Reynolds number is less than 2000 and $C=0.046$, $n=0.2$ for turbulent flow when Reynolds number is larger than 3000. The discontinuity of friction factor in the transition region between laminar flow and turbulent flow was addressed in Zhang *et al.* (2003) Unified Model by interpolation between laminar and turbulent flows.

The Reynolds number for the casing and tubing liquid film and gas core are defined as

$$\text{Re}_{FC} = \frac{4A_{FC}v_{FC}\rho_L}{S_{FC}\mu_L}, \quad (30)$$

$$\text{Re}_{FT} = \frac{4A_{FT}v_{FT}\rho_L}{S_{FT}\mu_L}, \quad (31)$$

$$\text{Re}_c = \frac{4A_c v_c \rho_G}{(S_c + S_l) \mu_L} \quad (32)$$

The other way to calculate the friction factor in annulus was proposed by Caetano (1986) by taking annulus configuration into account. In Caetano's method, the friction factor in concentric annulus is determined from solution of the continuity equation, equation of motion and Fanning equation. This friction factor is used in the new annulus flow model.

For Laminar flow:

$$f_{CA} = \frac{16}{\text{Re}} \frac{(1-K)^2}{\left[\frac{1-K^4}{1-K^2} - \frac{1-K^2}{\ln(1/K)} \right]} \quad (33)$$

For turbulent flow, there is a problem for fully eccentric annulus. When e equals 1, the friction factor goes infinity.

The variables A_{CF} , A_{TF} and A_c used in above equations refer to cross section areas occupied by the casing liquid film, tubing liquid film and the gas pocket:

$$A_{FC} = H_{LFC} A, \quad (34)$$

$$A_{FT} = H_{LFT} A, \quad (35)$$

$$A_c = (1 - H_{LFC} - H_{LFT}) A. \quad (36)$$

Closure Relationships

Interfacial Friction Factor for Slug Flow

According to Andritsos *et al.* (1987) correlation modified by Zhang *et al.* (2003), the interfacial friction factor can be written as

$$f_{IC} = f_c \left(1.0 + 15.0 \left(\frac{2\delta_T}{d_c} \right)^{0.5} \left(\frac{v_{SG}}{v_{SG,t}} - 1.0 \right) \right), \quad (37)$$

$$f_{IT} = f_c \left(1.0 + 15.0 \left(\frac{2.0\delta_T}{d_T} \right)^{0.5} \left(\frac{v_{SG}}{v_{SG,t}} - 1.0 \right) \right), \quad (38)$$

$$v_{SG,t} = 5.0 \sqrt{\frac{\rho_a}{\rho_g}}. \quad (39)$$

Interfacial Friction Factor for Annular Flow

Ambrosini *et al.* (1991) improved Asali (1984)

equation for interfacial friction factor in annular flow.

Casing Interfacial Friction Factor

$$f_{IC} = f_{GC} \left(1 + 13.8 \text{We}_{GC}^{0.2} \text{Re}_{GC}^{-0.6} (h_{FC}^+ - 200 \sqrt{\rho_G / \rho_L}) \right) \quad (40)$$

$$\text{We}_{GC} = \frac{\rho_G v_c^2 D_C}{\sigma} \quad (41)$$

$$\text{Re}_{GC} = \frac{\rho_G v_c d_C}{\mu_G} \quad (42)$$

$$h_{CF}^+ = \frac{\rho_G \delta_C v_c^*}{\mu_G} \quad (43)$$

$$v_c^* = \sqrt{\tau_{IC} / \rho_G} \quad (44)$$

$$f_{GC} = 0.046 \text{Re}_{GC}^{-0.2} \quad (45)$$

Tubing Interfacial Friction Factor

$$f_{IT} = f_{GT} \left(1 + 13.8 \text{We}_{GT}^{0.2} \text{Re}_{GT}^{-0.6} (h_{FT}^+ - 200 \sqrt{\rho_G / \rho_L}) \right) \quad (46)$$

$$\text{We}_{GT} = \frac{\rho_G v_c^2 d_T}{\sigma} \quad (47)$$

$$\text{Re}_{GT} = \frac{\rho_G v_c d_T}{\mu_G} \quad (48)$$

$$h_{FT}^+ = \frac{\rho_G \delta_T v_c^*}{\mu_G} \quad (49)$$

$$v_c^* = \sqrt{\tau_{IT} / \rho_G} \quad (50)$$

$$f_{GT} = 0.046 \text{Re}_{GT}^{-0.2} \quad (51)$$

Casing and Tubing Liquid Holdup Ratio

According to Caetano (1986) liquid film holdup equation and liquid film thickness ratio, the liquid holdup ratio can be written as

$$H_{LFC} = \frac{4\delta_c}{d_c} \frac{(1 + \frac{\delta_c}{d_T})}{(1 - K^2)}, \quad (52)$$

$$H_{LFT} = \frac{4\delta_T}{d_c} K \frac{(1 + \frac{\delta_T}{d_T})}{(1 - K^2)},$$

(53)

$$\frac{H_{LFT}}{H_{LFC}} = \frac{\delta_T}{\delta_C} \frac{K(1 + \frac{\delta_T}{d_T})}{(1 - \frac{\delta_C}{d_C})} \quad (54)$$

Since δ_C and δ_T are very small compared to casing and tubing diameter, $\frac{\delta_T}{d_T}$ and $\frac{\delta_C}{d_C}$ can be neglected and the Eq. (55) can be written as:

$$\frac{H_{LFT}}{H_{LFC}} = \frac{\delta_T}{\delta_C} K \quad (55)$$

Caetano developed the equation for the tubing and casing liquid film thickness ratio, which were expressed as:

$$\frac{\delta_T}{\delta_C} = \frac{W_T'}{(2\pi - W_T')K} \quad (56)$$

$$W_T' = \frac{1}{(1 - K^2)} (2 * \sin^{-1}(K) + 2K\sqrt{1 - K^2} - K^2\pi) \quad (57)$$

Wetted Wall Fraction and Interfacial Perimeter

Based on the annulus geometry and the assumption of uniform film thickness, the perimeters of casing liquid film, tubing liquid film and gas core are given, respectively, by

$$S_{IC} = \pi(d_C - 2\delta_C) \quad (58)$$

$$S_{IT} = \pi(d_T - 2\delta_T) \quad (59)$$

$$S_I = \pi d \quad (60)$$

where S_{IC} and S_{IT} are the interfacial perimeters for casing film and gas core and tubing film and gas core, respectively.

$$S_{FC} = \pi D_C \quad (61)$$

$$S_{FT} = \pi D_T \quad (62)$$

where S_{FC} and S_{FT} are the wetted wall perimeter for casing and tubing.

The hydraulic diameters for casing and tubing wetted wall and gas core are given, respectively.

$$D_{FC} = 4 \left(\frac{A_{FC}}{S_{FC} + S_{IC}} \right) \quad (63)$$

$$D_{FT} = 4 \left(\frac{A_{FT}}{S_{FT} + S_{IT}} \right) \quad (64)$$

$$D_C = 4 \left(\frac{A_C}{S_{CD} + S_I} \right) \quad (65)$$

Liquid Entrainment in Gas Core

Zhang *et al* (2003) modified Oliemans's *et al.* (1986) empirical correlation to estimate the liquid entrainment in gas core by using six non-dimensional groups, due to the three dimensions involved. This equation can be applied in annulus by applying hydraulic or representative diameter.

$$\frac{F_E}{1 - F_E} = 0.003 W_{eSG}^{1.8} Fr_{SG}^{-0.92} Re_{SG}^{-1.24} \left(\frac{\rho_L}{\rho_G} \right)^{0.38} \left(\frac{\mu_L}{\mu_G} \right)^{0.97} \quad (66)$$

where

$$W_{eSG} = \frac{\rho_G v_{SG}^2 d}{\sigma} \quad (67)$$

$$Fr = \frac{v_{SG}}{\sqrt{gd}} \quad (68)$$

$$Re_{SL} = \frac{\rho_L v_{SL} d}{\mu_L} \quad (69)$$

$$Re_{SG} = \frac{\rho_G v_{SG} d}{\mu_G} \quad (70)$$

Slug Liquid Holdup

Zhang *et al.* (2003) developed a mechanistic model to predict slug liquid holdup based on the balance between turbulent kinetic energy of the liquid phase and the surface free energy of dispersed gas bubbles in the slug body. This model can be used in annulus slug flow by applying representative diameter concept.

$$H_{LS} = \frac{1}{1 + \frac{T_{sm}}{3.16((\rho_L - \rho_G)g\sigma)^{1/2}}} \quad (71)$$

$$T_{sm} = \frac{1}{C_e} \left(\frac{\frac{f_S}{2} \rho_S v_S^2 + \frac{d}{4} \frac{\rho_L (H_{LFC} + H_{LFT}) (v_T - v_{CF}) (v_s - v_{CF})}{l_S}}{\frac{d}{4} \frac{\rho_C (1 - H_{LFC} - H_{LFT}) (v_T - v_C) (v_s - v_C)}{l_S}} \right) \quad (72)$$

and

$$C_e = \frac{2.5 - |\sin \theta|}{2} \quad (73)$$

$$\rho_S = \rho_L H_{LS} + \rho_G (1 - H_{LS}) \quad (74)$$

$$\text{Re} = \frac{\rho_S v_S d}{\mu_L} \quad (75)$$

Before solving the combined momentum equation, the slug liquid holdup must be estimated to calculate different closure relationships. The estimation can be made using the Gregory *et al.* (1978) correlation.

$$H_{LS} = \frac{1}{1 + \left(\frac{v_S}{8.66}\right)^{1.39}} \quad (76)$$

Translational Velocity and Slug Length

Hasan and Kabir (1990) proposed a new equation for drift velocity in upward annuli, and it proves to perform better than the Sadatomi *et al.* (1982) Taylor bubble rise velocity. The equation is expressed as

$$v_D = 0.345(1 + 0.1K)\sqrt{gd_c(\rho_L - \rho_G)/\rho_L} \quad (77)$$

The translational velocity can be expressed as

$$v_T = C_S v_S + v_D \quad (78)$$

The coefficient C_S is considered to be the ratio of the maximum to the mean velocity of a fully developed velocity profile and it varies with different conditions. According to Nicklin (1962), Bendiksen (1984) and Zhang *et al.* (2003), C_S equals to 2.0 in laminar flow, and 1.3 in turbulent flow. In the transition area ($2000 < \text{Re} < 4000$) between laminar and turbulent flow, C_S is given by

$$C_S = 2.0 - 0.7 * (\text{Re} - 2000) / 2000 \quad (79)$$

It has been proposed that the slug length is related to pipe diameter, but the closure relationship for slug flow varies with different models or correlations. According to Taitel *et al.* (1980) and Barnea and Brauner (1985), the slug length for vertical pipes can be estimated by applying representative diameter concept in annulus slug flow.

$$l_s = 16.0d \quad (80)$$

Reference Diameter

In present study, either the hydraulic diameter or the representative diameter was used in the hydrodynamic models, based on their performance.

Model Performance

The new model is tested against Caetano's (1986) experimental data. The two-phase fluids used in these experiments were air-water and air-kerosene. According to the characteristic configuration of annuli and the different fluids used in experiments, the experimental data include three sets: air and water in concentric annulus, air and water in fully eccentric annulus, air and kerosene in concentric annulus. The hydrodynamic models for slug flow, annular flow and churn flow are compared against Caetano's (1986) experimental data separately.

Slug Flow Model Performance

Figures 4 to 7 shows the comparisons for the liquid holdup and pressure gradient predicted by present hydrodynamic model and the Zhang *et al.* unified model for slug flow against Caetano's slug flow experimental data of air-water flow in concentric annulus. The absolute average error of the new model in predicting liquid holdup and pressure gradient are 9.31% and 12.47%. In comparison, the unified model average errors are 12.45% and 14.7%.

Figures 8 to 11 are the comparisons for both the liquid holdup and pressure gradient predicted by the present hydrodynamic model and the unified model against Caetano's slug flow experimental data of air-water in fully eccentric annulus. The absolute average errors of liquid holdup and pressure gradient predictions are 5.01% and 5.17%, comparing with the average errors of unified model 12.48% and 15.37%.

Figures 12 and 14 show the comparison for the liquid holdup and pressure gradient predicted by present hydrodynamic model against Caetano's slug flow experimental data of air and kerosene in concentric annulus. The comparison results for unified model were also given in Figures 13 and 15. The absolute average error of the new model in predicting liquid holdup and pressure gradient are 10.67% and 14.62%. The corresponding average errors for unified model are 19.02% and 23.09%.

The present hydrodynamic model for slug flow performs very well, with a slight over prediction of pressure gradient for air-water and air-kerosene in concentric annulus. The model performs best for fully eccentric annulus flow, suggesting that the

model accounts for eccentricity. There are still some large errors which might attribute to churn flow points.

Annular Flow Model Performance

For each simulation, four combinations of diameters and friction factors have been used, and they are hydraulic diameter/unified model friction factor, hydraulic diameter/Caetano's friction factor, representative diameter/unified model friction factor and representative diameter/Caetano's friction factor.

The table 1 shows the absolute average errors for liquid holdup and pressure gradient with different reference diameters and friction factors correlations. The combinations which perform best for each case are different.

In the following study, only the results from representative diameter and unified model friction factor are shown and the results from the present model are compared with the results from unified model.

Figures 16 to 19 show the comparisons for liquid holdup and pressure gradient predicted by the present model and the unified model against Caetano's (1986) experimental data of annular flow in concentric annulus. The absolute average errors of liquid holdup and pressure gradient predictions of the new model are 23.08% and 34.83%. The unified model average errors are 29.63% and 16.32%.

Figures 20 to 23 are the comparison results between present model prediction results and Caetano's (1986) experimental data and also for the unified model for air-water flow in fully eccentric annulus. The absolute average errors of the new model liquid holdup and pressure gradient prediction are 18.29% and 25.92%. In comparison, the unified model average errors are 26.65% and 33.30%.

Figures 24 to 27 show the comparisons for liquid holdup and pressure gradient prediction against Caetano's (1986) experimental data. The absolute average errors of liquid holdup and pressure gradient of present model are 24.26% and 24.87%. The corresponding average errors for unified model are 39.55%, 36.61%.

The new model gives big error points when the liquid velocity is high. Barnea's (1986) instability criteria may explain this trend. At this condition, the annular flow configuration is unstable with backward flow of the film, resulting in liquid accumulation and

blockage of the core and transition to slug flow.

The big errors might be also due to the accuracy of the experimental measurement for annular flow, mentioned by Caetano (1986). The quick-closing ball valves used to measure liquid holdup were less accurate than in other flow patterns due to the low liquid holdup value for annular flow, and the reported holdup values are sometimes below the 3% minimum value possible to measure. The system used to measure pressure gradient was not adequate for the cross-sectional and axial dependent annular flow pattern.

Another reason mentioned by Caetano (1986) in his thesis is film thickness ratio, which was used in the present study. Caetano (1986) pointed out that the no particle size and inherent type of deposition mechanism were considered in the deposition rate expression, which proved to affect the deposition rate by Gardner (1975).

Thus, more data of annular flow in concentric and eccentric annuli and modifications of some closure relationships are required to improve the model performance.

Churn Flow Model Performance

The hydrodynamic model for churn flow is used to predict the liquid holdup and pressure gradient. The performance of the model is obtained by comparing the model prediction results against Caetano's (1986) experimental results.

Figures 28 to 31 show the comparison results for liquid holdup and pressure gradient predictions by present model and unified model against Caetano's (1986) experimental results for air-water in concentric annulus. The absolute average errors of the liquid holdup and pressure drop prediction for the present model are 18.41% and 15.69%. The prediction errors of unified model are 26.93% and 34.53%.

Figures 32 to 35 show comparison for liquid holdup and pressure gradient predictions by the present model and the unified model against Caetano's (1986) experimental results for air-water in fully eccentric annulus. The absolute average errors of the present model are 16.02% and 18.03%, while the corresponding absolute average errors of unified model are 32.08% and 39.80%.

Figures 36 to 39 are the present model and the unified model performances for the liquid holdup and

pressure gradient predictions of air-kerosene flow in concentric annulus. The absolute average errors of the present model are 22.45% and 16.45%. In comparison, the average error of Unified Model 26.55% and 34.19%.

The agreement between experimental results and the churn flow model predictions is better than annular flow, but not as good as slug flow. The main reason is due to the application of slug flow model in churn flow with modification of closure relationships. The other reason may be due to the constant liquid holdup value used in the churn flow model. The liquid holdup may vary with the gas and liquid flow rate.

Future Studies

Flow Pattern Transition Models Development

The flow pattern transition model will be developed based on the Zhang et al. (2003) unified model

approach and slug-churn flow pattern transition will be included.

Hydrodynamic Models Improvement

The hydrodynamic models for slug flow, annular flow and churn flow still need to be improved. The problem of over prediction of pressure drop for slug flow model in concentric annulus needs to be addressed. The hydrodynamic model for annular flow requires improvement since the errors of liquid holdup and pressure gradient predictions are dissatisfactory. The churn flow model may be modified, if necessary.

New Model Validation with Data Available

The new model development or modification will be validated with Caetano's (1986) experimental data. Data from other sources will also be searched and collected.

Nomenclature

A	= cross section area
d	= pipe diameter
e	= eccentricity
f	= friction factor
Fe	= liquid entrainment
Fr	= Froude number
H	= liquid holdup
K	= pipe diameter ratio
l	= length of the slug unit
P	= pressure
Re	= Reynolds number
S	= perimeter
v	= velocity
We	= Weber number

Greek Letters

δ	= liquid film thickness
Θ	= pipe circumferential wetted fraction
μ	= viscosity
θ	= pipe inclination angle

ρ	= density
σ	= surface tension
τ	= shear stress

Subscripts

C	= casing or gas core
CA	= concentric annulus
D	= drift
FC	= casing film
FT	= tubing film
GC	= gas casing
GT	= gas tubing
H	= hydraulic diameter
IC	= casing interfacial
IT	= tubing interfacial
LS	= slug liquid holdup
LFC	= casing liquid film holdup
LFT	= tubing liquid film holdup
r	= representative diameter
S	= slug
SL	= liquid superficial
SG	= gas superficial
T	= tubing or translational velocity
U	= slug unit

References

- Ambrosini, W., Andreussi, P., and Azzopardi, B. J.: "A Physically Based Correlations for Drop Size in Annular Flow," *Int. J. Multiphase Flow* 17(4), 497-507 (1991).
- Andritsos, N. and Hanratty, T.J.: "Influence of Interfacial Waves in Stratified Gas-Liquid Flows," *AIChE J.*, 33(3), 444-454, (1987).
- Asali, J. C.: "Entrainment in Vertical Gas-Liquid Annular Flow," PH.D. Dissertation, U of Illinois, Urbana, (1984).
- Barnea, D.: "A Unified Model for Predicting Flow-Pattern Transition for the Whole Range of Pipe Inclinations," *Int. J. Multiphase Flow* 13, (1), 1-12 (1987).
- Barnea, D. and Brauner, N.: "Hold-Up of the Liquid Slug in Two Phase Intermittent Flow," *Int. J. Multiphase Flow* 11, 43-49 (1985).
- Bendiksen, K. H.: "An Experimental Investigation of The Motion of Long Bubbles in Inclined Tubes," *Int. J. Multiphase Flow* 10, 467-483 (1984).

- Caetano, E.F., Shoham, O. and Brill, J.P.: "Upward Vertical Two-Phase Flow through An Annulus Part I: Single phase Friction Factor, Taylor Bubble Velocity and Flow Pattern Prediction," *J. Energy Resources Technology*.114, 1-13 (1992).
- Caetano, E.F., Shoham, O. and Brill, J.P.: "Upward Vertical Two-Phase Flow through An Annulus Part II: Modeling Bubble, Slug and Annulus flow," *J. Energy Resources Technology*.114, 1-13 (1992).
- Gregory, G. A., Nicholson, M.K., and Aziz, K., "Correlations of the Liquid Volume Fraction in the Slug for Horizontal Gas-Liquid Slug Flow," *Int. J. Multiphase Flow*, 4, 33-39 (1978)
- Gomez, L.E., Shoham, O., Schmidt, Z. and Chokshi, R.N.: "A Unified Mechanistic Model for Steady-State Two-Phase Flow in Wellbores and Pipelines," paper SPE 56520 presented at 1999 Annual Technical Conference and Exhibition held in Houston, Texas 3-6 October.
- Hasan, A.R. and Kabir, C.S.: "Two-Phase Flow in Vertical and Inclined Annuli," *Int. J. Multiphase Flow* 18, 279-293 (1992).
- Kelessidis, C.: "Vertical Upward Gas-Liquid Flow in Concentric and Eccentric Annuli," PhD Dissertation, U. of Houston, Houston, TX (1986).
- Nicklin, D. J.: "Two-Phase Bubble Flow," *Chem. Eng. Sci.*, 17, 693-702 (1962)
- Olienabs, R. V., Pots, B. F. M., and Trompe, N.: "Modeling of Annular Dispersed Two-Phase Flow in Vertical Pipes," *Int. J. Multiphase Flow* 12, (5), 711-732 (1986).
- Omurlu, C.M. and Evren, M.O.: "Analysis of Two-Phase Fluid Flow through Fully Eccentric Horizontal Annuli," Proceedings BHRG Multiphase Technology Conference, Edinburgh, UK (2007)
- Sadatomi, M., Sato, Y. and Saruwatari, S.: "Two-phase Flow in Vertical Noncircular Channels," *Int. J. Multiphase Flow* 8, 641-655 (1982).
- Sunthankar, A.A.: "Study of the Flow of Aerated Drilling Fluids in Annulus under Ambient Temperature and Pressure Conditions," MS Thesis, U. Tulsa, Tulsa, OK (2002).
- Taitel, Y., Barnea, D., and Dukler, A.E.: "Modeling Flow Pattern Transition for Steady Upward Gas-Liquid Flow in Vertical Tubes," *AIChE J*, 26,345 (1980).
- Zhang H-Q., Wang, Q., Sarica C. and Brill, J.P.: "Unified Model for Gas-Liquid Pipe Flow Model via Slug Dynamics-Part I: Model Development," *J. Energy Resources Technology*, Vol. 125, 274-283 (2003).
- Zhang H-Q., Wang, Q., Sarica C. and Brill, J.P.: "A Unified Mechanistic Model for Slug Liquid Holdup and Transition between Slug and Dispersed Bubble Flows," *Int. J. Multiphase Flow*, 29, 97-107 (2003).

	Air and water in fully eccentric annulus		Air and kerosene in concentric annulus		Air and water in concentric annulus	
	Liquid holdup	Pressure drop	Liquid holdup	Pressure drop	Liquid holdup	Pressure drop
hy/Caetano's	26.10%	34.47%	30.81%	41.66%	15.79%	10.97%
hy/unified	16.14%	20.55%	44.54%	27.72%	56.40%	10.53%
re/Caetano's	23.65%	29.39%	36.29%	31.98%	42.26%	20.29%
re/unified model	18.29%	25.93%	26.76%	24.87%	23.08%	34.80%
unified model	25.80%	33.30%	39.55%	46.46%	29.26%	17.51%

Table 1 Annular Flow Model Results Comparison
(hy, re, Caetano's, unified refer to hydraulic diameter, representative diameter, Caetano's friction factor and unified model friction factor, respectively.)

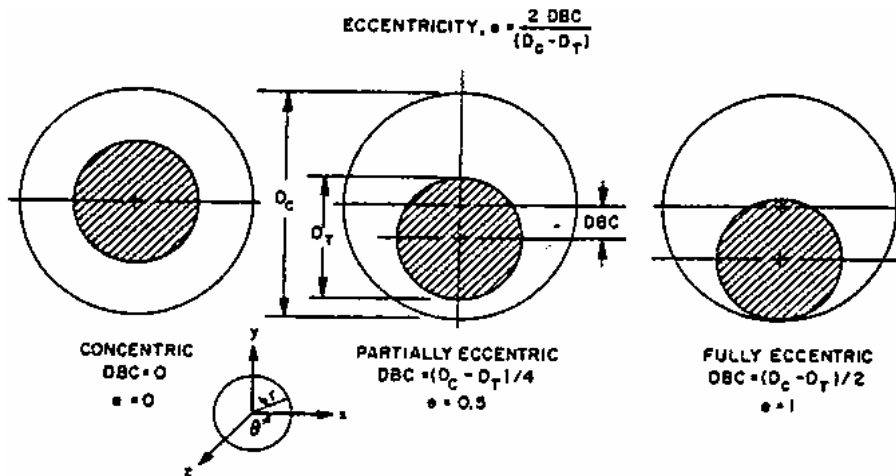


Figure 1: Annular Flow Configuration (Caetano, 1986)

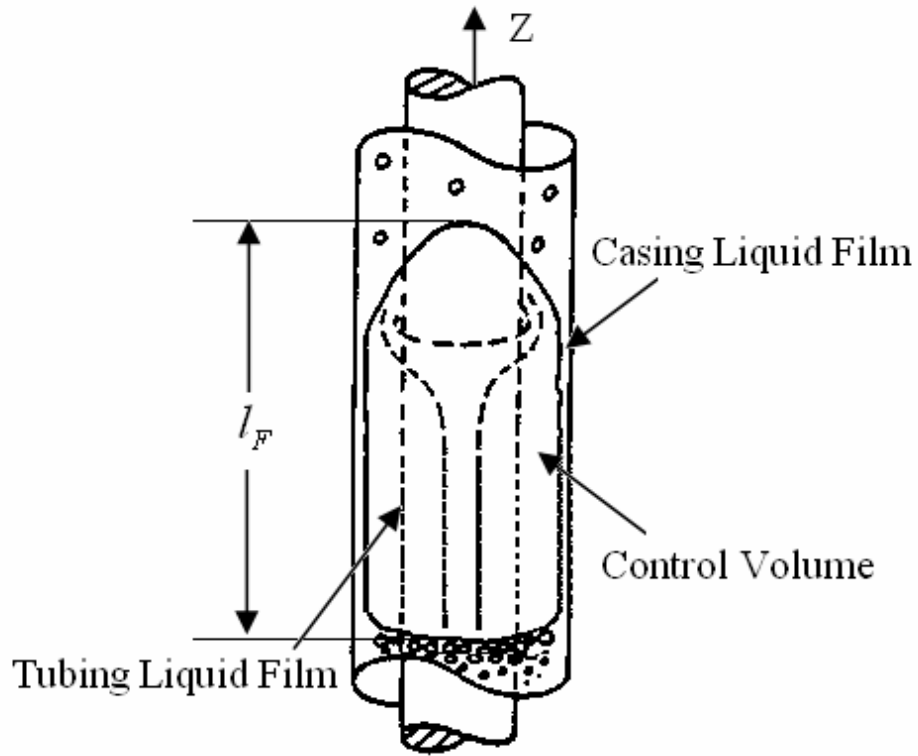


Figure 2: Control Volume Used in Slug Flow Modeling

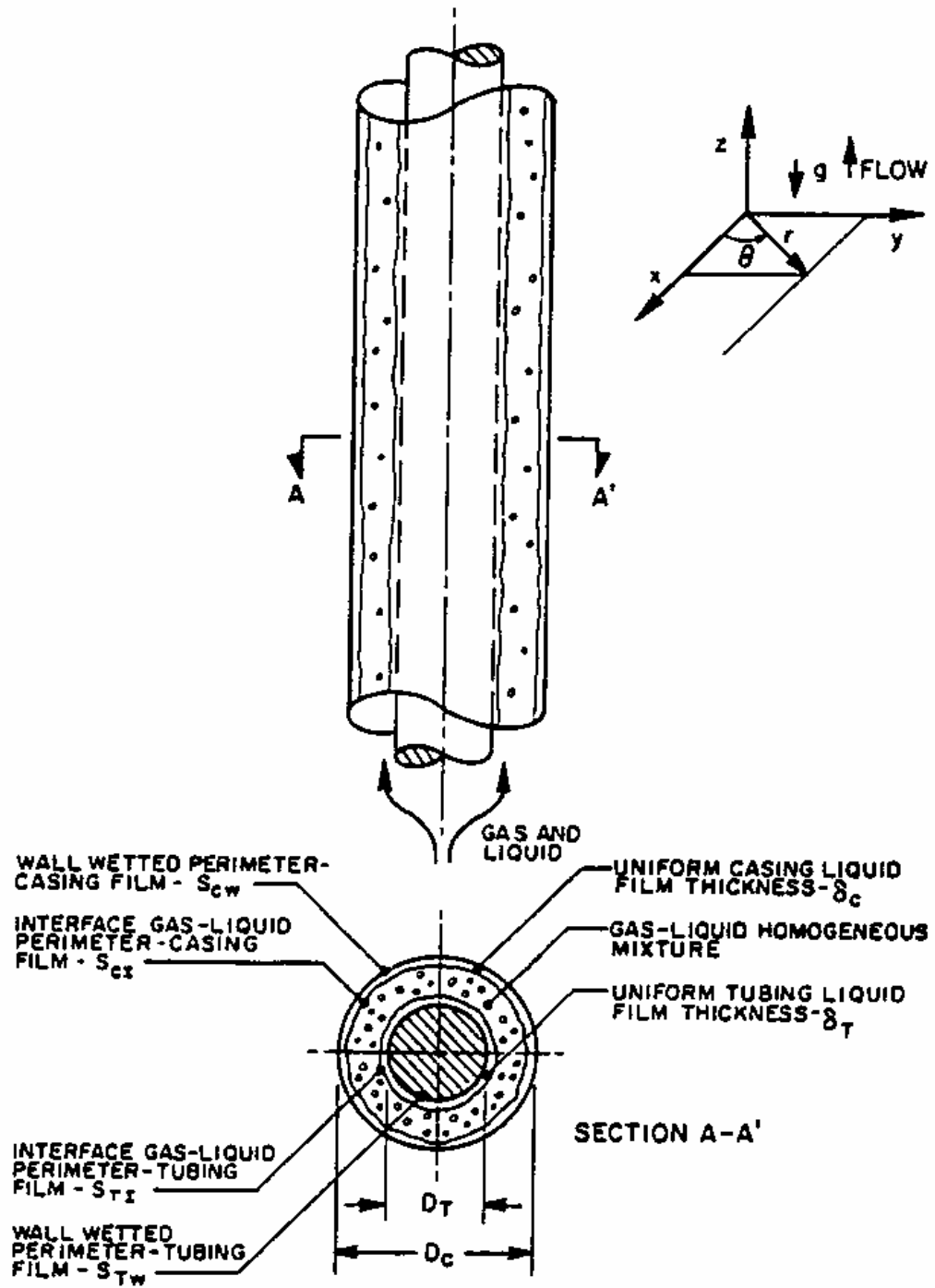


Figure 3: Idealized Annular Flow in Concentric Annulus-Geometry and Parameters
(Caetano, 1986)

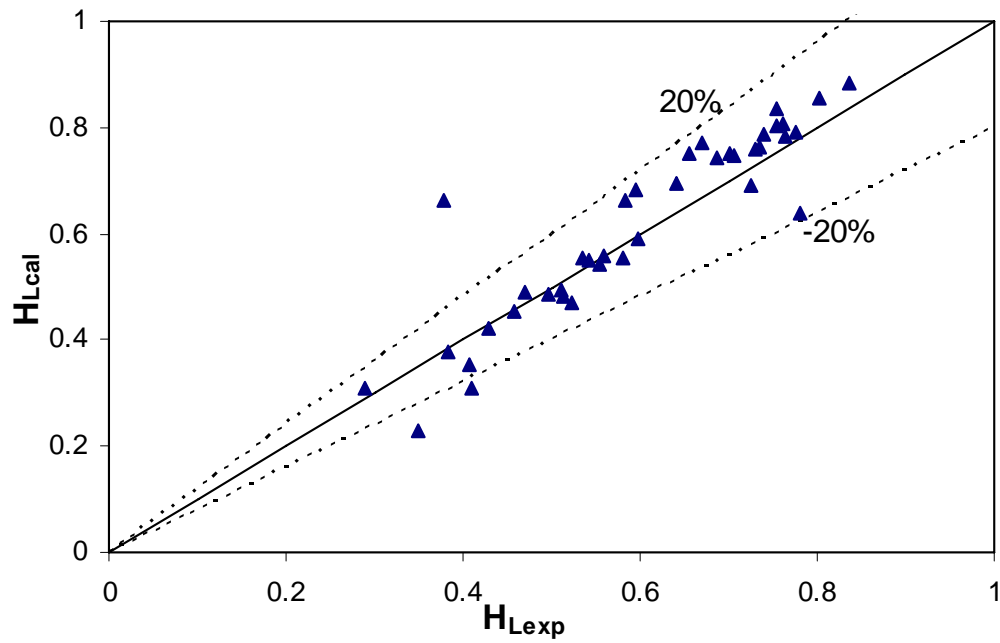


Figure 4: Present Slug Flow Model Performance for Liquid Holdup Prediction (Air and Water in Concentric Annulus)

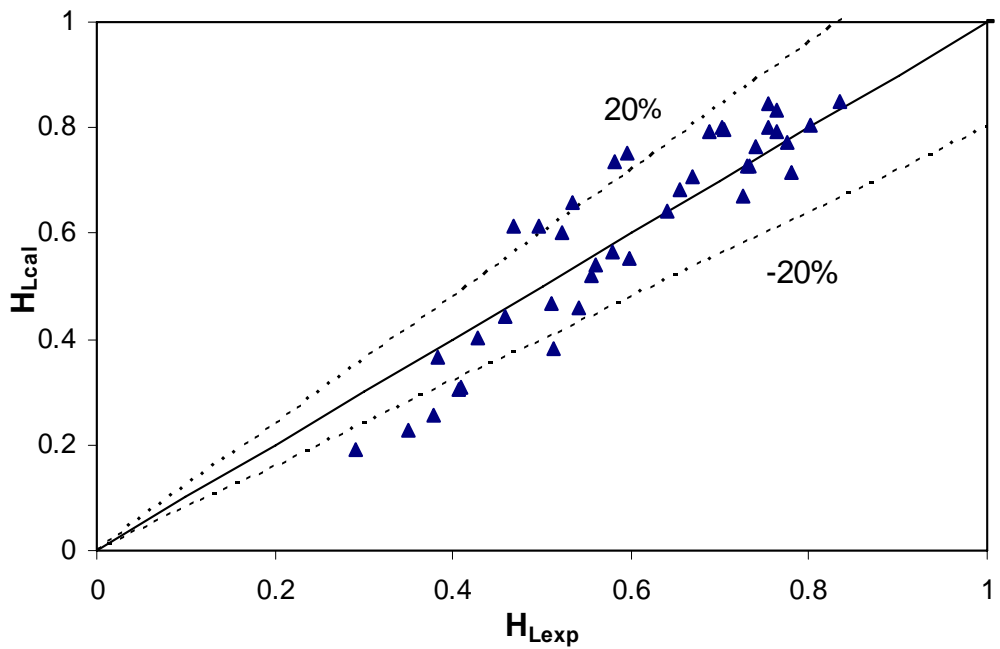


Figure 5: Zhang et al. unified model Performance for Liquid Holdup Prediction (Air and Water in Concentric Annulus)

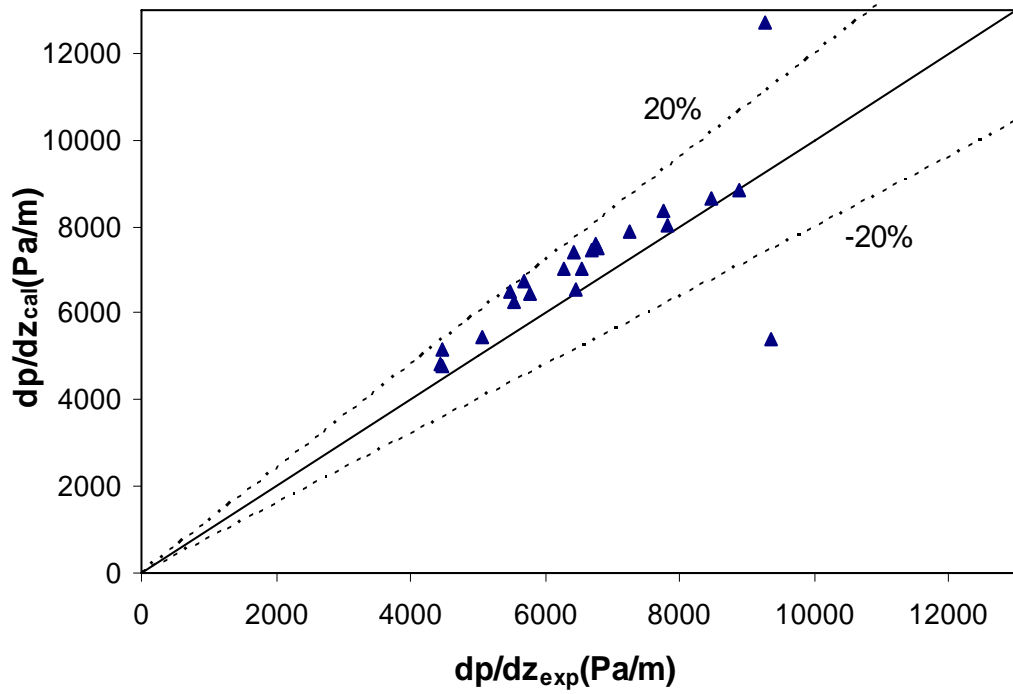


Figure6: Present Slug Flow Model Performance for Pressure Gradient Prediction
(Air and Water in Concentric Annulus)

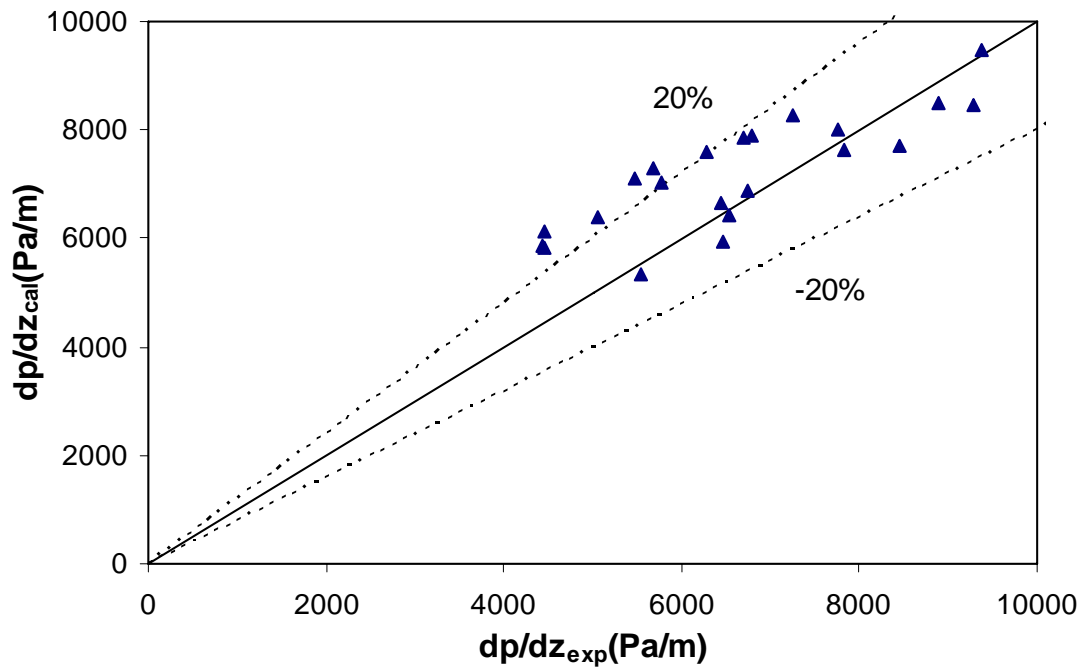


Figure 7: Zhang et al. Unified Model Performance for Pressure Gradient Prediction
(Air and Water in Concentric Annulus)

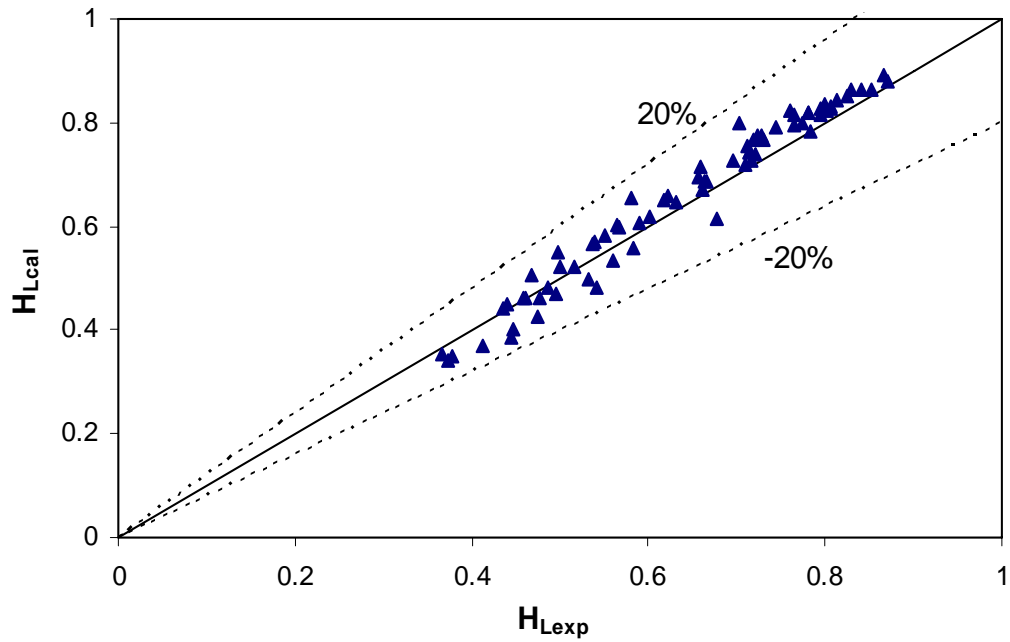


Figure 8: Present Flow Model Performance for Liquid Holdup Prediction (Air and Water in Fully Eccentric Annulus)

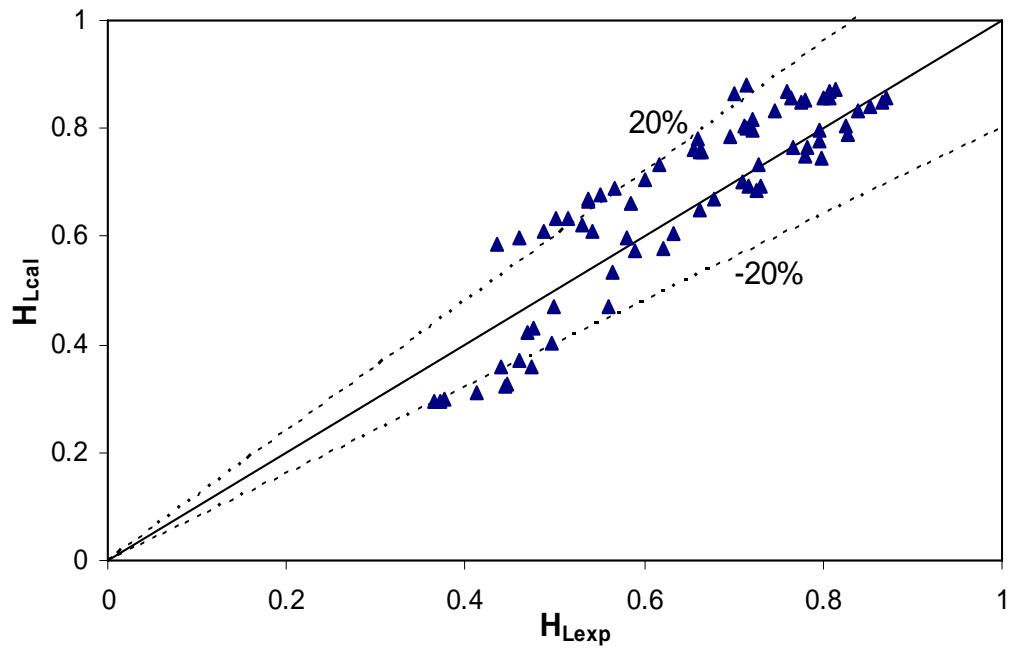


Figure 9: Zhang et al. Unified Model Performance for Liquid Holdup Prediction (Air and Water in Fully Eccentric Annulus)

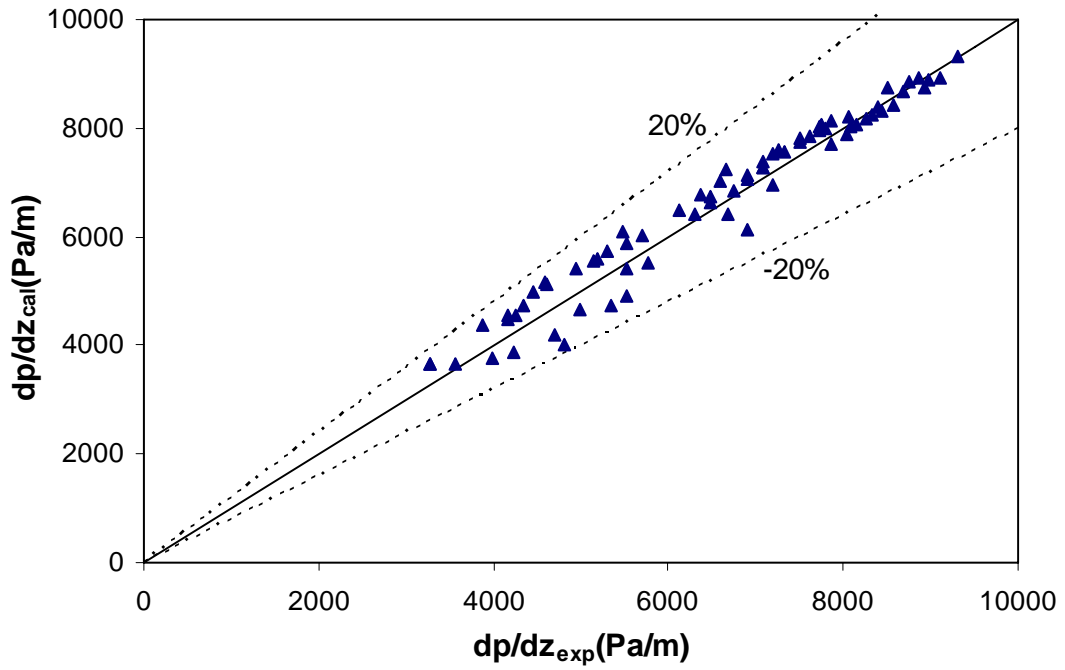


Figure 10: Present Slug Flow Model Performance for Pressure Gradient Prediction (Air and Water in Fully Eccentric Annulus)

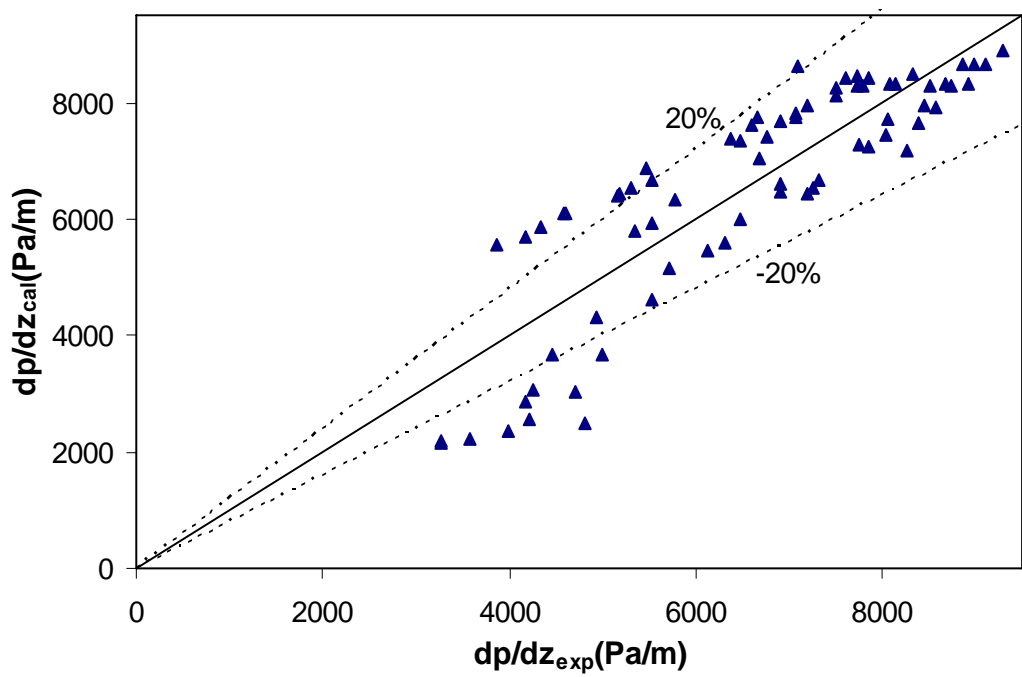


Figure 11: Zhang et al. Unified Model Performance for Pressure Gradient Prediction (Air and Water in Fully Eccentric Annulus)

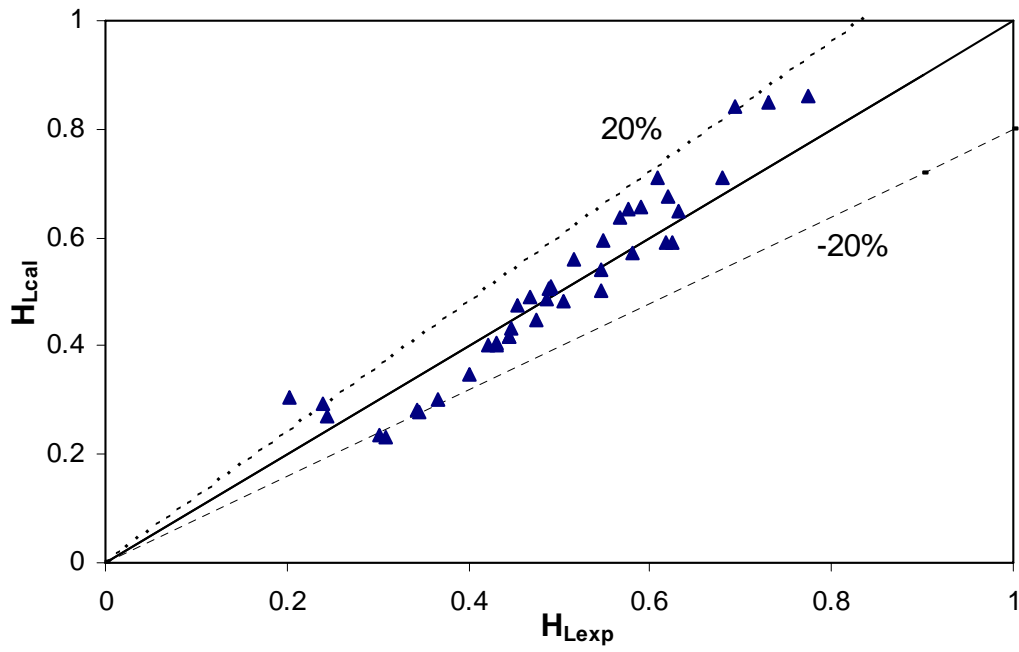


Figure 12: Present Slug Flow Model Performance for Liquid Holdup Prediction (Air and Kerosene in Concentric Annulus)

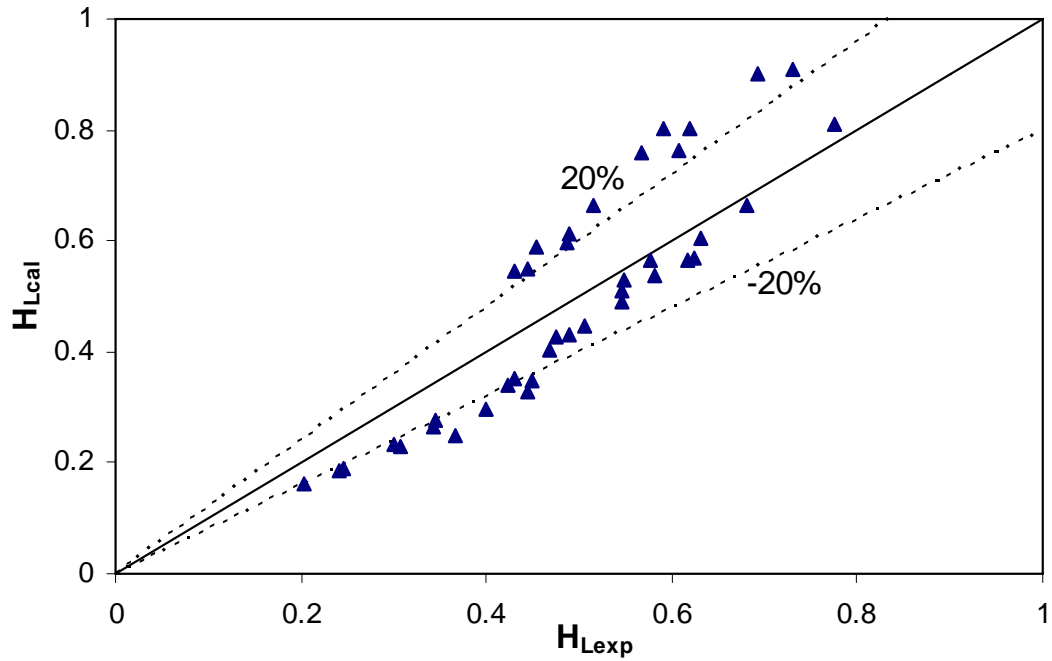


Figure 13: Zhang et al. Unified Model Performance for Liquid Holdup Prediction (Air and Kerosene in Concentric Annulus)

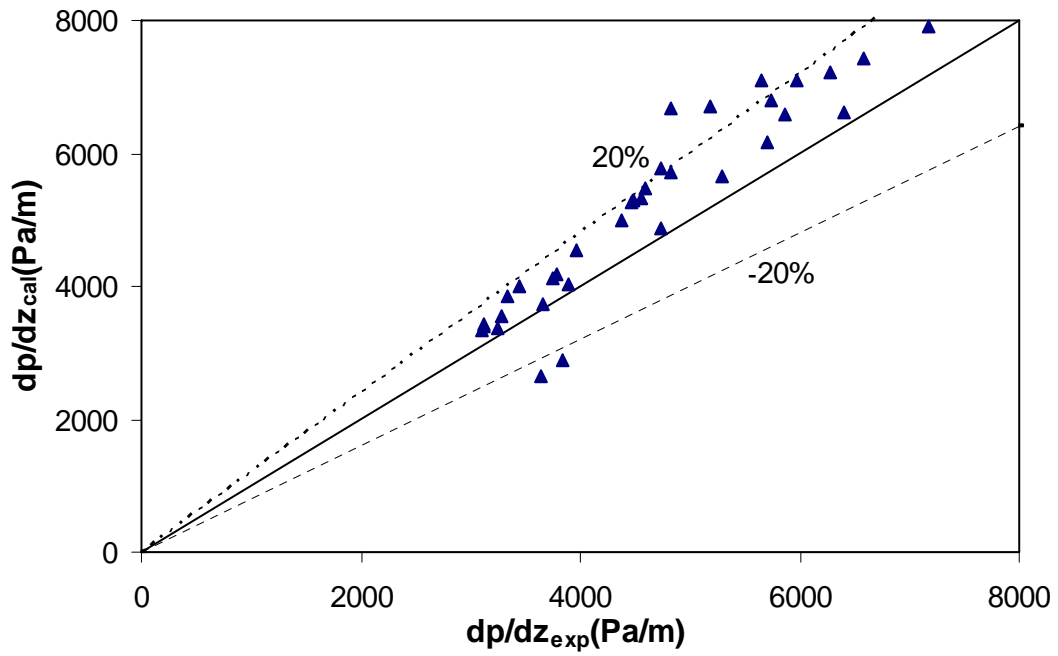


Figure 14: Present Slug Flow Model Performance for Pressure Gradient Prediction
(Air and Kerosene in Concentric Annulus)

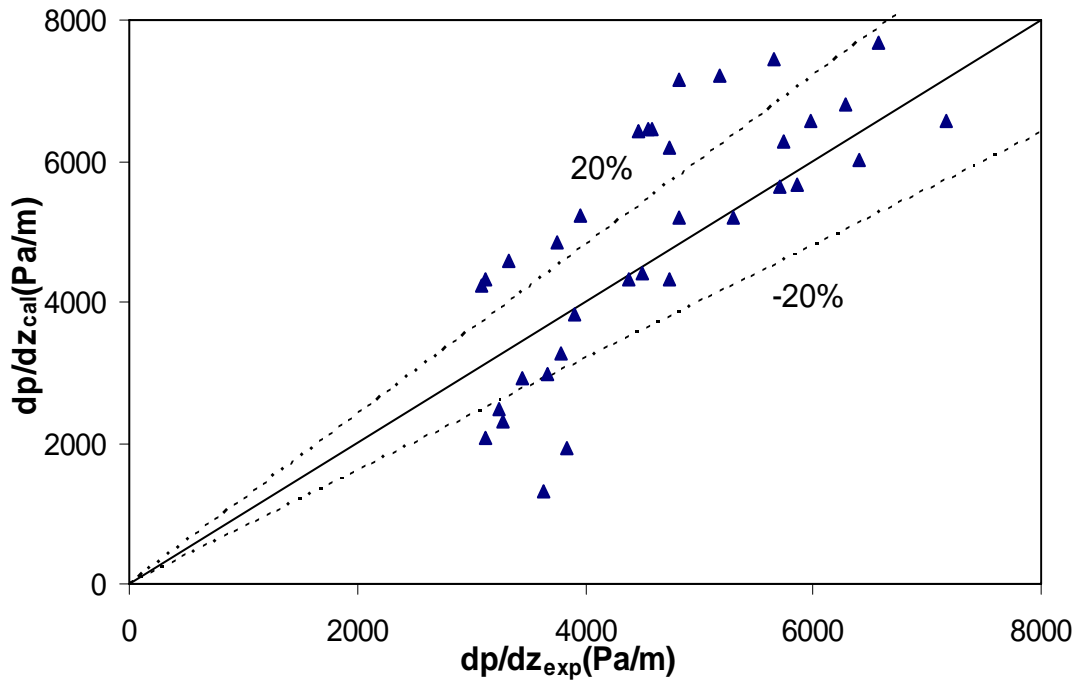


Figure 15: Zhang et al. Unified Model Performance for Pressure Gradient Prediction
(Air and Kerosene in Concentric Annulus)

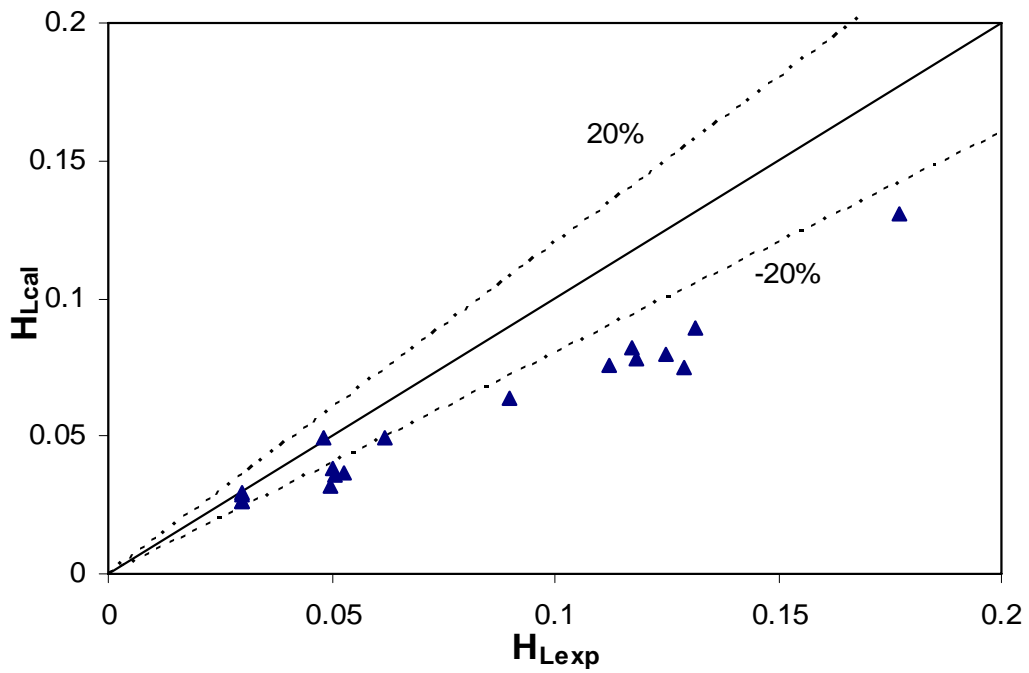


Figure 16: Present Annular Flow Model Performance for Liquid Holdup Prediction (Air and Water in Concentric Annulus)

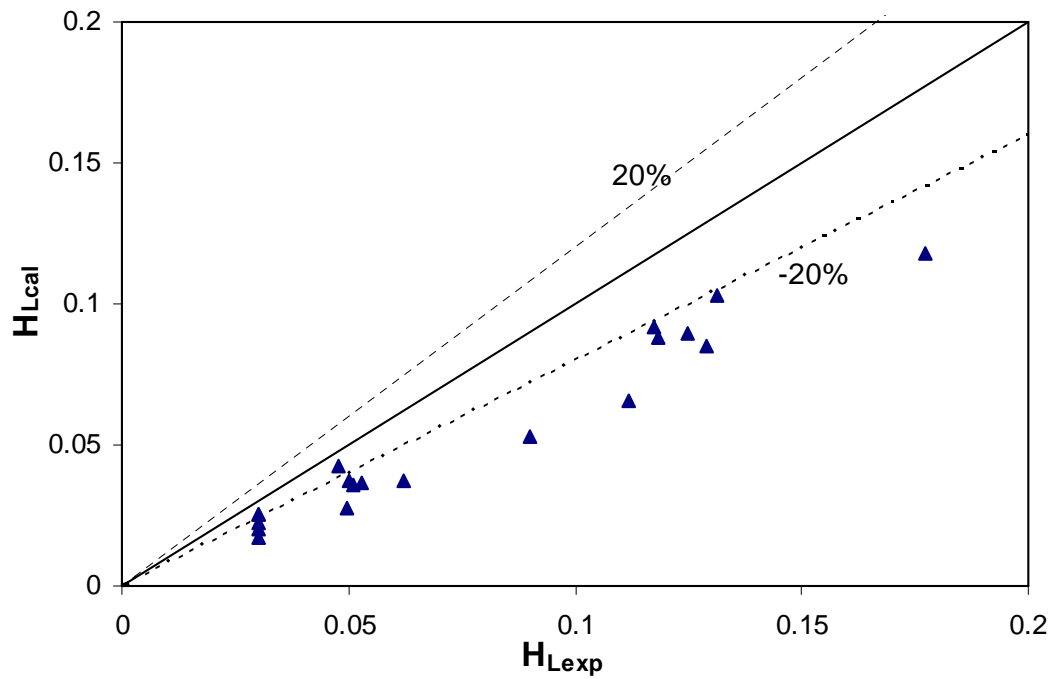


Figure 17: Zhang et al. Unified Flow Model Performance for Liquid Holdup Prediction (Air and Water in Concentric Annulus)

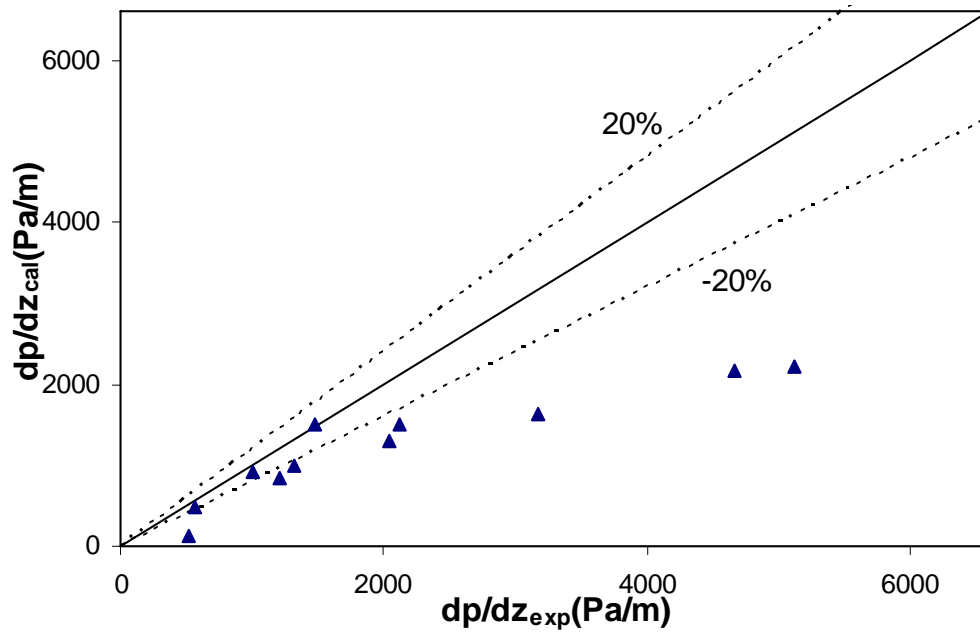


Figure 18: Present Annular Flow Model Performance for Pressure Gradient Prediction (Air and Water in Concentric Annulus)

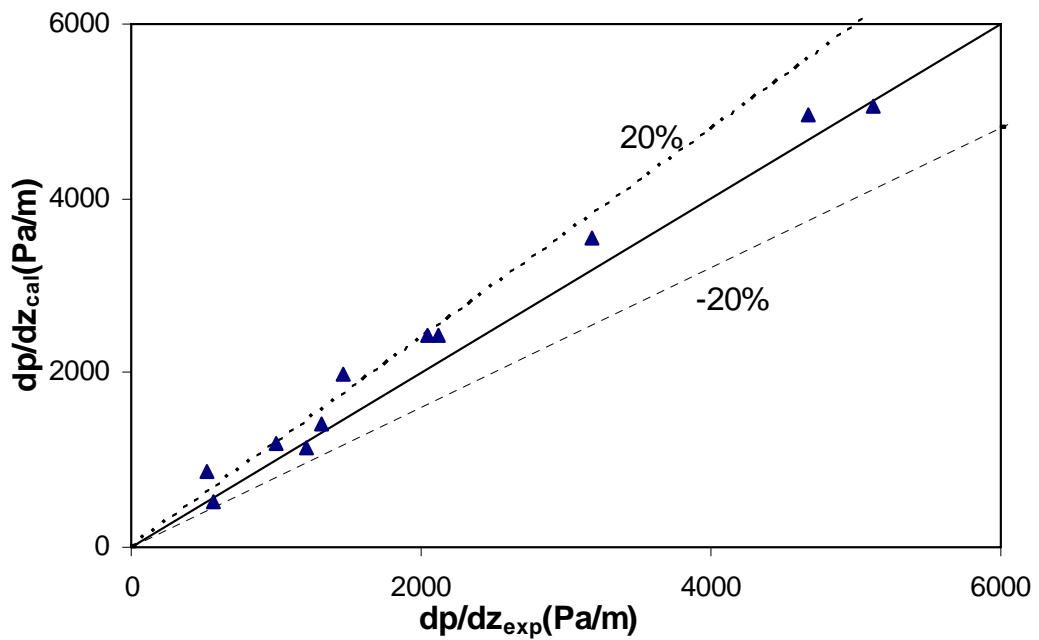


Figure 19: Zhang et al. Unified Model Performance for Pressure Gradient Prediction (Air and Water in Concentric Annulus)

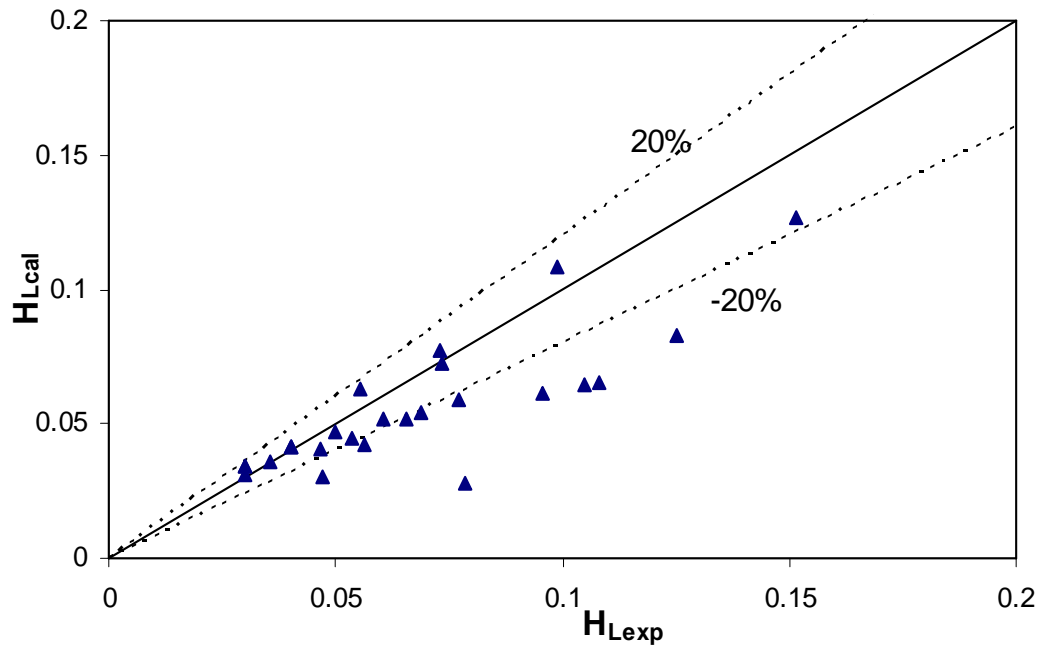


Figure 20: Present Annular Flow Model Performance for Liquid Holdup Prediction
(Air and Water in Fully Eccentric Annulus)

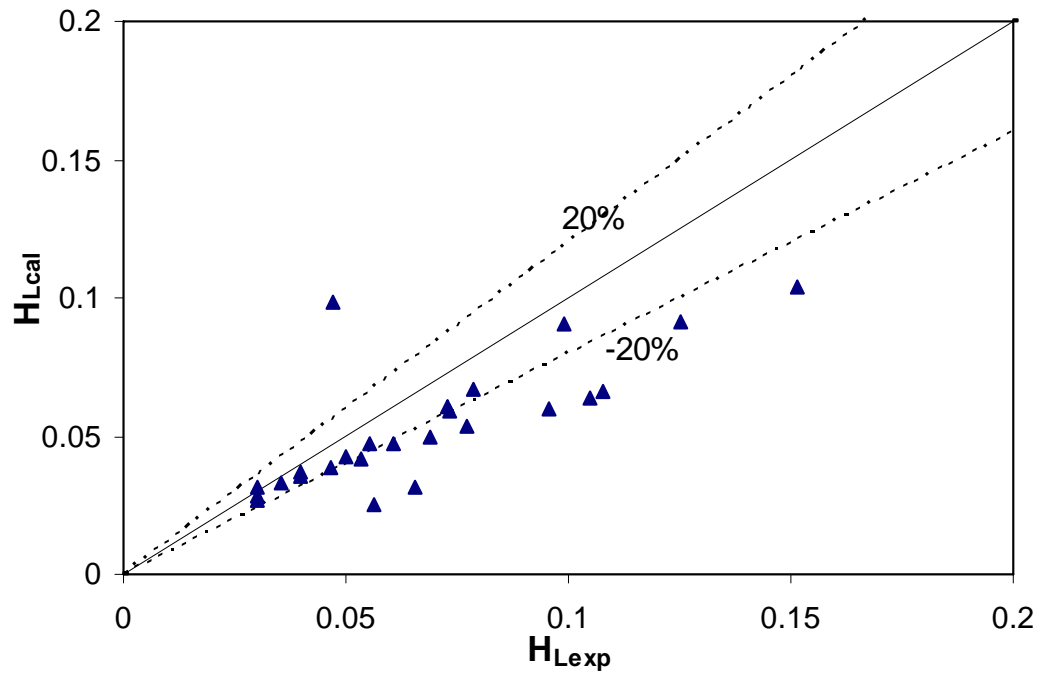


Figure 21: Zhang et al. Unified Model Performance for Liquid Holdup Prediction
(Air and Water in Fully Eccentric Annulus)

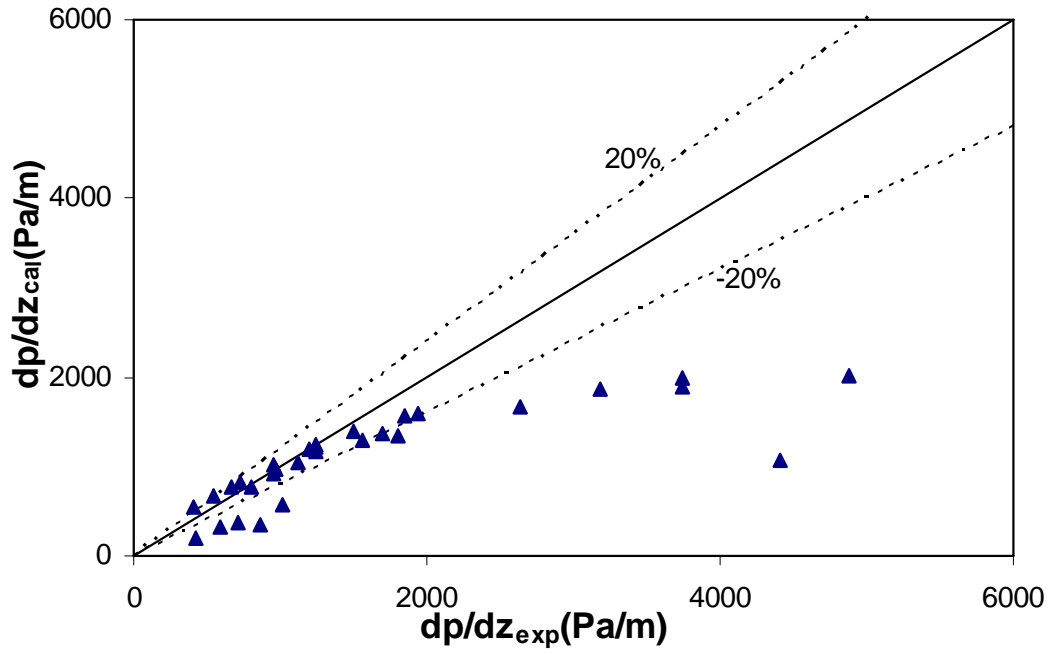


Figure 22: Present Annular Flow Model Performance for Pressure Gradient Prediction
(Air and Water in Fully Eccentric Annulus)

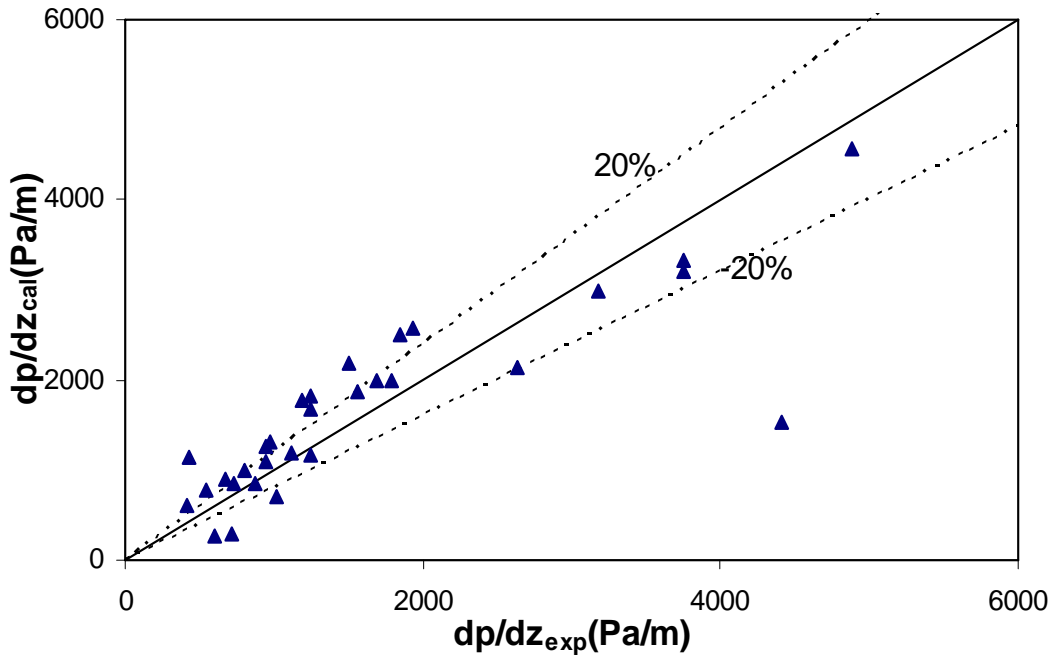


Figure 23: Zhang et al. Unified Model Performance for Pressure Gradient Prediction
(Air and Water in Fully Eccentric Annulus)

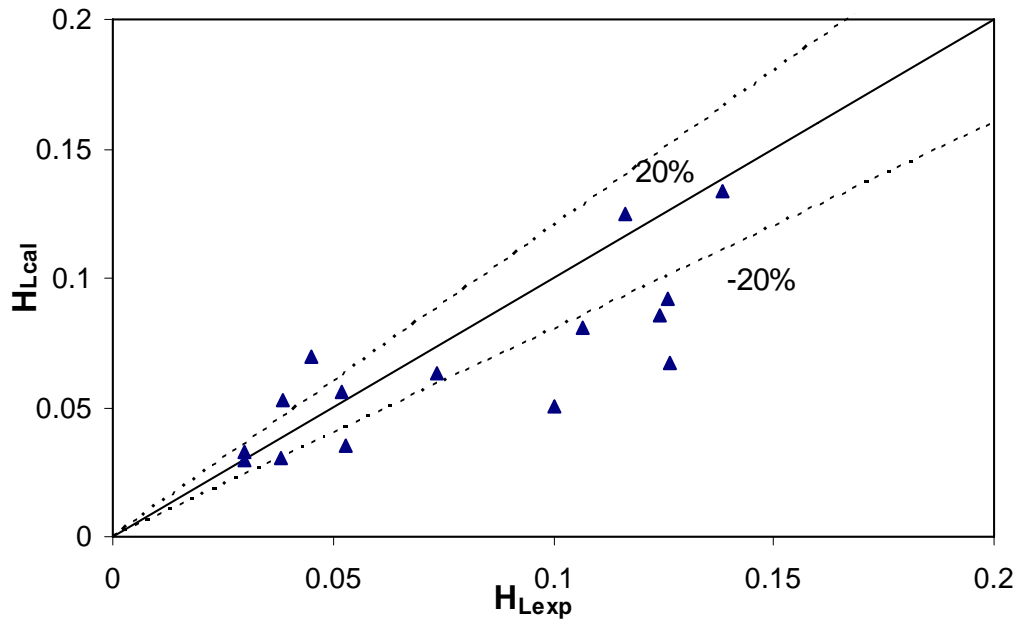


Figure 24: Present Annular Flow Model Performance for Liquid Holdup Prediction (Air and Kerosene in Concentric Annulus)

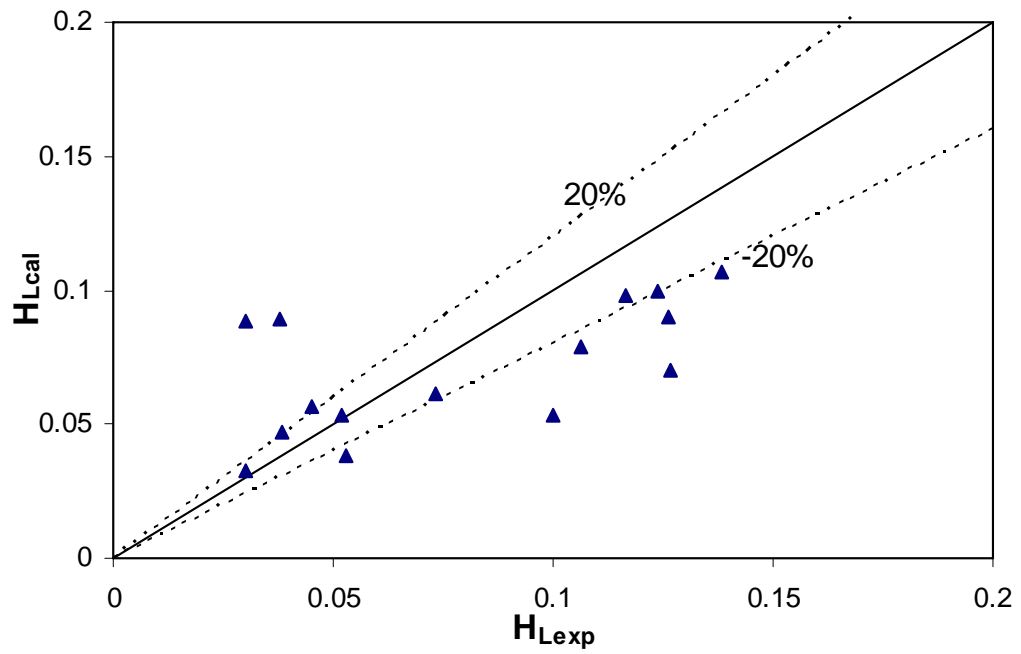


Figure 25: Zhang et al. Unified Flow Model Performance for Liquid Holdup Prediction (Air and Kerosene in Concentric Annulus)

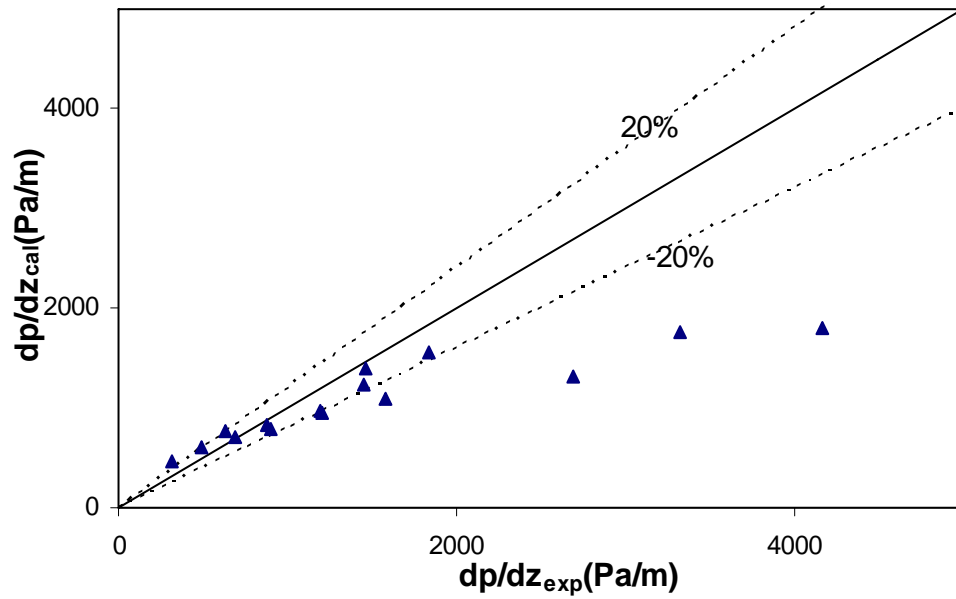


Figure 26: Present Annular Flow Model Performance for Pressure Gradient Prediction (Air and Kerosene in Concentric Annulus)

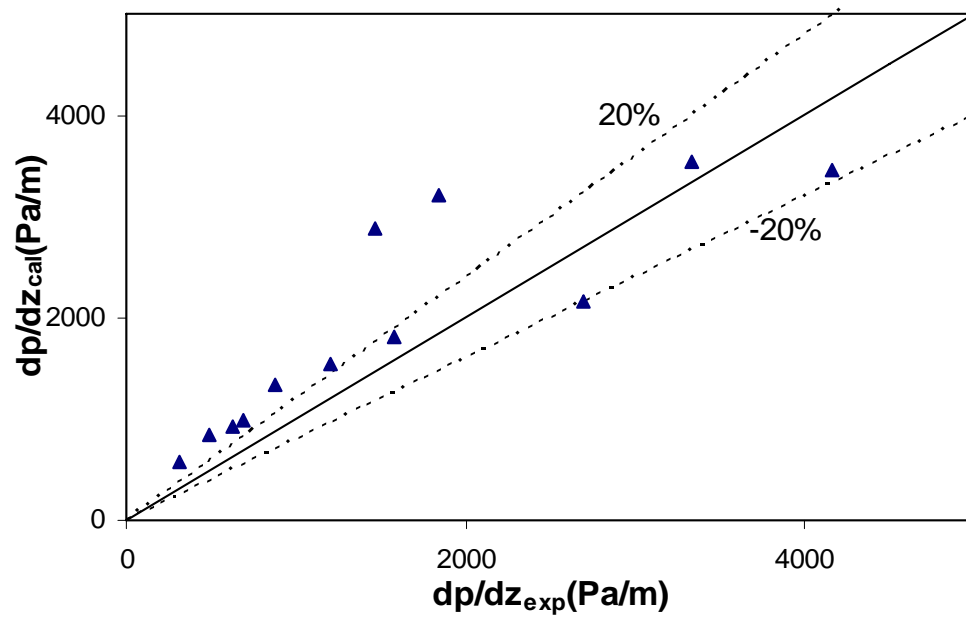


Figure 27: Zhang et al. Unified Model Performance for Pressure Gradient Prediction (Air and Kerosene in Concentric Annulus)

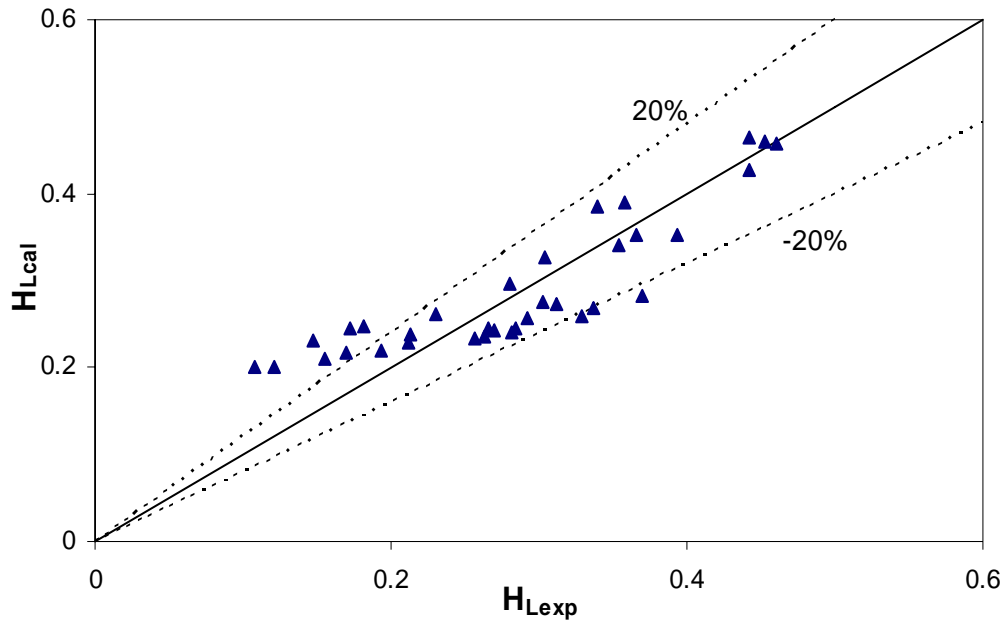


Figure 28: Present Churn Flow Model Performance for Liquid Holdup Prediction (Air and Water in Concentric Annulus)

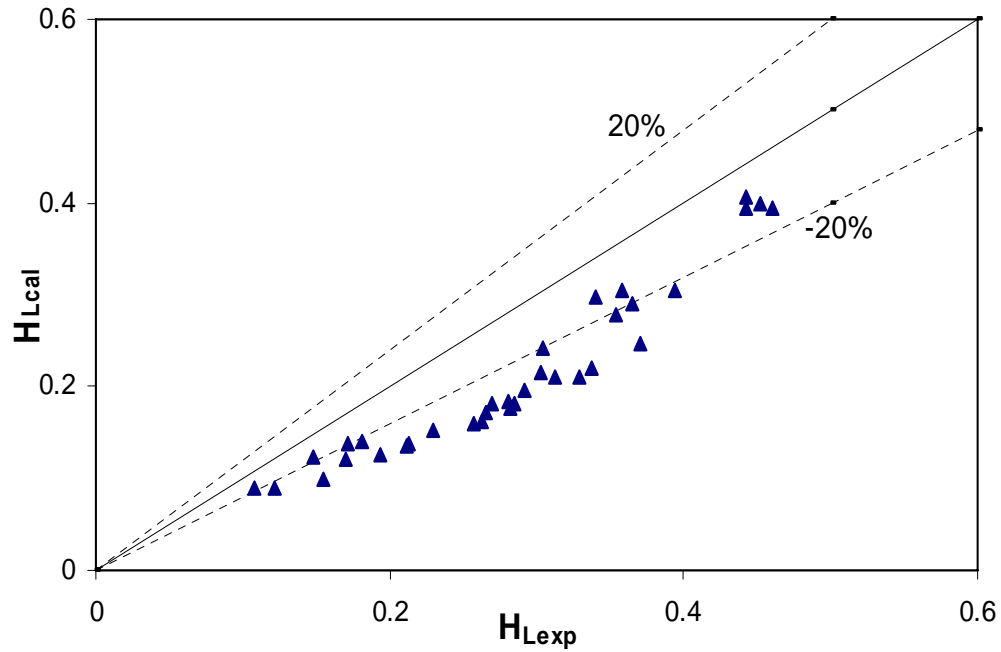


Figure 29: Zhang et al. Unified Model Performance for Liquid Holdup Prediction (Air and Water in Concentric Annulus)

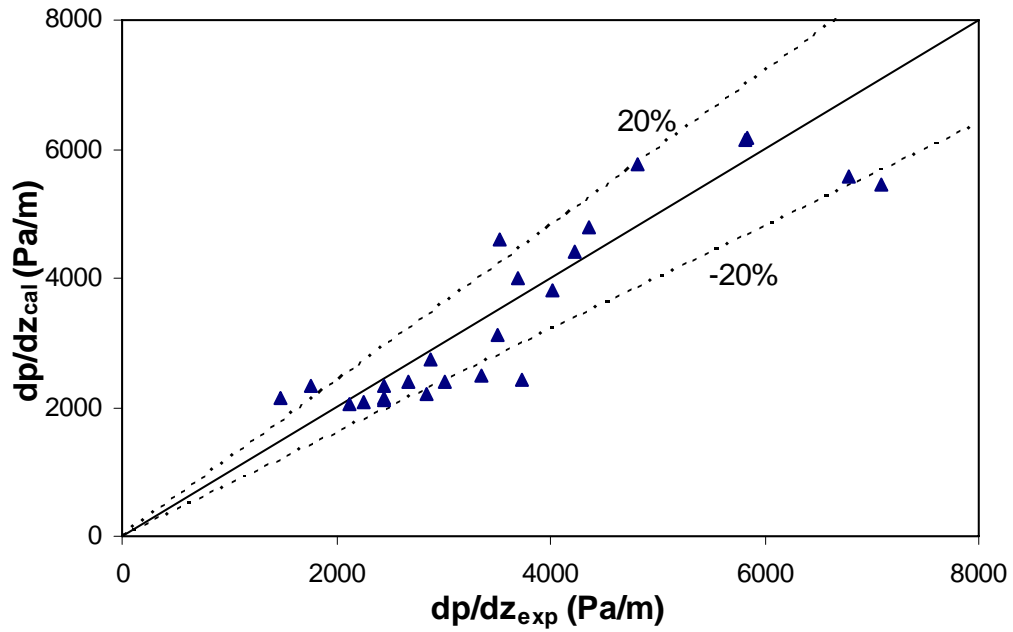


Figure 30-New Churn Flow Model Performance-Pressure Gradient for Air and Water in Concentric Annulus

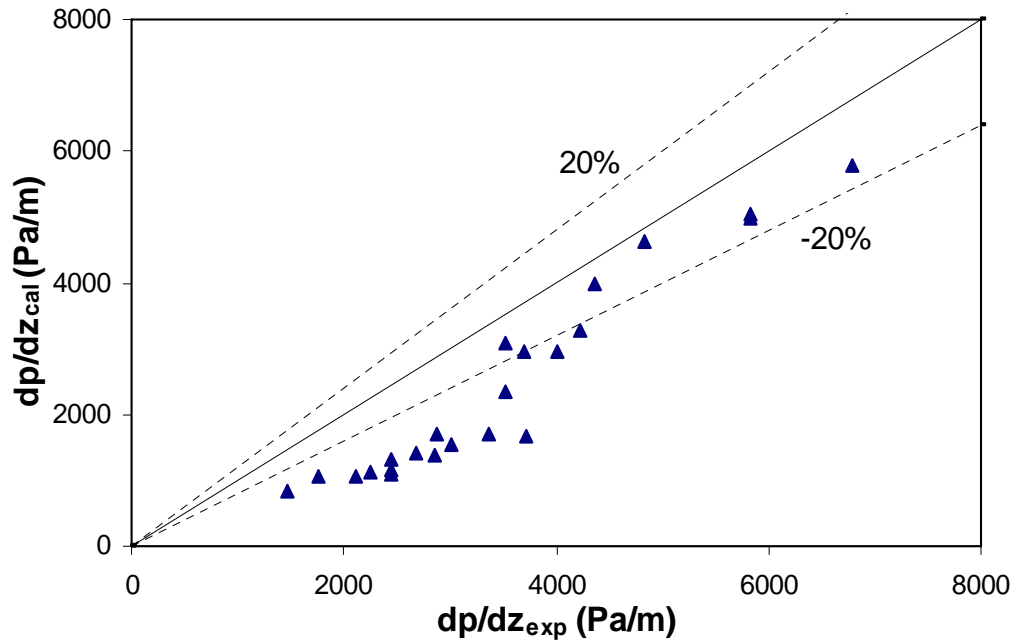


Figure 31: Zhang et al. Unified Model Performance for Pressure Gradient Prediction (Air and Water in Concentric Annulus)

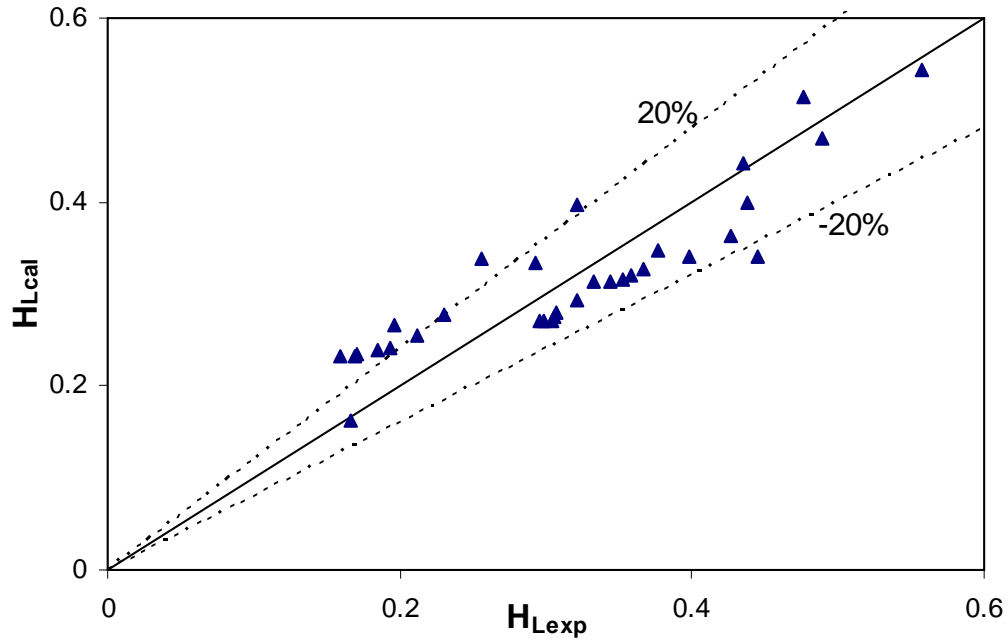


Figure 32: Present Churn Flow Model Performance for Liquid Holdup Prediction (Air and Water in Fully Eccentric Annulus)

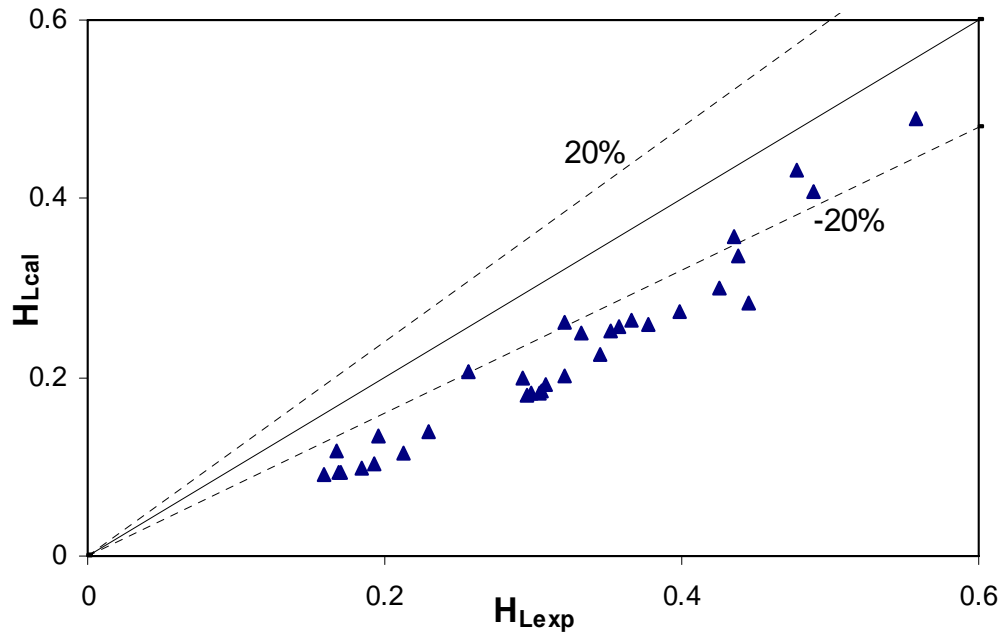


Figure 33: Zhang et al. Unified Model Performance for Liquid Holdup Prediction (Air and Water in Fully Eccentric Annulus)

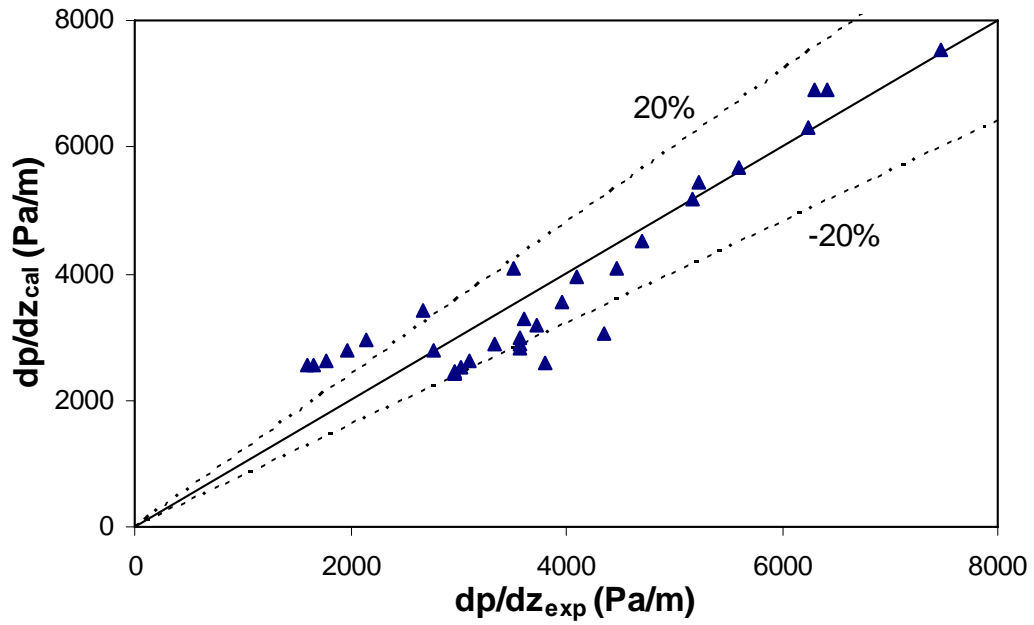


Figure 34 Present Churn Flow Model Performance for Pressure Gradient Prediction
(Air and Water in Fully Eccentric Annulus)

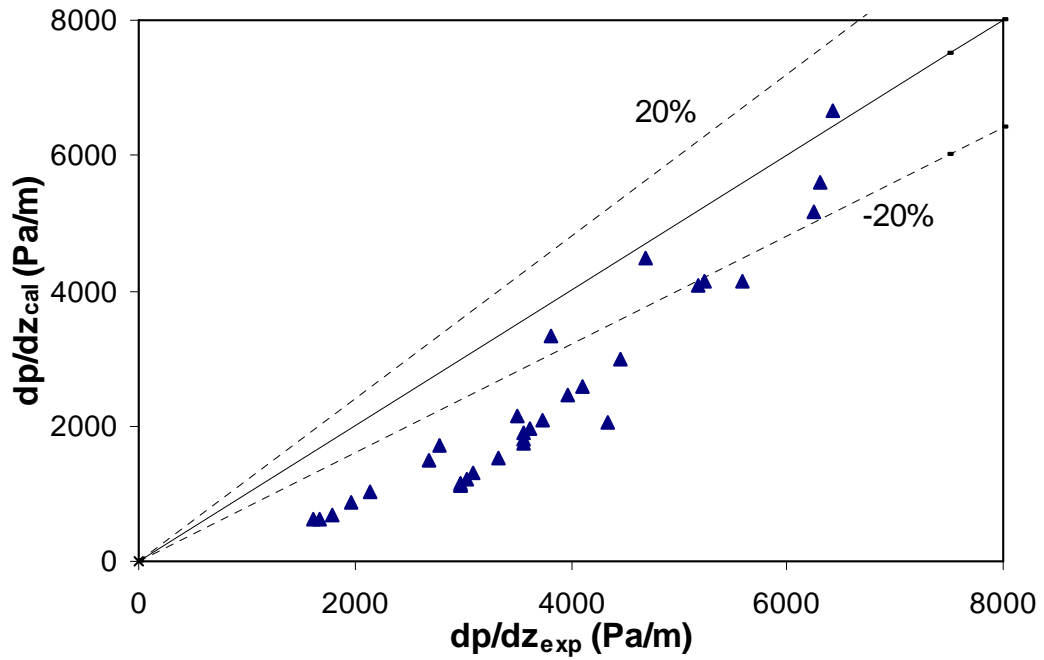


Figure 35: Zhang et al. Unified Model Performance for Pressure Gradient Prediction
(Air and Water in Fully Eccentric Annulus)

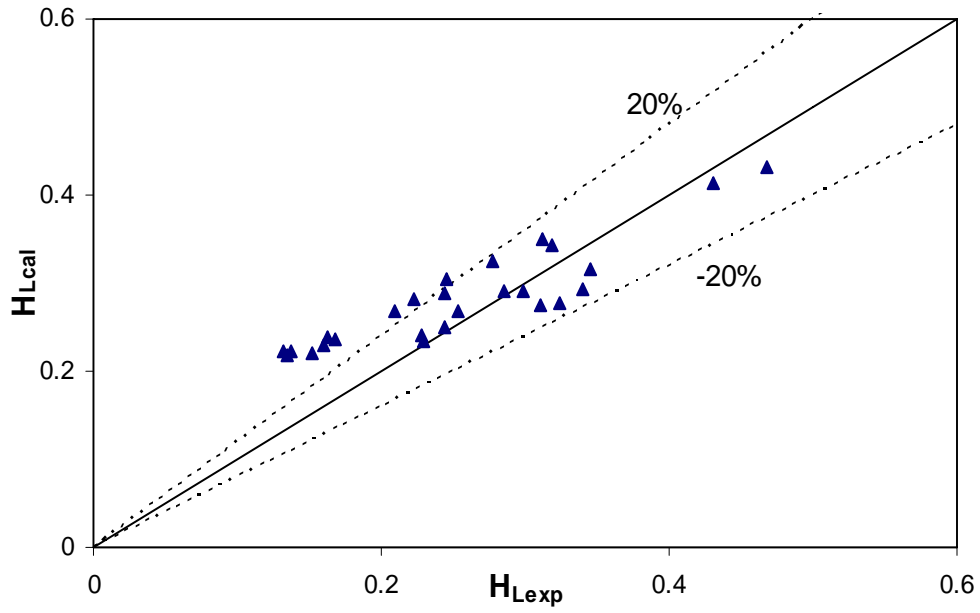


Figure 36: Present Churn Flow Model Performance for Liquid Holdup Prediction (Air and Kerosene in Concentric Annulus)

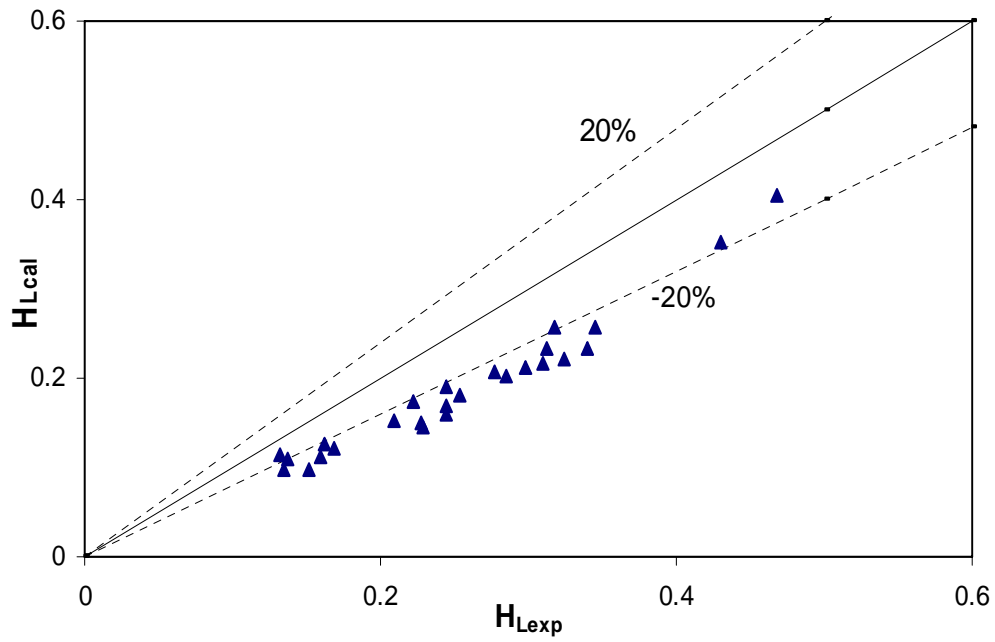


Figure 37: Zhang et al. Unified Model Performance for Liquid Holdup Prediction (Air and Kerosene in Concentric Annulus)

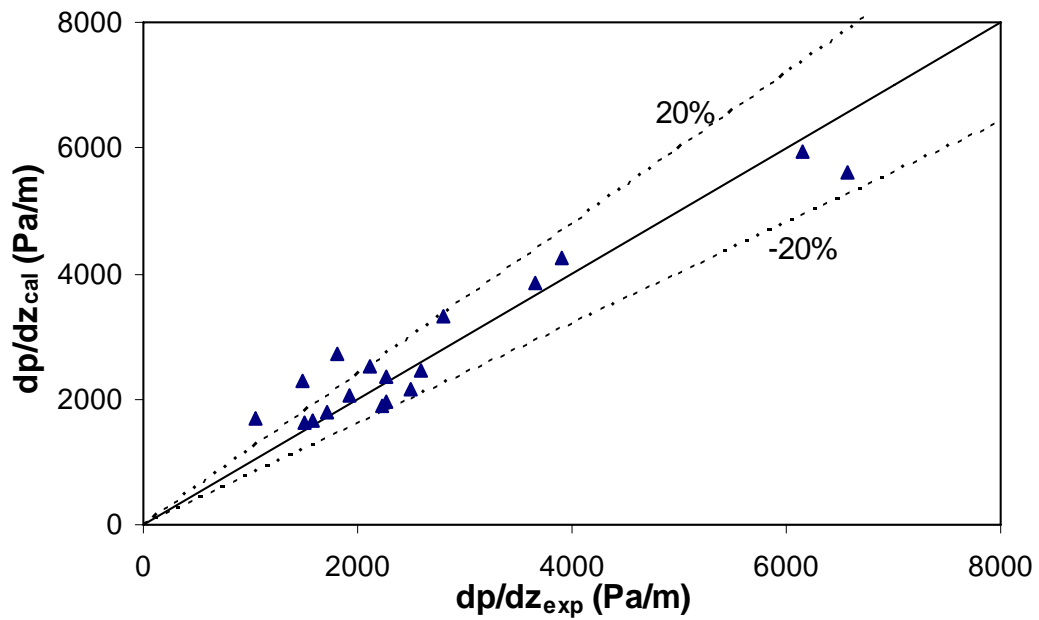


Figure 38: Present Churn Flow Model Performance for Pressure Gradient Presentation (Air and Kerosene in Concentric Annulus)

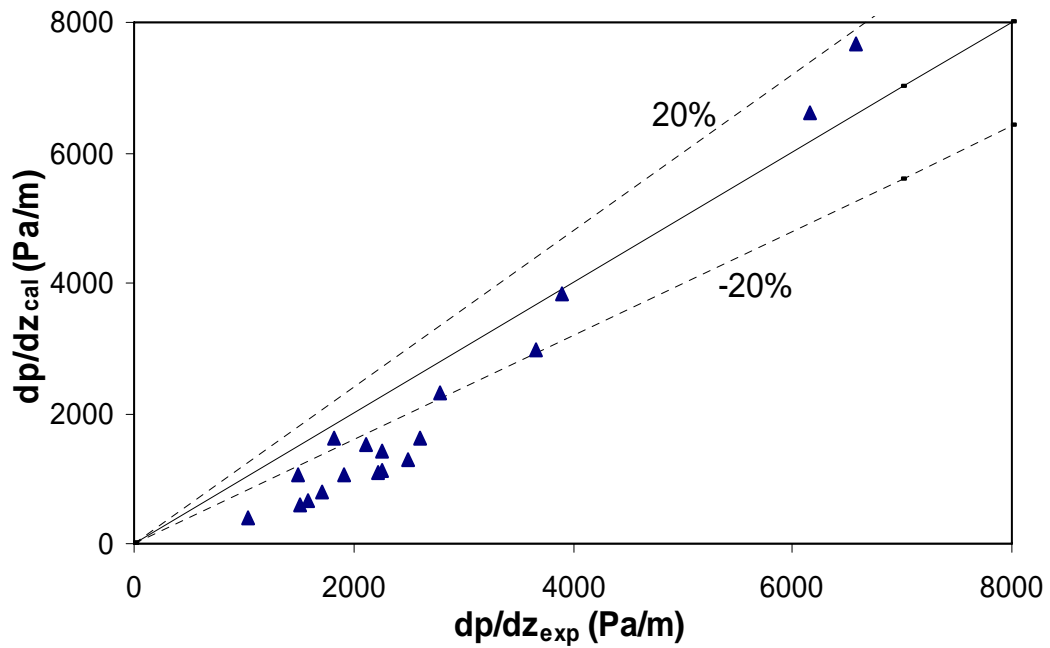


Figure 39: Zhang et al. Unified Model Performance-Pressure Gradient (Air and Kerosene in Concentric Annulus)

Low Liquid Loading Flow

◆ Significance

➤ Wet Gas Transportation

- ▲ Holdup and Pressure Drop Prediction
- ▲ Corrosion Inhibitor Delivery (Top of the Line Corrosion)

◆ Objectives

➤ Develop Better Predictive Tools

Low Liquid Loading Flow ...

◆ Past TUFFP Studies

➤ Two-phase, Small Diameter, Low Pressure

- ▲ Air-Water and Air-Oil
- ▲ 2-in. ID Pipe with $\pm 2^\circ$ Inclination Angles from Horizontal

➤ Two-phase, Large Diameter, Low Pressure

- ▲ Air-Water
- ▲ 6-in. ID and $\pm 2^\circ$ Inclination Angles from Horizontal

Low Liquid Loading Flow ...

◆ Past TUFFP Studies ...

➤ Three-phase, Large Diameter, Low Pressure

▲ Air-Mineral Oil-Water

▲ 6-in. ID, Horizontal Flow

▲ Findings

✦ Observed and Described Flow Patterns and Discovered a New Flow Pattern

✦ Acquired Significant Amount of Data on Various Parameters, Including Entrainment Fraction

▲ Remaining Tasks

✦ Development of Improved Closure Relationships

Low Liquid Loading Flow ...

◆ Current Study

➤ Three-phase, Large Diameter, Low Pressure Inclined Flow

▲ Air-Mineral Oil-Water

▲ 6-in. ID and $\pm 2^\circ$ Inclination Angles from Horizontal

▲ Objectives

✦ Acquire Similar Data as in Horizontal Flow Study

✦ Develop Improved Closure Relationships

Low Liquid Loading Flow ...



◆ Status

- On Hold Due to Insufficient Graduate Student Performance
- Study will be Continued Starting Spring 2009
 - ▲ New Ph.D. Student
 - ▲ Research Scholar, Professor Yuxing Li of China University of Petroleum

◆ Future Studies

- Two and Three-phase, Large Diameter, High Pressure Horizontal and Inclined Flow
 - ▲ Requires New High Pressure Facility

Up-Scaling Studies

- ◆ **Significance**
 - Better Design and Operation
- ◆ **Objective**
 - Testing and Improvement of Existing Models for Large Diameter and Relatively High Pressures
- ◆ **Past Studies**
 - Low Pressure and 6-in. ID Low Liquid Loading (Fan and Dong)
 - High Pressure 2-in. ID (Manabe, 2002)

Up-Scaling Studies ...

- ◆ **Current Project**
 - Construction of a New High Pressure, Large Diameter Facility
 - Extension of Low Liquid Loading Study to High Pressures is Envisioned as the First Study

Up-Scaling Studies ...

◆ Status

- Design is Complete
 - ▲ Operable with both Nitrogen and Natural Gas
- Professional Outside Evaluation of the Design is Complete
- P&ID Developed by EnSerca Engineering
- Fire Marshall was Contacted
 - ▲ Informal No Concern Response
- Long Lead Item Equipments Such As Compressor have been Ordered
 - ▲ Generator was Received

Up-Scaling Studies ...

◆ Near Future Activities

- SOP Preparation
- HAZOP Study
- Construction



Fluid Flow Projects

Up-scaling Studies in Multiphase Flow

Abdel Al-Sarkhi

Advisory Board Meeting, September 17, 2008

Outline

- ◆ Objectives
- ◆ Introduction
- ◆ High Pressure Large Diameter Facility
- ◆ Instrumentation
- ◆ Safety
- ◆ Capital Cost & Time Table
- ◆ Proposed Projects

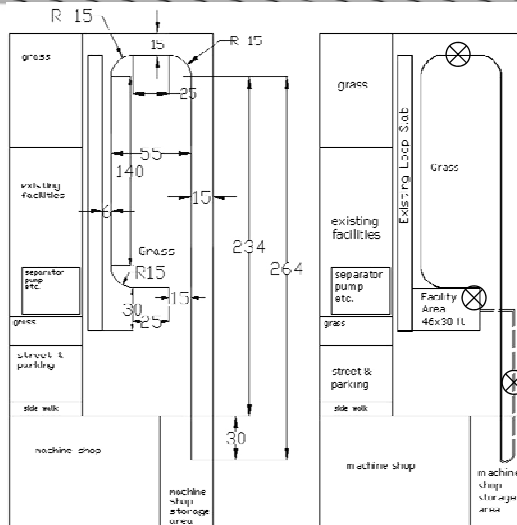
Objectives

- ◆ Investigate Effect of Pipe Diameter and Pressure on Multiphase Flow Behavior
- ◆ Verify and Improve Models/Correlations Against New Data

Introduction

- ◆ Pressure and Pipe Diameter Affect Flow Behavior in Multiphase Flow Significantly
- ◆ Most of Investigations are for Low Pressure and Small Diameter Conditions

High Pressure Facility (HFP) - Flow Loop Layout (Dimensions in Feet)



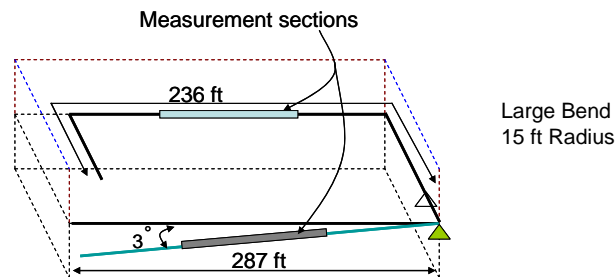
Fluid Flow Projects

Advisory Board Meeting, September 17, 2008

HPF - Test Section

Total Flow Loop Length = 523 ft = 160 m

Pipeline Diameter = 6 inch = 15.4 cm



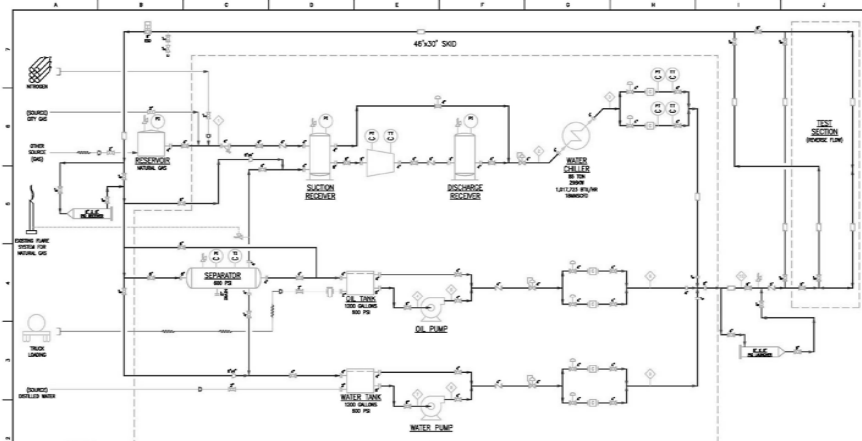
3° Upward /Downward Flow

Inclined Part Length = 287 ft = 87 m

Fluid Flow Projects

Advisory Board Meeting, September 17, 2008

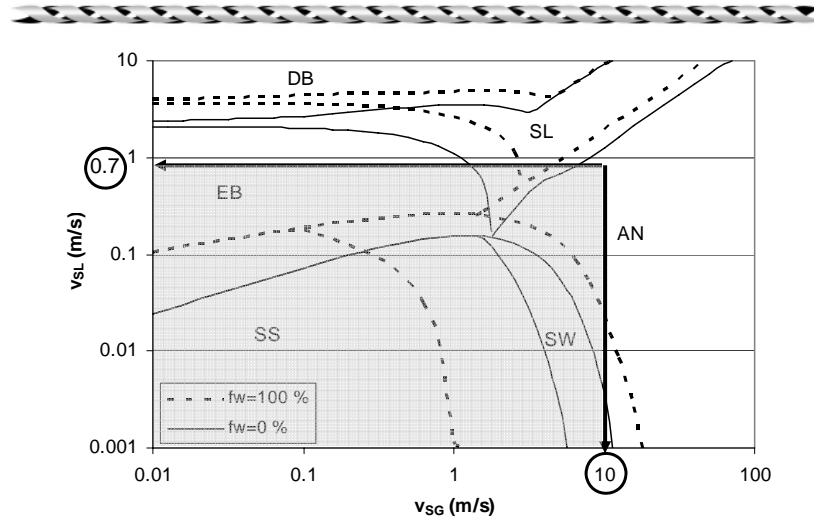
HPF Process Flow Diagram (PFD)



HPF- Fluids

- ◆ Gas Phase
 - Tulsa City Natural Gas
 - Nitrogen
- ◆ Oil Phase - Tulco Tech-80 Mineral Oil
- ◆ Water Phase - Distilled Water

HPF - Flow Pattern Maps



HPF - Operating Range

- ◆ Operating Pressure = 500 psig
- ◆ $v_{SL, max} = 0.7$ m/s; $v_{SG, max} = 10$ m/s
- ◆ f_w Between 0 and 100 %
- ◆ $q_{G, max} = 18$ MMSCFD
- ◆ $q_{L, max} = 200$ GPM
- ◆ Separator 54" x 10' @ 600 psig

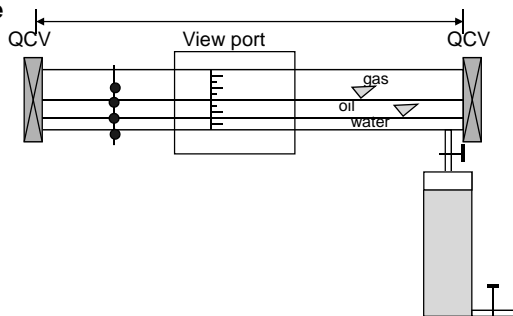
Instrumentation - Basic

	Pressure (psig)	Capacity (6 in. pipe)
Gas Flow Rate	600	18 MMSCFD
Water Flow Rate	600	200 GPM
Oil Flow Rate	600	200 GPM
Differential Pressure	500	0 – 50 in H ₂ O
Pressure	600	0 – 800 psi
Temperature	500	0-100 °C
Quick Closing Valves	600	6 in. ID

Instrumentation - Special

◆ Total Liquid Holdup

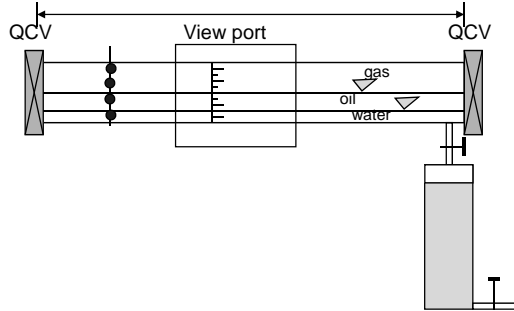
- Quick Closing Valve
- Viewing Window (Liquid Height Measurement)
- Two Lasers Sensor (Trial)
- Conductivity Probe for Water Height (?)
- Multipoint Densitometer



Instrumentation- Special

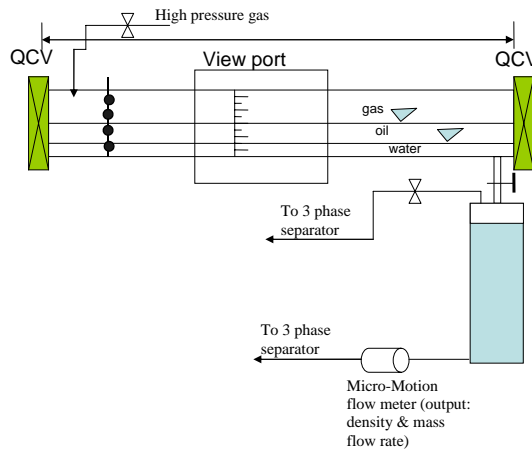
Oil/Water Holdup

- Quick Closing Valve
- High Pressure to Flush Liquid Out
- Wait for Separation of Oil and Water
- Multiple Point Densitometer to Get the Level
- Push Liquid Back to Separator Using Gas Line



Instrumentation- Special (Suggested By Fan)

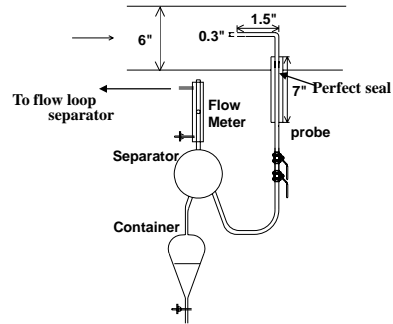
Oil/Water Holdup



Instrumentation- Special

◆ Liquid Entrainment

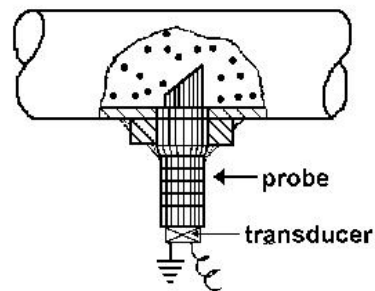
- Iso-kinetic Probe High Pressure Rating
- Gas Outlet to Separator
- Reaching Iso-kinetic Conditions is Expected to Be Challenging



Instrumentation- Special

◆ Liquid Entrainment

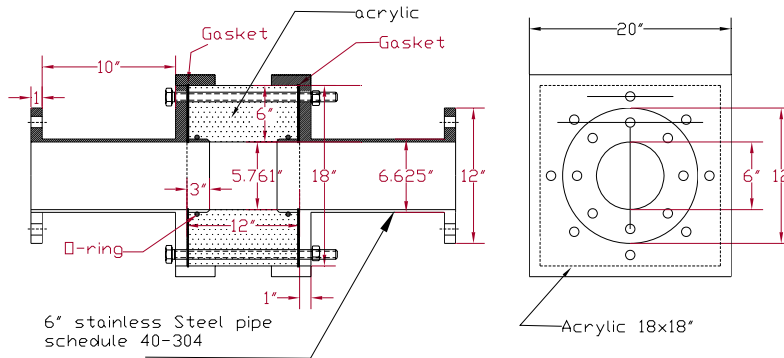
- Inline, Online Monitoring of Particle Flow
- Detection of Minute Shock Waves by the Impact of a Particle or Droplet on a Probe
- A Transducer Converts Waves, Which are Proportional to the Kinetic Energy, into Electrical Signals:
- $K.E. = \frac{1}{2} m v^2$
- Manufacturer Provides a Procedure to Accomplish Iso-kinetic Conditions



Instrumentation- Special

◆ Flow Pattern

➢ Visual Observation/Whole Perimeter Viewing Section

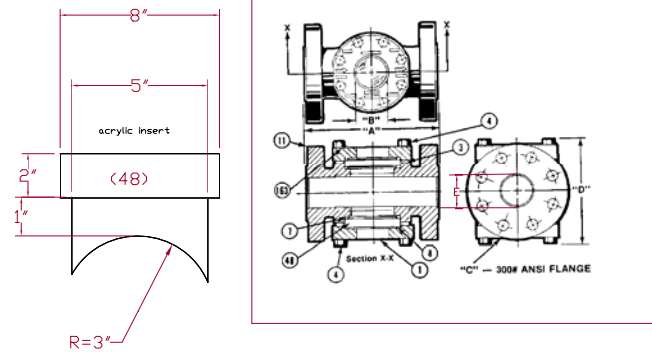


➢ Static Testing is Needed

Instrumentation- Special

◆ Flow Pattern

➢ Visual Observation/Partial Perimeter Viewing Section (Commercially Available)



Other Consideration

- ◆ **Insulating The Pipe For Better Temperature Control**
- ◆ **Stainless Steel Material Will Be Used (Previously Carbon Steel Was Suggested)**

Safety Issues

- ◆ **Residential Area Located on the East and North Side of the Pipeline Next to the Wooden Fence**
- ◆ **University Machine Shop Located in the South Side of the Pipe Line Area**
- ◆ **Onsite Control Room**
- ◆ **Finding the Right Safety Regulations**

Safety Considerations

◆ Three Steps:

- Hiring Professional Engineering Co. “Enserca Engineering”
- Use Nitrogen First
- Department of Transportation Safety Division Regulations

Safety Considerations

◆ Encerca Engineering

- P&ID Drawing and Process Flow Diagram
- Permit Review
- Civil / Structural Design and Drawing

Safety Considerations

- ◆ **Nitrogen Utilization**
 - **Master/Control All Sections at High Pressure for Issues of Seal and Instrumentation Connections Using Less Hazardous Gas**
 - **Establish Procedures for Using HFP**
 - **Train Our Staff and Student**
 - **Obtain Data at Higher Gas Density**

Safety Considerations

- ◆ **Department of Transportation – Safety Division:**
 - **Project does not Fall Under DOT Pipeline Safety Regulations**
 - **Design Pressure Formula**

$$P = \frac{2 \times S \times t}{D} F \times E \times T$$

S: Yield Strength; **t:** Nominal wall thickness; **D:** Outer Diameter;

F: Design Factor; **E:** Joint Factor; **T:** Temperature Derating Factor

- **P = 1,400 PSI >> 500 PSI (Operating Pressure)**

Capital Cost Analysis

- ◆ Option-1: Completion in 2009
- ◆ Option-2: Completion in 2010

Option-1

#	Component	Capacity	Cost (K \$)
1	Compressor	18 MMSCFD	242
2	Heat Exchanger	720,000 BTU/HR/Pass	20
3	Chiller	90 ton	67
4	Valves	2	20
5	Water pump	200 GPM	20
6	Oil pump	200 GPM	20
7	Separator	54" x 10' x 600	36
8	Water tank	1200 gallon	33
9	Oil tank	1200 gallon	33
10	Pipeline (SS)	6-in. ID, 540 ft	90
11	Densitometer	Multipoint	10

Option-1 ...

#	Component	Capacity	Cost (K \$)
12	Gas flow rate	18 MMSCFD	20
13	Water flow rate	200 GPM	20
14	Oil flow rate	200 GPM	20
15	Diff. pressure	0 – 50 in H ₂ O (8)	8
16	Pressure	0 – 800 psi (8)	5
17	Temperature	0-100 C (8)	5
18	QCV	6 in ID (5)	15
19	Power generator	500 KW	65
20	Steel structure/Tilting		50
21	Pressure regulator	3 (Oil, Water & Gas)	5
22	Concrete foundation	600 ft by 6 ft	50
23	Comp. Surge control	Daul loop	25
24	Data Acquisition system		10

Option-1 ...

#	Component	Capacity	Cost (K \$)
25	Pipe Insulation	540 ft	10
26	Geo-Tech-Exploration	3 points	2.4
27	Enserca Engineering		
	P&ID and PFD		27.4
	Permit Review		6.4
	Civil/Structural Design		31.5
	Total		967

Option-1 ...

- ◆ **Currently Spent \$400,000**
- ◆ **Requires \$567,000 Capital Expenditures**
- ◆ **Without Disruption of the Other TUFFP Projects, \$414,000 can be Spent**
- ◆ **Requires Supplemental One Time \$153,000 Capital Infusion**

Option-2

- ◆ **Complete on Oil-Gas in 2009**
- ◆ **Add Water Phase in 2010**

Option-2 ...

#	Component	Capacity	Cost (K \$)
1	Compressor	18 MMSCFD	242
2	Heat Exchanger	720,000 BTU/HR/Pass	20
3	Chiller	90 ton	67
4	Valves	2	20
5	Water pump	200 GPM	20
6	Oil pump	200 GPM	20
7	Separator	54" x 10' x 600	36
8	Water tank	1200 gallon	33
9	Oil tank	1200 gallon	33
10	Pipeline (SS)	6-in. ID, 540 ft	90
11	Densitometer	Multipoint	10



Fluid Flow Projects

Advisory Board Meeting, September 17, 2008

Option-2 ...


#	Component	Capacity	Cost (K \$)
12	Gas flow rate	18 MMSCFD	20
13	Water flow rate	200 GPM	20
14	Oil flow rate	200 GPM	20
15	Diff. pressure	0 – 50 in H ₂ O (8)	8
16	Pressure	0 – 800 psi (8)	5
17	Temperature	0-100 C (8)	5
18	QCV	6 in ID (5)	15
19	Power generator	500 KW	65
20	Steel structure/Tilting		50
21	Pressure regulator	3 (Oil, Water & Gas)	5
22	Concrete foundation	600 ft by 6 ft	50
23	Comp. Surge control	Daul loop	25
24	Data Acquisition system		10



Fluid Flow Projects


Advisory Board Meeting, September 17, 2008

Option-2 ...



#	Component	Capacity	Cost (K \$)
25	Pipe Insulation	540 ft	10
26	Geo-Tech-Exploration	3 points	2.4
27	Enserca Engineering		
	P&ID and PFD		27.4
	Permit Review		6.4
	Civil/Structural Design		31.5
	Total		967

Option-2 ...

- 
- ◆ **Currently Spent \$400,000**
 - ◆ **Spend \$414,000 in 2009 and Complete two-phase Gas-Oil**
 - ◆ **Spend \$153,000 in 2010 to Add Water Phase**

Time Table for Option-1

Tasks	Status	Completing time/ or required time
Quotation & Order	Under way	November 30, 2008
Engineering Design, Review	underway	2 weeks
Equipment Manufacture		
Compressor	Order Placed	28 -30 weeks
Pump	Quote U.	13 weeks
Heat Exchanger	Quote R.	15 weeks
Chiller	Quote R.	15 weeks
Separator	Quote R.	14 weeks
Tank	Quote R.	15 weeks
Power Generator		Received
Construction		March, 1, 2009
Calibration & Shake Down Tests		June 30, 2009

Quote R.: Quote Received

Quote U.: Quote Under way

Proposed Projects

- ◆ **Investigation of 2 phase Low Liquid Loading at High Pressures**
- ◆ **Investigation of 3 phase Low Liquid Loading at High Pressures**

Up-scaling Studies



Questions?

Upscaling Studies in Multiphase Flow

Abdel Al-Sarkhi

Objectives

Scaling up of small diameter and low pressure results to the large diameter and high pressure conditions is very important in multiphase flow research studies. Studies with a large diameter facility would significantly improve our understanding (and modeling) of flow characteristics in actual field conditions. Therefore, our main objective in this project is to be able to investigate the effect of pipe diameter and pressures on flow behavior using a large diameter and high pressure flow loop.

Introduction

Gas-liquid pipe flow characteristics, such as flow patterns, pressure drop and liquid holdup, have been mostly investigated with small-diameter pipes (2 or 3 in.) and low pressure conditions (lower than 100 psig). Two-phase flow behavior in large diameter pipes, under high pressure condition is different from those under these experimental conditions. It is important to validate the applicability of the models with experimental results obtained for conditions similar to those experienced in a real field.

A new facility with large pipe diameter and high pressure is proposed to investigate the effects of pipe diameter and pressure on two-phase and three-phase flow behaviors. Experimental data from this facility can be used to evaluate the existing models and correlations. New models and closure relationships can be developed if needed.

New Flow Loop

Fluids

The facility is designed for gas-oil-water three-phase flow. Tulco Tech-80 Mineral oil and distilled water are the liquid phases. The facilities, equipment and instrumentation are designed to have the ability to work on either Tulsa City Natural gas or Nitrogen. Initially, Nitrogen is planned to be used due to its relatively low safety risk. In fact, Nitrogen has a higher density than natural gas at the same operating condition (Table 1). Next will be the natural gas. The current flare system will be checked before

switching to the natural gas in terms of capacity, and duration.

Experimental Setup

The facility is composed of gas, oil, water system and separation systems and test section. The operating pressure will be 500 psig. The flow loop length will be 523 ft approximately. The last section will have the ability to be inclined 3° downward and for the upward flow the direction of the flow will be reversed. The inclined section starts at a distance of 236 ft from the pipe inlet.

The inclinable section length will approximately be 287 ft. The L/D ratio at the beginning of the inclination part of the pipe will be around 472. The test section of the inclined part of the pipe will be 140 ft away from the pipe outlet which makes the L/D ratio on the inclinable section only (from starting point of the inclined section to the test section) around 280 to ensure a fully developed flow.

The process flow diagram (PFD) of the facility with all its components is shown in Figs. 1A, 1B and 1C. Figure 2 shows the layout, the space available for the flow loop and the location of the borings for the geotechnical exploration of the loop area. Figure 3 shows the location and details of the inclinable part.

The natural slope of the ground will be taken into consideration. The support system will be constructed on pillars support made of I-beams.

Operating Conditions Range

Flow pattern maps have been generated using Barnea model with two water cuts (0 % and 100%) for a 6 in. pipe at 500 psig system operating pressure as shown in Fig. 4. The operating range of the facility can be decided based on the flow pattern maps.

The maximum superficial gas velocity will be 10 m/s at 500 psig. The maximum superficial liquid velocity will be 0.7 m/s with water cut from 0 to 100%. With these superficial velocities, the flow patterns will be mainly stratified flow and intermittent flow.

Gas, Oil, Water and Separation Systems

According to maximum gas and liquid superficial velocities, the capacities of compressor, pumps, separator, heat exchanger, chiller and tanks can be decided. For the compressor, the design flow rate, discharge and suction pressures are 18 MMSCFD, 500 psig and 400 psig, respectively. For the pumps, the design flow rate is 200 GPM with the same discharge and suction pressures as for compressor. The volume of oil tank and water tank should be 1200 gallons and have pressure rating of 600 psig. The dimensions of the cylindrical three-phase separator will be 54" x 10'. The separator will have a pressure rating of 600 psig. Separator and tanks will be coated against corrosion.

Using gas liquid separator followed by lower pressure liquid-liquid separator for high viscosity oil has been suggested. The flow loop components have been designed for low viscosity. However, in case of running high viscosity liquid a parallel separating system and pumps have to be considered.

Heat Exchanger & Chiller

Based on the Sundyne compressor specification sheet for the inlet condition 414 psia and 100 F, the outlet condition will be 515.7 psia and the outlet temperature will be 138.2 °F. There will be an increase in the temperature of about 38 °F. A heat exchanger must be designed and installed to fix the gas temperature same as the inlet temperature. Based on all parameters summarized in Table 1 for the natural gas (Methane), a heat exchanger with maximum (at maximum flow rate) heat duty of 210 KW (720,000 BTU/HR) is required. Chilled water must be provided to the heat exchanger. Based on the maximum operating condition, a 60-ton Chiller must be used. For the Nitrogen as gas phase, a heat exchanger with heat duty of 298 kW (1017723 BTU/HR) is required and a chiller with 85 ton capacity is needed to provide the chilled water to the heat exchanger at maximum flow rate.

Test section

The inner diameter of test section will be 6 in. The flow developing section will be longer than existing low pressure test section. The inclination angle can be changed from 0 to -3 degree and for the upward flow (0 to +3), the direction of the flow will be reversed. Two measurement sections are planned. The first will be placed at 135 ft (L/D=270) from the entrance and the second will be placed at 440 ft (L/D=880) from the entrance. To minimize the effect

of pipe bend on the flow, a wide bend with 15 ft turning radius will be installed.

Basic Instrumentation

The following are proposed instrumentation for the high-pressure flow loop.

Pressure and Temperature

Flow rates for gas, oil and water phase will be measured by Micro Motion flow meters separately. Pressure and temperature will be measured by pressure and temperature transducers, respectively. Differential pressure transducers will be mounted on the test section and developing section to measure the pressure gradient and to monitor the flow development. These instruments will be high pressure rated.

Liquid Holdup

Total Liquid Holdup

Quick closing valves will be used to measure the total liquid holdup. A trapped-liquid measurement vessel needs to be designed to measure the volume of the trapped liquid for two-phase flow (gas and water), see Fig. 5. In addition, the liquid level in the pipe will be measured through the viewing window. For three-phase flow of water, oil and gas especially at low water cut some of the residual oil may remain in the pipe, this will be checked using Gamma Ray Densitometer and viewing port. Uncertainty analysis will be also performed to get the residual amount of oil (if exist) statistically. Moreover, a measurement of the height of the liquid level and the wetted pipe perimeter will be used to calculate the total liquid holdup in some cases (high and low water cuts). Different view port designs will be discussed later. Multiple point densitometer may be used to measure the liquid height and density of the trapped liquid between the two Quick closing valves.

Oil and Water Holdup

Oil and water holdup measurements will be one of the most difficult tasks. Using the scale on the view port may not give the oil or water holdup separately since the distribution of oil and water (at certain water cuts) may take different shapes and not just two segregated liquid layer on top of each other. If the two liquid phases were completely segregated, we can use the height measurement to calculate the liquid holdup. A new technique will also be developed to measure the height of the water and oil based on two laser sensors one from the top and another from the bottom in case of the segregation. This technique will be developed and tested in house.

The height of the water film will be also measured by the conductance probe technique. It is worth mentioning that at low pressure experiments we have used pigging system to push all liquid out of the trapped space between the two Quick closing valves (specially at low water cut). High pressure may be used to flush the liquids out to an external lower pressure vessel. If necessary a pigging system can be installed and used. At the end, any separation technique can be used to get phase fractions. After flushing all the liquid out of the trapped space between the two Quick closing valves, a densitometer detector will be used to scan the area between the quick closing valves to make sure that there is no residual liquid left. Uncertainty analysis will be conducted to evaluate any oil residual. In some cases, Gamma-Ray densitometer may give the holdup measurement. At least one multiple point densitometer will be installed to give the height and the density of the trapped liquid between the quick closing valves. All techniques will be implemented and compared to achieve accurate measurements.

Another possible procedure suggested by Yongqian Fan of, ConocoPhillips as shown in Fig. 5B envisions using a collecting container (500 psi rated) and a Micro-Motion flow meter. The collecting container is actually a small 2-phase separator, which consists a cylinder, an inlet (connected to drainage pipe from test section), a gas outlet at top (connected to the 3-phase separator), and a liquid outlet at bottom (connected to a Micro-Motion flow meter, then merge with the pipe from gas outlet to the 3-phase separator). Additional piping is needed to connect the high pressure gas to the part between quick closing valves, to drain liquid from test section to the collecting container, and to push the liquid from the collecting container through the Micro-Motion flow meter to the 3-phase separator.

Film Thickness

The film thickness of the water will be measured using conductivity probe, and the total film thickness will be measured visually by measuring the height of liquid using the scale pasted on the viewing port. The accuracy of this measurement will depend on the interface shape between the liquid and the gas.

Moreover, film thickness and wetted perimeter can be measured by using Gamma Ray Densitometer.

Liquid Velocity

The liquid velocity will be measured by injecting a cold liquid at the same pressure or slightly higher pressure. The injected cold water will be supplied by

a pump or a pressurized tank as shown in Fig. 6. The difference in temperature along a certain distance over a period of time will be used to calculate the liquid velocity. The time difference between the temperature peaks detected by two temperature probes will be recorded with a high-speed data acquisition system.

Liquid Entrainment

Iso-Kinetic Probe

Liquid entrainment will be measured by using Iso-kinetic probe high pressure rating as shown in Fig. 7A. The stagnation probe, separator, and the container will be high pressure rated. The gas outlet will be connected to the flow loop separator, which is the lowest pressure point in the system. The challenge in this technique is the probe tube seal into the pipeline must be perfect and the high-pressure rating of the other components.

Droplet Monitor

A new measurement technique, inline, online monitoring of particle flow and concentration will be considered. The new device, as shown in Fig. 7B, is claimed to measure the number and average mass of particles, and the mass of each individual particulate and calculate particle size. The monitoring method is based on detection of minute shock waves produced by the impact of a particle or droplet on a probe. A transducer converts these waves, which are proportional to the kinetic energy, into electrical signals:

Flow pattern

The visual observation of the flow pattern will be done through viewing port or/and through a video Borescope with built in lightning system. The commercial viewing ports or sight indicator available in the market are not made with careful attention of flow pattern. The available sight indicators in the market usually disturb the flow pattern either by the expansion of the inside diameter right at the viewing window or by the flat glass (sapphire) piece on a round pipeline surface.

Different designs for the viewing port are considered and presented below:

Design A: Whole perimeter viewing section

This design made of a thick piece of polycarbonate acrylic that covers the whole parameter of the pipe as shown in Fig. 8A. The thick piece of acrylic will be fixed by two flanges as shown in the figure. A

destructive test will be performed to make sure that this design will handle more than 500 psig.

Design B: Partial perimeter viewing section

This design based on the sight indicator available in the market with some modification to remove all the flow disturbance sources from their design (Fig. 8B). It consists of two pieces of polycarbonate acrylic inserted inside a containing flange. The inserted acrylic piece will have the same curvature as the inside pipe diameter so it will not cause any flow disturbance.

More instrumentation will be implemented depending on the research needed

Temperature Control

For better temperature control the pipe will be insulated and the temperature will be monitored at different sections. Chiller-heat exchanger system will be used to control the excess temperature from the compression stage.

Pipe Material

Stainless steel material will be used instead of previously selected carbon steel as the pipe material to eliminate corrosion. Although the price of the stainless steel is about 3 times higher than the carbon steel and the machining cost is also higher, the pipe cost is not a major compared to the total project investment.

Liquid monitoring and Sampling

Liquid sampling vs. monitoring of water in oil or oil in water techniques. These two techniques are considered, we will be able to get sample from the liquid between two quick closing valves if required and we will be able to monitor the oil water mixture.

Safety Issues

Several feedbacks from members about the safety requirement of the facility were received. The challenges are mainly comes from the location and space available and if the loop will have enough distance to nearest office trailer, machines-shop and residential area. A residential area located on the east and north side of the pipeline next to the wooden fence (the pipe is 15 ft away from the fence). The University machine shop located in the south side of the pipeline area (the pipe is 20 ft away from the machine shop). On-site control room at the center of the loop area as shown in Fig. 2.

In considering the safety concern, the following actions are completed, underway, or will be completed in near future:

Hiring a Professional Engineering Company

Enserca Engineering is hired to help us in completing this project. The scope outsources to Enserca consists of the creation of the Preliminary Process Flow Diagram (PFD), Process and Instrumentation Diagram (P&ID), Civil/Structural design and drawing for equipment building and piping support and Permit Review.

Design Considerations for Use Nitrogen and Natural gas

Initially Nitrogen will be used as a gas phase instead of Methane with the following objectives:

- To master/control all sections at high pressure for issues of seal and instrumentation connections using less hazardous gas.
- To train our staff and student and establish a procedure for using the high pressure facility
- To obtain data at higher gas density especially for entrainment for comparison purposes.

The final stage of this project will use the Methane as a gas phase with the following precautions:

- A line from the flow loop to the existing flare system needs to be installed. The methane pressure will be reduced by passing it to a tank (this tank will be located close to the existing flare system), then the new reduced pressure will be bleed to the low flaring pressure by using two needle valves and pressure regulator.
- Several emergencies quick closing valves will be installed and by which the flow loop can be separated into sections in case of any leakages.
- The electrical power generator will be installed away from the flow loop and then there will be no source of ignition around.
- A restricted running procedure and training will be established for the safety of the operator and the facility.

Department of Transportation Part 192 Regulations and Basic Calculation

Department of Transportation-Pipeline Safety Division has been contacted to check if they have any regulations to follow. They indicated that the available regulations do not apply to our case because of the fact that the facility is a research laboratory and not in a transportation state, not affecting other commerce and not going to sale any product.

In addition Williams Brothers' lead facility engineer in exploration and production division was contacted. The engineer referred us to the safety regulation part 192 from Department of Transportation - Transportation of Natural and other Gas by Pipeline. Based on the recommended calculations the maximum operating pressure for the selected piping is 1400 psi. Our operating pressure is 500 psi significantly lower than the maximum.

Solubility Issues

A concern about using the Nitrogen as a gas phase and if the Nitrogen will have similar behavior as the methane has been raised because of the lower solubility of the Nitrogen compared to the Methane. The solubility of the Methane is about 4 times that of the nitrogen on the Mole bases and it is about twice on the mass bases due to the difference in their molecular weights. The solubility will mainly affect the viscosity of the flowing liquid but at the end the flow behavior will be almost comparable. Regarding the entrainment fraction, the main factor is the difference in the gas density at the operating pressure which will be recorded.

Geo-Technical Analysis of Loop Area

Terracon Consulting Engineering and Scientists has conducted the subsurface geo-technical analysis for

the facility. Recommendations regarding the design and construction of the foundations and the support of the floor slabs, relative to the subsurface conditions encountered in the borings are contained in their report. The borings locations are shown in Fig. 2.

Capital investment

The design and construction of a high pressure and large diameter facility is a very significant capital investment for TUFFP. All the equipment are being shopped around and negotiated with suppliers. The estimated costs for the three phase facilities are listed in Table 2. Labor cost is not included.

Time Table

The completion of the design and construction of the facility is expected to be ready to operate by June 2009 (see Table 3). The most time consuming item is the Compressor. The compressor is ordered, and expected to be received shortly.

Proposed Initial Project

Investigation of low liquid loading at high pressures is proposed to be investigated as the first research project for this facility.

Table 1: Methane Properties and Flow Conditions for Heat Exchanger Design

	Methane		Nitrogen	
	English Units	SI Units	English Units	SI Units
Outlet Temperature	100 F	311 K	132.6 F	329 K
Intlet Temperature	138 F	332 K	60 F	288 K
Pressure	500 psig	3447.4 KPa	500 psig	3447.4 KPa
Gas Constant	0.124 BTU/lbm-R	0.518 kJ/Kg-K	0.071 BTU/lbm-R	0.297 kJ/Kg-K
Critical Temperature	343.9 R	191.1 K	227.16 R	126.2 K
Critical Pressure	673 psia	4.64 MPa	491.67 psia	3.39 MPa
Compressibility factor	0.95	0.95	1	1
Density	1.45 Lb/Ft ³	23.2 Kg/m ³	2.4 Lb/Ft ³	38.5 Kg/m ³
Mass Flow Rate at v_{SG} =10 m/s	9.32 lb/s	4.23 Kg/s	15.43 lb/s	7 Kg/s
Specific Heat at 300 K, Cp	0.532 BTU/lbm-R	2.2537 KJ/Kg-K	0.248 BTU/lbm-R	1.039 KJ/Kg-K
Heat Exchanger Duty Per Pass	720,000 BTU/HR	210 KW	1017723 BTU/HR	298 KW
Chiller Capacity	60 ton	60 ton	95 ton	95 ton

Table 2. Facility Capital Cost Analysis (in \$1000)

	Component	Capacity	Cost	Status*
1	Compressor	18 MMSCFD	242	Q. P.
2	Compressor Surge Control	Dual loop controller	25	Q.R.
3	Heat Exchanger	1017723 BTU/HR/pass	20	Q. R.
4	Chiller	95 ton	67	Q. R.
5	Safety Valves, others		20	
6	Water Pump	200 GPM	20	Q.U.
7	Oil Pump	200 GPM	20	Q.U.
8	Separator-Coated	54" x 10' @ 600 psig	36	Q. R.
9	Water Tank-Coated	1200 gallon	33	Q. R.
10	Oil Tank-Coated	1200 gallon	33	Q. R.
11	Test Section	6 in. ID	20	
12	Gas Flow Metering	18 MMSCFD	20	
13	Water Flow Metering	200 GPM	20	
14	Oil Flow Metering	200 GPM	20	
15	Differential Pressure	(8) with proper range	8	
16	Pressure	(8) with proper range	5	
17	Temperature	0-100 °C (8)	5	
18	QCV	6 in ID (7)	15	
19	Power Generator	500 KW	65	Received
20	Steel structure & Tilting		50	
21	Stainless steel pipe	Schedule 40 304 SS	70	
22	Pipe Insulation		10	
23	Pressure Regulator	3 (oil, water & gas)	5	
24	Concrete Foundations and Pillars	600 ft by 5 ft	50	Q.U.
25	Data Acquisition System		10	
26	Densitometer	Multipoint	10	
27	Geo-Tech. Analysis		2.4	Received
28	P&ID and PFD		27.4	O.P.
29	Permit Review		6.4	O.P.
30	Civil Structural Design & Drawing		31.5	O.P.
	Total		\$ 967K	

Q. R.: Quote Received ; Q. U.: Quote Underway; O.P.: Order Placed

Table 3: Time Table for Facility Construction

Tasks	Status	Completing or Required Time
Quotation & order	Underway	June 30, 2008
Engineering design, review	Underway	8-10 weeks
Equipment manufacture		
Compressor	O.P.	28 -30 weeks
Pump	Q. U.	13 weeks
Heat Exchanger	Q. R.	15 weeks
Chiller	Q. R.	15 weeks
Separator	Q. R.	20 weeks
Tank	Q. R.	15 weeks
Power generator	Q. R.	16 weeks
Construction		October 30, 2008
Calibration & shake down tests		June 30, 2009

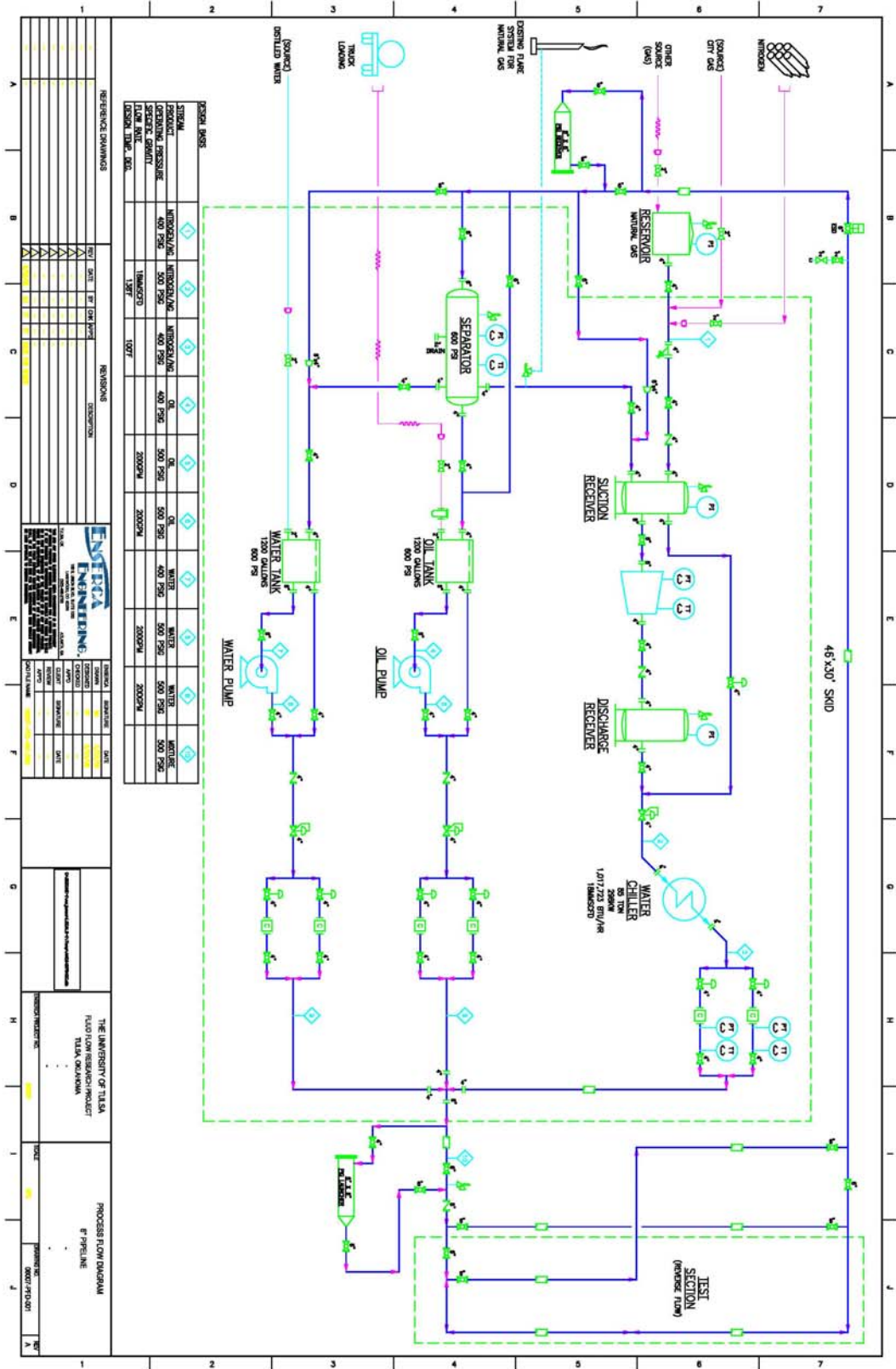
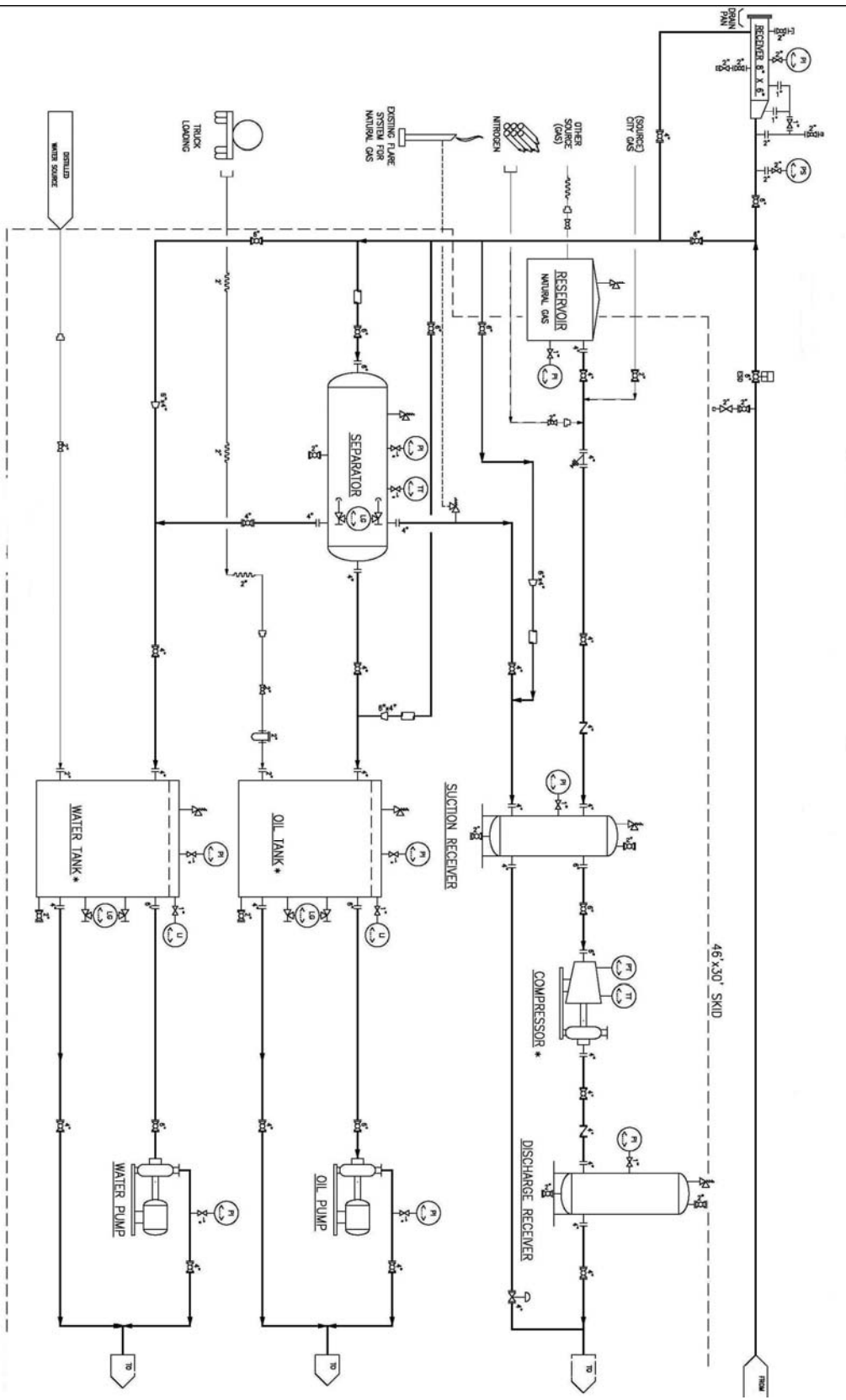


Figure 1A: Process Flow Diagram (PFD)



Process Flow Diagram Detail, Part 1/2

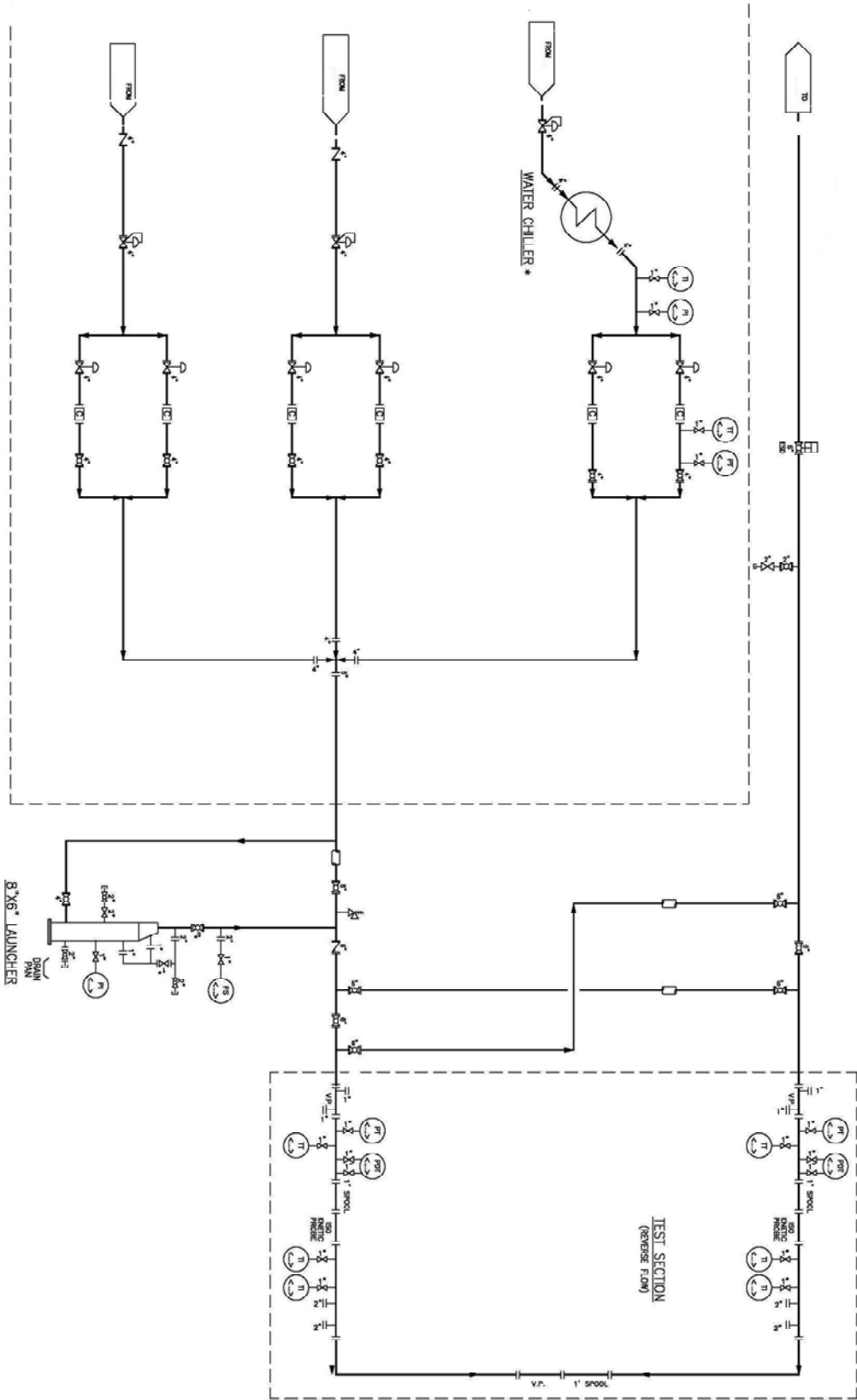


Figure 1B: Process Flow Diagram Detail - Part 2/2

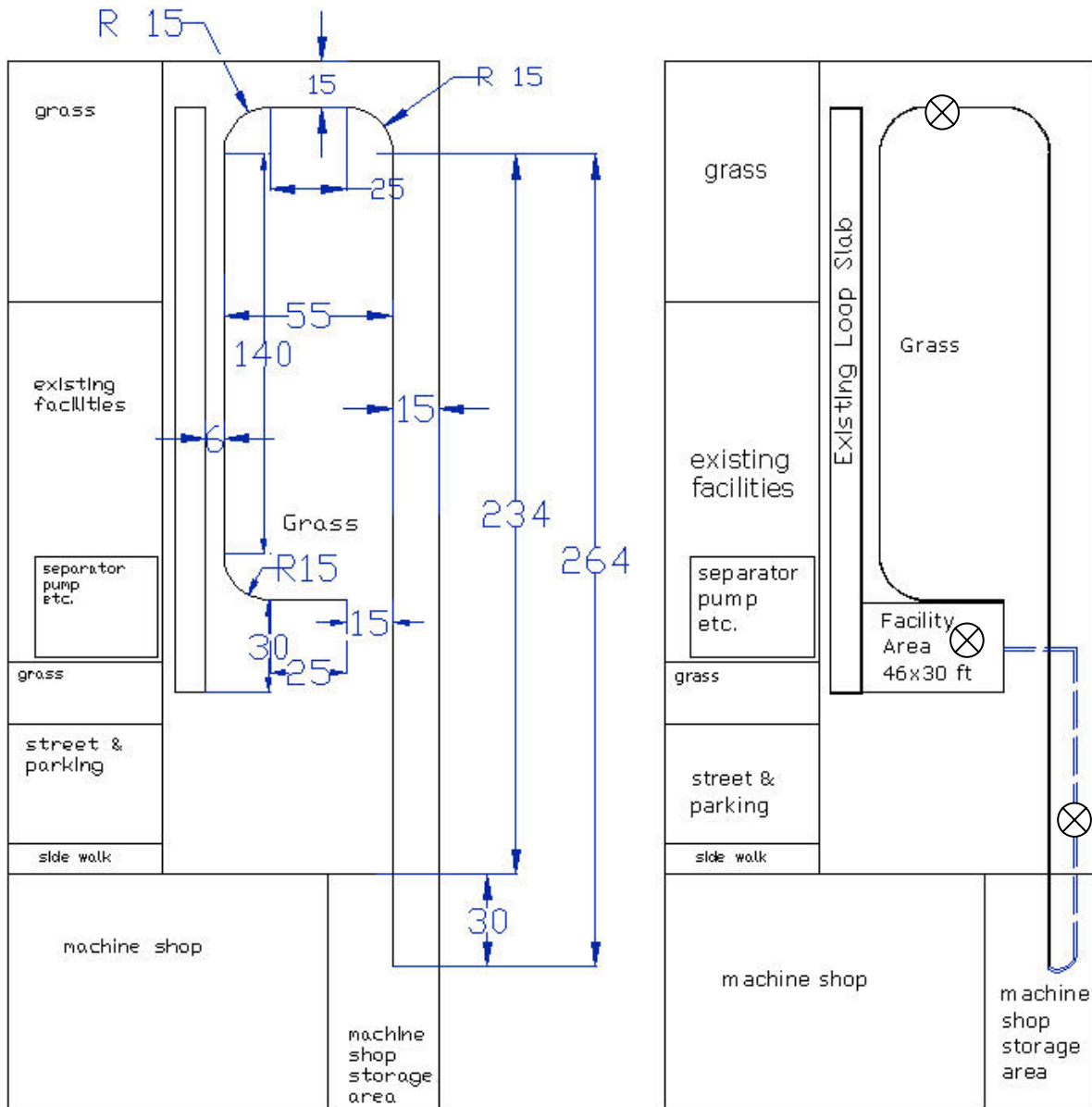


Figure 2: Flow Loop Layout and Available Space (Dimensions in feet)

⊗ Borings Location for Geotechnical Analysis

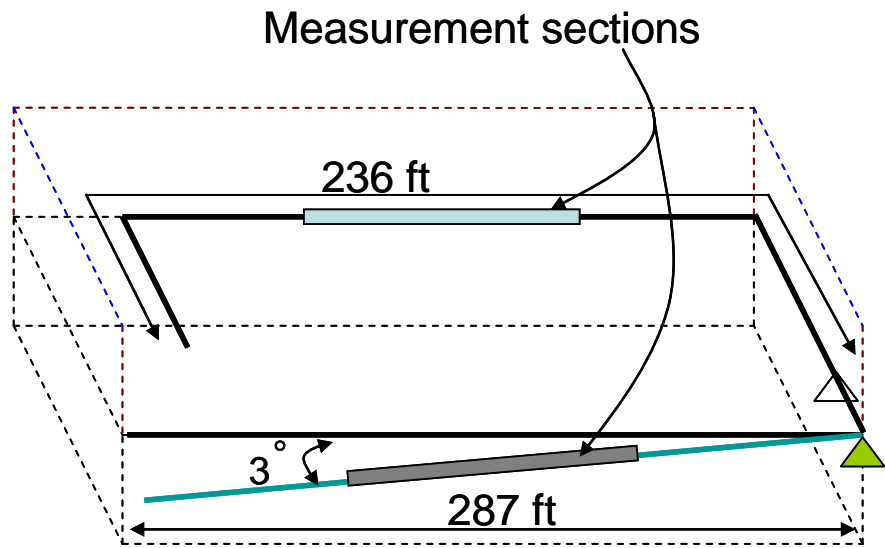


Figure 3: Pipe Inclination Details

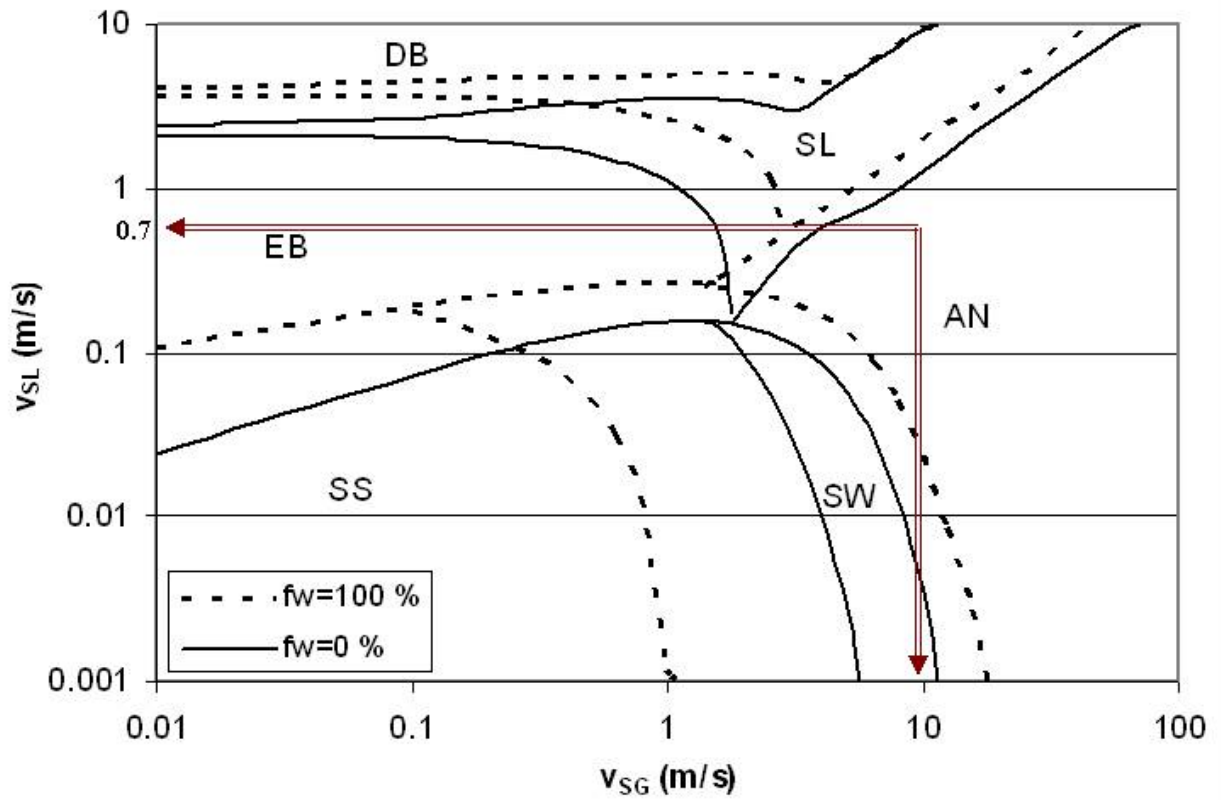


Figure 4. Flow Pattern Map for 100% and 0% Water Cut at 500 psig, 6 in. Pipe

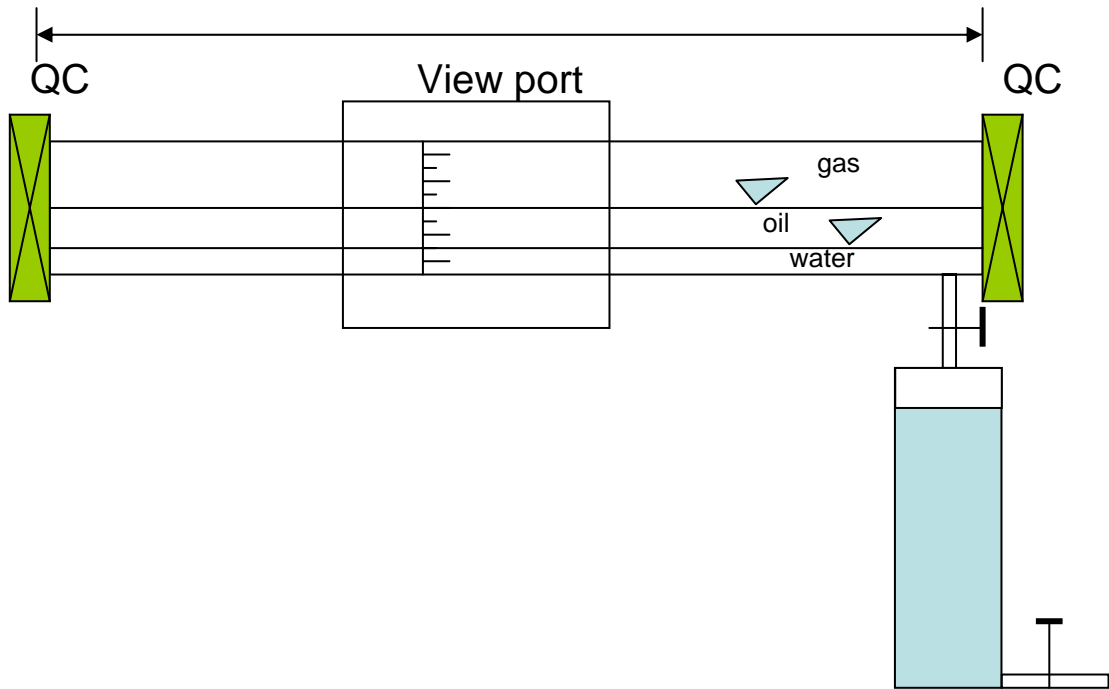


Figure 5A: Liquid Holdup Measurement Technique

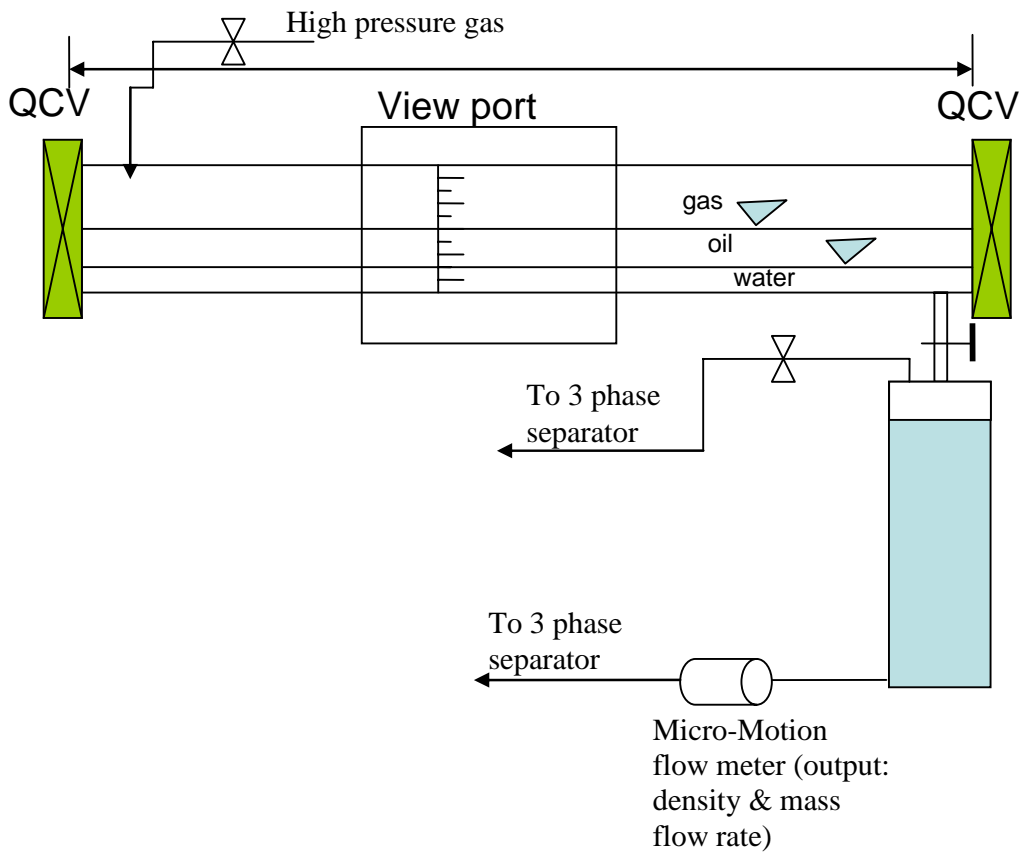


Figure 5B: Liquid Holdup Measurement Technique (Yongqian Fan's suggestion)

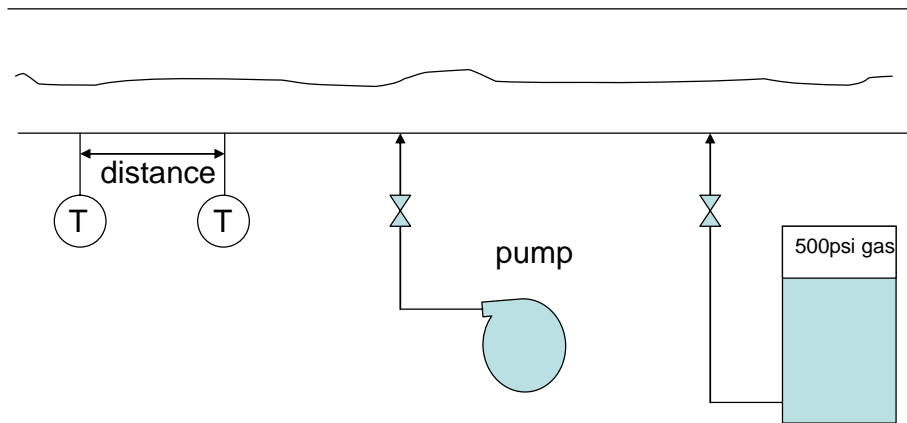


Figure 6: Liquid Film Velocity Method (Cold Liquid Injected Either by a Pump or a Pressurized Tank)

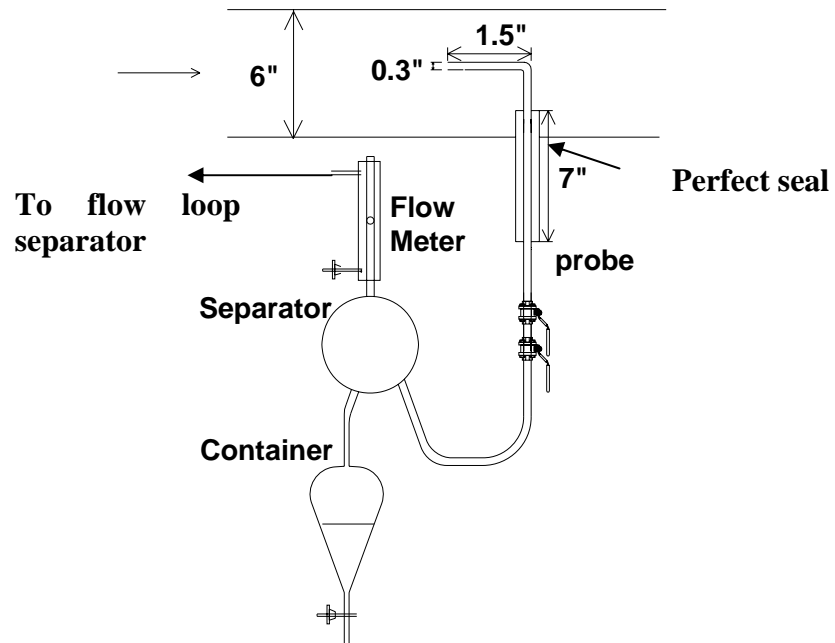


Figure 7A: Iso-kinetic Probe - High Pressure Rating

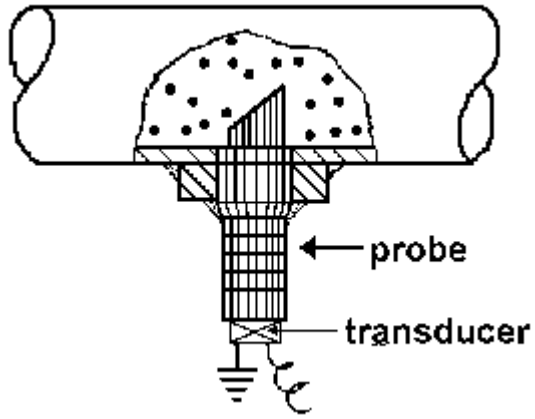


Figure 7B: Particulate Monitor Device

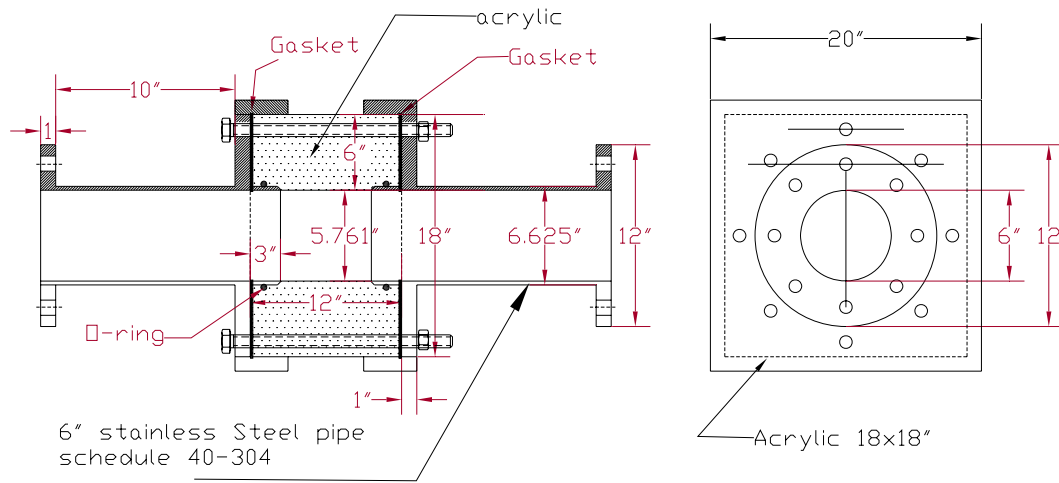
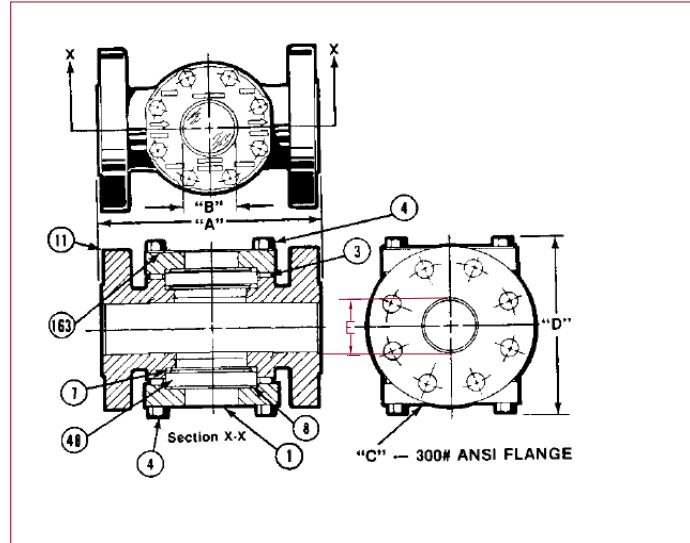
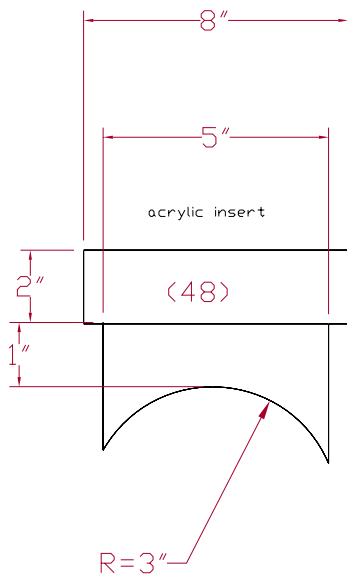


Figure 8A: Viewing Port (*Design A: Whole perimeter viewing section*)



- A: 21 inch
 - B: 6 inch
 - C: 17 inch
 - D: 17 inch
 - E: 6 inch
- the inner pipe diameter is 6 inch
ANSI class 300# flange will allow
up to 500 psig

Figure 8B: Viewing Port (*Design B: Partial Perimeter Viewing Section*)

Transient Modeling

◆ Significance

- Industry has Capable All Purpose Transient Software
 - ▲ OLGA, PLAC, TACITE
- Efforts are Well Underway to Develop Next Generation All Purpose Transient Simulators
 - ▲ Horizon, LEDA
- Need for a Simple Transient Flow Simulator

Transient Modeling ...

◆ Objective

- Development and Testing of a Simple Transient Flow Simulator

◆ Past Studies

- TUFFP has Conducted Many Transient Multiphase Studies
 - ▲ Scoggins, Sharma, Dutta-Roy, Taitel, Vierkandt, Sarica, Vigneron, Minami, Gokdemir, Zhang, Tengedal, and Beltran

Transient Modeling ...

- ◆ **Current Study**
 - **Kwonil Choi is Focusing on Development of a Lagrangian-Eulerian Model**
 - ▲ Simplified and Applicability Will be Limited
- ◆ **Status**
 - **Mr. Choi has Spent His Allowed 3 Years in US**
 - **Returned to Brazil**
 - **Plans to Pursue His Studies from Brazil**
- ◆ **Future Studies**
 - **Simplified Model**
 - ▲ Relatively Fast
 - ▲ Usable as a Screening Tool
 - ▲ Project Proposal Rated High in Recent TUFFP Questionnaire

Instrumentation Development

- ◆ **TUFFP Constantly Looks for Better Instrumentation**
- ◆ **Capacitance Sensor Development is Currently Underway**
- ◆ **Will be Used in Several Projects**
- ◆ **Progress**
 - **New Circuit (Insensitive to Environment)**
 - **New Housing**
 - **Works Fine for Oil-Gas**
 - **Has Its Challenges with Water**



Fluid Flow Projects

Capacitance Sensor

Scott Graham

Advisory Board Meeting, September 17, 2008

Background

- ◆ **At Spring 2008 Advisory Board Meeting**
 - **Previous Work with the Conductivity Probes Showed They Were Only Applicable for Separated Flow Patterns**
 - **Need For Better Measurement of Water Fraction During Three-phase Flow**
 - **Capacitance Measurement is Identified as Possible Technique**

Common Knowledge

- ◆ **Oil-Gas**
 - Works Fine
- ◆ **Oil-Water-Gas**
 - Works for Trending Information in Regards to Water Concentration
 - Never Intended for Precision Measurement of Holdup

Objective

- ◆ **Develop New Generation of Capacitance Sensors for Use in Various TUFFP Projects**

Design Criteria

- ◆ Weather Proof
- ◆ Easy to Relocate
- ◆ Stable Over Temperature and Humidity
- ◆ Easily Tuned for Different Applications
- ◆ Repeatable Measurements

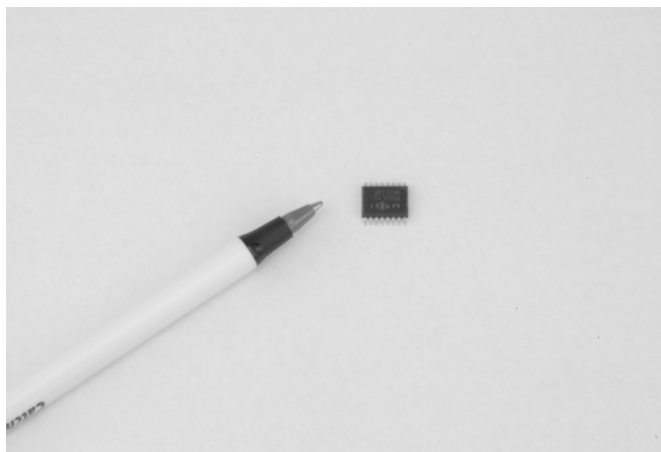
Old Faithful



The Guts



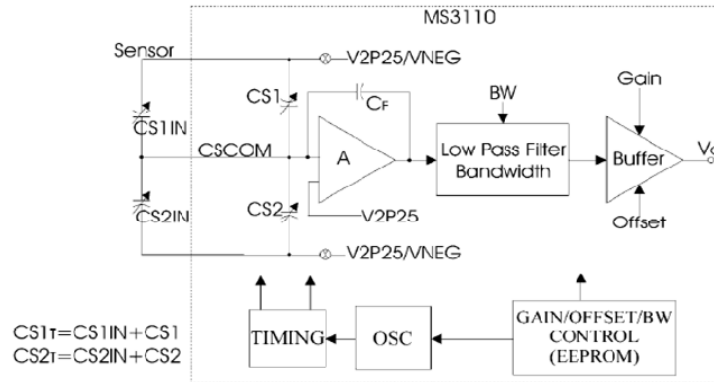
IC from Irvine Sensor



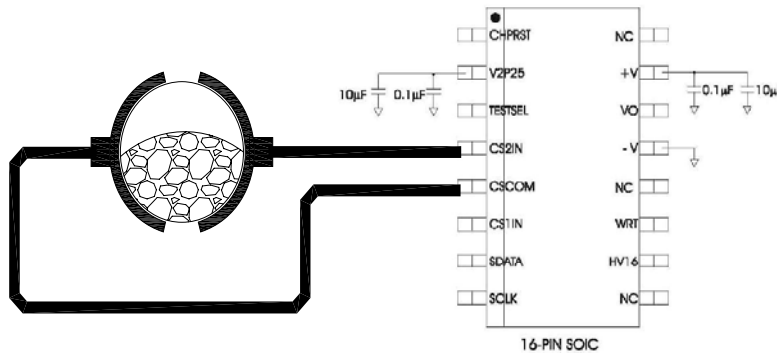
Block Diagram

MS3110 Universal Capacitive Readout^{IM} IC

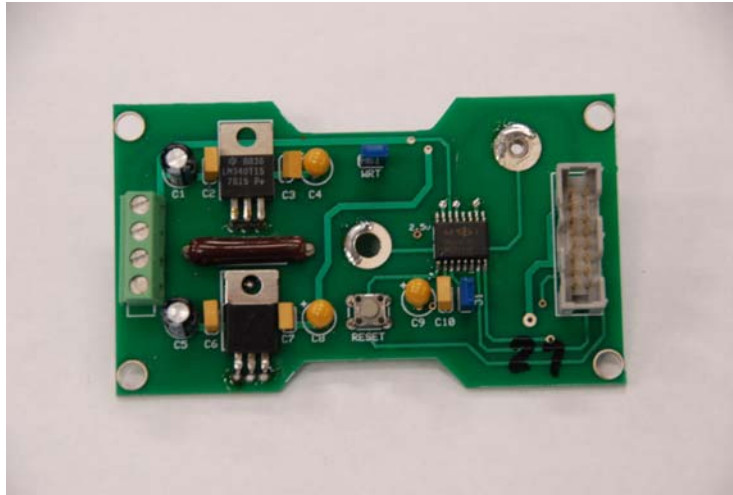
Functional Block Diagram:



System Components

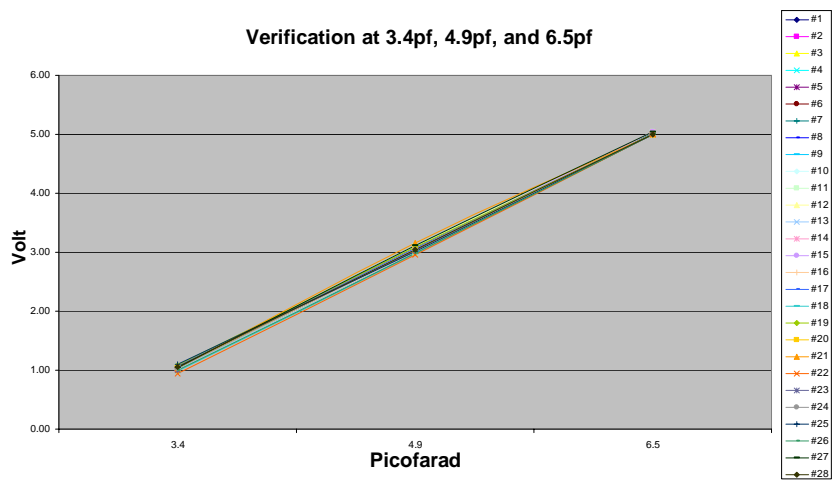


Actual Circuit Board

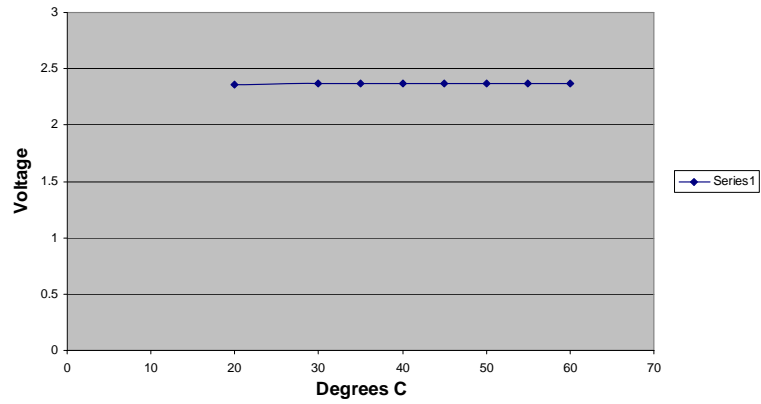


Repeatability Between Circuits

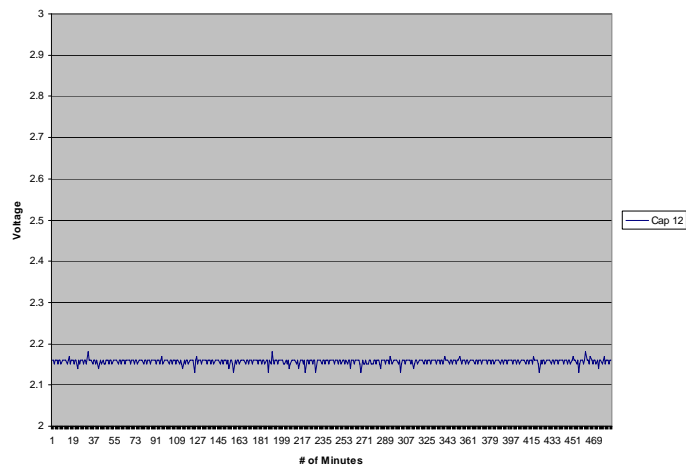
Verification at 3.4pf, 4.9pf, and 6.5pf



Temperature Stability



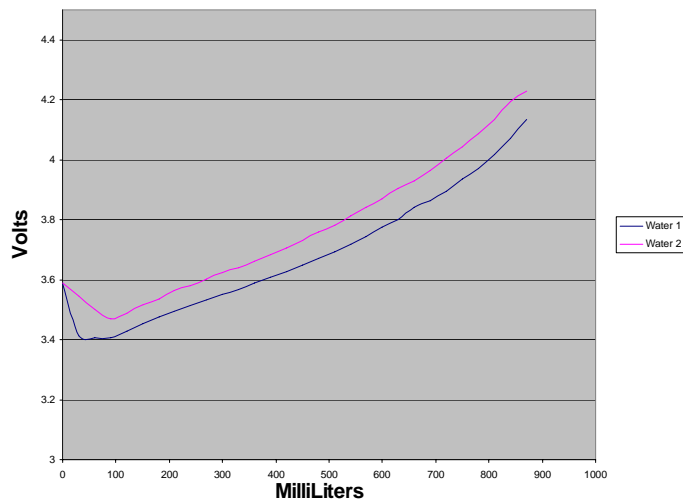
Long Term Stability Test



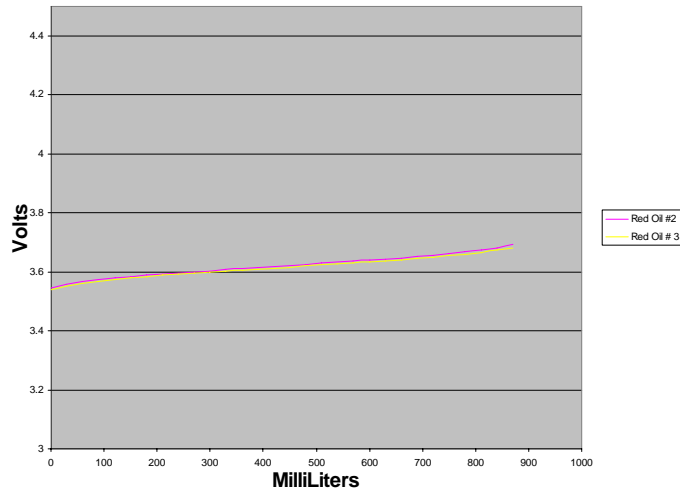
New Capacitance Probes



Water 0 – 100%



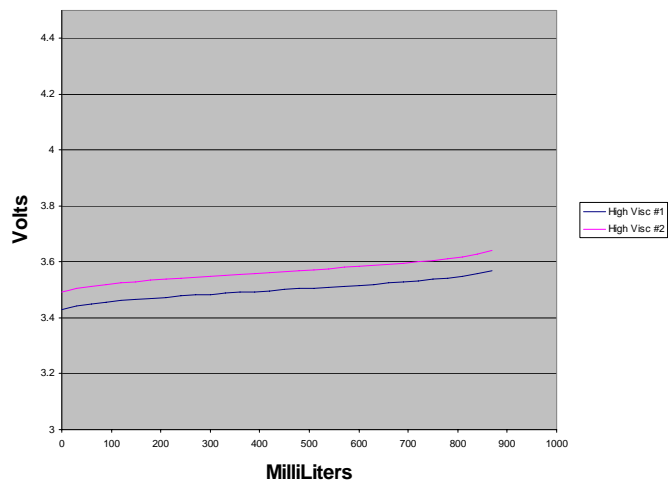
Low Viscosity Oil 0 – 100%



 Fluid Flow Projects

Advisory Board Meeting, September 17, 2008

High Viscosity Oil 0 – 100%



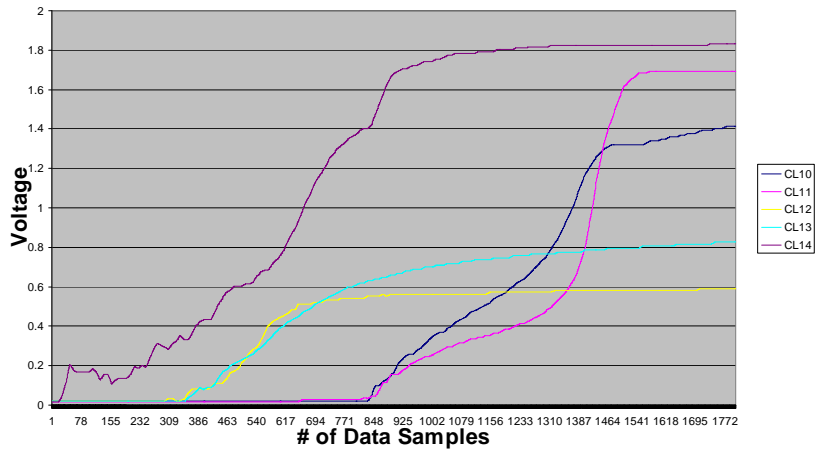
 Fluid Flow Projects

Advisory Board Meeting, September 17, 2008

Dynamic Repeatability



Dynamic Conditions

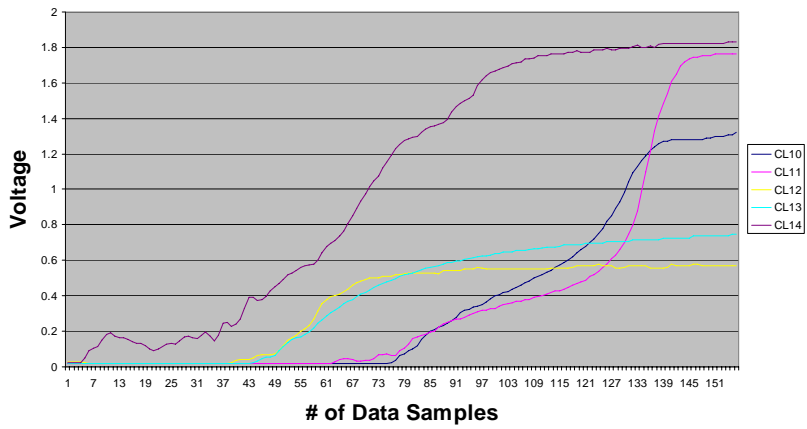


Fluid Flow Projects

Dynamic Repeatability



Dynamic Conditions

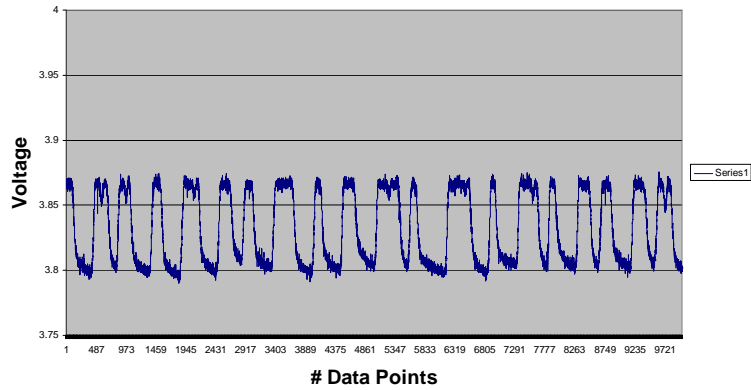


Fluid Flow Projects

Slug Flow Data



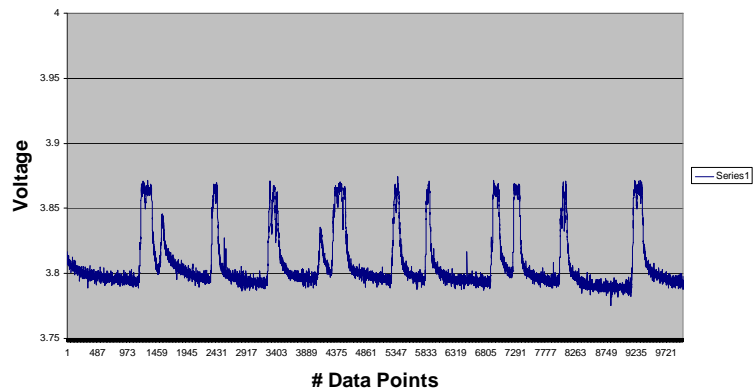
LOW GAS VELOCITY



Slug Flow Data



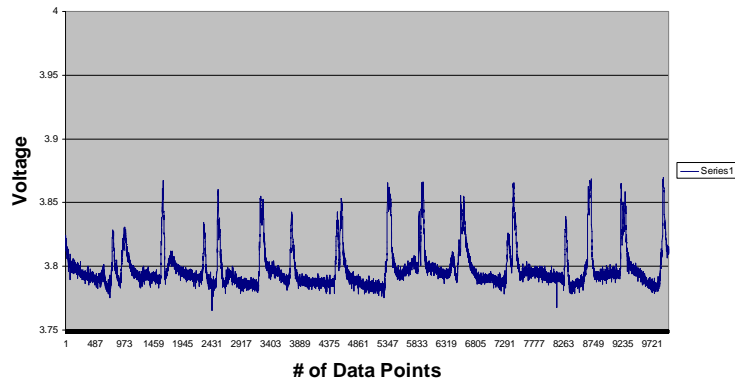
Medium Gas Velocity



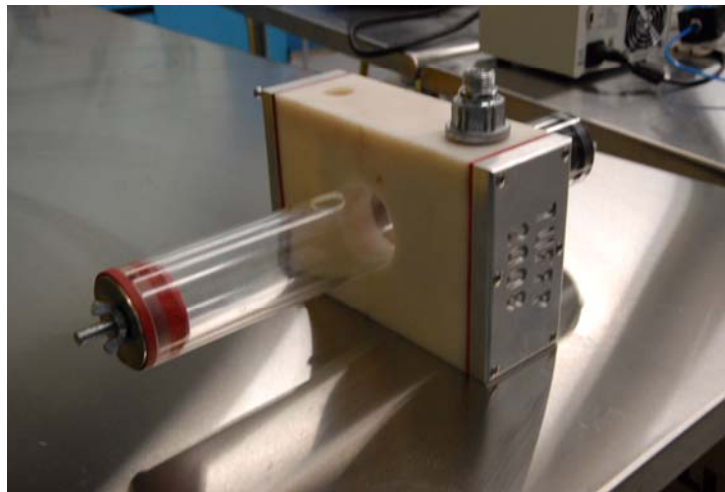
Slug Flow Data



High Gas Velocity



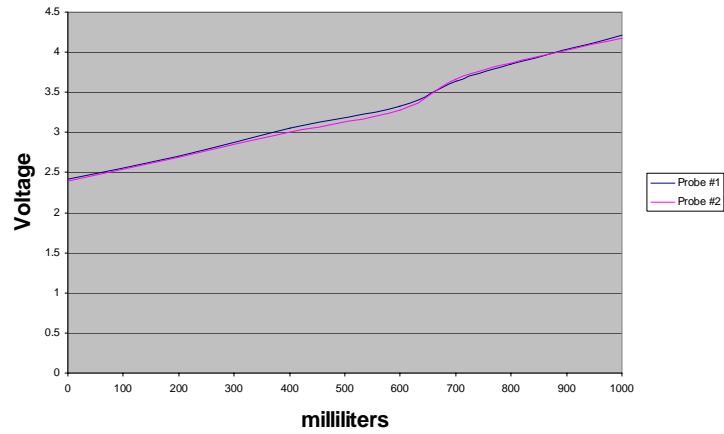
Calibration Fixture



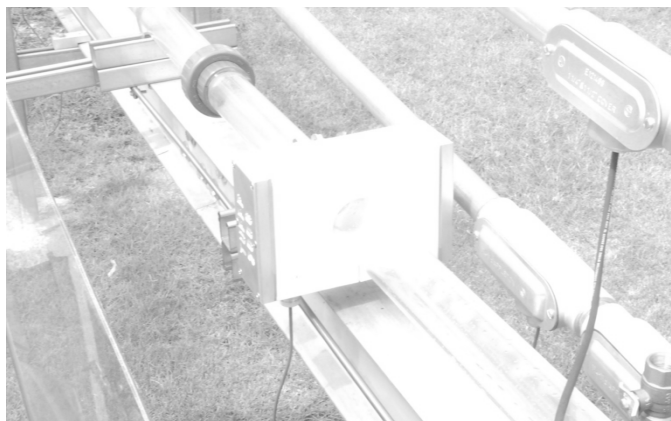
Bench Calibration



Calibration with Water



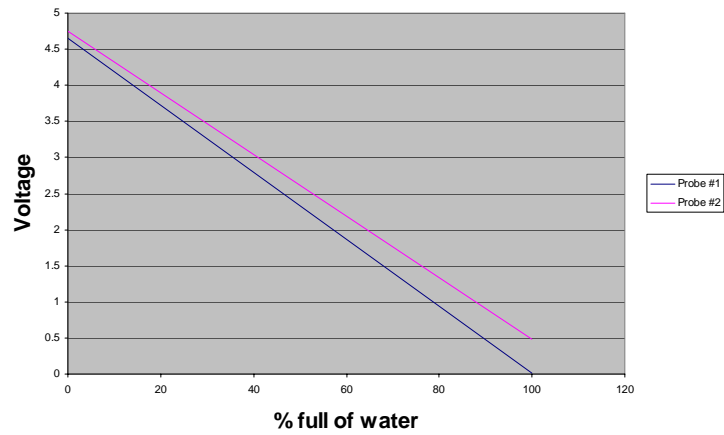
Capacitance Sensor



Installed on Flow Loop



Installed on Flow Loop with Water



Why



?

Capacitance Sensor

- ◆ Measures Amount of Energy That can be Stored in Process Fluid Currently within the Probe
- ◆ It is Determined by the Average Dielectric Constant (DC) of Whatever Mixture Currently Within the Probe

Correlation of Capacitance to Water-Cut

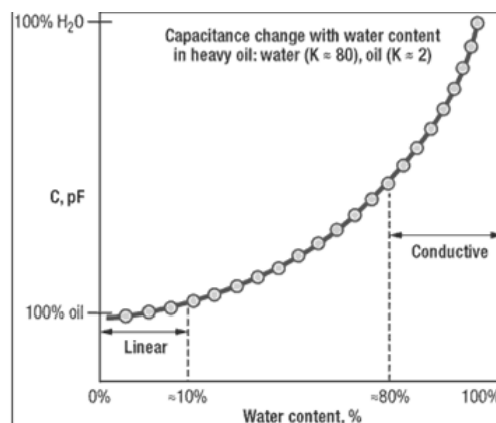
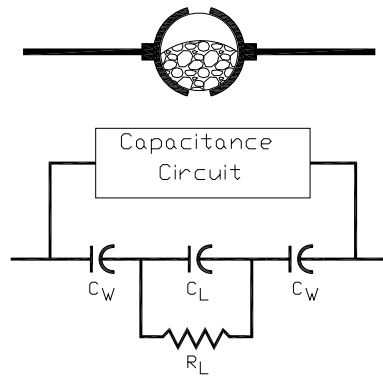


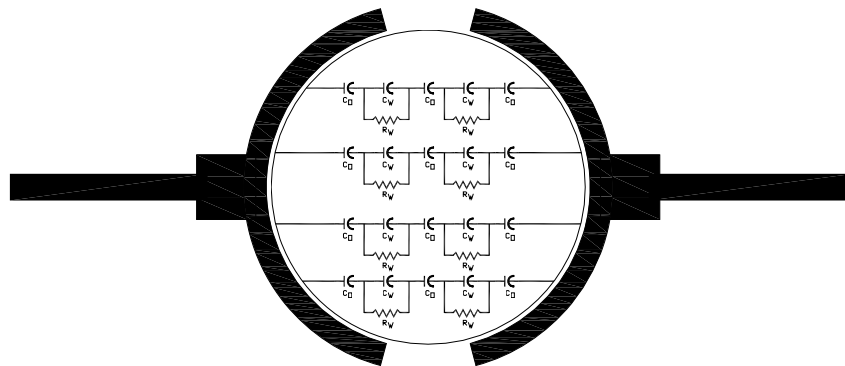
Fig. 2. Correlation of capacitance to water content.

Equivalent Circuit

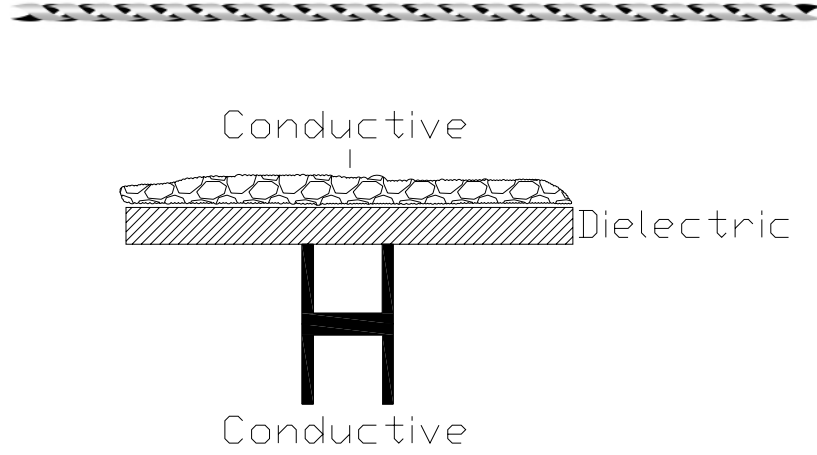


External Electrode

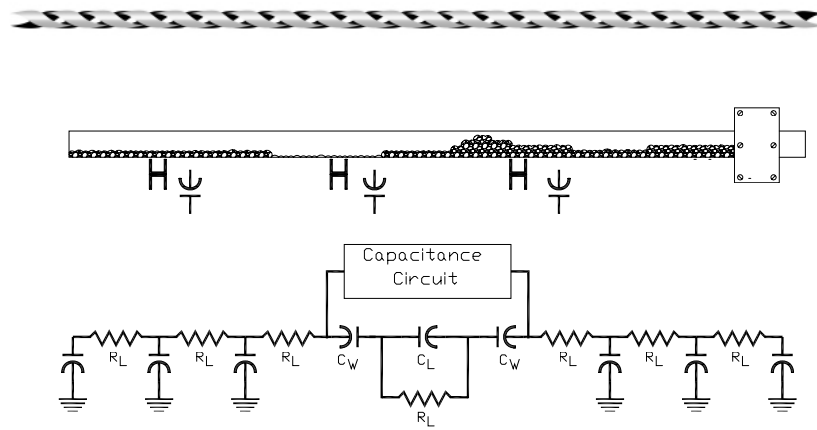
Equivalent Circuit



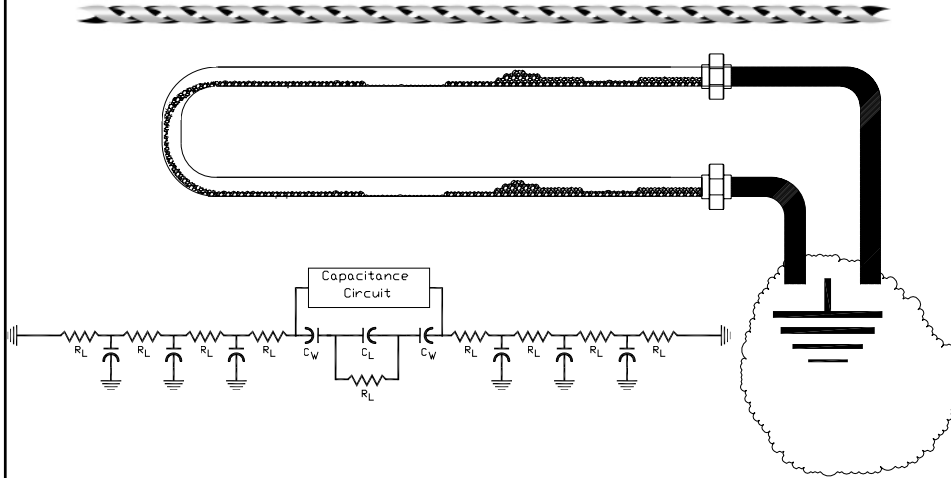
Wall Capacitance



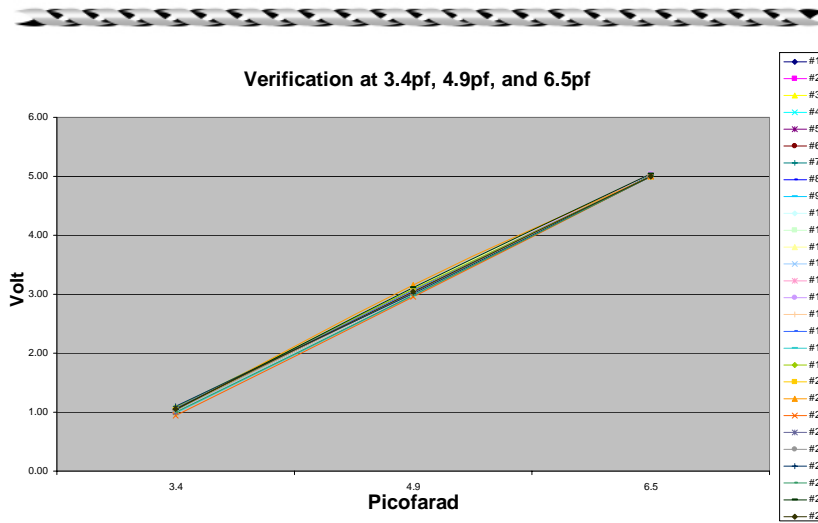
Equivalent Circuit



Equivalent Circuit



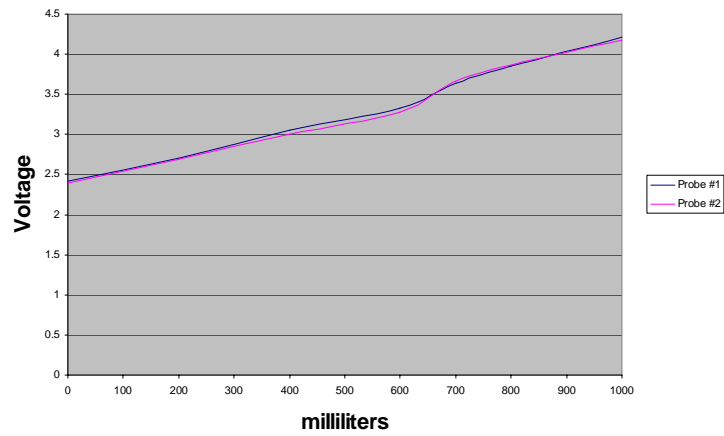
Repeatability Between Circuits



Bench Calibration



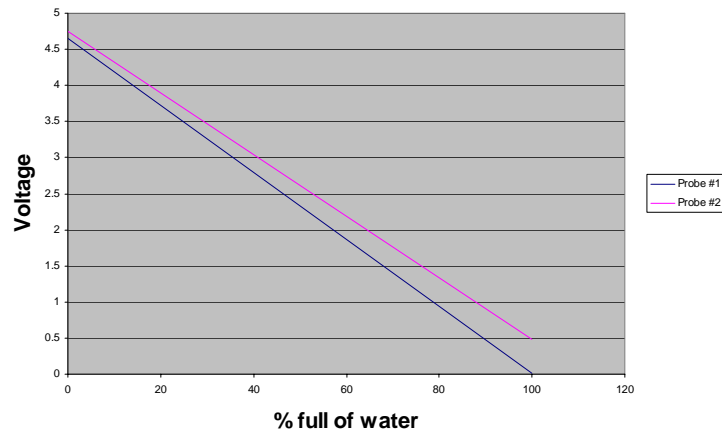
Calibration with Water



Installed on Flow Loop



Installed on Flow Loop with Water



Conclusions

- ◆ **Measured capacitance is a function of both fluid conductivity and permittivity**

- ◆ **Being Conducting Means**
 - **Current Present Whenever an Electric Field is Applied**
 - **Current Means Charge "Leaking"**
 - **Generation of Additional Wall Capacitances If the Piping is Supported by a Metal Structure**

Conclusions ...

- ◆ **Measurement of Capacitance Will Only Work in Oil Continuous Phase**
- ◆ **Once Mixture Becomes Water Continuous**
 - **Conductivity Dramatically Increases, Creating an Electrical Short to Ground**

 - **As a Result Capacitance Measurement Between the Plates Breaks Down**

Side Notes

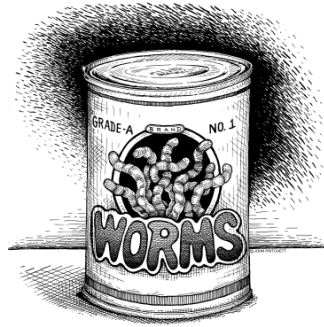
- ◆ A material's polarization does not respond instantaneously to an applied field
 - The response will always be *causal* (arising after the applied field)
- ◆ Due to the different local velocity of the fluids, the holdup of a particular fluid is not the same as the proportion of the total flow rate due to that fluid

Side Notes

- ◆ The measurement sensitivity distribution of the probe still needs to be investigated.
- ◆ If it is not homogenous the measured capacitance will be dependant on both the concentration of water and its location in the pipe.
- ◆ Water conductivity changes significantly with temperature and impurities

Questions ????????

Capacitance



Conductive Fluids

Unified Model

- ◆ **Objective**
 - **Develop and Maintain an Accurate and Reliable Steady State Multiphase Simulator**
- ◆ **Past Studies**
 - **Zhang et al. Developed “Unified Model” in 2002 for Two-phase Flow**
 - ▲ **Became TUFFP’s Flagship Steady State Simulator**
 - ▲ **Applicable for All Inclination Angles**
 - **“Unified Model was Extended to Three-phase in 2006**

Unified Model ...

- ◆ **Current Activities**
 - **Development of a Better Wetted Wall Fraction Model**
 - **Code and Software Improvement Efforts**

Unified Model ...



- ◆ **Future Activities**
 - **Continue Improvements in Both Modeling and Software Development**



Fluid Flow Projects

A Model for Wetted Wall Fraction and Gravity Center of Liquid Film in Gas-Liquid Pipe Flow

Holden Zhang

Advisory Board Meeting, September 17th, 2008

Outline

- ◆ Introduction
- ◆ Relationship between Film Gravity Center and Wetted Wall Fraction
- ◆ Gravity Center Modeling
- ◆ Comparisons with Experimental Results
- ◆ Concluding Remarks



Introduction

- ◆ **Wetted Wall Fraction (WWF) is an Important Closure Relationship in Mechanistic Modeling of Gas-liquid Pipe Flow**
- ◆ **For Transient Flow, Gravitational Term must be Considered in Momentum Equations**

Introduction ...

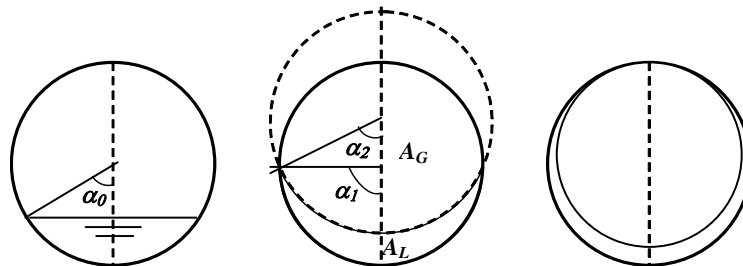
- ◆ **Gravitational Term Dependent on the Change of Film Gravity Center (FGC)**
- ◆ **Wetted Wall Fraction, Film Gravity Center and Flow Pattern Transition Interrelated**

Introduction ...

- ◆ Unified Approach Presented for Prediction of FGC Based on Taitel and Dukler (1976) Model for Flow Pattern Transitions Between Stratified and Annular Flows
- ◆ FGC is Used to Calculate WWF Based on Chen et al. (1997) “Double Circle” Model

Relationship between FGC and WWF

- ◆ Change from Flat to Concave Interface and Finally Transition to Annular Flow Caused by Increase of Gas Velocity
- ◆ Wetted Wall Fraction Increases and Film Gravity Center Elevated



Relationship between FGC and WWF ...

- ◆ Chen et al. (1997) Proposed “Double Circle” Method to Represent Liquid Film Thickness Distribution by Assuming Interface as Part Of a Second Circle
- ◆ Radius of This Circle is Determined by WWF and Liquid Film Holdup

Relationship between FGC and WWF ...

- ◆ Location of FGC is Defined as Its Location Relative to Pipe Central Axis
- ◆ Value is Negative If FGC is Below Pipe Central Axis
- ◆ FGC Corresponding to Flat Interface Expressed as

$$\frac{y_0}{D} = -\frac{\sin^3(\alpha_0)}{3\pi H_{LF}}$$

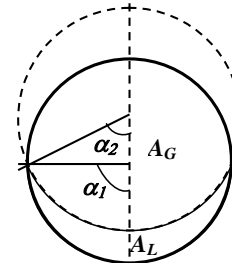
$$\alpha_0 = \pi H_{LF} + \frac{\sin(2\alpha_0)}{2}$$

Relationship between FGC and WWF ...

- Using Chen et al. (1997) "Double Circle" Model, FGC Corresponding to Concave Interface Expressed As

$$\frac{y}{D} = \frac{\sin^3 \alpha_1}{2\pi H_{LF} \sin^2 \alpha_2} (\text{ctg } \alpha_2 - \text{ctg } \alpha_1) \left[\frac{1}{2} \sin(2\alpha_2) - \alpha_2 \right]$$

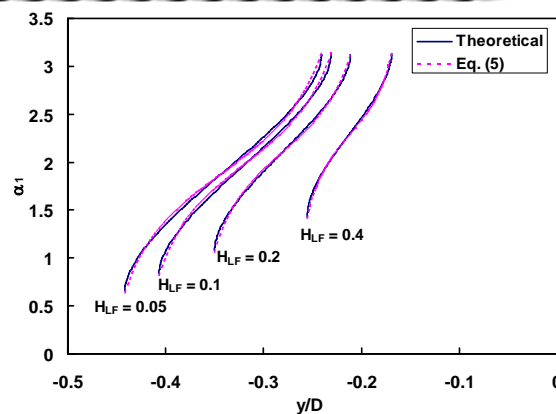
$$\alpha_1 - \frac{1}{2} \sin(2\alpha_1) - \frac{\sin^2 \alpha_1}{\sin^2 \alpha_2} \left[\alpha_2 - \frac{1}{2} \sin(2\alpha_2) \right] = \pi H_{LF}$$



Correspondence between FGC and WWF

- Relationship Approximated As:

$$\alpha_1 = \frac{\pi + \alpha_0}{2} + \frac{\pi - \alpha_0}{3.464} \text{tg} \left[\frac{\pi(2y - y_1 - y_0)}{3(y_1 - y_0)} \right]$$

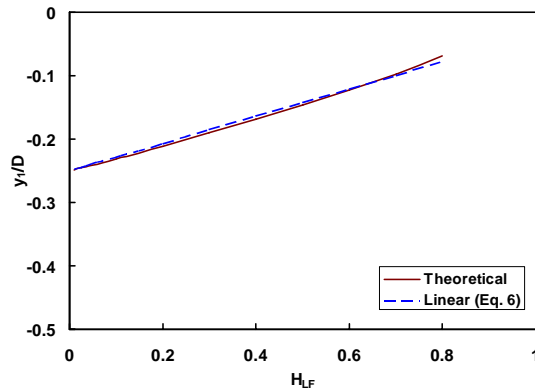
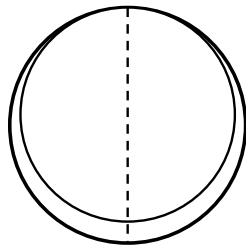


FGC Corresponding to Bridging

◆ y_1 can be Obtained When α_1 Approaches π

➤ Transition to Annular Flow

➤ Function of Film Holdup



Fluid Flow Projects

FGC Corresponding to Bridging ...

◆ This Relationship can be Approximated With a Linear Equation

$$\frac{y_1}{D} = 0.215H_{LF} - 0.25$$

◆ Wetted Wall Fraction

$$\Theta = \frac{\alpha_1}{\pi}$$

Fluid Flow Projects

Advisory Board Meeting, September 17th, 2008

Gravity Center Modeling

- ◆ Taitel and Dukler (1976) Criterion for Transition Between Stratified and Non-stratified Flows (Including Slug And Annular)

$$Fr_{GC} \frac{\sqrt{1 - \left(\frac{2h_L}{D} - 1\right)^2}}{\frac{\pi}{4}(1 - H_{LF})} = 1$$

- ◆ Froude Number

$$Fr_G = \frac{\rho_G v_G^2}{(\rho_L - \rho_G)gD \cos \theta}$$

Critical Froude Number

- ◆ If Film Holdup, H_{LF} , is Used to Replace h_L/D , Critical Froude Number for Flow Pattern Transition can be Estimated As

$$Fr_{GC} = \frac{\pi}{8} \left(\frac{1 - H_{LF}}{H_{LF}} \right)^{0.5}$$

Froude Number Used

- ◆ When Compared With Experimental Results, Critical Froude Number is Estimated As

$$Fr_{GC} = 0.7 \left(\frac{1 - H_{LF}}{H_{LF}} \right)^{0.5}$$

- ◆ Froude Number is Also Slightly Different

$$Fr_G = \frac{\rho_G (v_G - v_F)^2}{(\rho_L - \rho_G) g D \cos \theta}$$

FGC vs. R_{Fr}

- ◆ Using Ratio of Froude Number to Critical Froude Number ($R_{Fr} = Fr_G / Fr_{GC}$), Film Gravity Center may be Expressed As

$$y = \frac{y_0}{e^{AR_{Fr}^B}}$$

- ◆ When $R_{Fr} = 0$, $y = y_0$

- ◆ When $R_{Fr} = 1$, $y = \frac{y_0}{e^A} = y_1$

FGC vs. R_{FR} ...

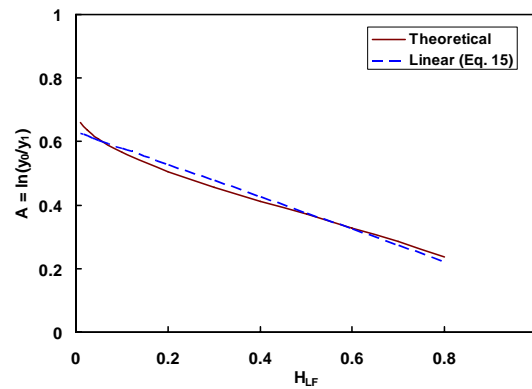


$$A = \ln\left(\frac{y_0}{y_1}\right)$$

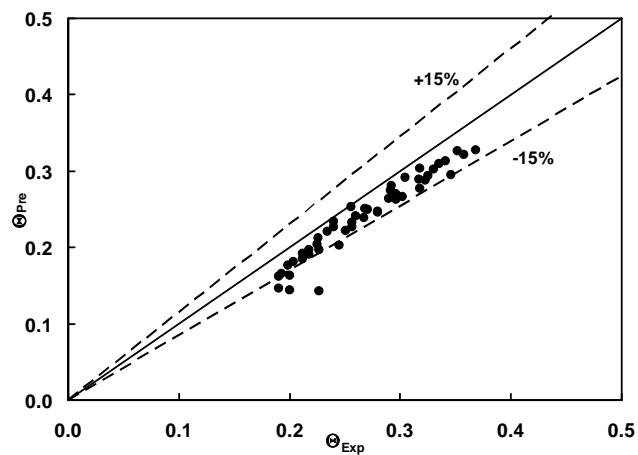
- ◆ Approximation with a Linear Equation

$$A = 0.63 - 0.51H_{LF}$$

$$B = 1.4$$

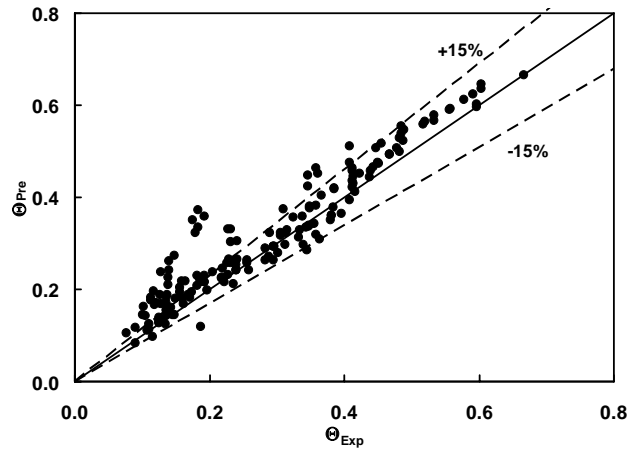


Comparisons with Experiments



Predicted Wetted Wall Fraction Compared with Measurements of Chen et al. (1997)
(air/kerosene, 3-in ID, horizontal)

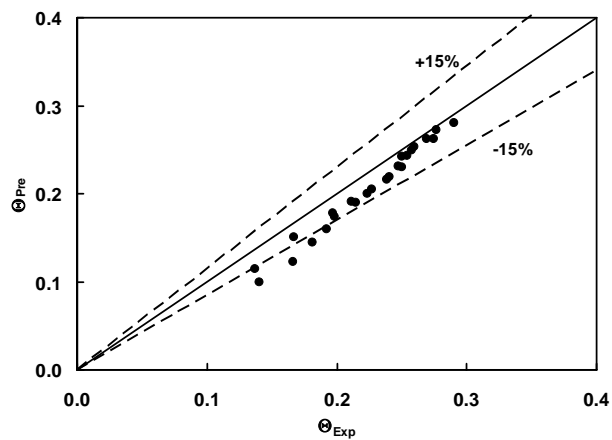
Comparisons with Experiments ...



Predicted Wetted Wall Fraction Compared with Measurements by Fan (2005)
(air/water, 2-in ID, -2 to 20 inclined)

 Fluid Flow Projects

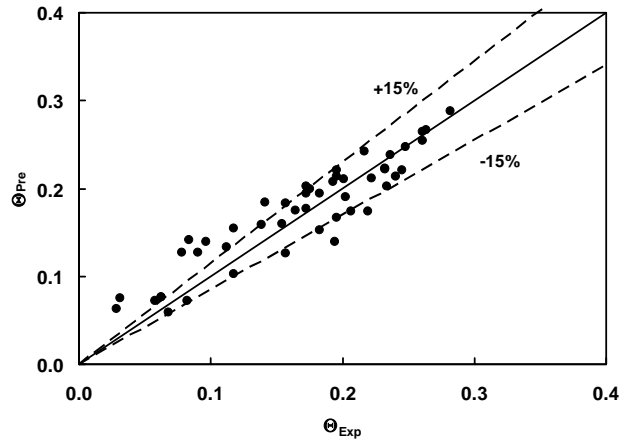
Comparisons with Experiments ...



Predicted Wetted Wall Fraction Compared with Measurements by Fan (2005)
(air/water, 6-in ID, horizontal)

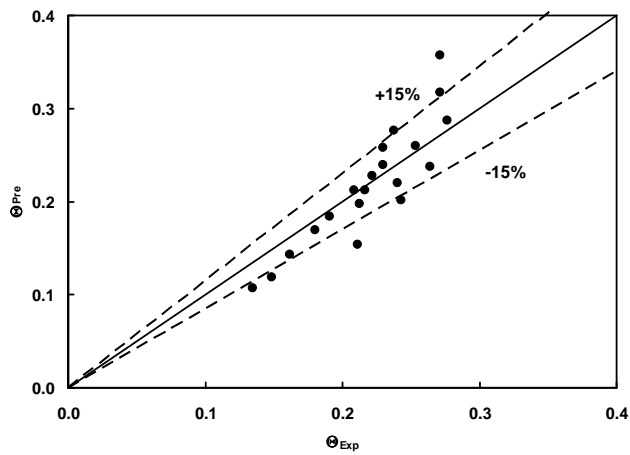
 Fluid Flow Projects

Comparisons with Experiments ...



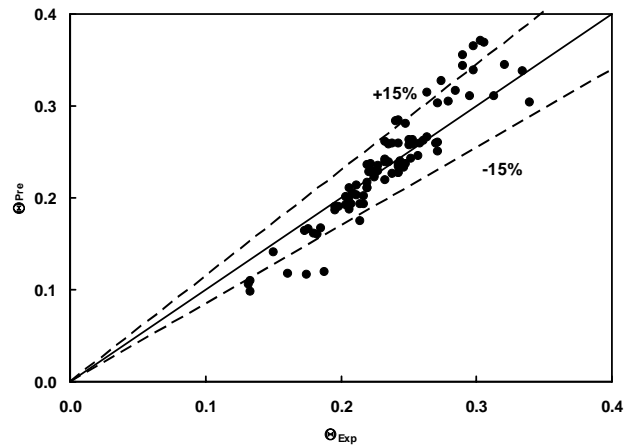
Predicted Wetted Wall Fraction Compared with Measurements by Dong (2007)
(air/water, 6-in ID, horizontal)

Comparisons with Experiments ...



Predicted Wetted Wall Fraction Compared with Measurements by Dong (2007)
(air/oil, 6-in ID, horizontal)

Comparisons with Experiments ...



Predicted Wetted Wall Fraction Compared with Measurements by Dong (2007)
(air/oil/water, 6-in ID, horizontal)

 Fluid Flow Projects

Comparisons with Experiments ...

Model Prediction Compared with Different Data Sets

Statistical Parameters	Chen et al. Air/Kerosene 3-in ID	Fan Air/Water 2-in ID	Fan Air/Water 6-in ID	Dong Air/Water 6-in ID	Dong Air/Oil 6- in ID	Dong Air/Oil/Water 6-in ID	Overall
ϵ_1 %	-11.74	11.82	-10.77	7.85	-3.14	-1.22	3.41
ϵ_2 %	11.74	14.88	10.77	17.20	11.50	8.54	12.95
ϵ_3 %	7.45	18.11	8.36	23.09	14.51	11.98	15.95

 Fluid Flow Projects

Concluding Remarks

- ◆ **Model Developed for Prediction of Wetted Wall Fraction Based on the Taitel and Dukler (1976) Model for Flow Pattern Transitions Between Stratified and Annular Flows**
- ◆ **Froude Number Reflects Competition Between Spreading and Settling of Liquid Across Pipe**

Concluding Remarks ...

- ◆ **New Model Unifies Predictions of Liquid Film Gravity Center, Wetted Wall Fraction and Flow Pattern Transitions From Stratified Flow to Annular Flow**
- ◆ **Predictions Compared With Measurements and Good Agreements Observed**

A Model for Wetted Wall Fraction and Gravity Center of Liquid Film in Gas-Liquid Pipe Flow

Holden Zhang

Abstract

A model is developed for predictions of wetted wall fraction and gravity center of liquid film in gas-liquid pipe flow under different flow conditions. This model is based on the instability of the liquid film in an equilibrium stratified flow proposed by Taitel and Dukler (1976) for flow pattern transition prediction from stratified flow to non-stratified flows. The relationship between the wetted wall fraction and the gravity center of the liquid film is based on the double circle model proposed by Chen et al. (1997) for the liquid film distribution. The present model unifies the predictions of liquid wetted wall fraction, film gravity center and flow pattern transition between stratified and annular flows. It can also be used to predict the wetted wall fraction in the film region of a slug flow and stratified flow with droplet entrainment

Introduction

The wetted wall fraction is an important closure relationship in mechanistic modeling of gas-liquid pipe flow. It determines the lengths of the pipe inside perimeters contacted by liquid and gas, respectively. The shear forces acting on the liquid and gas phases at the wall are then calculated using the shear stresses and the perimeters wetted by the liquid and gas. Together with the liquid film holdup, the wetted wall fraction is also used to estimate the interfacial length and to determine the interfacial shear force.

For transient gas-liquid pipe flow, the gravitational term due to the liquid film holdup and distribution changes must be considered in the momentum equations. This gravitational term is directly dependent on the change of the liquid film gravity center. The liquid film gravity center change is resulted from the local hydrodynamics including changes in fluid velocities, pressure, liquid holdup and flow pattern. During the transition from stratified to annular, gas and liquid interface changes from flat to concave and eventually the liquid film covers the entire pipe wall. Simultaneously, the film gravity center is also elevated. Therefore, the wetted

wall fraction, film gravity center and the flow pattern transition are interrelated. However, these relationships have not been emphasized in the previous developments of correlations for wetted wall fraction prediction.

Taitel and Dukler (1976) model of flow pattern transition from stratified flow to non-stratified flows (including slug and annular flows) was developed based on the instability of an equilibrium stratified flow perturbed with a solitary wave. Good agreements were observed by Barnea (1987) when this model was compared with experimental data under different flow conditions. The unified hydrodynamic model developed by Zhang et al. (2003) is based on slug dynamics. Flow pattern transitions from slug flow to non-slug flows (including stratified, annular and dispersed bubble flows) are predicted with the change of the length of the liquid film region in slug flow. The transition from stratified flow to annular flow is predicted by using a correlation of wetted wall fraction, i.e. the transition happens as the wetted wall fraction approaches to 1.

In this study, a unified approach is presented for the prediction of the liquid film gravity center in gas liquid pipe flow based on the Taitel and Dukler (1976) model for flow pattern transitions between stratified and annular flows. Then, the liquid film gravity center is used to calculate the wetted wall fraction based on the Chen et al. (1997) "double circle" model for the liquid film distribution. This model can also be used to predict the flow pattern transition between stratified and annular flows.

Relationship between Film Gravity Center and Wetted Wall Fraction

Figure 1 shows stratified flows with flat and curved interfaces. The change from flat to concave interface and finally the transition to annular flow is caused by the increase of the gas velocity. During this change, the wetted wall fraction by liquid film increases and

the film gravity center is elevated. The relationship between the wetted wall fraction and gravity center is dependent on the liquid film distribution. Chen et al. (1997) proposed a “double circle” method to represent the liquid film thickness distribution by assuming the interface as part of a second circle. The radius of this circle is determined by the wetted wall fraction and liquid film holdup.

In this study, the location of the gravity center of the liquid film is defined as its location relative to the pipe central axis. The value is negative if the gravity center is below the pipe central axis. The gravity center of the liquid film corresponding to a flat interface can be expressed as

$$y_0 = -\frac{D \sin^3(\alpha_0)}{3\pi H_{LF}}, \quad (1)$$

where D is pipe inner diameter, and α_0 is half of the wetted angle corresponding to flat interface. α_0 can be calculated with the film holdup H_{LF} ,

$$\alpha_0 = \pi H_{LF} + \frac{\sin(2\alpha_0)}{2}. \quad (2)$$

Using the Chen et al. (1997) “double circle” model, the film gravity center corresponding to the concave interface can be expressed as

$$\frac{y}{D} = \frac{\sin^3 \alpha_1}{2\pi H_{LF} \sin^2 \alpha_2} \left[\text{ctg} \alpha_2 - \text{ctg} \alpha_1 \right] \left[\frac{1}{2} \sin(2\alpha_2) - \alpha_2 \right], \quad (3)$$

where α_1 is half of the wetted angle by the liquid film, and α_2 is half of the angle occupied by the concave interface as part of the second circle. α_2 can be calculated from the following relationship:

$$\alpha_1 - \frac{1}{2} \sin(2\alpha_1) - \frac{\sin^2 \alpha_1}{\sin^2 \alpha_2} \left[\alpha_2 - \frac{1}{2} \sin(2\alpha_2) \right] = \pi H_{LF}. \quad (4)$$

Obviously, for a given liquid film holdup, the gravity center can be calculated using the wetted angle (or wetted wall fraction), or vice versa. Figure 2 shows the changes of the half wetted angle with the changes of the gravity center corresponding to different film holdups.

Based on its similarity to a tangent curve, the relationship between the wetted wall angle and gravity center can be approximated as

$$\alpha_1 = \frac{\pi + \alpha_0}{2} + \frac{\pi - \alpha_0}{3.464} \text{tg} \left[\frac{\pi(2y - y_1 - y_0)}{3(y_1 - y_0)} \right]. \quad (5)$$

y_1 is the gravity center when the liquid film becomes bridged at the top of the pipe. The approximation is compared with the original relationship in Fig. 2.

y_1 can be obtained when α_1 approaches π . Figure 3 shows its change with the film holdup. This relationship can also be approximated with a linear equation,

$$\frac{y_1}{D} = 0.215 H_{LF} - 0.25. \quad (6)$$

The wetted wall fraction is

$$\Theta = \frac{\alpha_1}{\pi}. \quad (7)$$

Gravity Center Modeling

The Taitel and Dukler (1976) criterion for transition between stratified and non-stratified flows (including slug and annular) is

$$Fr_{GC} \frac{\sqrt{1 - \left(\frac{2h_L}{D} - 1 \right)^2}}{\frac{\pi}{4}(1 - H_{LF})} = 1, \quad (8)$$

where h_L is the liquid film height corresponding to the flat interface. Fr_{GC} is the critical Froude number corresponding to the transition. The Froude number, Fr_G , is defined as

$$Fr_G = \frac{\rho_G v_G^2}{(\rho_L - \rho_G) g D \cos \theta}, \quad (9)$$

where v_G is gas velocity in a stratified flow, ρ_G and ρ_L are gas and liquid densities, and θ is the pipe inclination angle from horizontal. If the film holdup, H_{LF} , is used to replace h_L/D , the critical Froude number for flow pattern transition can be roughly estimated as

$$Fr_{GC} = \frac{\pi}{8} \left(\frac{1 - H_{LF}}{H_{LF}} \right)^{0.5}. \quad (10)$$

When compared with experimental results later in this paper, the critical Froude number will be estimated as

$$Fr_{GC} = 0.7 \left(\frac{1 - H_{LF}}{H_{LF}} \right)^{0.5}. \quad (11)$$

The Froude number used in this study is also slightly different and given by with

$$Fr_G = \frac{\rho_G (v_G - v_F)^2}{(\rho_L - \rho_G) g D \cos \theta}, \quad (12)$$

where v_F is the film velocity.

Naturally, the transition from stratified flow to annular flow must correspond to the liquid film bridging at the top of the pipe. Therefore, with the increase of the Froude number from 0 to the critical value, the liquid film with flat interface will spread around the pipe and reach to the top of the pipe. The liquid film will become more uniform if the Froude number is further increased. During this process, the film gravity center will also experience an elevation. If the ratio of the Froude number to the critical Froude number ($R_{Fr} = Fr_G / Fr_{GC}$) is used, the film gravity center may be expressed in the following form:

$$y = \frac{y_0}{e^{AR_{Fr}^B}}. \quad (13)$$

When $R_{Fr} = 0$, $y = y_0$.

When $R_{Fr} = 1$, $y = \frac{y_0}{e^A} = y_1$.

Then A becomes

$$A = \ln \left(\frac{y_0}{y_1} \right). \quad (14)$$

A is a function of film holdup. It can be estimated using Eqs. (1) and (6). As shown in Fig. 4, this relationship can be approximated with a linear equation,

$$A = 0.63 - 0.51 H_{LF}. \quad (15)$$

The B value in Eq. (13) is set as 1.4 based on comparisons with experimental data.

Comparisons with Experimental Results

Figure 5 shows the comparison between the wetted wall fractions predicted by the present model and the

experimental measurements by Chen et al. (1997). In their experimental study, Chen et al. observed the interfacial behavior of air-kerosene stratified-wavy flow in a 77.9-mm (3-in) inner diameter (ID), 420-m long horizontal pipeline. The liquid film-wetted wall fraction was measured using a tape attached on the outside of the transparent test section. The pressure in the test section was about 50 psig and the temperature was close to ambient temperature. The air and kerosene superficial velocities ranged from 3.7 to 12.7 m/s and from 0.004 to 0.046 m/s, respectively. It is seen that most of the comparisons fall inside the $\pm 15\%$ error band.

Fan (2005) conducted low liquid loading two-phase flow experiments on a 50.8-mm (2-in) ID flow loop and a 149.6-mm (6-in) ID flow loop with air and water. The wetted wall fractions were also measured from outside of the pipe using a tape. For the 2-in pipe flow, the superficial air velocity ranged from 5 to 25 m/s, and the superficial water velocity ranged from 0.01 to 0.052 m/s. The inclination angles were 0, ± 1 and ± 2 degrees. Figure 6 shows the comparison between the predicted wetted wall fractions by the present model and the experimental measurements. For the 6-in pipe flow, the superficial air velocity ranged from 10 to 14 m/s, and the superficial water velocity ranged from 0.002 to 0.05 m/s. Stratified smooth and stratified wavy flows were observed. Figure 7 shows the comparison between the predicted wetted wall fractions by the present model and the experimental measurements.

It needs to be pointed out that significant uncertainties may exist in the wetted wall fraction measurements. First of all, the wetted wall fraction is very difficult to be measured due to the turbulence and the irregularities of the film boundaries. Secondly the pipe wall diffraction may also contribute to the uncertainty if the measurements are conducted with a tape from outside. The last but not the least factor is the human errors. Different observers may use different criteria to determine the boundaries of the liquid film.

Dong (2007) conducted low liquid loading three-phase flow experiments on a 149.6-mm (6-in) ID horizontal flow loop with air, oil and water. The oil density and viscosity at 25 °C were 854.0 kg/m³ and 22.0 mPa-s, respectively. At the same temperature, the oil surface tension was 29.0 dynes/cm, and the oil-water interfacial tension was 16.3 dynes/cm. For the measurement of the wetted wall fraction, the transparent acrylic pipe was marked on the inside to give a direct reading of the wetted perimeter. This significantly reduced the reading uncertainty. The superficial air velocity ranged from 5 to 20 m/s, and

the superficial oil and water velocities ranged from 0.002 to 0.04 m/s. Figure 8 shows the comparison between the predicted wetted wall fractions by the present model and the experimental measurements for air and water flow. Figure 9 shows the comparison for air and oil flow. Figure 10 shows the comparison for air, oil and water flow.

Statistical parameters are used to examine the performance of the present model against the previously mentioned experimental results. These statistical parameters are calculated from the relative error, e_1 ,

$$(e_1)_i = \left[\left(\frac{\Theta_{\text{Pre}} - \Theta_{\text{Exp}}}{\Theta_{\text{Pre}} + \Theta_{\text{Exp}}} \right) \times 200 \right]_i. \quad (16)$$

Θ_{Exp} is the experimental measurement, and Θ_{Pre} is the model prediction. From the above error, three statistical parameters are defined (N is the data number). The average relative error is

$$\varepsilon_1 = \frac{1}{N} \sum_{i=1}^N (e_1)_i. \quad (17)$$

The absolute average error is

$$\varepsilon_2 = \frac{1}{N} \sum_{i=1}^N |(e_1)_i|. \quad (18)$$

The standard deviation about average relative error is

$$\varepsilon_3 = \sqrt{\frac{\sum_{i=1}^N ((e_1)_i - \varepsilon_1)^2}{N - 1}}. \quad (19)$$

Table 1 lists the comparisons between the model predictions and the experimental measurements of the wetted wall fraction under different flow

conditions. For the Chen et al. (1997) air/kerosene flow in a 3-in ID pipe and Fan (2005) air/water flow in a 6-in ID pipe, the model slightly under predicts the wetted wall fraction. For the Fan air/water flow in a 2-in ID pipe and the Dong (2007) air/water flow in a 6-in ID pipe, the model slightly over predicts the experimental results. The overall comparison is good.

Concluding Remarks

A model for prediction of wetted wall fraction in gas-liquid stratified flow is developed based on the Taitel and Dukler (1976) model for flow pattern transitions between stratified and annular flows. Apparently, the Froude number which is the ratio of the kinetic energy of the gas flow and the gravitational potential of the liquid phase in a pipe reflects the competition between spreading and settling of the liquid across the pipe. The new model unifies the predictions of liquid film gravity center, wetted wall fraction and flow pattern transitions from stratified flow to annular flow. Predictions by the present model have been compared with the measurements of wetted wall fraction by Chen et al. (1997), Fan (2005) and Dong (2007), and good agreements have been observed.

The present model serves as a closure relationship for unified steady state and transient multiphase flow simulators. It can also be used to predict the gravity center and the wetted wall fraction in the film region of slug flow by use of the local holdup and gas/liquid velocities. In this model, the liquid entrainment in gas core may also be considered. The Froude number can be calculated using gas core mixture density. Then, the transition from stratified flow to annular flow will be altered due to the droplet entrainment. More experimental observations and measurements need to be carried out to validate these aspects of the model.

References

- Barnea, D., 1987. A Unified Model for Predicting Flow-Pattern Transitions for the Whole Range of Pipe Inclinations. *Int. J. Multiphase Flow* 13, 1-12.
- Chen, X.T., Cai, X.D., Brill, J.P., 1997. Gas-liquid stratified-wavy flow in horizontal pipelines. *J. Energy Resources Technology* 119, 209-216.
- Dong, H, 2007. An Experimental Study of Low Liquid Loading Gas-Oil-Water Flow in Horizontal Pipes. Master Thesis, U. of Tulsa, Tulsa, OK, USA.
- Fan, 2005. An Investigation of Low Liquid Loading Gas-Liquid Stratified Flow in Near-Horizontal Pipes. Ph.D. Dissertation, U. of Tulsa, Tulsa, OK, USA.
- Taitel, Y., and Dukler, A.E., 1976. A Model for Predicting Flow Regime Transition in Horizontal and Near Horizontal Gas-Liquid Flow. *AIChE Journal* 22, 47-55.
- Zhang, H.-Q., Wang, Q. and Brill, J.P., 2003. Unified Model for Gas-Liquid Pipe Flow via Slug Dynamics – Part 1: Model Development. *J. Energy Resources Technology* 125, 266-273.

Table 1. Model Prediction Compared with Different Data Sets

Statistical Parameters	Chen et al. Air/Kerosene 3-in ID	Fan Air/Water 2-in ID	Fan Air/Water 6-in ID	Dong Air/Water 6-in ID	Dong Air/Oil 6-in ID	Dong Air/Oil/Water 6-in ID	Overall
ε_1 %	-11.74	11.82	-10.77	7.85	-3.14	-1.22	3.41
ε_2 %	11.74	14.88	10.77	17.20	11.50	8.54	12.95
ε_3 %	7.45	18.11	8.36	23.09	14.51	11.98	15.95

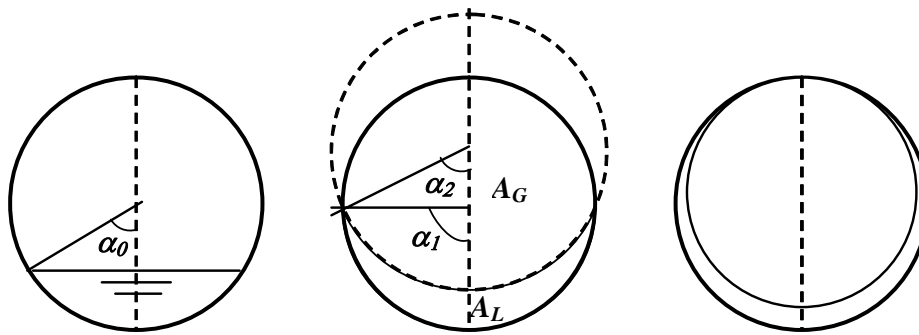


Figure 1. Liquid Film Interface Approximated as Part or Whole of Second Circle

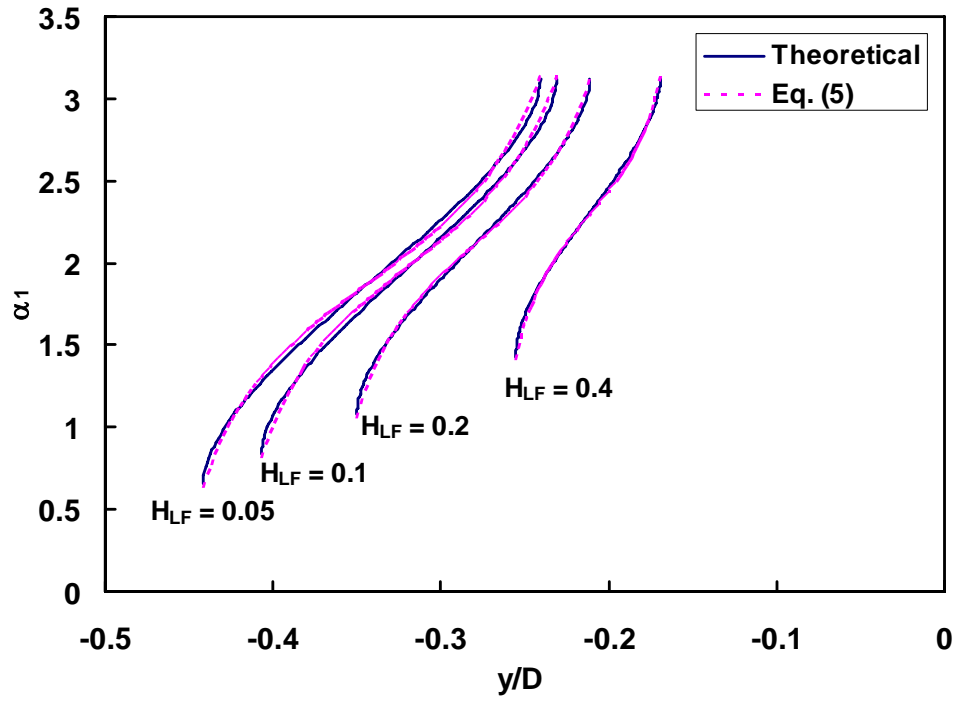


Figure 2. Wetted Angle vs. Gravity Center at Different Film Holdups

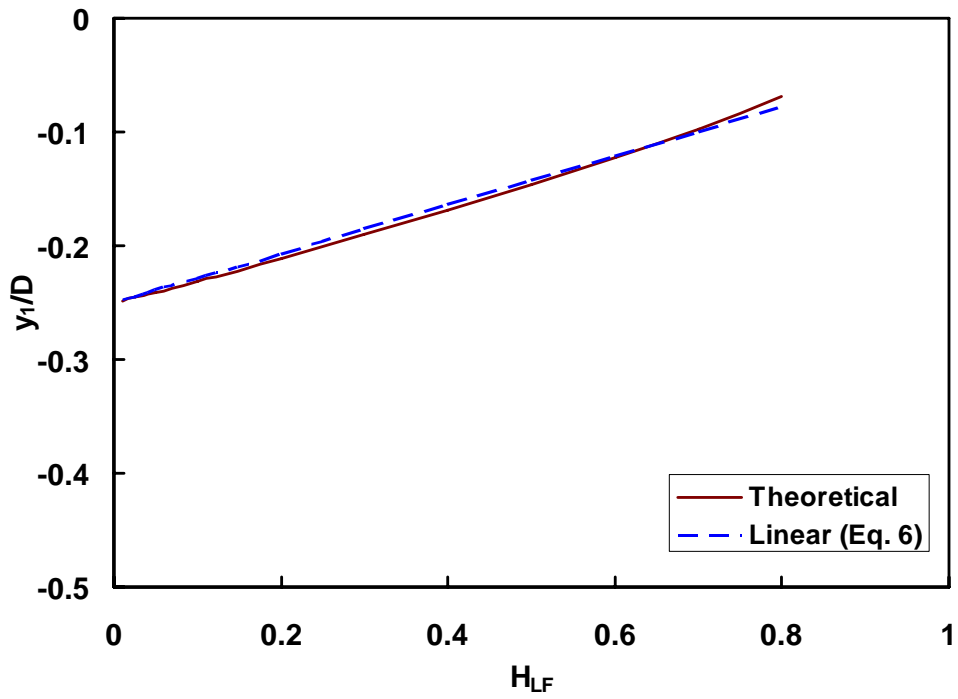


Figure 3. Gravity Center of Film Reaching to Top of Pipe vs. Liquid Holdup

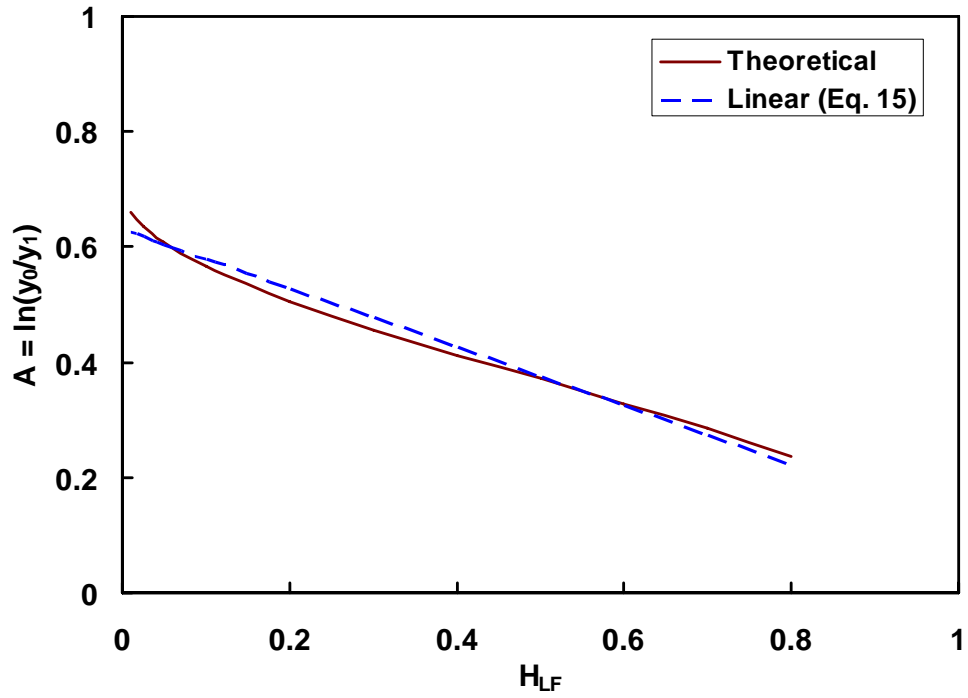


Figure 4. $\ln(y_0/y_1)$ vs. Film Holdup

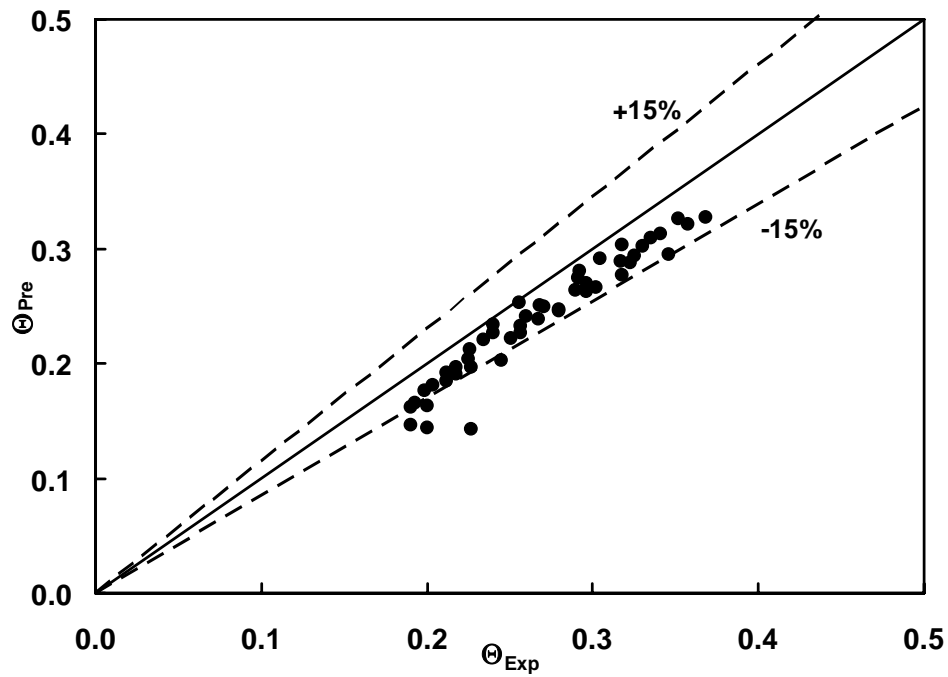


Figure 5. Predicted Wetted Wall Fraction Compared with Measurements of Chen et al. (1997) (air/kerosene, 3-in ID, horizontal)

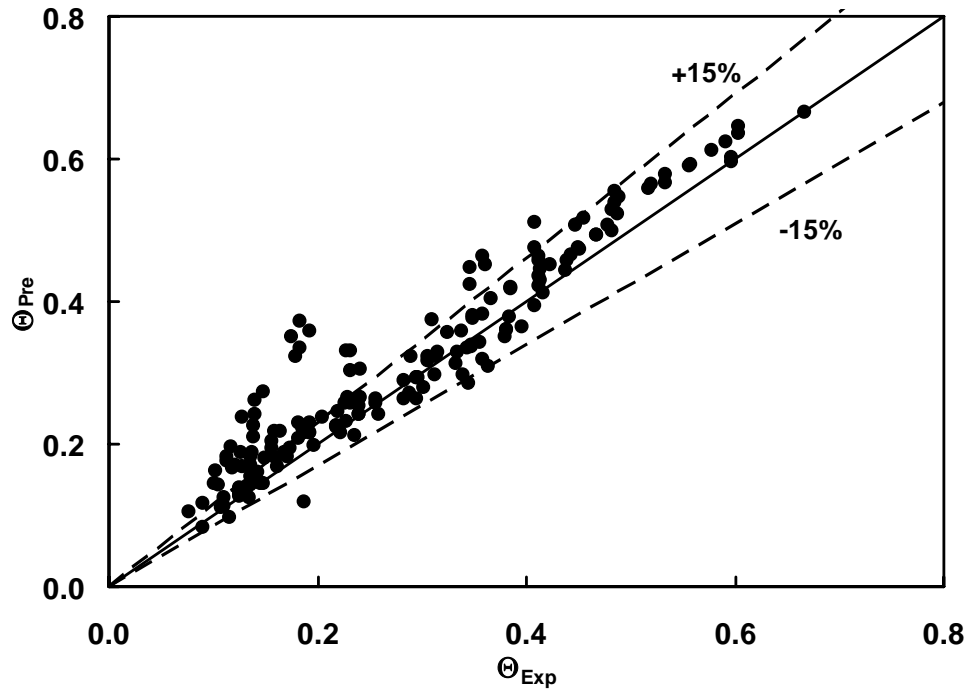


Figure 6. Predicted Wetted Wall Fraction Compared with Measurements by Fan (2005)
(air/water, 2-in ID, -2 to 2° inclined)

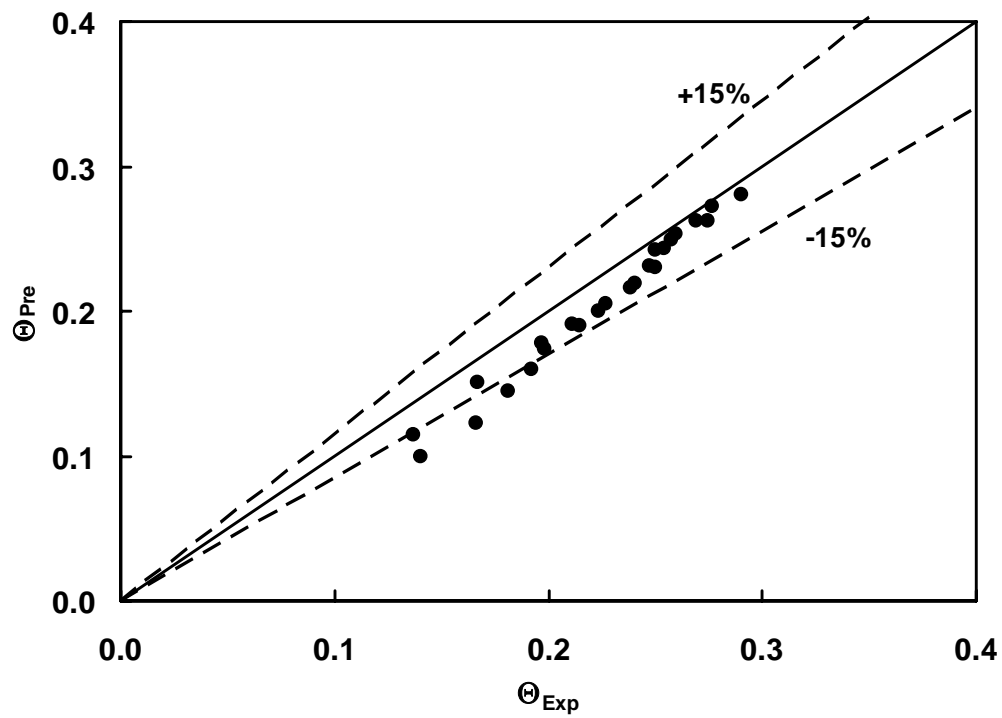


Figure 7. Predicted Wetted Wall Fraction Compared with Measurements by Fan (2005)
(air/water, 6-in ID, horizontal)

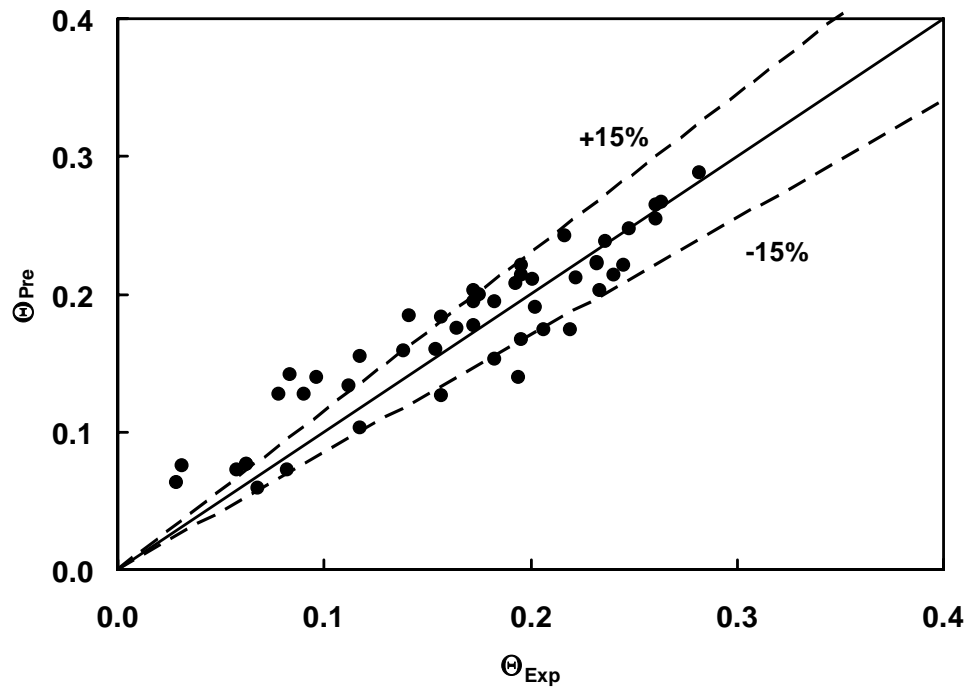


Figure 8. Predicted Wetted Wall Fraction Compared with Measurements by Dong (2007)
(air/water, 6-in ID, horizontal)

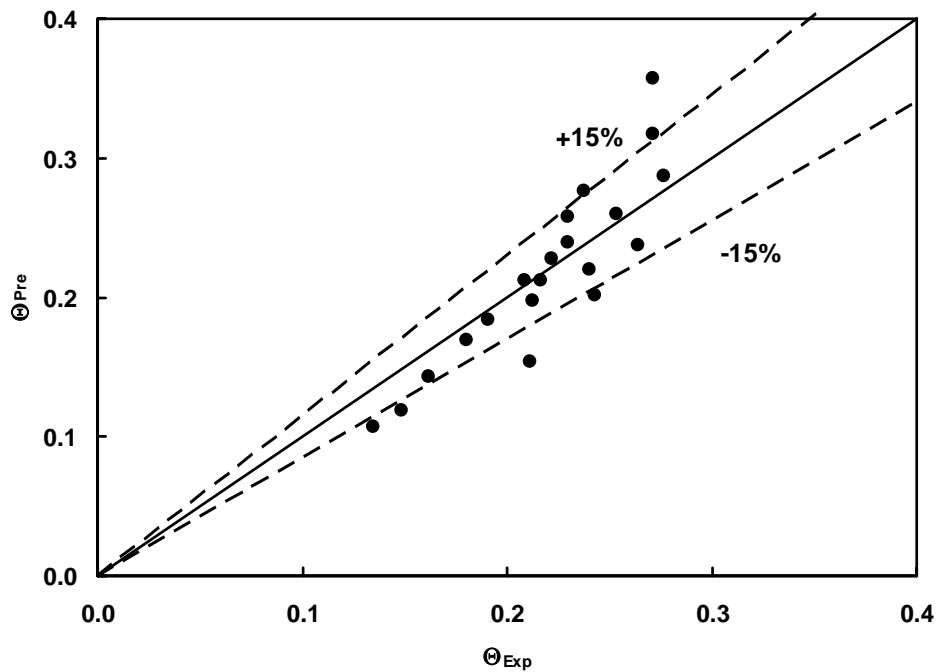


Figure 9. Predicted Wetted Wall Fraction Compared with Measurements by Dong (2007)
(air/oil, 6-in ID, horizontal)

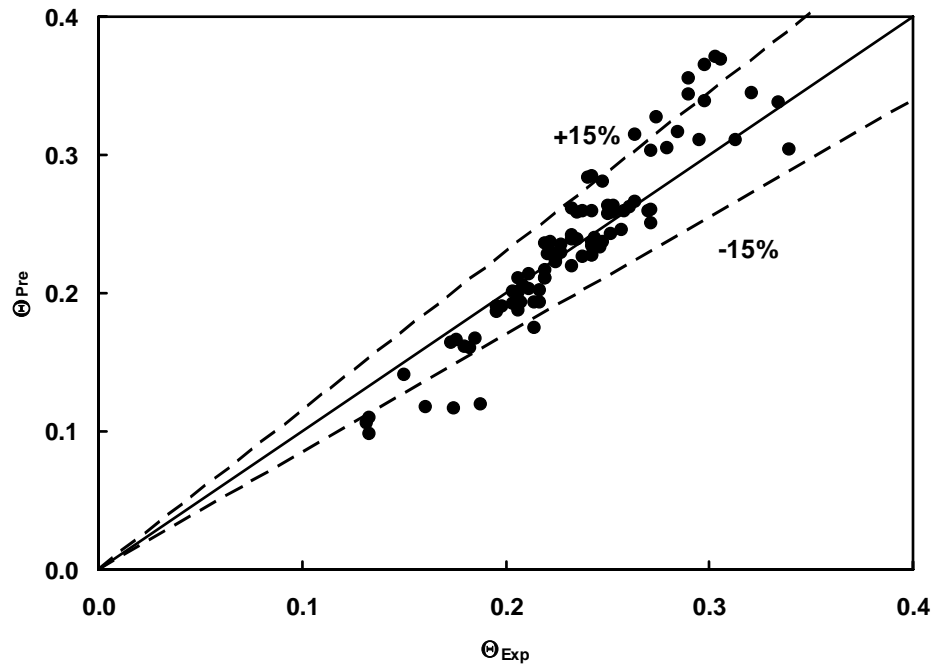


Figure 10. Predicted Wetted Wall Fraction Compared with Measurements by Dong (2007)
 (air/oil/water, 6-in ID, horizontal)



Fluid Flow Projects



TUFFPT Updates

Holden Zhang

Advisory Board Meeting, September 17th, 2008

Pipeline and Well Module Improved



- ◆ Use Black Oil Model to Update Fluid Properties for Each Segment during Integration
- ◆ Pressure Drop Prediction Improved

Documentations

◆ Modeling Methods Documented

- Living Document
- All Basic Equations and Closure Relationships in Current Model
- Gas-Liquid Model, Oil-Water Model and Three-phase Model
- Available on TUFFP Website

Excel VBA Interface Improvement

- ◆ Execution Process Hidden with a Progress Indication Bar
- ◆ Execution Made Faster



Fluid Flow Projects

2008 Questionnaire

Holden Zhang

Advisory Board Meeting, September 17th, 2008

2008 Questionnaire Results

#	Research Title	Status	Baker Atlas	BP	Chevron	ConocoPhillips	ExxonMobil	JOGMEC	Kuwait Oil Co.	Marathon	MMS	Penex	Petrobras	Petronas	Rosneft	Schlumberger	Shell	Tenaris	Total	Total Scores	Priority Ranking	Ranking(2007)
5	Effect of High Viscosity on Multiphase Flow Behavior	O	3	5	5	4	3	5	5	4	3		5			3			45	1	3	
9	Up-scaling Studies in Multiphase Flow	O	5	4	4	5	5	4	3	4	3		4			3			44	2	2	
3	Unified Modeling of Multiphase Pipe Flows (Including Gas-Liquid, Oil-Water and Gas-Oil-Water)	O	5	4	4	4	1	3	4	5	4		3			5			42	3	5	
1	Gas-Oil-Water Flow in Pipes	O	5	4	4	5	2	3	3	5	4		3			3			41	4	1	
8	Simplified Transient Multiphase Flow Model	O	4	5	3	5	3	4	2	3	3		3			5			40	5	14	
7	Three-Phase Flow in Near-Horizontal Pipelines with Low Oil-Water Loadings	O	3	3	3	5	5	3	3	3	5		3			2			38	6	6	
2	Oil-Water Flow	O	4	4	3	4	2	2	4	5	3		3			3			37	7	4	
6	Closure Laws for Droplet-Homophase Interaction	O	4	2	4	4	2	4	2	3	4		4			3			36	8	10	
10	Two-Phase Downward Flow and Gas Carryunder	P	2	3	3	4	3	5	2	5	4		4			1			36	8	9	
18	Investigation of High Viscosity Two-Phase Flow Pattern in	P	3	2	4	5	3	5	3	3	4		3			1			36	8		

#	Research Title	Status	Baker Atlas	BP	Chevron	ConocoPhillips	ExxonMobil	JOGMEC	Kuwait Oil Co.	Marathon	MMS	Pemex	Petrobras	Petronas	Rosneft	Schlumberger	Shell	Tenaris	Total	Total Scores	Priority Ranking	Ranking(2007)
4	Multiphase Flow in Hilly Terrain Pipelines	O	5	2	4	4	1	4	2	3	4		4			1				34	11	9
13	Investigation of Four-Phase Solid, Water, Oil and Gas Flow	P	2	4	2	4	3	4	3	2	3		4			3				34	11	4
19	Investigation of Gas Well Unloading	P	3	2	4	3	3	4	1	5	2		2			5				34	11	12
16	Modeling of Foam Flow in Wells	P	2	1	3	3	3	4	4	5	2		5			1				33	14	
22	Integration of Multiphase Flows Modeling From Reservoir, Wellbore and Pipelines to Surface Facilities	P	4	1	2	4	2	2	4	2	5		1			5				32	15	
14	Gas-Liquid Flow in Undulating Horizontal Wells	P	5	2	3	3	1	3	1	2	5		3			3				31	16	11
15	Investigation of Inversion Point in Oil-Water Flow	P	4	4	2	3	2	2	2	2	3		2			5				31	16	7
17	Effect of Drag-Reducing Polymers on Gas-Oil-Water Pipe Flow	P	2	2	3	5	4	4	2	2	3		2			1				30	18	11
20	Multiphase Flow Metering	P	4	1	2	3	2	4	4	2	5		2			1				30	18	
21	Pumps Selection for the Applicable Flow System and	P	2	1	1	3	1	4	5	2	5		1			5				30	18	
11	Closure Relationship Study and Numerical Simulation of Slug Flow	P	4	1	3	3	1	3	2	2	4		3			3				29	21	8
12	Effect of Wave Characteristics on Interfacial Shear Stress	P	3	2	2	5	4	2	2	2	2		3			1				28	22	12



Fluid Flow Projects

Business Report

Cem Sarica

Advisory Board Meeting, September 17, 2008

Membership Status

◆ Current Status

- Membership Stands at 17
 - ▲ 16 Industrial and MMS
- Efforts Continue to Increase Membership
 - ▲ SPT
 - ▲ CNOOC

Membership Status ...

- ◆ **DOE Support**
 - **Started June 2003**
 - **\$731,995 Over Five Years**
 - **Gas-Oil-Water Flow Research**
 - ▲ **Development of Next Generation Multiphase Prediction Tools**
 - **Completed**

Personnel Changes

- ◆ **Dr. Abdel Salam Al-Sarkhi Resigned Due to Family Reasons**
 - **Search is Underway to Fill His Position**
- ◆ **Mr. Feng Xiao's Research Assistantship is Terminated**
- ◆ **Ms. Ceyda Kora Joins TUFFP Team to Pursue MS Degree in Petroleum Engineering**

Conferences

- ◆ **BHRg 2008 Production Technology Conference**
 - **Banff, Alberta, Canada June 4 – 6, 2008**
 - **Dr. Sarica was Technical Chair**
 - **Paper from TUFFP Research Projects**
 - ▲ **Gokcal, B. Al-Sarkhi, A., Sarica, C.: Effects of High Oil Viscosity on Drift Velocity for Horizontal Pipes**

Next Advisory Board Meetings

- ◆ **Tentative Schedule**
 - **March 17, 2009**
 - ▲ TUHOP Meeting
 - ▲ TUFFP Workshop
 - ▲ Facility Tour
 - ▲ TUHOP/TUFFP Social Function
 - **March 18, 2009**
 - ▲ TUFFP Meeting
 - ▲ TUFFP/TUPDP Reception
 - **March 19, 2009**
 - ▲ TUPDP Meeting
- ◆ **Venue TBD**

Financial Report

◆ Year 2008

- TUFFP Industrial Account
- TUFFP MMS Account
- TUFFP DOE Account

◆ Year 2009 Proposed

- TUFFP Industrial Account
- TUFFP MMS Account

2008 TUFFP Industrial Account Budget Summary (Prepared September 8, 2008)

Anticipated Reserve Fund Balance on January 1, 2008				610,365.69
Uncollected 2007 Membership Fees (2 @ \$40,000)				(80,000.00)
				530,365.69
Income for 2008				
2008 Membership Fees (15 @ \$48,000 - excludes MMS)				\$720,000
2008 Membership Fees (1 @ 38,000)				\$38,000
Total Budget				1,288,365.69
Projected Budget/Expenditures for 2008				
	Budget	Revised Budget 4/08	Expenses 9/8/08	Anticipated 2008 Expenses
90101 Principal Investigator - Sarica	24,392.00	25,907.00	13,973.33	27,930.48
90103 Co-Principal Investigator - Zhang	19,665.00		3,622.50	3,622.50
90600 Professional Salary - Jones	5,141.00	7,330.00	5,540.21	8,472.20
90601 Professional Salary - Li	13,505.00	28,854.00	21,432.31	24,651.07
90602 Professional Salary - Graham	5,237.00	15,785.00	8,345.12	15,505.93
90603 Professional Salary - Al-Sarkhi	32,500.00	38,750.00	21,812.52	6,458.34
90701 Technician - Miller	15,065.00			
90702 Technician - Waldron	6,575.00	11,428.00	5,193.03	9,869.21
90703 Technician - Kelsey	9,750.00	10,154.00	9,099.72	12,754.00
90800 Salaries - Part-time	4,290.00			
91000 Graduate Students - Monthly	50,100.00	65,000.00	41,433.32	60,745.44
91100 Students - Hourly	15,000.00	15,000.00	9,564.63	14,064.63
91800 Fringe Benefits (33%)	50,910.83	45,609.00	29,376.18	36,057.04
93100 General Supplies	3,000.00	3,000.00	222.43	500.00
93101 Research Supplies	100,000.00	100,000.00	82,672.88	100,000.00
93102 Copier/Printer Supplies	500.00	500.00	169.05	280.00
93104 Computer Software	4,000.00	4,000.00	502.18	1,200.00
93106 Office Supplies	2,000.00	2,000.00	2,070.79	3,000.00
93200 Postage/Shipping	500.00	500.00	531.82	650.00
93300 Printing/Duplicating	2,000.00	2,000.00	1,292.37	2,000.00
93400 Telecommunications	3,000.00	3,000.00	1,166.54	1,766.00
93500 Membership/Subscriptions	1,000.00	1,000.00	181.50	400.00
93601 Travel - Domestic	14,000.00	10,000.00	4,289.48	10,000.00
93602 Travel - Foreign	10,000.00	10,000.00	10,946.46	10,946.46
93606 Visa			241.35	241.35
93700 Entertainment (Advisory Board Meetings)	10,000.00	10,000.00	5,780.37	10,000.00
94803 Consultants	16,000.00		7,708.35	18,500.00
94813 Outside Services	20,000.00	20,000.00	68,278.29	68,278.29
95200 P&A (55.6%)	119,456.33	121,324.00	75,006.49	102,344.00
98901 Employee Recruiting	3,000.00	3,000.00		147.00
99001 Equipment	600,000.00	200,000.00	93,401.74	263,500.00
99002 Computers	8,000.00	8,000.00	768.70	4,000.00
99300 Bank Charges	40.00	40.00		
81801 Tuition/Fees	30,306.00	53,103.00	55,342.00	55,342.00
81806 Graduate Fellowship			933.03	1,809.22
Total Expenditures	1,182,933.16	831,284.00	\$80,898.69	875,035.16
Anticipated Reserve Fund Balance as of 12/31/08				413,330.53

2008 MMS Account Summary



(Prepared July 28, 2008)

Reserve Balance as of 12/31/07		\$5,322
2008 Budget		40,000
Total Budget		45,322
Projected Budget/Expenditures for 2008		
	Budget	2007 Anticipated Expenditures
91000 Students - Monthly	25,600.00	28,800.00
95200 F&A	14,233.60	15,696.00
81801 Tuition/Fees		
Total Anticipated Expenditures as of 12/31/08	39,833.60	44,496.00
Total Anticipated Reserve Fund Balance as of 12/31/08		825.94

2008 DOE Account Summary



(Prepared July 28, 2008)

Award Amount		\$731,995
Amount Invoiced (June 1, 2003 - December 31, 2007)		625,397.81
Total Budget		106,597.19
Projected Budget/Expenditures for 2008		
	2008 Budget	2008 Expenditures
90600 Professional Salary - Jones	6,279.00	7,451.33
90600 Professional Salary - Graham	12,514.00	13,567.73
90601 Professional Salary - Alsarkhi	22,958.33	21,812.49
90602 Professional Salary - Li		2,253.13
90702 Technician - Mechanical	3,644.00	3,953.56
90703 Technician - Mechanical	6,825.00	2,148.58
91000 Graduate Students - Monthly	7,000.00	8,215.22
91800 Fringe Benefits (35%)	17,232.50	16,891.65
95200 F&A (51%)	30,202.50	30,295.04
Total Anticipated Expenditures as of 5/31/08	106,655.33	106,588.73
Anticipated Fund Balance on 8/31/08		\$ 8.46

2009 TUFFP Industrial Account Budget Summary (Prepared September 8, 2008)

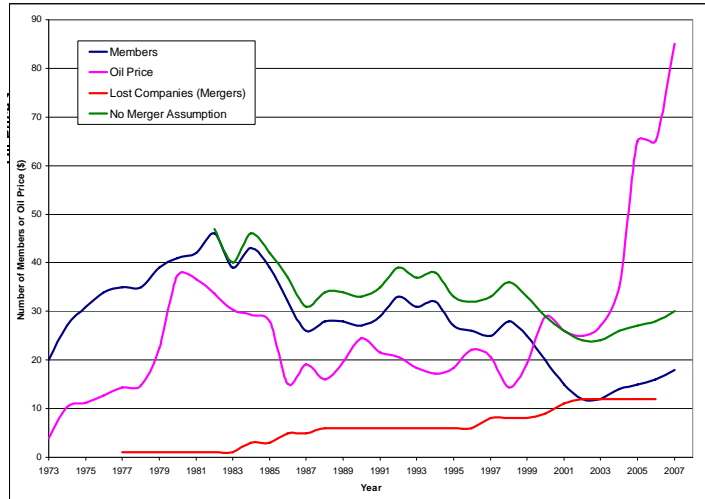
Anticipated Reserve Fund Balance on January 1, 2009	\$413,330.00
Income for 2009	
2009 Anticipated Membership Fees (16 @ \$48,000 - excludes MMS)	\$768,000.00
Total Income	\$1,181,330.00
2009 Anticipated Expenditures	Projected Budget
90101-90103 Faculty Salaries	29,251.82
90600-90609 Professional Salaries	106,676.24
90700-90703 Staff Salaries	45,866.46
91000 Graduate Students	58,100.00
91100 Undergraduate Students	15,000.00
91800 Fringe Benefits (33%)	59,992.19
93100 General Supplies	3,000.00
93101 Research Supplies	100,000.00
93102 Copier/Printer Supplies	500.00
93104 Computer Software	4,000.00
93106 Office Supplies	2,000.00
93200 Postage/Shipping	500.00
93300 Printing/Duplicating	2,000.00
93400 Telecommunications	3,000.00
93500 Memberships/Subscriptions	1,000.00
93601 Travel - Domestic	10,000.00
93602 Travel - Foreign	10,000.00
93700 Entertainment (Advisory Board Meetings)	10,000.00
81801 Tuition/Student Fees	30,665.00
94803 Consultants	16,000.00
94813 Outside Services	20,000.00
95200 Indirect Costs (55.6%)	141,721.35
98901 Employee Recruiting	3,000.00
99001 Equipment	600,000.00
99002 Computers	8,000.00
99300 Bank Charges	40.00
Total Expenditures	\$1,280,313.05
Anticipated Reserve Fund Balance on December 31, 2009	-\$98,983.05

2009 Proposed MMS Account Summary

(Prepared September 8 2008)

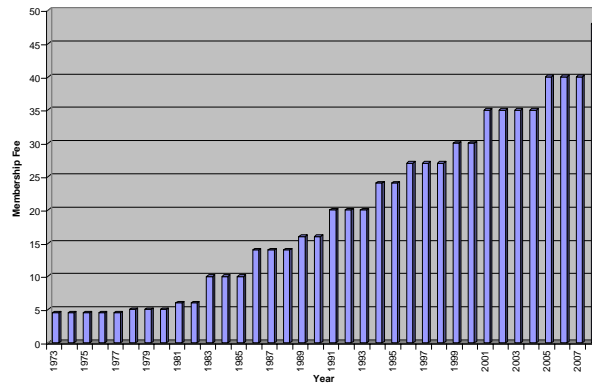
Account Balance - January 1, 2009	\$825.94
Income for 2009	
2009 Membership Fee	\$48,000.00
Remaining Balance	\$48,825.94
2009 Anticipated Expenditures	Projected Budget
90101-90103 Faculty Salaries	0.00
90600-90609 Professional Salaries	0.00
90700-90703 Staff Salaries	0.00
91000 Graduate Students	27,900.00
91800 Fringe Benefits (33%)	0.00
95200 Indirect Costs (55.6%)	15,512.40
Total Expenditures	\$43,412.40
Anticipated Reserve Fund Balance on December 31, 2009	\$5,413.54

History – Membership



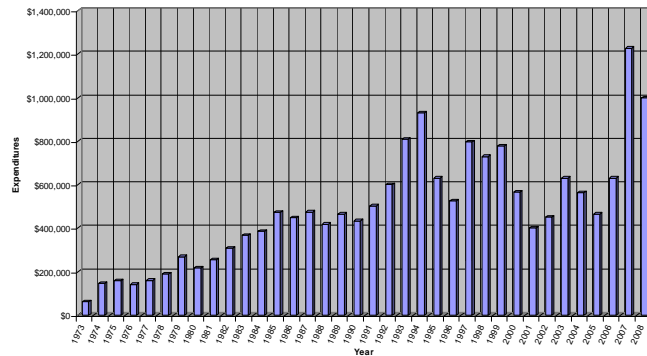
History – Membership Fees

Figure II - Membership Fee History



History - Expenditures

Figure III - History of TUFFP Expenditures



Membership Fees

- ◆ **2007 Membership Dues**
 - 2 Unpaid
 - Expect to Be Paid Shortly
- ◆ **2008 Membership Dues**
 - 12 of 17 Paid as of September 1
 - Need your prompt payments

Introduction

This semi-annual report is submitted to Tulsa University Fluid Flow Projects (TUFFP) members to summarize activities since the April 15, 2008 Advisory Board meeting and to assist in planning for the next six months. It also serves as a basis for reporting progress and generating discussion at the 71st semi-annual Advisory Board meeting to be held in Tulsa Learning Center at Doubletree Hotel at Warren Place, 6110 South Yale Avenue, Tulsa, OK on Thursday, September 17, 2008.

The activities will start with Tulsa University High Viscosity Projects (TUHOP) Advisory Board meeting on September 16, 2008 between 8:30 a.m. and noon in Salon-A at Doubletree Hotel at Warren Place. Between 1:00 and 3:00 p.m. on September 17, 2008, there will be TUFFP workshop in the same room. There will be presentations made by TUFFP member companies. Simultaneously, Tulsa University Hydrate Flow Performance JIP (TUHFP) Advisory Board meeting will be held between 8:30 a.m. and 3:00 p.m. in Tulsa Learning Center at Doubletree Hotel at Warren Place. A facility tour will be held on September 17, 2008 between 4:00 and 6:00 p.m. Following the tour, there will be a TUHOP/TUHFP/TUFFP reception between 6:30 and 9:00 p.m. in Salon-A of Doubletree Hotel at Warren Place.

TUFFP Advisory Board meeting will convene at 8:00 a.m. on September 17th and will adjourn at approximately 5:00 p.m. Following the meeting, there will be a joint TUFFP and TUPDP reception between 6:00 and 9:00 p.m. in Parkview East at Doubletree Hotel at Warren Place.

The Tulsa University Paraffin Deposition Projects (TUPDP) Advisory Board meeting will be held on September 18th in Salon-A at Doubletree Hotel at Warren Place between 8:30 a.m. and 1:00 p.m.

The reception and the social function will provide an opportunity for informal discussions among members, guests, and TU staff and students.

Several TUFFP facilities will be operating during the tour. An opportunity will also be available to view the single-phase, multiphase, and small scale paraffin deposition test facilities and the hydrate flow loop.

The following dates have tentatively been established for spring 2009 Advisory Board meetings. The venue for spring 2009 Advisory Board meetings will be determined later.

2009 Spring Meetings

March 17, 2009	Tulsa University High Viscosity Oil Projects (TUHOP) JIP Meeting Tulsa University Fluid Flow Projects (TUFFP) Workshop Facility Tour TUHOP – TUFFP Reception
March 18, 2009	Tulsa University Fluid Flow Projects (TUFFP) Advisory Board Meeting TUFFP – TUPDP Reception
March 19, 2009	Tulsa University Paraffin Deposition Projects (TUPDP) Advisory Board Meeting

Personnel

Dr. Cem Sarica, Professor of Petroleum Engineering, continues as Director of TUFFP and TUPDP, and as Co-Principal Investigator of TUHFP and TUHOP.

Dr. Holden Zhang, Assistant Professor of Petroleum Engineering, serves as Principal Investigator of TUHOP and Associate Director of TUFFP.

Dr. Brill serves as a Research Professor of Petroleum Engineering on a part-time basis.

Dr. Abdel Salam Al-Sarkhi served as the lead research associate for TUFFP for 1 ½ years. Abdel resigned his position effective August 26, 2008 due to family obligations in Jordan. He has contributed significantly to TUFFP during his short stay with us. He will be missed. We wish him well in his future endeavors. A search is currently underway to fill his position.

Dr. Mingxiu (Michelle) Li continues to serve as a Research Associate for TUHOP, TUFFP, and related projects. Michelle received her Ph.D. from The University of Edinburgh in Bio-Fluid Dynamics – Department of Mechanical Engineering in March 2007. She has an M.Phil in Engineering Thermophysics from Department of Energy and Power Engineering of Xia'Tong University.

Mr. Scott Graham continues to serve as Project Engineer. Scott oversees all of the facility operations and continues to be the senior electronics technician for TUFFP, TUPDP, and TUHOP.

Mr. Craig Waldron continues as Research Technician, addressing our needs in mechanical areas. He also serves as a flow loop operator for TUPDP and Health, Safety, and Environment (HSE) officer for TUFFP, TUPDP and TUHOP.

Mr. Brandon Kelsey serves as an electro-mechanical technician serving TUFFP, TUPDP, and TUHOP projects. Brandon is a graduate of OSU Okmulgee with a BS degree in instrumentation and automation degree.

Ms. Linda Jones continues as Project Coordinator of TUFFP, TUPDP and TUHOP projects. She keeps the project accounts in addition to other responsibilities such as external communications, providing computer support for graduate students, publishing and distributing all research reports and

deliverables, managing the computer network and web sites, and supervision of part-time office help.

Mr. James Miller, Computer Manager, and TUFFP TUPDP and TUHOP Web Administrator, is currently on military leave. He is expected to return in November 2008.

Table 1 updates the current status of all graduate students conducting research on TUFFP projects for the last six months.

Mr. Bahadir Gokcal continues his Ph.D. degree studies conducting research on High Viscosity Two-phase Flow research. He is concentrating his efforts on Slug Flow for High Viscosity Two-phase Flow. Bahadir is expected to defend his Ph.D. dissertation after the Advisory Board meetings. He has already accepted a position with Technip in Houston.

Mr. Kwonil Choi is pursuing his Ph.D degree in Petroleum Engineering. He is fully supported by PETROBRAS. He is conducting a research project titled "Lagrangian-Eulerian Transient Two-phase Flow Model". His allowed time in Tulsa has expired and he will continue his research from Brazil.

Mr. Xiao Feng was studying Three-phase Low Liquid Loading Flow in Inclined Pipes towards a MS degree in Petroleum Engineering. Due to unsatisfactory progress, his MS program is converted to Master of Engineering requiring no research. Research on Low Liquid Loading will be assigned to a new Research Assistant in spring 2009.

Mrs. Gizem Ersoy Gokcal, from Turkey, started her Ph.D. degree studies. She is working on the project titled "Three-phase Gas-Oil-Water Flow in Hilly Terrain Pipelines". Gizem received a BS degree in Petroleum and Natural Gas Engineering from Middle East Technical University and an MS degree in Petroleum Engineering from The University of Tulsa.

Mr. Kyle Magrini, a US National, received a BS degree in Electrical Engineering from The University of Tulsa. Kyle is working on the project titled "Liquid Entrainment in Annular Two-phase in Inclined Pipes".

Mr. Anoop Sharma, from India, has a BS degree in Chemical Engineering from National Institute of Technology Karnataka, India. He has also involved in research at other universities such as Indian Institute of Science, Bangalore, India. He is studying to improve the

two-phase oil-water flow modeling and closure relationship development.

Ms. Tingting Yu graduated in 2007 from China University of Petroleum (East China), majored in Oil and Gas Storage and Transportation. Tingting is now a teaching assistant for the Petroleum Engineering Department. She is working on a project investigating multiphase flow in annulus.

Ms. Ceyda Kora, from Turkey, has recently joined the TUFFP to pursue her MS degree in Petroleum Engineering. Ceyda has received a BS degree in Petroleum and Natural Gas Engineering from Middle East Technical University in 2008.

A list of all telephone numbers and e-mail addresses for TUFFP personnel are given in Appendix D.

Table 1***2008 Fall Research Assistant Status***

<i>Name</i>	<i>Origin</i>	<i>Stipend</i>	<i>Tuition</i>	<i>Degree Pursued</i>	<i>TUFFP Project</i>	<i>Completion Date</i>
Kwon Il Choi	Brazil	No – Petrobras	No – Petrobras	Ph.D. – PE	Lagrangian-Eulerian Transient Two-Phase Flow Model	Spring 2009
Gizem Ersoy	Turkey	Yes – TUFFP	Yes – TUFFP	Ph.D. – PE	Multiphase Flow in Hilly Terrain Pipelines	Spring 2009
Bahadir Gokcal	Turkey	Yes – TUFFP	Waived	Ph.D. – PE	High Viscosity Oil Multiphase Flow Behavior	Fall 2008
Ceyda Kora	Turkey	Yes – TUFFP	Yes - TUFFP	MS. – PE	To Be Assigned	Fall 2010
Kyle Magrini	USA	Yes – TUFFP	Yes – TUFFP	MS – PE	Entrainment Fraction in Annular Two-phase Flow in Inclined Pipes	Spring 2009
Anoop Sharma	India	Yes – TUFFP	Yes – TUFFP	MS – PE	Development of Oil-Water Flow Closure Relationships	Spring 2009
Tingting Yu	PRC	Partial – TUFFP	No – PE Depart.	MS – PE	Multiphase Flow in a Vertical Annulus	Spring 2009

Membership

The current membership of TUFFP stands at 16 industrial members and Mineral Management Services of Department of Interior (MMS).

DOE project titled “The development of new generation multiphase flow predictive tools for three-phase flow” has effectively ended at the end of summer 2008. DOE’s support translated into the equivalent four members for the past five years.

Our efforts to increase the TUFFP membership level continues. SPT will be joining TUFFP this year. The paper work is currently underway. A new five years membership contract with MMS will be

finalized soon. Drs. Cem Sarica and Holden Zhang visited PetroChina and Chinese National Offshore Oil Company (CNOOC) in June to establish relationships and solicit membership in our research programs. They have shown significant interest. It is expected that we will have CNOOC be part of TUFFP soon.

Table 2 lists all the current 2008 TUFFP members. A list of all Advisory Board representatives for these members with pertinent contact information appears in Appendix B. A detailed history of TUFFP membership is given in Appendix C.

Table 2

2008 Fluid Flow Projects Membership

Baker Atlas	PEMEX
BP Exploration	Petrobras
Chevron	Petronas
ConocoPhillips	Rosneft
Exxon Mobil	Schlumberger
JOGMEG	Shell Global Solutions
KOC	Tenaris
Marathon Oil Company	Total
Minerals Management Service	

Equipment and Facilities Status

Test Facilities

The high viscosity two-phase flow loop is equipped with capacitance sensors in addition to laser sensors to measure the slug characteristics.

The three-phase facility modifications to accommodate Three-phase Gas-oil-water Flow in Hilly Terrain Pipelines have been completed.

The severe slugging facility is modified for the Liquid Entrainment project. The new liquid film removal device is constructed for 3 in. pipe. .

The design of a high pressure (500 psi operating pressures) and large diameter (6 in. ID) facility were completed and presented at the last Advisory Board meeting. The facility P&ID is prepared by an independent engineering company. The final stage before construction will be the HAZOP exercise with the help of one of the member company HAZOP engineers.

New generation capacitance sensors are developed and are being used in various projects.

Detailed descriptions of these modification efforts appear in the progress reports given in this brochure. A site plan showing the location of the various TUFFP and TUPDP test facilities on the North Campus is given in Fig. 1.

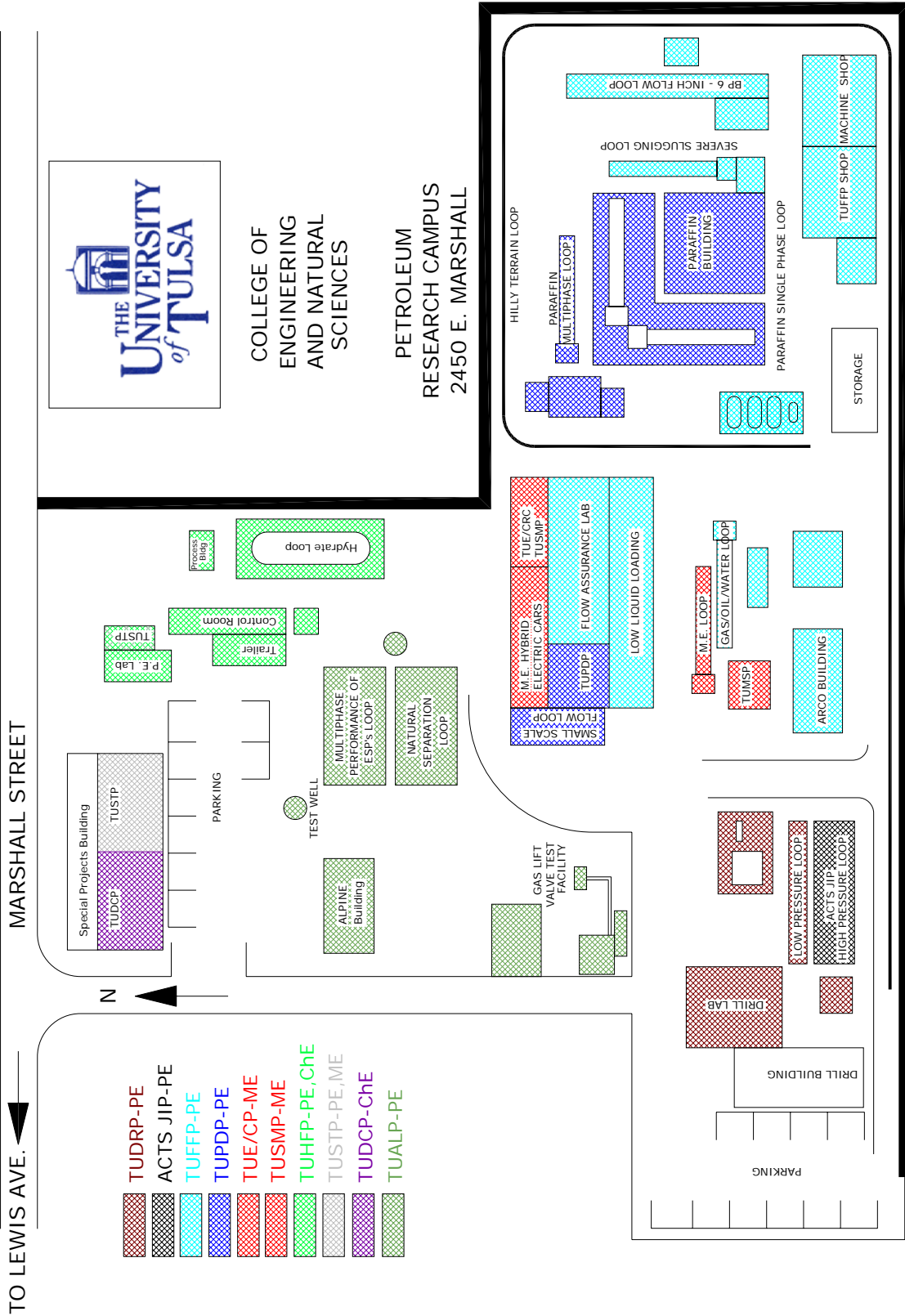


Figure 1 – Site Plan for the North Campus Research Facilities

Financial Status

TUFFP maintains separate accounts for industrial and U.S. government members. Thus, separate accounts are maintained for the MMS and DOE funds.

As of September 8, 2008, 16 of the 18 TUFFP members had paid their 2007 membership fees. The members who have not paid their membership fee were informed, and we expect expedited payments. Moreover, 12 of the 17 TUFFP members paid their 2008 membership fees. We really appreciate your prompt payment of the membership dues.

Table 3 presents a financial analysis of income and expenditures for the 2008 Industrial member account as of September 8, 2008. Also shown are previous 2008 budgets that have been reported to the members. The total industry expenditures for 2008 are projected to be \$875,035. The industry reserve account is expected to be \$413,330 at the end of 2008 if the two unpaid membership dues could not be collected.

Table 4 presents a financial analysis of expenditures and income for the MMS Account for 2008. This account is used primarily for graduate student stipends. A balance of \$826 will be carried over to 2009.

Table 5 presents a financial analysis of expenditures and income for the DOE Account for 2008. The

DOE Award is \$731,995 over five years. The start date of the award was July 2003. A total of \$106,589 will be spent in 2008, leaving an award balance of \$8 at the end of 2008.

The University of Tulsa waives up to 19 hours of tuition for each graduate student that is paid a stipend from the United States government, including both MMS and DOE funds. A total of 45 hours of tuition (equivalent of \$32,850) was waived for 2008.

Tables 6-7 present the projected budgets and income for the Industrial, and MMS accounts for 2009. The 2009 TUFFP industrial membership is assumed to stay at 17 in this analysis. This will provide \$816,000 of industrial membership income for 2008. The sum of the 2008 income and the reserve account is projected to be \$1,181,330. The expenses for the industrial member account are estimated to be \$1,280,313 leaving a deficit of \$98,983 if all of the expenses on High Pressure Test Facility are made in 2009. TUFFP can not operate with deficit. We will either need an additional one time facility enhancement contribution from our members or we can shift some of the facility construction cost to 2010 by delaying the completion the construction. The MMS account is expected to have a carryover of \$5,414.

Table 3: TUFFP 2008 Industrial Budget

**2008 TUFFP Industrial Account Budget Summary
(Prepared September 8, 2008)**

Anticipated Reserve Fund Balance on January 1, 2008	610,365.69
Uncollected 2007 Membership Fees (2 @ \$40,000)	(80,000.00)
	530,365.69
Income for 2008	
2008 Membership Fees (15 @ \$48,000 - excludes MMS)	\$720,000
2008 Membership Fees (1 @ 38,000)	\$38,000
Total Budget	1,288,365.69

Projected Budget/Expenditures for 2008

	Budget	Revised Budget 4/08	Expenses 9/8/08	Anticipated 2008 Expenses
90101 Principal Investigator - Sarica	24,392.00	25,907.00	13,973.33	27,930.48
90103 Co-Principal Investigator - Zhang	19,665.00		3,622.50	3,622.50
90600 Professional Salary - Jones	5,141.00	7,330.00	5,540.21	8,472.20
90601 Professional Salary - Li	13,505.00	28,854.00	21,432.31	24,651.07
90602 Professional Salary - Graham	5,237.00	15,785.00	8,345.12	15,505.93
90603 Professional Salary - Al-Sarkhi	32,500.00	38,750.00	21,812.52	6,458.34
90701 Technician - Miller	15,065.00		-	-
90702 Technician - Waldron	6,575.00	11,428.00	5,193.03	9,869.21
90703 Technician - Kelsey	9,750.00	10,154.00	9,099.72	12,754.00
90800 Salaries - Part-time	4,290.00		-	-
91000 Graduate Students - Monthly	50,100.00	65,000.00	41,433.32	60,745.44
91100 Students - Hourly	15,000.00	15,000.00	9,564.63	14,064.63
91800 Fringe Benefits (33%)	50,910.83	45,609.00	29,376.18	36,057.04
93100 General Supplies	3,000.00	3,000.00	222.43	500.00
93101 Research Supplies	100,000.00	100,000.00	82,672.88	100,000.00
93102 Copier/Printer Supplies	500.00	500.00	169.05	280.00
93104 Computer Software	4,000.00	4,000.00	502.18	1,200.00
93106 Office Supplies	2,000.00	2,000.00	2,070.79	3,000.00
93200 Postage/Shipping	500.00	500.00	531.82	650.00
93300 Printing/Duplicating	2,000.00	2,000.00	1,292.37	2,000.00
93400 Telecommunications	3,000.00	3,000.00	1,166.54	1,766.00
93500 Membership/Subscriptions	1,000.00	1,000.00	181.50	400.00
93600 Travel			-	-
93601 Travel - Domestic	14,000.00	10,000.00	4,289.48	10,000.00
93602 Travel - Foreign	10,000.00	10,000.00	10,946.46	10,946.46
93606 Visa			241.35	241.35
93700 Entertainment (Advisory Board Meetings)	10,000.00	10,000.00	5,780.37	10,000.00
94803 Consultants		16,000.00	7,708.35	18,500.00
94813 Outside Services	20,000.00	20,000.00	68,278.29	68,278.29
95200 F&A (55.6%)	119,456.33	121,324.00	75,006.49	102,344.00
98901 Employee Recruiting	3,000.00	3,000.00		147.00
99001 Equipment	600,000.00	200,000.00	93,401.74	263,500.00
99002 Computers	8,000.00	8,000.00	768.70	4,000.00
99300 Bank Charges	40.00	40.00	-	-
81801 Tuition/Fees	30,306.00	53,103.00	55,342.00	55,342.00
81806 Graduate Fellowship			933.03	1,809.22
Total Expenditures	1,182,933.16	831,284.00	580,898.69	875,035.16

Anticipated Reserve Fund Balance as of 12/31/08	413,330.53
---	------------

Table 4: TUFFP 2008 MMS Budget

2008 TUFFP MMS Budget Summary

(Prepared July 28, 2008)

Reserve Balance as of 12/31/07	\$5,322
2008 Budget	40,000

Total Budget	45,322
---------------------	---------------

Projected Budget/Expenditures for 2008

	Budget	2007 Anticipated Expenditures
91000 Students - Monthly	25,600.00	28,800.00
95200 F&A	14,233.60	15,696.00
81801 Tuition/Fees		
Total Anticipated Expenditures as of 12/31/08	39,833.60	44,496.00
Total Anticipated Reserve Fund Balance as of 12/31/08		825.94

Table 5: TUFFP 2008 DOE Budget

**2008 TUFFP DOE Budget
(Prepared July 28, 2008)**

Award Amount	\$731,995
Amount Invoiced (June 1, 2003 - December 31, 2007)	625,397.81
Total Budget	106,597.19

Projected Budget/Expenditures for 2008

	2008 Budget	2008 Expenditures	
90600 Professional Salary - Jones	6,279.00	7,451.33	
90600 Professional Salary - Graham	12,514.00	13,567.73	
90601 Professional Salary - Wang/Abdel	22,958.33	21,812.49	
90602 Professional Salary - Li		2,253.13	
90702 Technician - Mechanical	3,644.00	3,953.56	
90703 Technician - Mechanical	6,825.00	2,148.58	
91000 Graduate Students - Monthly	7,000.00	8,215.22	
91800 Fringe Benefits (35%)	17,232.50	16,891.65	
95200 F&A (51%)	30,202.50	30,295.04	
Total Anticipated Expenditures as of 5/31/08	106,655.33	106,588.73	
Anticipated Fund Balance on 8/31/08			\$ 8.46

Table 6: 2009 Projected TUFFP Industrial Budget

2009 TUFFP Industrial Account Budget Summary

(Prepared September 8, 2008)

Anticipated Reserve Fund Balance on January 1, 2009	\$413,330.00
Income for 2009	
2009 Anticipated Membership Fees (16 @ \$48,000 - excludes MMS)	\$768,000.00
Total Income	\$1,181,330.00
2009 Anticipated Expenditures	Projected Budget
90101-90103 Faculty Salaries	29,251.82
90600-90609 Professional Salaries	106,676.24
90700-90703 Staff Salaries	45,866.46
91000 Graduate Students	58,100.00
91100 Undergraduate Students	15,000.00
91800 Fringe Benefits (33%)	59,992.19
93100 General Supplies	3,000.00
93101 Research Supplies	100,000.00
93102 Copier/Printer Supplies	500.00
93104 Computer Software	4,000.00
93106 Office Supplies	2,000.00
93200 Postage/Shipping	500.00
93300 Printing/Duplicating	2,000.00
93400 Telecommunications	3,000.00
93500 Memberships/Subscriptions	1,000.00
93601 Travel - Domestic	10,000.00
93602 Travel - Foreign	10,000.00
93700 Entertainment (Advisory Board Meetings)	10,000.00
81801 Tuition/Student Fees	30,665.00
94803 Consultants	16,000.00
94813 Outside Services	20,000.00
95200 Indirect Costs (55.6%)	141,721.35
98901 Employee Recruiting	3,000.00
99001 Equipment	600,000.00
99002 Computers	8,000.00
99300 Bank Charges	40.00
Total Expenditures	\$1,280,313.05
Anticipated Reserve Fund Balance on December 31, 2009	-\$98,983.05

Table 7: TUFFP Projected 2009 MMS Budget

2009 TUFFP MMS Account Budget Summary

(Prepared September 8 2008)

Account Balance - January 1, 2009	\$825.94
Income for 2009	
2009 Membership Fee	\$48,000.00
Remaining Balance	\$48,825.94
2009 Anticipated Expenditures	Projected Budget
90101-90103 Faculty Salaries	0.00
90600-90609 Professional Salaries	0.00
90700-90703 Staff Salaries	0.00
91000 Graduate Students	27,900.00
91800 Fringe Benefits (33%)	0.00
95200 Indirect Costs (55.6%)	15,512.40
Total Expenditures	\$43,412.40
Anticipated Reserve Fund Balance on December 31, 2009	\$5,413.54

Miscellaneous Information

Fluid Flow Projects Short Course

The 33rd TUFFP “Two-Phase Flow in Pipes” short course offering was offered to 17 attendees (12 from member companies) May 12-16, 2008. The 34th short course is scheduled for May 18-22, 2009. We urge you to sign-up potential participants early. We need at least 10 attendees for the course to be offered.

Jim Brill to Receive Prestigious SPE Award

Jim Brill, the founder and the director emeritus of TUFFP, will receive Society of Petroleum Engineers’ (SPE) 2008 DeGolyer Distinguished Service Award at the 2008 SPE Annual Technical Conference and Exhibition. The DeGolyer Distinguished Service Medal recognizes distinguished and outstanding service to SPE, the professions of engineering and/or geology, and to the petroleum industry.

BHR Group Conference on Multiphase Technology

Since 1991, TUFFP has participated as a co-sponsor of BHR Group Conferences on Multiphase Production. TUFFP personnel participate in reviewing papers, serving as session chairs, and advertising the conference to our members. This conference has become one of the premier international event providing delegates with opportunities to discuss new research and developments, to consider innovative solutions in multiphase production area.

6th North American Conference on Multiphase Technology, supported by Neotechnology Consultants of Calgary, Canada, New Technology Magazine, SPT Group and TUFFP, was successfully held 4-6 of June 2008 in Banff, Canada. Over 80 delegates participated in the conference. Cem Sarica served as the technical chair of the conference. Dr. James P. Brill gave the Opening Address. Mr. Bahadir Gokcal made a technical paper presentation discussing some of his findings on drift velocity for high viscosity oils.

14th International Conference on Multiphase Technology, supported by IFP, Technology Initiatives and TUFFP, will be held 17-19 of June 2009 in Cannes, France. The conference will benefit anyone engaged in the application, development and research of multiphase technology for the oil and gas

industry. Applications in the oil and gas industry will also be of interest to engineers from other industries for which multiphase technology offers a novel solution to their problems. The conference will also be of particular value to designers, facility and operations engineers, consultants and researchers from operating, contracting, consultancy and technology companies. The conference brings together experts from across the American Continents and Worldwide.

The scope of the conference includes variety of subjects pertinent to Multiphase Production in both technology development and applications of the existing technologies. The theme of the conference is “*Bigger, Deeper, Longer*”. The abstract deadline is October 6, 2008. The detailed information about the conference can be found in BHRg’s (www.brhgroup.com).

Publications & Presentations

Since the last Advisory Board meeting, the following publications and presentations are made.

- 1) Gokcal, B., Wang, Q., Zhang, H. Q., and Sarica, C.: “Effects of High Oil Viscosity on Oil-Gas Flow Behavior in Horizontal Pipes,” SPE 102727, *SPE Projects, Facilities & Construction Journal*, June 2008.
- 2) Vielma, M., Atmaca, S., Zhang, H. Q., and Sarica, C.: “Characterization of Oil/Water Flows in Horizontal Pipes,” SPE 109591, Accepted for Publication in *SPE Projects, Facilities & Construction Journal*, 2008.
- 3) Al-Safraan, E. Kappos, L. and Sarica, C. “Experimental and Numerical Investigation of Separator Pressure Fluctuation Effect on Terrain Slugging in a Hilly-Terrain Two-phase Flow Pipeline,” *Journal of Energy Resources Technology* September 2008.
- 4) Gokcal, B., Alsarkhi, A., and Sarica, C.: “Experimental Effects of High Viscosity on Drift Velocity for Horizontal Pipes,” 6th North American Conference on Multiphase Technology, June 4 – 6, 2008, Banff, Canada.

Paraffin Deposition Projects Activities

The third three year phase of TUPDP continues. The studies concentrate on the paraffin deposition characterization of single-phase turbulent flow, oil-

water paraffin deposition, gas-oil-water paraffin deposition.

TU CoRE Activities

The Center of Research Excellence (TUCoRE) initiated by Chevron at The University of Tulsa funds several research projects on flow assurance topics. TUFFP researchers are involved in various TUCoRE activities. One such activity is on High Viscosity Multiphase Flow (TUHOP). Up to this date, Chevron has provided TU to \$680,000 for

improvement of an existing high pressure multiphase flow facility. Moreover, this research is being leveraged by forming a Joint Industry Project. Current members of the JIP are BP, Chevron and Petrobras.

Two-Phase Flow Calendar

Several technical meetings, seminars, and short courses involving two-phase flow in pipes are scheduled for 2008 and 2009. Table 9 lists meetings that would be of interest to TUFFP members.

Table 9

Meeting and Conference Calendar**2008**

September 4-7	Offshore Europe, Aberdeen, Scotland
September 16	TUHOP Fall Advisory Board meeting, Tulsa, OK
September 16	TUHFP Fall Advisory Board meeting, Tulsa, OK
September 16	TUFFP Fall Workshop, Tulsa, OK
September 17	TUFFP Fall Advisory Board meeting, Tulsa, OK
September 18	TUPDP Fall Advisory Board meeting, Tulsa, OK
September 21 – 24	SPE Annual Technical Conference and Exhibition, Denver, Colorado, USA
October 20 – 23	SPE International Thermal Operations and Heavy Oil Symposium
December 3 – 5	International Petroleum Technology Conference, Kuala Lumpur, Malaysia

2009

January 27 – 29	Bridging the Divide: Improving the Reservoir/Facilities Interface – SPE Workshop, London, England
March 17	TUHOP Spring Advisory Board meeting, Tulsa, OK
March 17	TUFFP Spring Workshop, Tulsa, OK
March 18	TUFFP Spring Advisory Board meeting, Tulsa, OK
March 19	TUPDP Fall Advisory Board meeting, Tulsa, OK
April 4 – 8	SPE Productions and Operations Symposium, Oklahoma City, OK, USA
April 20 -22	SPE International Symposium on Oil Field Chemistry, the Woodlands, TX, USA
May 4 – 7	Offshore Technology Conference, Houston, TX, USA
June 17 – 19	BHRg Multiphase Production Technology, Cannes, France

Appendix A

Fluid Flow Projects Deliverables¹

1. "An Experimental Study of Oil-Water Flowing Mixtures in Horizontal Pipes," by M. S. Malinowsky (1975).
2. "Evaluation of Inclined Pipe Two-Phase Liquid Holdup Correlations Using Experimental Data," by C. M. Palmer (1975).
3. "Experimental Evaluation of Two-Phase Pressure Loss Correlations for Inclined Pipe," by G. A. Payne (1975).
4. "Experimental Study of Gas-Liquid Flow in a Pipeline-Riser Pipe System," by Z. Schmidt (1976).
5. "Two-Phase Flow in an Inclined Pipeline-Riser Pipe System," by S. Juprasert (1976).
6. "Orifice Coefficients for Two-Phase Flow Through Velocity Controlled Subsurface Safety Valves," by J. P. Brill, H. D. Beggs, and N. D. Sylvester (Final Report to American Petroleum Institute Offshore Safety and Anti-Pollution Research Committee, OASPR Project No. 1; September, 1976).
7. "Correlations for Fluid Physical Property Prediction," by M. E. Vasquez A. (1976).
8. "An Empirical Method of Predicting Temperatures in Flowing Wells," by K. J. Shiu (1976).
9. "An Experimental Study on the Effects of Flow Rate, Water Fraction and Gas-Liquid Ratio on Air-Oil-Water Flow in Horizontal Pipes," by G. C. Laflin and K. D. Oglesby (1976).
10. "Study of Pressure Drop and Closure Forces in Velocity- Type Subsurface Safety Valves," by H. D. Beggs and J. P. Brill (Final Report to American Petroleum Institute Offshore Safety and Anti-Pollution Research Committee, OSAPR Project No. 5; July, 1977).
11. "An Experimental Study of Two-Phase Oil-Water Flow in Inclined Pipes," by H. Mukhopadhyay (September 1, 1977).
12. "A Numerical Simulation Model for Transient Two-Phase Flow in a Pipeline," by M. W. Scoggins, Jr. (October 3, 1977).
13. "Experimental Study of Two-Phase Slug Flow in a Pipeline-Riser Pipe System," by Z. Schmidt (1977).
14. "Drag Reduction in Two-Phase Gas-Liquid Flow," (Final Report to American Gas Association Pipeline Research Committee; 1977).
15. "Comparison and Evaluation of Instrumentation for Measuring Multiphase Flow Variables in Pipelines," Final Report to Atlantic Richfield Co. by J. P. Brill and Z. Schmidt (January, 1978).
16. "An Experimental Study of Inclined Two-Phase Flow," by H. Mukherjee (December 30, 1979).

¹ Completed TUFFP Projects – each project consists of three deliverables – report, data and software. Please see the TUFFP website

17. "An Experimental Study on the Effects of Oil Viscosity, Mixture Velocity and Water Fraction on Horizontal Oil-Water Flow," by K. D. Oglesby (1979).
18. "Experimental Study of Gas-Liquid Flow in a Pipe Tee," by S. E. Johansen (1979).
19. "Two Phase Flow in Piping Components," by P. Sookprasong (1980).
20. "Evaluation of Orifice Meter Recorder Measurement Errors in Lower and Upper Capacity Ranges," by J. Fujita (1980).
21. "Two-Phase Metering," by I. B. Akpan (1980).
22. "Development of Methods to Predict Pressure Drop and Closure Conditions for Velocity-Type Subsurface Safety Valves," by H. D. Beggs and J. P. Brill (Final Report to American Petroleum Institute Offshore Safety and Anti-Pollution Research Committee, OSAPR Project No. 10; February, 1980).
23. "Experimental Study of Subcritical Two-Phase Flow Through Wellhead Chokes," by A. A. Pilehvari (April 20, 1981).
24. "Investigation of the Performance of Pressure Loss Correlations for High Capacity Wells," by L. Rosslund (1981).
25. "Design Manual: Mukherjee and Brill Inclined Two-Phase Flow Correlations," (April, 1981).
26. "Experimental Study of Critical Two-Phase Flow through Wellhead Chokes," by A. A. Pilehvari (June, 1981).
27. "Experimental Study of Pressure Wave Propagation in Two-Phase Mixtures," by S. Vongvuthipornchai (March 16, 1982).
28. "Determination of Optimum Combination of Pressure Loss and PVT Property Correlations for Predicting Pressure Gradients in Upward Two-Phase Flow," by L. G. Thompson (April 16, 1982).
29. "Hydrodynamic Model for Intermittent Gas Lifting of Viscous Oils," by O. E. Fernandez (April 16, 1982).
30. "A Study of Compositional Two-Phase Flow in Pipelines," by H. Furukawa (May 26, 1982).
31. "Supplementary Data, Calculated Results, and Calculation Programs for TUFFP Well Data Bank," by L. G. Thompson (May 25, 1982).
32. "Measurement of Local Void Fraction and Velocity Profiles for Horizontal Slug Flow," by P. B. Lukong (May 26, 1982).
33. "An Experimental Verification and Modification of the McDonald-Baker Pigging Model for Horizontal Flow," by S. Barua (June 2, 1982).
34. "An Investigation of Transient Phenomena in Two-Phase Flow," by K. Dutta-Roy (October 29, 1982).
35. "A Study of the Heading Phenomenon in Flowing Oil Wells," by A. J. Torre (March 18, 1983).
36. "Liquid Holdup in Wet-Gas Pipelines," by K. Minami (March 15, 1983).
37. "An Experimental Study of Two-Phase Oil-Water Flow in Horizontal Pipes," by S. Arirachakaran (March 31, 1983).

38. "Simulation of Gas-Oil Separator Behavior Under Slug Flow Conditions," by W. F. Giozza (March 31, 1983).
39. "Modeling Transient Two-Phase Flow in Stratified Flow Pattern," by Y. Sharma (July, 1983).
40. "Performance and Calibration of a Constant Temperature Anemometer," by F. Sadeghzadeh (August 25, 1983).
41. "A Study of Plunger Lift Dynamics," by L. Rosina (October 7, 1983).
42. "Evaluation of Two-Phase Flow Pressure Gradient Correlations Using the A.G.A. Gas-Liquid Pipeline Data Bank," by E. Caetano F. (February 1, 1984).
43. "Two-Phase Flow Splitting in a Horizontal Pipe Tee," by O. Shoham (May 2, 1984).
44. "Transient Phenomena in Two-Phase Horizontal Flowlines for the Homogeneous, Stratified and Annular Flow Patterns," by K. Dutta-Roy (May 31, 1984).
45. "Two-Phase Flow in a Vertical Annulus," by E. Caetano F. (July 31, 1984).
46. "Two-Phase Flow in Chokes," by R. Sachdeva (March 15, 1985).
47. "Analysis of Computational Procedures for Multi-Component Flow in Pipelines," by J. Goyon (June 18, 1985).
48. "An Investigation of Two-Phase Flow Through Willis MOV Wellhead Chokes," by D. W. Surbey (August 6, 1985).
49. "Dynamic Simulation of Slug Catcher Behavior," by H. Genceli (November 6, 1985).
50. "Modeling Transient Two-Phase Slug Flow," by Y. Sharma (December 10, 1985).
51. "The Flow of Oil-Water Mixtures in Horizontal Pipes," by A. E. Martinez (April 11, 1986).
52. "Upward Vertical Two-Phase Flow Through An Annulus," by E. Caetano F. (April 28, 1986).
53. "Two-Phase Flow Splitting in a Horizontal Reduced Pipe Tee," by O. Shoham (July 17, 1986).
54. "Horizontal Slug Flow Modeling and Metering," by G. E. Kouba (September 11, 1986).
55. "Modeling Slug Growth in Pipelines," by S. L. Scott (October 30, 1987).
56. "RECENT PUBLICATIONS" - A collection of articles based on previous TUFFP research reports that have been published or are under review for various technical journals (October 31, 1986).
57. "TUFFP CORE Software Users Manual, Version 2.0," by Lorri Jefferson, Florence Kung and Arthur L. Corcoran III (March 1989)
58. "Simplified Modeling and Simulation of Transient Two Phase Flow in Pipelines," by Y. Taitel (April 29, 1988).
59. "RECENT PUBLICATIONS" - A collection of articles based on previous TUFFP research reports that have been published or are under review for various technical journals (April 19, 1988).

60. "Severe Slugging in a Pipeline-Riser System, Experiments and Modeling," by S. J. Vierkandt (November 1988).
61. "A Comprehensive Mechanistic Model for Upward Two-Phase Flow," by A. Ansari (December 1988).
62. "Modeling Slug Growth in Pipelines" Software Users Manual, by S. L. Scott (June 1989).
63. "Prudhoe Bay Large Diameter Slug Flow Experiments and Data Base System" Users Manual, by S. L. Scott (July 1989).
64. "Two-Phase Slug Flow in Upward Inclined Pipes", by G. Zheng (Dec. 1989).
65. "Elimination of Severe Slugging in a Pipeline-Riser System," by F. E. Jansen (May 1990).
66. "A Mechanistic Model for Predicting Annulus Bottomhole Pressures for Zero Net Liquid Flow in Pumping Wells," by D. Papadimitriou (May 1990).
67. "Evaluation of Slug Flow Models in Horizontal Pipes," by C. A. Daza (May 1990).
68. "A Comprehensive Mechanistic Model for Two-Phase Flow in Pipelines," by J. J. Xiao (Aug. 1990).
69. "Two-Phase Flow in Low Velocity Hilly Terrain Pipelines," by C. Sarica (Aug. 1990).
70. "Two-Phase Slug Flow Splitting Phenomenon at a Regular Horizontal Side-Arm Tee," by S. Arirachakaran (Dec. 1990)
71. "RECENT PUBLICATIONS" - A collection of articles based on previous TUFFP research reports that have been published or are under review for various technical journals (May 1991).
72. "Two-Phase Flow in Horizontal Wells," by M. Ihara (October 1991).
73. "Two-Phase Slug Flow in Hilly Terrain Pipelines," by G. Zheng (October 1991).
74. "Slug Flow Phenomena in Inclined Pipes," by I. Alves (October 1991).
75. "Transient Flow and Pigging Dynamics in Two-Phase Pipelines," by K. Minami (October 1991).
76. "Transient Drift Flux Model for Wellbores," by O. Metin Gokdemir (November 1992).
77. "Slug Flow in Extended Reach Directional Wells," by Héctor Felizola (November 1992).
78. "Two-Phase Flow Splitting at a Tee Junction with an Upward Inclined Side Arm," by Peter Ashton (November 1992).
79. "Two-Phase Flow Splitting at a Tee Junction with a Downward Inclined Branch Arm," by Viswanatha Raju Penmatcha (November 1992).
80. "Annular Flow in Extended Reach Directional Wells," by Rafael Jose Paz Gonzalez (May 1994).
81. "An Experimental Study of Downward Slug Flow in Inclined Pipes," by Philippe Roumazelles (November 1994).
82. "An Analysis of Imposed Two-Phase Flow Transients in Horizontal Pipelines Part-1 Experimental Results," by Fabrice Vigneron (March 1995).

83. "Investigation of Single Phase Liquid Flow Behavior in a Single Perforation Horizontal Well," by Hong Yuan (March 1995).
84. "1995 Data Documentation User's Manual", (October 1995).
85. "Recent Publications" A collection of articles based on previous TUFFP research reports that have been published or are under review for various technical journals (February 1996).
86. "1995 Final Report - Transportation of Liquids in Multiphase Pipelines Under Low Liquid Loading Conditions", Final report submitted to Penn State University for subcontract on GRI Project.
87. "A Unified Model for Stratified-Wavy Two-Phase Flow Splitting at a Reduced Tee Junction with an Inclined Branch Arm", by Srinagesh K. Marti (February 1996).
88. "Oil-Water Flow Patterns in Horizontal Pipes", by José Luis Trallero (February 1996).
89. "A Study of Intermittent Flow in Downward Inclined Pipes" by Jiede Yang (June 1996).
90. "Slug Characteristics for Two-Phase Horizontal Flow", by Robert Marcano (November 1996).
91. "Oil-Water Flow in Vertical and Deviated Wells", by José Gonzalo Flores (October 1997).
92. "1997 Data Documentation and Software User's Manual", by Avni S. Kaya, Gerad Gibson and Cem Sarica (November 1997).
93. "Investigation of Single Phase Liquid Flow Behavior in Horizontal Wells", by Hong Yuan (March 1998).
94. "Comprehensive Mechanistic Modeling of Two-Phase Flow in Deviated Wells" by Avni Serdar Kaya (December 1998).
95. "Low Liquid Loading Gas-Liquid Two-Phase Flow in Near-Horizontal Pipes" by Weihong Meng (August 1999).
96. "An Experimental Study of Two-Phase Flow in a Hilly-Terrain Pipeline" by Eissa Mohammed Al-Safran (August 1999).
97. "Oil-Water Flow Patterns and Pressure Gradients in Slightly Inclined Pipes" by Banu Alkaya (May 2000).
98. "Slug Dissipation in Downward Flow – Final Report" by Hong-Quan Zhang, Jasmine Yuan and James P. Brill (October 2000).
99. "Unified Model for Gas-Liquid Pipe Flow – Model Development and Validation" by Hong-Quan Zhang (January 2002).
100. "A Comprehensive Mechanistic Heat Transfer Model for Two-Phase Flow with High-Pressure Flow Pattern Validation" Ph.D. Dissertation by Ryo Manabe (December 2001).
101. "Revised Heat Transfer Model for Two-Phase Flow" Final Report by Qian Wang (March 2003).
102. "An Experimental and Theoretical Investigation of Slug Flow Characteristics in the Valley of a Hilly-Terrain Pipeline" Ph.D. Dissertation by Eissa Mohammed Al-safran (May 2003).
103. "An Investigation of Low Liquid Loading Gas-Liquid Stratified Flow in Near-Horizontal Pipes" Ph.D. Dissertation by Yongqian Fan.

104. "Severe Slugging Prediction for Gas-Oil-Water Flow in Pipeline-Riser Systems," M.S. Thesis by Carlos Andrés Beltrán Romero (2005)
105. "Droplet-Homophase Interaction Study (Development of an Entrainment Fraction Model) – Final Report," Xianghui Chen (2005)
106. "Effects of High Oil Viscosity on Two-Phase Oil-Gas Flow Behavior in Horizontal Pipes" M.S. Thesis by Bahadır Gokcal (2005)
107. "Characterization of Oil-Water Flows in Horizontal Pipes" M.S. Thesis by Maria Andreina Vielma Paredes (2006)
108. "Characterization of Oil-Water Flows in Inclined Pipes" M.S. Thesis by Serdar Atmaca (2007).
109. "An Experimental Study of Low Liquid Loading Gas-Oil-Water Flow in Horizontal Pipes" M.S. Thesis by Hongkun Dong (2007).

Appendix B

2008 Fluid Flow Projects Advisory Board Representatives

Baker Atlas

Dan Georgi
Baker Atlas
2001 Rankin Road
Houston, Texas 77073
Phone: (713) 625-5841
Fax: (713) 625-6795
Email: dan.georgi@bakeratlas.com

Datong Sun
Baker Atlas
2001 Rankin Road
Houston, Texas 77073
Phone: (713) 625-5791
Fax: (713) 625-6795
Email: datong.sun@bakeratlas.com

BP

Official Representative & UK Contact

Phil Sugarman
BP
Upstream Technology Group
Chertsey Road
Sunbury-on-Thames, Middlesex TW 16 7LN
England
Phone: (44 1 932) 762882
Fax: (44 1 932) 763178
Email: sugarman@bp.com

US Contact

George Shoup
BP
501 Westlake Park Blvd.
Houston, Texas 77079
Phone: (281) 366-7238
Fax:
Email: shoupgj@bp.com

Oris Hernandez
Flow Assurance Engineer
BP
501 Westlake Park Blvd.
Houston, Texas 77079
Phone: (281) 366-5649
Fax:
Email: oris.hernandez@bp.com

Alternate UK Contact

Paul Fairhurst
BP
Flow Assurance Engineering – UTG
Building H
Chertsey Road
Sunbury on Thames, Middlesex TW16 7LN
England
Phone: (44 1 932) 774818
Fax: (44 7 787) 105183
Email: fairhucp@bp.com

Andrew Hall
BP
Pipeline Transportation Team, EPT
1H-54 Dyce
Aberdeen, AB21 7PB
United Kingdom
Phone: (44 1224) 8335807
Fax:
Email: halla9@bp.com

Chevron

Lee Rhyne
Chevron
Flow Assurance Team
1500 Louisiana Street
Houston, Texas 77002
Phone: (832) 854-7960
Fax: (832) 854-7900
Email: lee.rhyne@chevron.com

Sam Kashou
Chevron
1500 Louisiana Street
Houston, Texas 77002
Phone: (832) 854-3917
Fax: (832) 854-6425
Email: samkashou@chevron.com

Jeff Creek
Chevron
1500 Louisiana Street
Houston, Texas 77002
Phone: (832) 854-7957
Fax: (832) 854-7900
Email: lcrc@chevron.com

ConocoPhillips, Inc.

Tom Danielson
ConocoPhillips, Inc.
600 N. Dairy Ashford
1036 Offshore Building
Houston, Texas 77079
Phone: (281) 293-6120
Fax: (281) 293-6504
Email: tom.j.danielson@conocophillips.com

Kris Bansal
ConocoPhillips, Inc.
1034 Offshore Building
600 N. Dairy Ashford
Houston, Texas 77079
Phone: (281) 293-1223
Fax: (281) 293-3424
Email: kris.m.bansal@conocophillips.com

Richard Fan
ConocoPhillips, Inc.
600 N. Dairy Ashford
1052 Offshore Building
Houston, Texas 77079
Phone: (281) 293-4730
Fax: (281) 293-6504
Email: yongqian.fan@conocophillips.com

Department of Energy

Chandra Nautiyal
National Petroleum Technology Office
Williams Center Tower One
One West Third Street, Suite 1400
Tulsa, Oklahoma 74108
Phone:
Fax:
Email: chandra.nautiyal@netl.doe.gov

ExxonMobil

Don Shatto
ExxonMobil
P. O. Box 2189
Houston, Texas 77252-2189
Phone: (713) 431-6911
Fax: (713) 431-6387
Email: don.p.shatto@exxonmobil.com

Jiyong Cai
ExxonMobil
P. O. Box 2189
Houston, Texas 77252-2189
Phone: (713) 431-7608
Fax: (713) 431-6387
Email: jiyong.cai@exxonmobil.com

JOGMEC

Tomoko Watanabe
JOGMEC
1-2-2, Hamada, Mihama-ku
Chiba, 261-0025 Japan
Phone: (81 43) 2769281
Fax: (81 43) 2764063
Email: watanabe-tomoko@jogmec.go.jp

Masaru Nakamizu
JOGMEC
One Riverway, Suite 450
Houston, Texas 77056
Phone: (713) 622-0204
Fax: (713) 622-1330
Email: nakamizu-masaru@jogmec.jo.jp

Kuwait Oil Company

Eissa Alsafran
Kuwait University
Email: eisa@kuc01.kuniv.edu.kw

Adel Al-Abbasi
Manager, Research and Technology
Kuwait Oil Company (K.S.C.)
P. O. Box 9758
Ahmadi – Kuwait 61008
Phone: (965) 398-8158
Fax: (965) 398-2557
Email: aabbasi@kockw.com

Abdullatif Y. Al-Kandari
Team Leader
Research and Technology Group
Industrial Area
Kuwait Oil Company
P. O. Box 9758
Ahmadi – Kuwait 61008
Phone: (965) 3984132
Fax: (965) 3984138
Email: almohamm@kockw.com

Marathon Oil Company

Rob Sutton
Marathon Oil Company
P. O. Box 3128
Room 3343
Houston, Texas 77253
Phone: (713) 296-3360
Fax: (713) 296-4259
Email: rpsutton@marathonoil.com

Minerals Management Services

Sharon Buffington
Minerals Management Services
Technology Research Assessment Branch
381 Elden Street
Mail Stop 2500
Herndon, VA 20170-4817
Phone: (703) 787-1147
Fax: (703) 787-1555
Email: sharon.buffington@mms.gov

Pemex

Miguel Hernandez
Pemex
1er Piso Edificio Piramide
Blvd. Adolfo Ruiz Cortines No. 1202
Fracc. Oropeza CP
86030 Villahermosa, Tabasco,
Mexico
Phone:
Fax:
Email: mhernandezga@pep.pemex.com

Dr. Heber Cinco Ley
Pemex Exploracion y Produccion
Subdireccion de la Coordinacion Tecnica de Explotacion
Gerencia de Sistemas de Produccion
Av. Marina Nacional Num 329
Torre Ejecutiva Piso 41
Colonia Huasteca C. P. 11311
Mexico D.F.

Jose Francisco Martinez
Pemex
Phone:
Fax:
Email: fmartinezm@pep.pemex.com

Petrobras

Rafael Mendes
Petrobras
Cidade Universitaria – Quadra 7 – Ilha do Fundao
CENPES/PDEP/TEEA
Rio de Janeiro 21949-900
Brazil
Phone: (5521) 38652008
Fax:
Email: rafael.mendes@petrobras.com.br

Marcelo Goncalves
Petrobras
Cidade Universitaria – Quadra 7 – Ilha do Fundao
CENPES/PDEP/TEEA
Rio de Janeiro 21949-900
Brazil
Phone: (5521) 38656712
Fax: 5521) 38656796
Email: marcelog@petrobras.com.br

Kazuioishi Minami
Petrobras
Av. Republica do Chile
65 – 17° Andar – Sala 1703
Rio de Janeiro 20035-900
Brazil
Phone: (55 21) 5346020
Fax: (55 21) 5341128
Email: minami@petrobras.com.br

Ibere Alves
Petrobras
Phone: (55 21) 5343720
Email: ibere@petrobras.com.br

Petronas

Sukor B. Ahmad
Materials & Facilities
Novel Process and Advanced Engineering
Petronas
Lot 3288 & 3289 Off Jalan Ayer Itam
Kawasan Institusi Bangi
43000 Kajang, Selangor Darul Ehsan
Malaysia
Phone: (603) 89281031
Fax:
Email: sukor@petronas.com.my

Feroz Sultan
Project Engineer
(Instrumentation and Control)
Facilities Engineering Group
Plant & Engineering Division
Petronas
Lot 3288 & 3289 Off Jalan Ayer Itam
Kawasan Institusi Bangi
43000 Kajang, Selangor Darul Ehsan
Malaysia
Phone: (603) 89281233
Fax: (603) 89253146
Email: maungmyothant@petronas.com.my

Rosneft

Vitaly Krasnov
Rosneft Oil Company
Sofiyskaya embankment 26/1
115998 Moscow
Russia
Phone:
Fax:
Email: v_krasnov@rosneft.ru

Vitaly Yelitcheff
Rosneft Oil Company
450092 ufa
Revolutionnaya Str, 96/2
Russia
Phone: (73472) 289900
Fax: (73472) 289900
Email: vitaly@ufanipi.ru
vyelitcheff@gmail.com

Schlumberger

Mack Shippen
Schlumberger
5599 San Felipe
Suite 1700
Houston, Texas 77056
Phone: (713) 513-2532
Fax: (713) 513-2042
Email: mshippen@slb.com

Nina Vielma
Schlumberger Information Services
5599 San Felipe
Suite 1700
Houston, Texas 77063
Phone: (713) 513-1533
Fax:
Email: mvielma@slb.com

Sammy Haddad
GFM Reservoir Domain Champion & Res. Eng. Advisor
Schlumberger Middle East S.A.
Mussafah
P. O. Box 21
Abu Dhabi, UAE
Phone: (971 2) 5025212
Fax:
Email: shaddad@abu-dhabi.oilfield.slb.com

William Bailey
Principal
Schlumberger – Doll Research
1 Hampshire Street, MD-B213
Cambridge, MA 02139
Phone: (617) 768-2075
Fax:
Email: wbailey@slb.com

Shell Global Solutions

Rusty Lacy
Fluid Flow (OGUF)
Shell Global Solutions (US) Inc.
Westhollow Technology Center
3333 Hwy 6 South
Houston, Texas 77082-3101
Phone: (281) 544-7309
Fax: (281) 544-8427
Email: ulf.andresen@shell.com

Ulf Andresen
Fluid Flow Engineer
Shell Global Solutions (US) Inc.
Westhollow Technology Center
3333 Hwy 6 South
Houston, Texas 77082
Phone: (281) 544-6424
Fax:
Email: ulf.andresen@shell.com

Tenaris

Teresa Perez
Tenaris
Dr. Jorge A. Simini 250
(B2804MHA) Campana
Buenos Aires, Argentina
Phone: (54) 3489 433012
Fax:
Email: tperez@tenaris.com

Claudio Morales
Senior Researcher
Center for Industrial Research
Tenaris
Dr. Jorge A. Simini 250
(B2804MHA) Campana
Buenos Aires, Argentina
Phone: (54) 3489 433100 ext. 34313
Fax: (54) 3489 427928
Email: clmorales@tenaris.com

TOTAL

Alain Ricordeau
TOTAL

Phone: (33 559) 836997
Fax:
Email: alain.ricordeau@total.com

Benjamin Brocart
Research Engineer
Rheology and Disperse Systems
TOTAL Petrochemicals France
Research & Development Centre Mont/Lacq
B. P. 47 – F – 64170
Lacq, France
Phone: (33 559) 926611
Fax: (33 559) 926765
Email: Benjamin.brocart@total.com

Appendix C

History of Fluid Flow Projects Membership

1973		
1.	TRW Reda Pump	12 Jun. '72 T: 21 Oct. '77
2.	Pemex	15 Jun. '72 T: 30 Sept. '96 R: Dec '97 Current
3.	Getty Oil Co.	19 Jun. '72 T: 11 Oct. '84 with sale to Texaco
4.	Union Oil Co. of California	7 Jul. '72 T: for 2001
5.	Intevep	3 Aug. '72 TR: from CVP in '77; T: 21 Jan '05 for 2006
6.	Marathon Oil Co.	3 Aug. '72 T: 17 May '85 R: 25 June '90 T: 14 Sept. '94 R: 3 June '97 Current
7.	Arco Oil and Gas Co.	7 Aug. '72 T: 08 Dec. '97
8.	AGIP	6 Sep. '72 T: 18 Dec. '74
9.	Otis Engineering Corp.	4 Oct. '72 T: 15 Oct. '82
10.	ConocoPhillips, Inc.	5 Oct. '72 T: Aug. '85 R: 5 Dec. '86 Current
11.	Mobil Research and Development Corp.	13 Oct. '72 T: 27 Sep. 2000
12.	Camco, Inc.	23 Oct. '72 T: 15 Jan. '76 R: 14 Mar. '79 T: 5 Jan. '84
13.	Crest Engineering, Inc.	27 Oct. '72 T: 14 Nov. '78 R: 19 Nov. '79 T: 1 Jun. '84
14.	Chevron	3 Nov. '72 Current
15.	Aminoil	9 Nov. '72 T: 1 Feb. '77

16.	Compagnie Francaise des Petroles (TOTAL)	6 Dec. '72	T: 22 Mar. '85 R: 23 Oct. '90 T: 18 Sep. '01 for 2002 R: 18 Nov. '02 Current
17.	Oil Service Co. of Iran	19 Dec. '72	T: 20 Dec. '79
18.	Sun Exploration and Production Co.	4 Jan. '73	T: 25 Oct. '79 R: 13 Apr. '82 T: 6 Sep. '85
19.	Amoco Production Co. (now as BP Amoco)	18 May '73	
20.	Williams Brothers Engrg. Co.	25 May '73	T: 24 Jan. '83

1974

21.	Gulf Research and Development Co.	20 Nov. '73	T: Nov. '84 with sale to Chevron
22.	El Paso Natural Gas Co.	17 Dec. '73	T: 28 Oct. '77
23.	Arabian Gulf Exploration Co.	27 Mar. '74	T: 24 Oct. '82
24.	ExxonMobil Upstream Research	27 Mar. '74	T: 16 Sep. '86 R: 1 Jan. '88 T: 27 Sep. 2000 R: 2007 Current
25.	Bechtel, Inc.	29 May '74	T: 14 Dec. '76 R: 7 Dec. '78 T: 17 Dec. '84
26.	Saudi Arabian Oil Co.	11 Jun. '74	T: for 1999
27.	Petrobras	6 Aug. '74	T: for 2000 R: for 2005 Current

1975

28.	ELF Exploration Production (now as TotalFina Elf)	24 Jul. '74	T: 24 Feb. '76 Tr. from Aquitaine Co. of Canada 19 Mar. '81 T: 29 Jan. '87 R: 17 Dec. '91
29.	Cities Service Oil and Gas Corp.	21 Oct. '74	T: 25 Oct. '82 R: 27 Jun. '84 T: 22 Sep. '86

30.	Texas Eastern Transmission Corp.	19 Nov. '74	T: 23 Aug. '82
31.	Aquitaine Co. of Canada, Ltd.	12 Dec. '74	T: 6 Nov. '80
32.	Texas Gas Transmission Corp.	4 Mar. '75	T: 7 Dec. '89

1976

33.	Panhandle Eastern Pipe Line Co.	15 Oct. '75	T: 7 Aug. '85
34.	Phillips Petroleum Co.	10 May '76	T: Aug. 94 R: Mar 98 T: 2002

1977

35.	N. V. Nederlandse Gasunie	11 Aug. '76	T: 26 Aug. '85
36.	Columbia Gas System Service Corp.	6 Oct. '76	T: 15 Oct. '85
37.	Consumers Power Co.	11 Apr. '77	T: 14 Dec. '83
38.	ANR Pipeline Co.	13 Apr. '77	TR: from Michigan- Wisconsin Pipeline Co. in 1984 T: 26 Sep. '84
39.	Scientific Software-Intercomp	28 Apr. '77	TR: to Kaneb from Intercomp 16 Nov. '77 TR: to SSI in June '83 T: 23 Sep. '86
40.	Flopetrol/Johnston-Schlumberger	5 May '77	T: 8 Aug. '86

1978

41.	Norsk Hydro a.s	13 Dec. '77	T: 5 Nov. '82 R: 1 Aug. '84 T: 8 May '96
42.	Dresser Industries Inc.	7 Jun. '78	T: 5 Nov. '82

1979

43.	Sohio Petroleum Co.	17 Nov. '78	T: 1 Oct. '86
44.	Esso Standard Libya	27 Nov. '78	T: 2 Jun. '82
45.	Shell Internationale Petroleum MIJ B.V. (SIPM)	30 Jan. '79	T: Sept. 98 for 1999

1980

46.	Fluor Ocean Services, Inc.	23 Oct. '79	T: 16 Sep. '82
47.	Texaco	30 Apr. '80	T: 20 Sep. '01 for 2002
48.	BG Technology (Advantica)	15 Sep. '80	T: 2003

1981		
-------------	--	--

49.	Det Norske Veritas	15 Aug. '80	T: 16 Nov. '82
-----	--------------------	-------------	----------------

1982		
-------------	--	--

50.	Arabian Oil Co. Ltd.	11 May '82	T: Oct.'01 for 2002
-----	----------------------	------------	---------------------

51.	Petro Canada	25 May '82	T:28 Oct. '86
-----	--------------	------------	---------------

52.	Chiyoda	3 Jun. '82	T: 4 Apr '94
-----	---------	------------	--------------

53.	BP	7 Oct. '81	Current
-----	----	------------	----------------

1983		
-------------	--	--

54.	Pertamina	10 Jan. '83	T: for 2000 R: March 2006
-----	-----------	-------------	------------------------------

1984		
-------------	--	--

55.	Nippon Kokan K. K.	28 Jun. '83	T: 5 Sept. '94
-----	--------------------	-------------	----------------

56.	Britoil	20 Sep. '83	T: 1 Oct. '88
-----	---------	-------------	---------------

57.	TransCanada Pipelines	17 Nov. '83	T:30 Sep. '85
-----	-----------------------	-------------	---------------

58.	Natural Gas Pipeline Co. of America (Midcon Corp.)	13 Feb. '84	T:16 Sep. '87
-----	---	-------------	---------------

59.	JGC Corp.	12 Mar. '84	T: 22 Aug. '94
-----	-----------	-------------	----------------

1985		
-------------	--	--

60.	STATOIL	23 Oct. '85	T:16 Mar. '89
-----	---------	-------------	---------------

1986		
-------------	--	--

61.	JOGMEC (formerly Japan National Oil Corp.)	3 Oct. '86	T: 2003 R: 2007 Current
-----	--	------------	--------------------------------------

1988		
-------------	--	--

62.	China National Oil and Gas Exploration and Development Corporation	29 Aug. '87	T:17 Jul. '89
-----	--	-------------	---------------

63.	Kerr McGee Corp.	8 Jul. '88	T:17 Sept. '92
-----	------------------	------------	----------------

1989		
-------------	--	--

64.	Simulation Sciences, Inc.	19 Dec. '88	T: for 2001
-----	---------------------------	-------------	-------------

1991		
-------------	--	--

65.	Advanced Multiphase Technology	7 Nov. '90	T:28 Dec. '92
-----	--------------------------------	------------	---------------

66.	Petronas	1 Apr. '91	T: 02 Mar. 98 R: 1 Jan 2001 Current
-----	----------	------------	--

1992

67.	Instituto Colombiano Del Petroleo	19 July '91	T: 3 Sep. '01 for 2002
68.	Institut Francais Du Petrole	16 July. '91	T: 8 June 2000
69.	Oil & Natural Gas Commission of India	27 Feb. '92	T: Sept. 97 for 1998

1994

70.	Baker Jardine & Associates	Dec. '93	T: 22 Sept. '95 for 1996
-----	----------------------------	----------	--------------------------

1998

71.	Baker Atlas	Dec. 97	Current
72.	Minerals Management Service (Department of Interior's)	May. 98	Current

2002

73.	Schlumberger Overseas S.A.	Aug. 02	Current
74.	Saudi Aramco	Mar. 03	T: for 2007

2004

75.	YUKOS	Dec. '03	T: 2005
76.	Landmark Graphics	Oct. '04	T: 2008

2005

77.	Rosneft	July '05	Current
-----	---------	----------	----------------

2006

78.	Tenaris		Current
79.	Shell Global		Current
80.	Kuwait Oil Company		Current

Note: T = Terminated; R = Rejoined; and TR = Transferred

Appendix D

Contact Information

Director

Cem Sarica

(918) 631-5154
cem-sarica@utulsa.edu

Associate Director

Holden Zhang

(918) 631-5142
hong-quan-zhang@utulsa.edu

Director Emeritus

James P. Brill

(918) 631-5114
brill@utulsa.edu

Project Coordinator

Linda M. Jones

(918) 631-5110
jones@utulsa.edu

Project Engineer

Scott Graham

(918) 631-5147
sdgraham@utulsa.edu

Research Associates

Mingxiu (Michelle) Li

(918) 631-5107
michelle-li@utulsa.edu

Research Technicians

Brandon Kelsey

(918) 631-5133
brandon-kelsey@utulsa.edu

Craig Waldron

(918) 631-5131
craig-waldron@utulsa.edu

Research Assistants

Kwonil Choi

(918) 631-5146
kwon-choi@utulsa.edu

Gizem Ersoy

(918) 631-5117
gizem-ersoy@utulsa.edu

Bahadir Gokcal

(918) 631-5119
bahadir-gokcal@utulsa.edu

Ceyda Kora

(918) 631-5117
ceyda-kora@utulsa.edu

Kyle Magrini

(918) 631-5119
kyle-magrini@utulsa.edu

Anoop Sharma

(918) 631-5124
anoop-sharma@utulsa.edu

Feng Xiao

(918) 631-5117
feng-xiao@utulsa.edu

Tingting Yu

(918) 631-5124
tingting-yu@utulsa.edu

Computer Resource Manager
James Miller

(918) 631-5115
james-miller@utulsa.edu

Fax Number:
Web Sites:

(918) 631-5112
www.tuffp.utulsa.edu